The adhesion G protein-coupled receptor BAI1 regulates the innate immune response to Gram-negative bacteria in macrophages

Emily Alyssa Billings
Bartlett, Illinois

Bachelor of Science, University of Illinois Urbana-Champaign, 2005

A Dissertation presented to the Graduate Faculty
of the University of Virginia in Candidacy for the Degree of
Doctor of Philosophy

Department of Microbiology, Immunology, and Cancer Biology

University of Virginia
May, 2016

Abstract

The early innate immune response is a critical component of host defense, driving the activation of early inflammatory signaling and cytokine responses that lead to cellular activation, cellular recruitment, and microbicidal activity to aid in the clearance of invading microbes and the resolution of inflammatory states. The detection of microbes and initiation of an innate immune response occurs through pattern recognition receptors (PRRs). It is unlikely that innate immune cells are presented with a single inflammatory stimulus during infection. Instead, the host is primed to detect several microbe associated molecular patterns (MAMPs) through the use of many PRRs, a feature thought to provide further specificity to the cellular response. Thus, the engagement of PRRs and the initiation of an immune response is a collaborative and coordinated process.

Brain angiogenesis inhibitor 1 (BAI1) is an adhesion heterotrimeric G-protein coupled receptor (GPCR) expressed in various tissues and cell types including myeloid lineage cells. In addition to negatively regulating neovascularization in brain tumor models, it was previously characterized as a phagocytic receptor for apoptotic cells. More recently, BAI1 has been shown to mediate the recognition and internalization of Gram-negative bacteria through an interaction with bacterial lipopolysaccharide (LPS). Prior to this study, the role of BAI1 during the recognition and response to Gram-negative bacteria in macrophages was largely unknown. The work presented in this thesis provides advances to our understanding of the ligand specificity of the TSR domains, the impact of BAI1-mediated phagocytosis on the fate of the internalized microbe, and the interaction of BAI1 with inflammatory signaling and transcriptional responses. BAI1, through the five TSR domains in the extracellular region, recognizes the negatively charged

phosphorylated L-glycero-d-manno-heptose sugars in the inner core oligosaccharide of LPS in the Gram-negative bacterial outer membrane. This suggests that BAI1-mediated detection is broadly relevant for bacterial recognition, as the phosphorylation of the inner core oligosaccharide is critical for membrane stability and is conserved across many Gram-negative bacterial species, commensals and pathogens alike.

The fate of a microbe upon contact with a host cell is determined by the local inflammatory environment and the route of cellular entry. The role and impact of BAI1-mediated recognition in the immune response of macrophages was previously undetermined. Here, we show that BAI1-driven Rac activation promotes the phagocyte NADPH oxidase-dependent ROS response, resulting in oxidative bacterial killing in vitro, and protection in an in vivo bacterial challenge model. This provides mechanistic insight into how upstream signals from non-opsonic phagocytic receptors, like BAI1, couple to the activation of critical microbicidal machinery in the context of several representative Gram-negative microbes.

We further characterized the impact of BAI1 on innate inflammatory signaling pathways and assessed the means of receptor crosstalk and interaction. We found that BAI1 selectively promotes intracellular signaling and transcriptional responses of toll-like receptor (TLR) 4 by enhancing the downstream phosphorylation and activation of TBK1 and IRF3. TRIF-dependent type-I IFN-β, IL-10, and CCL5 induction were all reduced in macrophages lacking BAI1, indicating a selective role for BAI1 in critical early innate responses that drive local cellular activation and regulate inflammatory responses. Moreover, TLR4 and BAI1 physically associate in a manner dependent upon an interaction with the cytoplasmic region of BAI1, and the spatial interaction between

Gram-negative bacteria and TLR4 is enhanced by BAI1 co-expression. The direct mechanisms of this interaction remain to be explored, but likely involve BAI1-dependent signaling that modulates either the local recruitment or activation of TLR4 signaling partners.

Collectively, this highlights the critical and unique specificity and function of BAI1 during TLR4-driven bacterial recognition and early innate responses and suggests that the phagosome serves as a multifunctional and heterogeneous organelle that is distinct from other innate signaling compartments within macrophages.

Table of Contents

List of Figures and Tables

List of Abbreviations

ADGRB1	Adhesion G protein-coupled receptor B1
ADP	Adenosine diphosphate
ATP	Adenosine triphosphate
αMem	Alpha minimal essential medium
ANOVA	Analysis of variance
ALR	Absent in melanoma 2 (AIM-2)-like receptor
AP-1	Activating protein-1
Arf6	ADP ribosylation factor 6
ASK1	Apoptosis signal-regulating kinase-1
BAI	Brain angiogenesis inhibitor
BAIAP	BAI1 associated protein
BAP	BAI1 associated protein
BMDM	bone marrow derived macrophage
BSA	bovine serum albumin
CARD	Caspase activation and recruitment domain
CCL5	C-C motif ligand 5
CD14	Cluster of differentiation 14
CFU	Colony-forming unit
CGD	Chronic granulomatous disease
CHO	Chinese hamster ovary cells
cIAP	Cell inhibitor of apoptosis
CLR	C-type lectin receptor

CR	Complement receptor
CSF1	Colony stimulating factor-1
CXCL1	C-X-C motif ligand 1
DAMP	Damage associated molecular pattern
DC-SIGN (SIGNR-1)	Dendritic cell-specific intercellular adhesion molecule-3-grabbing non-integrin
DMEM	Dulbecco's modified Eagle medium
DPI	Diphenyleneiodonium
DUOX	Dual oxidase
EGF	Epidermal growth factor
ELMO	Engulfment and cell motility protein
EMR2	EGF-like module containing mucin-like hormone receptor 2
ERC	Endocytic recycling compartment
ERK	Extracellular signal-regulated kinase
FBS	Fetal bovine serum
FcγR	Fc gamma receptor
FIP	Family of Rab11 interacting protein
GAIN	GPCR autoproteolysis-inducing domain
GAP	GTPase activating protein
GDI	Guanosine-nucleotide dissociation inhibitors
GDP	Guanosine diphosphate
GEF	Guanosine nucleotide exchange factors

GFP	Green fluorescent protein
GPCR	Heterotrimeric guanine nucleotide-binding protein-coupled receptor
GPS	GPCR proteolytic site
GTP	Guanosine triphosphate
GTPase	Guanosine triphosphate hydrolase
GST	Glutathione-*S*-transferase
HA	Hemagglutinin
HBD	Hormone binding domain
HBSS	Hanks' balanced salt solution
HIA	Heat inactivated
IFN	Interferon
IRAK	IL-1 receptor associated kinase
IRF	Interferon regulatory factor
IKK	IκB kinase
iNOS (NOS2)	Nitric oxide synthase 2
ISG	IFN stimulated gene
ITAM	Immunoreceptor tyrosine-based activating motif
ITIM	Immunoreceptor tyrosine-based inhibitory motif
JNK	c-Jun N-terminal kinase
KDO	3-deoxy-D-manno-otulosonic acid
KO	Knockout
LARG	Leukemia-associated RhoGEF

LB	Luria-bertani
LBC	lymphoid blast crisis
LBP	LPS binding protein
LDCL	Luminol-dependent chemiluminescence
LDL	Low density lipoprotein
LPA	Lysophosphatidic acid
LPS	Lipopolysaccharide
LRR	Leucine rich repeat
MAGI	Membrane associated guanylate kinase, WW and PDZ domain containing protein
MAMP	Microbe associated molecular pattern
MAPK	Mitogen-activated protein kinase
MARCO	Macrophage associated receptor with collagenous structure
MBL	Mannose binding lectin
MD2	Myeloid differentiation factor 2
MFI	Mean fluorescence intensity
MKK	MAPK kinase
MOI	Multiplicity of infection
MyD88	Myeloid differentiation primary response factor 88
NAC	N-acetylcysteine
NADPH	Nicotinamide adenine dinucleotide phosphate
NAP1	NF-κB-activating kinase-associated protein
NFAT	Nuclear factor of T cells

NF-κB	Nuclear factor-kappa B
NGS	Normal goat serum
NLR	Nucleotide oligomerization domain (NOD)-like receptor
NOS2 (iNOS)	Nitric oxide synthase 2
NOX	NADPH oxidase
NRAMP1	Natural resistance-associated macrophage protein 1
PAK	p-21 activating kinase
PBD	p-21-binding domain of PAK
PBS	Phosphate-buffered saline
PDZ	PSD-95/Disc-large/ZO-1 homology
PEM	Peritoneal macrophage
PFA	Paraformaldehyde
PI3K	Phosphoinositide 3-kinase
PI(4,5)P_2	Phosphatidylinositol (4,5) bisphosphate-2
PI(3)P	Phosphatidlyinositol 3-phosphate
PI(4)P	Phosphatidlyinositol 4-phosphate
PI5K	Phosphoinositide 4 phosphate 5-kinase
PKC	Protein kinase C
PLCγ2	Phospholipase C, gamma 2
PMA	Phorbol myristate acetate
PRR	Pattern recognition receptor
PSD	Post synaptic density
PYD	Pyrin domain

qRT-PCR	Quantitative real-time polymerase chain reaction
RGS	Regulator of G protein signaling
RIP1 (RIPK1)	Receptor interacting protein-1
ROI	Region of interest
ROS	Reactive oxygen species
RNS	Reactive nitrogen species
RLR	Retinoic acid-inducible gene I (RIG-I)-like receptor
SDS-PAGE	SDS-polyacrylamide gel electrophoresis
SEM	Standard error of the mean
shRNA	Short hairpin RNA
SH3	SRC-homology 3 domain
SIGNR-1(DC-SIGN)	Dendritic cell-specific intercellular adhesion molecule-3-grabbing non-integrin
SINTBAD	Similar to NAP1 TBK1 adaptor
SP-D	Surfactant protein D
SPI	*Salmonella* pathogenicity island
SR-A	Scavenger receptor A
STAT1	Signal transducer and activator of transcription 1
TAB	TAK1 binding protein 1
TAK1	Transforming growth factor β-activated kinase 1
TANK	TRAF family member-associated NF-κB activator
TBK1	Tank binding kinase 1
TIR	Toll/Interleukin-1 receptor homology

TIRAP	TIR domain-containing adaptor protein
TLR	Toll-like receptor
TNF-α	Tumor necrosis factor-α
TRAM	TRIF-related adaptor molecule
TRAF	Tumor necrosis factor receptor associated factor
TRIF	TIR domain-containing adaptor protein inducing IFN-β
TSP-1	Thrombospondin-1
TSR	Type-I thrombospondin repeat
T3SS	Type three-secretion system
V-ATPase	Vacuolar adenosine triphosphate hydrolases
WASP/N-WASP	Wiskott-Alrich Syndrome Protein
WAVE/Scar	WASP-family verprolin-homologous protein
WT	Wild type
WGA	Wheat germ agglutinin

Acknowledgements

"How wonderful it is to follow a thought quietly to its logical end. I have done this a few times. But mostly I just stand in the dark field, in the middle of the world, breathing in and out." Mary Oliver

To my advisor, Dr. Jim Casanova—Thank you for your mentorship and guidance. Your passion for basic research and love for science and learning is contagious. Your continuous support of my endeavors both inside the lab and in a variety of extracurricular activities (clubs, organizations, and internships alike), even when it was not the easiest course, has enabled me to become the scientist, professional, and person I am at the end of this journey.

To my thesis committee, Drs. Alison Criss, Young Hahn, Norbert Leitinger, and Kodi Ravichandran—Thank you for challenging me and supporting my growth. Your time and effort have truly helped me to think critically about science and to take a step back from the details, to which I am so easily drawn.

To the University of Virginia community—Thank you for cultivating a research environment of excellence that still maintains its enthusiasm and collaborative spirit. Thank you especially for supporting graduate student development outside of the classroom and the lab. I know this has impacted my course, and I think it will continue to impacts others.

To the members of the Casanova Lab, Kathryn Conger, Adam Greene, and Tori Weprinsky, and Drs. Ryan D'Souza, Christy Nichols, Corey Meyer, Ken Myers, Radim

Moravec, and Kate Owen—Your unique talents are so impressive and inspirational, and your support scientifically, professionally, and personally has meant so much.

To my friends—Thank you for enriching my life. Our many adventures and conversations will stay with me. When things seemed tough, your presence helped me remember how worthwhile this experience has been independent of everything else.

To my family—To my extended family, I am fortunate to have grown up in such a supportive and connected environment. Thank you for that, even when months and miles may separate us. To my sister, Alexandra, thank you for growing up by my side. I am grateful for all of your stories, advice, and support, and I am also so proud of the person you have become. To my parents, Jack and Bridget, thank you for your constant and unwaivering support. It is undeniable that without it, I would not be here. You instilled a sense of wonder for life and biology in me, from flowers to snakes to microbes, at an early age—and now here I am.

To my husband, Stephan—Thank you for being there for me through all of the challenges and successes and so many light and dark conversations. You will always be the best (and most exuberant) dance partner, personal chef, and friend.

The work presented here would not have been possible without the support of you all. For that, you have all my gratitude. Although this seemed to take so long, it went by so quickly, so "celebrate we will." Dave Matthews Band

Chapter 1:

Introduction

Chapter 1 Introduction

Innate immunity: Early perspectives and evolution of a field

Although the concepts of cellular and humoral innate immunity and the underlying cell biological processes (e.g. phagocytosis) were coined over a century ago, the field has recently evolved with the discovery and characterization of pattern recognition receptors (PRR) (1-4). It is now well appreciated that the innate immune system is a vital component of multicellular life, contributing to the maintenance and homeostasis of local environments enriched in crosstalk between host and microbes, the initiation of early inflammatory responses, the education of adaptive immunity, and the resolution of inflammation. Conceptually, this field went through a "reawakening" with the identification of germ-line encoded receptors that couple the detection of microbes to early inflammatory responses. Charles Janeway first proposed this concept in 1989, where he coined the term PRRs to refer to the sensors of the immune system that distinguish friend from foe to mount inflammatory signaling and priming of adaptive immunity (5). In this simplified model, these receptors distinguish between "self" and "non-self" by recognition of motifs uniquely expressed in microbes to mount an immune response. Early work led to the discovery of the *Drosophila* Toll protein (6), the mammalian homologue thereof (7, 8), and the identification of the mammalian gene required for inflammatory signaling in response to lipopolysaccharide (LPS) (9), which turned out to be Toll-like receptor (TLR) 4 and myeloid differentiation primary response factor 88 (MyD88), respectively.

Since this advance, the field of innate immunity has expanded to better define how the cumulative signals from the local environment, host receptors, and host-microbe

interactions affect the host in health and disease. In addition to "self" from "non-self" signals, other molecular information is interpreted by components of innate and adaptive immunity. This includes the detection of "altered self," such as oxidized low-density lipoprotein (LDL), or "missing self," such as the loss of markers normally expressed during homeostasis (10). Conceptually similar, models of innate immune activation include the danger model, where the host senses cellular and tissue damage induced by infection (11). Interestingly, the immune system utilizes overlapping cell subsets and receptors in the recognition and clearance of "altered self" and "non-self" stimuli, posing the challenge of using the same machinery for disparate outcomes. This is further complicated by the need to distinguish pathogens from resident non-pathogenic microbes. Accordingly, the local environment also plays a role in defining immune responses (12-14). Despite the shared use of receptors in these contexts, downstream responses differ, indicating an elegant level of control. Collectively, the fine tuning of the innate response by the coordinated actions of several receptors and the constant communication between the host environment, immune cells, and microbes provides a method for maintaining homeostasis, mounting effective immune responses during infection, and resolving inflammation. As such, defining the mechanisms contributing the specificity and regulation of innate immunity has further expanded this area of investigation (15-17). In particular, a better understanding of the interactions between innate receptors and the cellular compartmentalization and subcellular context of immune responses is needed.

PRRs

The sensing of microbes and pathogens initially occurs through a limited set of germ-line encoded receptors, defined as PRRs, which are an integral part of the innate

immune system. These receptors detect conserved structural and physical motifs called MAMPs present on distinct classes of microbes (5, 10, 17, 18). There are five major classes of PRRs including TLRs, C-type lectin receptors (CLR), retinoic acid inducible gene I (RIG-I)-like receptors (RLR), nucleotide oligomerization domain (NOD)-like receptors (NLRs), and absent in melanoma 2 (AIM-2)-like receptors (ALR) (15, 18) (**Fig. 1-1**). TLRs and CLRs are transmembrane proteins found on the cell surface and within endosomal compartments where they mediate the recognition of extracellular and internalized MAMPs. Alternatively, RLRs, NLRs, and ALRs are expressed in the cytosol, primed for the recognition of intracellular pathogens. Each of these contains a conserved domain that mediates ligand recognition and a domain that mediates cellular signaling for the development of an inflammatory phenotype. Scavenger receptors (e.g. CD36 and macrophage receptor with collagenous structure (MARCO)) are a distinct subclass of transmembrane PRRs that display broad specificity and are structurally heterogeneous (19, 20). Unlike the major classes of PRRs described above, these proteins are well characterized for their role in the clearance of altered-self ligands or danger associated molecular patterns (DAMP) at steady state and also contribute to recognition of microbes during infection (21-25) (**Fig. 1-1**).

Immune cells like macrophages and monocytes interpret the signals from PRRs to induce inflammatory signaling leading to the local induction of cytokines, chemokines, and type I-interferons (IFN). The coordinated actions of several receptors drive the specificity of the immune response, and loss of these receptors can render hosts highly susceptible to pathogens. This complex and dynamic process serves as the host's first line of defense against infection and is critical for the initiation of protective inflammatory

responses. Overlap amongst the different PRRs conveys enhanced sensitivity and specificity to the innate immune response. While the initiation of an immune response is critical to fight infection, overly robust or unchecked inflammation can also be detrimental to the host. As such, the magnitude and kinetics of the early inflammatory response are tightly regulated by the coordinated actions of several receptors, signaling, and transcriptional responses.

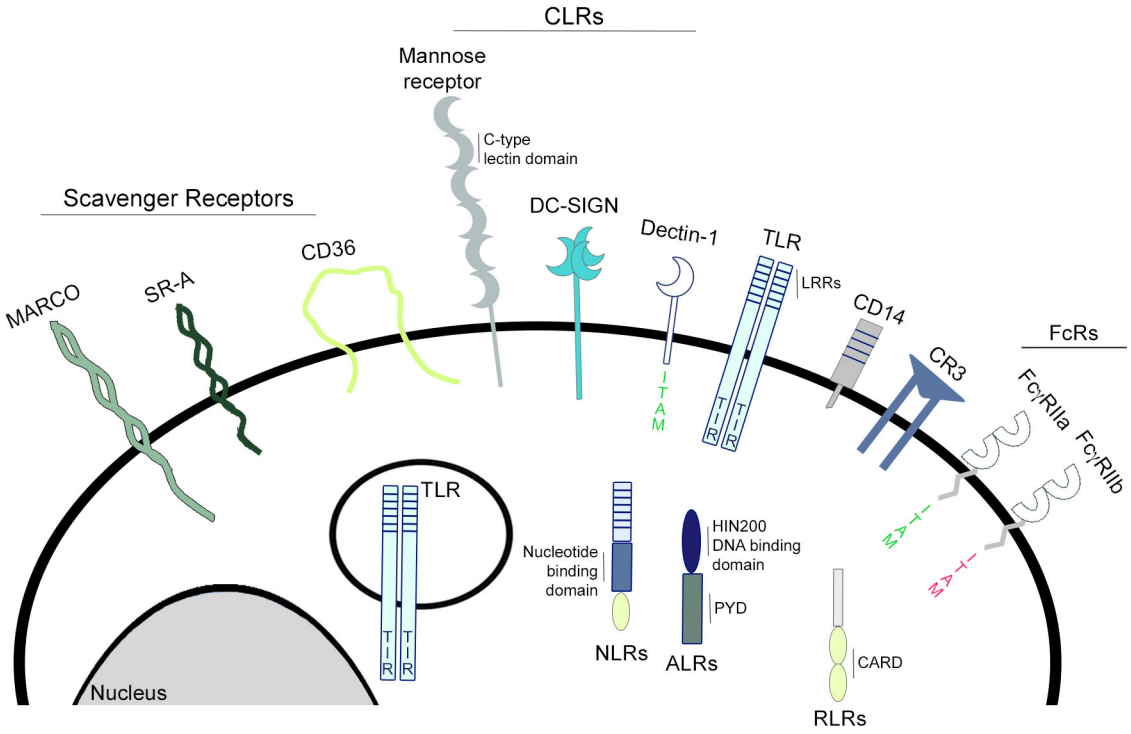
CLRs
Mannose receptor
C-type lectin domain
Scavenger Receptors
DC-SIGN
Dectin-1
TLR
LRRs
CD36
MARCO
SR-A
CD14
CR3
FcRs
FcγRIIa
FcγRIIb
ITAM
TLR
Nucleotide binding domain
HIN200 DNA binding domain
PYD
NLRs
ALRs
CARD
RLRs
Nucleus

Figure 1-1. Representative PRRs expressed on the cell surface and in the host cytoplasm

PRRs expressed on the cell surface are primed for detection of extracellular microbes and surface expressed MAMPs, while cytosolic receptors are biased for the recognition of intracellular microbes. Recognition occurs through conserved domains (e.g. LRR) or C-type lectin domains, which couple to signaling domains (e.g. TIR domain, ITAM, or ITIM). **Fig. 1-1** depicts representative examples of macrophage PRRs and their recognition and signaling domains. Phagocytic receptors, including CLRs and scavenger receptors, drive the phagocytosis and delivery of microbes to an intracellular compartment. Similarly, complement receptors (CRs) and Fc gamma receptors (FcγRs) facilitate the internalization of opsonized particulate ligands. TLRs, expressed on the cell surface and within endosomal compartments, mediate inflammatory signaling responses. NLRs (26, 27), RLRs (28, 29), and ALRs (30, 31) as cytosolic receptors recognize microbial nucleic acids and other stimuli to coordinate inflammatory signaling. In this case, caspase recruitment and activation domains (CARD) and pyrin domains (PYD) mediate activation of the inflammasome (18, 32). (Adapted from Plüddman et al 2010 (33))

Toll-like receptors

The first recognized family of PRRs is the TLRs. These are type-I transmembrane proteins that have a conserved extracellular domain containing leucine-rich repeats (LRR), which functions as the recognition domain, and a conserved Toll/Interleukin-1 receptor homology (TIR) domain, which mediates inflammatory signaling (17). Humans express TLR1-10, while mice express TLR1-9 and TLR11-13. The cell-specific expression patterns of these proteins coincide with specialized functions. For example, plasmacytoid dendritic cells express significantly more TLR7 and TLR9 relative to other innate cell subsets, making them particularly suited for early inflammatory responses to viral infection. Subcellular compartmentalization also plays a critical role in regulating the activation and function of TLRs. As mentioned previously, surface expressed receptors are primed to detect extracellular microbes and surface exposed or accessible MAMPs. TLR1, TLR2, and TLR6 form heterodimers in a stimulus-specific manner to detect lipopeptides, peptidoglycan, and lipoarabinomannans of bacterial cell walls, as well as components of the fungal cell wall (e.g. zymosan and mannans). TLR4 and TLR5 recognize Gram-negative bacterial LPS and flagellin, respectively (17). Other TLRs, including TLR3, TLR7, TLR8, TLR9, and TLR13 are selectively expressed in intracellular compartments to recognize microbial nucleic acid signatures. TLR9 recognizes unmethylated CpG motifs in dsDNA commonly found in viral and bacterial genomes (34-36). TLR3 recognizes dsRNA, while TLR7 and TLR8 recognize ssRNA structures (17). The compartmentalization of these receptors both impacts and reflects the role of a particular TLR, but also aids in preventing deleterious autoimmune responses.

TLR signaling

TLRs initiate inflammatory signaling through the selective use of four adaptor proteins: TIR domain-containing adaptor protein (TIRAP, Mal), MyD88, TRIF-related adaptor molecule (TRAM, TICAM2), and TIR domain-containing adaptor protein inducing IFN-β (TRIF, TICAM1) (8, 37-41). TIRAP and TRAM are considered sorting adaptors, as they regulate the association of signaling adaptors in a stimulus and TLR-specific manner. Ligand binding initiates receptor dimerization and recruitment of adaptor proteins to the TIR domain, which serves as a signaling platform (42). Activation of TLRs leads to signaling cascades converging on the activation of transcription factors (e.g. nuclear factor-kappa B (NF-κB), activating protein-1 (AP-1), interferon regulatory factor 3 (IRF3), and IRF7 and the induction of pro-inflammatory cytokine or type-I IFN transcriptional responses (see **Fig. 1-2** for further detail on TLR signaling). The relative induction and magnitude of inflammatory cytokines and type-I IFNs can have distinct consequences, making its precise regulation highly important (43). TLR1, TLR2, TLR4, and TLR6 initiate signaling from the cell surface, while TLR3, TLR4, TLR7, TLR8, and TLR9 signal from intracellular compartments. With the exception of TLR3, all TLRs signal through MyD88, while TLR4 and TLR3 signal through TRIF-dependent mechanisms. For example, TLR7 and TLR9 mediate MyD88-dependent activation of IRF7 via activation of IkB kinase alpha (IKKα) to induce type-I IFNs (44). Alternatively, TLR3 and TLR4 utilize TRIF to activate IRF3 and type-I IFN production. Notably, TLR4 is unique from other members of this family in that it couples to all sorting and signaling adaptors in a subcellular compartment-specific manner, as discussed in greater detail below. However, recent evidence suggests that TLR2 signaling is also initiated from intracellular compartments after trafficking events (45, 46). Polyubiquitinylation and the

formation of a signaling platform downstream of TLR activation are shared across all TLR signaling cascades.

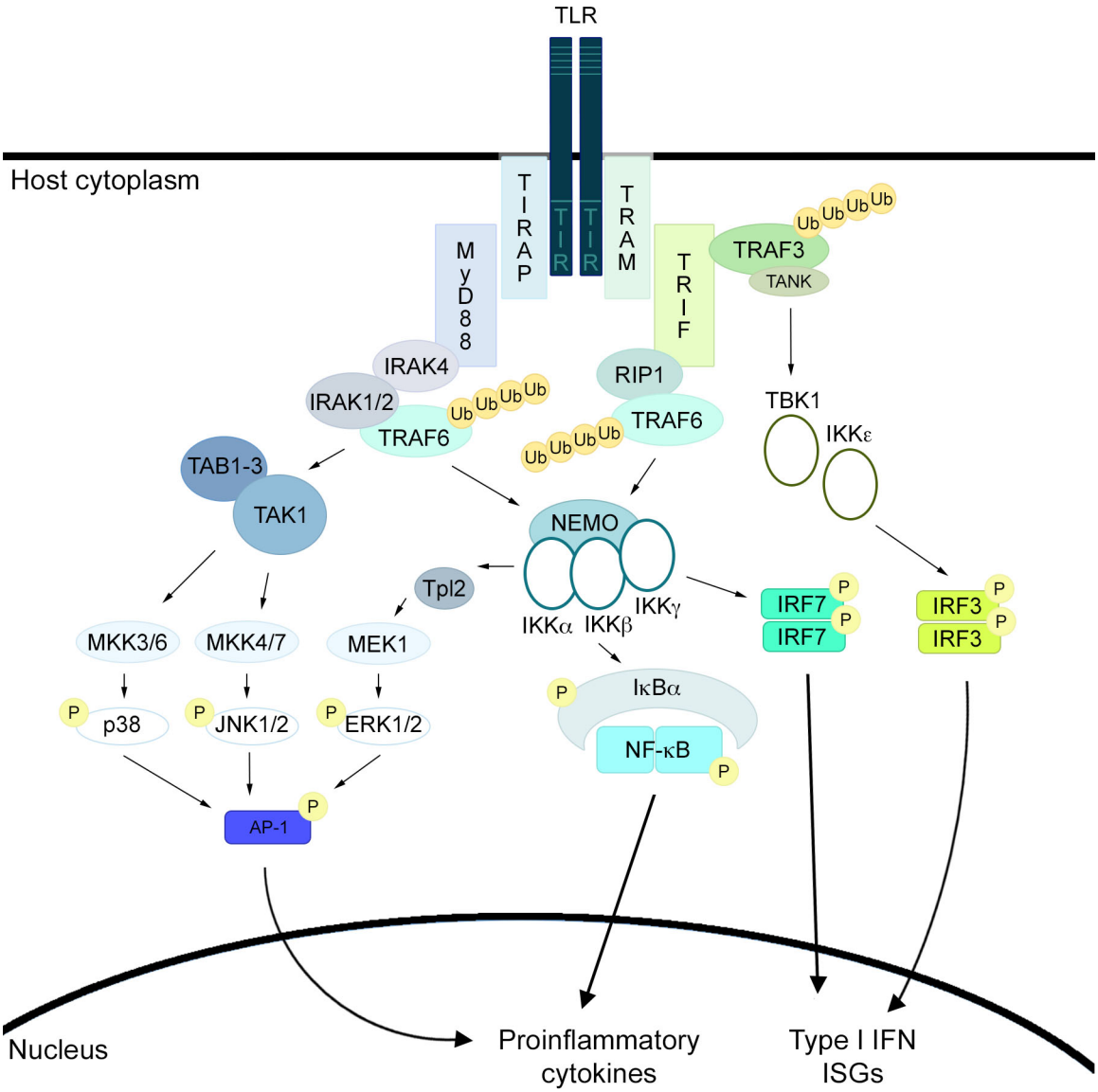
TLR
Host cytoplasm
TIRAP
TRAM
MyD88
TRIF
TRAF3
TANK
Ub
IRAK4
IRAK1/2
RIP1
TRAF6
TBK1
IKKε
TAB1-3
TAK1
NEMO
Tpl2
IKKα
IKKβ
IKKγ
IRF7
IRF3
P
MKK3/6
MKK4/7
MEK1
p38
JNK1/2
ERK1/2
IκBα
NF-κB
AP-1
Nucleus
Proinflammatory cytokines
Type I IFN ISGs

Figure 1-2. TLR activation promotes inflammatory signaling and transcriptional programs in the context of cognate MAMPs

Ligand recognition and binding leads to the recruitment of select adaptor proteins facilitating the formation of signaling complexes (47, 48). The association of MyD88 in a TIRAP-dependent and independent manner recruits and promotes activation of IRAK family members. This leads to the recruitment of TRAF6, an E3 ubiquitin ligase that generates a polyubiquitinylated signaling platform that promotes interaction with TAK1 and members of the IKK complex. Active IKK phosphorylates IκBα, the inhibitory molecule of NF-κB, resulting in its degradation and allowing for the subsequent activation of NF-κB. This complex also mediates the downstream activation of ERK1/2. TAK1, a MAPK kinase kinase, also promotes the activation of MAPKs through association with MKK3/6 and MKK4/7, leading to the activation of AP-1. MyD88-dependent signaling can lead to the activation of IRF7 in select cell subsets (49). TRIF signaling, with or without TRAM, leads to the recruitment of TRAF6 and RIP1 promoting NF-κB and MAPK activation as described above. TRIF also leads to the recruitment of TRAF3, another E3 ubiquitin ligase, which is critical for promoting the activation of non-canonical IKK family members, IKKε and TBK1, leading to the phosphorylation and activation of IRF3. The activation of pro-inflammatory cytokines or type-I IFNs occurs in a TLR-dependent manner. (Adapted from Morgensen 2009 (47))

TLR4

TLR4 is critical for initiating immune responses to Gram-negative bacteria. It was the first defined mammalian TLR responsible for the recognition of LPS, the main component of the bacterial outer membrane. TLR4-deficient cells display a loss of inflammatory signaling and cytokine production in response to LPS (50). Accordingly, TLR4-knockout or TLR4-defective animals are highly susceptible to bacterial challenge due to an inability to mount an effective immune response (51-53). This is also observed in human populations expressing polymorphisms in TLR4. For example, the Asp299Gly or Thr399Ile polymorphisms in TLR4 reduce responsiveness to LPS (54). Similar to mice, this is associated with altered inflammatory responses and enhanced susceptibility to Gram-negative bacterial infections. It has been linked to sepsis, meningococcal infection, chronic periodontitis, as well as other infectious diseases and inflammatory conditions (e.g. ulcerative colitis) (54-58). Although the strength and type of associations between known polymorphisms and disease states vary across studies, there is clearly a trend that highlights the importance of TLR4-dependent LPS responsiveness on inflammation and immunity against Gram-negative bacteria.

Accessory molecules play a critical role in LPS recognition and immune responses to Gram-negative bacteria. Recognition of LPS at the cell surface occurs through the sequential interaction with several accessory proteins. LPS binding protein (LBP), a soluble serum protein, isolates LPS monomers from aggregates present in the extracellular space and facilitates the delivery to a second protein, cluster of differentiation 14 (CD14). CD14 is expressed in both a soluble and membrane associated GPI-anchored form, which transfers LPS monomers to a third protein, myeloid

differentiation factor-2 (MD2) for presentation. In this capacity, CD14 is a critical adaptor protein, required for responsiveness to lower concentrations of LPS and to smooth LPS structures, which are defined by their highly variable polysaccharide O-antigen (59-61). MD2 and TLR4 form a complex under steady state conditions, however conformational changes occur upon ligand binding resulting in higher affinity interactions that promote downstream signaling and receptor trafficking (62-65).

Cellular compartmentalization and trafficking

Subcellular compartmentalization and trafficking are critical for regulating signaling responses to microbial stimuli. In macrophages, TLR4 is functionally expressed at the cell surface and within the endocytic recycling compartment (ERC) (66-69). As mentioned above, TLR4 couples to all four adaptor proteins in a manner dependent on subcellular localization, leading to distinct signaling outputs (**Fig. 1-3**). At the cell surface, TLR4 signals through an interaction with the sorting adaptor TIRAP and the signaling adaptor MyD88. The recruitment of TIRAP is driven through an association with phosphatidyl inositol (4,5) bisphosphate-2 ($PI(4,5)P_2$) at the plasma membrane (70-72). Adenosine diphosphate ribosylation factor 6 (Arf6) promotes this pathway through the activation of PI 4 phosphate 5-kinase (PI5K), which drives the enrichment of $PI(4,5)P_2$ at the membrane (71). The TIR domains present in the cytoplasmic domain of TLR4 and within TIRAP and MyD88 facilitates the formation of a multi-protein scaffold for the recruitment and activation of downstream signaling partners (62, 73). Collectively, this leads to the activation of NF-κB and mitogen-activated protein kinases (MAPK) and the production of inflammatory cytokines and IFNs as discussed in **Fig. 1-2**.

TLR4 is internalized from the plasma membrane to an endosomal compartment resulting in shut-down of the early activation of NF-κB and MAPKs and the upregulation of MyD88-independent signaling responses (**Fig. 1-3**). This event is critical for controlling overly robust inflammatory responses by eventually leading to receptor degradation upon trafficking to the highly degradative lysosomal compartment (68). CD14 promotes the internalization of TLR4 through a direct interaction with LPS-activated TLR4-MD2 homodimers (63). In this capacity, CD14 is required for the activation of Syk and phospholipase C, gamma 2 (PLCγ2) in an immunoreceptor tyrosine-based activating motif (ITAM)-dependent manner (74). Several signaling responses have been implicated in the internalization of TLR4-MD2 complexes from the cell surface. Dynamin, a large guanosine triphosphate hydrolase (GTPase) that regulates membrane pinching, and clathrin-mediated endocytosis have both been associated with receptor uptake (68). Additionally, Arf6, p120catenin, Annexin A2, and the p110δ isoform of phosphoinositide 3-kinase (PI3K) have also been associated with TLR4-MD2 delivery to an intracellular compartment (69, 75-77).

Upon receptor internalization, TLR4 initiates signaling through the association with the sorting adaptor TRAM and the signaling adaptor TRIF. The mechanisms defining the recruitment of TRAM and TRIF and the form and function of multimeric signaling complexes in the context of intracellular TLR4-MD2 are comparatively less understood than that for MyD88-dependent signaling. However, evidence suggests that the myristoylation motif in TRAM contributes to its localization and subsequent recruitment of TRIF to TLR4 (78). Signaling initiated from the endosomal compartment leads to the delayed or late activation of NF-κB and MAPKs in a tumor necrosis factor

receptor associated factor (TRAF) 6 and receptor interacting protein-1 (RIP1)-dependent manner (79-85), while association with TRAF3 leads to IRF3 activation downstream of tank binding kinase 1 (TBK1) and IKKε, two non-canonical IKK kinases (79-82, 85-89). This results in the production of type-I IFNs and MyD88-independent cytokines and chemokines (e.g. IL-10, CCL5, CXCL10) (**Fig. 1-3**).

The plasma membrane is not the only cellular source of TLR4 for driving intracellular signaling responses. The trafficking of TLR4 from intracellular compartments, such as the ERC, has only recently been identified as critical regulatory component of TLR4-dependent activity. In this context, functional TLR4-MD2 is selectively and specifically recruited to phagosomes containing Gram-negative bacteria. Husebye et al showed that the delivery of TLR4 to the phagosome requires the GTPase Rab11a (67). The activation of IRF3 and TRIF-dependent responses to *E. coli* is diminished without this trafficking event, suggesting that the phagosome is another critical subcellular compartment for TLR4-dependent innate immune responses. Arf6 has also been implicated in the regulation of delivery of TLR4 and adaptor proteins to intracellular signaling compartments, independent of the plasma membrane (90). The mechanisms initiating activation and recruitment of Rab11a, and perhaps Arf6, are unknown. Given the distinct signaling outputs, the distribution of TLR4-MD2 complexes and LPS within a cell can have a drastic effect on the downstream inflammatory response. Accordingly, defining the mechanisms and impact of TLR4 trafficking during the immune response to Gram-negative bacteria is of great interest.

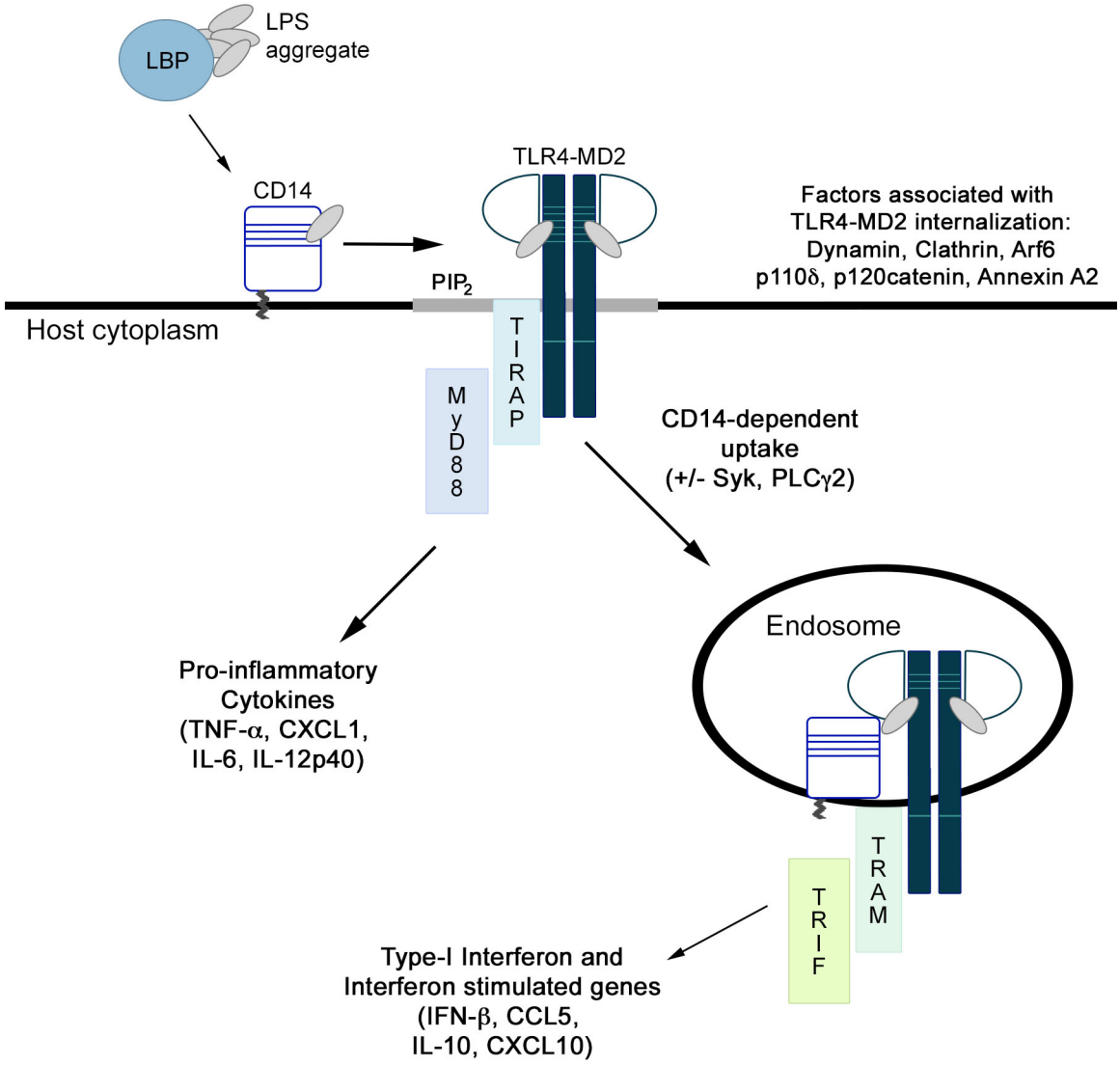
LBP
LPS
aggregate
CD14
TLR4-MD2
Factors associated with
TLR4-MD2 internalization:
Dynamin, Clathrin, Arf6
p110δ, p120catenin, Annexin A2
PIP2
Host cytoplasm
TIRAP
MyD88
CD14-dependent
uptake
(+/- Syk, PLCγ2)
Endosome
Pro-inflammatory
Cytokines
(TNF-α, CXCL1,
IL-6, IL-12p40)
TRAM
TRIF
Type-I Interferon and
Interferon stimulated genes
(IFN-β, CCL5,
IL-10, CXCL10)

Figure 1-3. Cellular compartmentalization of TLR4 signaling

Accessory proteins LBP and CD14 facilitate the delivery of monomeric LPS at the cell surface (91). At the plasma membrane, TLR4-MD2 signaling couples to TIRAP and MyD88 to initiate signaling and production of inflammatory cytokine, including TNF-α, CXCL1, IL-6, and IL-12p40. $PI(4,5)P_2$ enrichment at the plasma membrane promotes the recruitment of TIRAP via the PX domain, which drives the localization of the signaling adaptor MyD88 (70-72). TLR4-MD2 complexes are internalized from the plasma membrane to an early endocytic compartment. There, signaling through TRAM and TRIF leads to distinct signaling responses culminating in the production of IFN-β, ISGs, CCL5, IL-10, and CXCL10 (79-89, 92). Several mechanisms of internalization from the cell surface have been proposed. CD14 promotes the internalization of CD14-TLR4-MD2 signaling complexes by signaling through ITAM-mediated Syk and PLCγ2 activation (63, 74). Internalization of TLR4-MD2 requires Dynamin, a large GTPase that regulates membrane pinching during endocytosis, and clathrin mediated endocytosis (68, 92). Other proteins implicated in receptor uptake include: Arf6 (90), p120catenin (77), Annexin A2 (76), and the p110δ isoform of PI3K (75). (Adapted from Płóciennikowska 2015 (93))

Evolving themes in innate immunity—PRR coordination and crosstalk

It is unlikely that innate immune cells are presented with a single inflammatory stimulus during infection. Instead, the innate immune system is primed to detect several MAMPs through the use of many PRRs, a feature thought to provide further specificity to the cellular response. The dual sensing of soluble (e.g. LPS) or particulate ligands (e.g. bacteria) further complicates the signals deciphered by these immune receptors. Thus, the engagement of PRRs and the initiation of an immune response is a collaborative and coordinated process.

Ligand Delivery

Receptor crosstalk occurs via several mechanisms and is demonstrated in the context of phagocytosis, bacterial killing, and inflammatory signaling and cytokine responses. This interaction can occur directly through physical interactions, for example through the formation of signaling complexes or co-receptors (94-96). Some molecules promote and aid in the delivery and presentation of ligands to other PRRs. For example, LBP and CD14 aid in the delivery and presentation of first aggregate and then soluble LPS to TLR4-MD2 (97-101). Phagocytic receptors also interact to function as co-receptors to aid in ligand delivery and presentation. CD36, a class B scavenger receptor, facilitates the delivery of TLR2 ligands to endosomal compartments (102, 103).

Signaling crosstalk

Signaling crosstalk is another commonly employed mechanism of PRR interaction, whereby signaling responses intersect either directly or indirectly to amplify or dampen a pathway. This type of interaction can be in the context of spatial and

physical interactions that promote signaling crosstalk, particularly when one receptor initiates signaling that generates a local environment that modulates the signaling potential of another receptor. Alternatively, signaling crosstalk can occur downstream from signaling complex formation. For example, C-type lectin receptors (CLRs), like Dectin-1, synergize with TLR2-driven fungal responses through the activation of the non-receptor tyrosine kinase Syk, converging on the activation of NF-κB (104, 105). Similarly, dendritic cell-specific intercellular adhesion molecule-3-grabbing non-integrin (DC-SIGN, SIGNR-1) enhances the transcriptional activity of NF-κB downstream of TLRs by promoting acetylation of the p65 subunit (106). Activation of scavenger receptor A (SR-A) has been shown to synergize with TLR4-dependent LPS responses, but has also been shown to indirectly negatively regulate inflammatory signaling by scavenging and neutralizing inflammatory stimuli (107-109).

Receptor trafficking and subcellular compartmentalization

A novel area of investigation relevant for PRR crosstalk is the role of subcellular compartmentalization and trafficking. It is now evident that the subcellular location of both the receptor and ligand impacts the cellular response (15, 110). For example, in addition to mediating ligand delivery, CD14 acts as an accessory protein required for the internalization of CD14-TLR4-MD2 signaling complexes. TLR complexes can also be targeted to intracellular compartments during phagocytosis by direct and indirect association with phagocytic receptors (21, 111, 112). Early work suggested that TLRs were passively recruited to phagosomes, as they could be seen associated with phagosomal compartments that lacked microbial ligands entirely (34, 111). However, new evidence suggests that the recruitment of surface TLRs to intracellular compartments

is critical for optimal responses. TLR2-dependent activity has been shown to require phagocytosis, in part by facilitating microbe degradation promoting MAMP accessibility (21, 46, 113). Notably, mannose binding lectin (MBL) selectively promotes TLR2-dependent inflammatory responses in the phagosome (113). The sterile inflammatory response to oxidized LDL and β-amyloid by CD36-TLR4-TLR6 heterocomplexes also requires internalization (112). Thus, the phagosome is uniquely tailored to context-dependent immune responses.

A Functional definition—Phagocytic PRRs

Phagocytic receptors play a critical role in the immune response. TLRs are not inherently phagocytic, further emphasizing the unique importance of receptor driven internalization. Instead, several lines of evidence indicate that TLRs contribute to phagocytosis indirectly by modulating transcriptional programs leading to the upregulation of phagocytic receptors that clear microbes and apoptotic cells (114-116). Phagocytic receptors modulate inflammatory responses, drive microbicidal activity, promote adaptive immunity, and aid in the resolution of the inflammatory response (117). Representative examples of receptors that mediate uptake of non-opsonized microbes include CLRs (118) (mannose receptor (119), Dectin-1(120)) and scavenger receptors (19, 20) (CD36 (121), MARCO (122)). Other examples of phagocytic receptors include Fc-gamma receptors (FcγR) and complement receptor 3 (CR3), which mediate the uptake of particles opsonized with soluble IgG or complement and other ligands, respectively (123). Collectively, these proteins mediate the delivery of microbes to an intracellular compartment, the phagosome, that upon signaling and membrane trafficking events matures to a highly degradative compartment within the cell. This results in bacterial

killing and antigen presentation in a cell subset specific manner (117). Interestingly, some evidence suggests that the route of cell entry impacts the potential for microbial activity within the phagosome (124). Additionally, the inflammatory response and microbicidal activity intersect in the context of these phagocytic receptors, which play a critical role in the processing, presentation, and compartmentalization of MAMPs and TLRs (46, 67, 117). In some cases, these receptors function in an inhibitory context to clear MAMPs from the host, thereby limiting further inflammation (108, 109). The role and impact of these phagocytic receptors is variable and complex and likely depends on the microbial, subcellular, and cell subset-specific context.

Cell biology of phagocytosis

The cell biological process of phagocytosis includes a synchronized series of events including attachment, cytoskeletal rearrangement, and membrane remodeling that conclude in the internalization of large particles. Receptor driven phagocytosis has classically been studied in the context of FcγR or CR mediated internalization (125, 126). During FcγR-driven phagocytosis, membrane extends out and around the attached particle, while in CR-mediated events the attached particle appears to sink into the cell (**Fig. 1-4**). Alternatively, particles can be ingested in a non-specific manner through macropinocytosis, which involves large membrane ruffling leading to the bulk sampling of the extracellular space (**Fig. 1-4**). LPS stimulates membrane ruffling, which likely contributed to early observations that suggested TLRs were associated with phagocytic processes. Generally, receptor signaling triggers and couples with phospholipid remodeling to facilitate uptake (127). Lipid dynamics are a critical and conserved

component of phagocytosis, however the direct mediators and the impact of such changes are not fully understood.

Small GTPases play a critical role in internalization by regulating actin and microtubule dynamics. Activation via guanine nucleotide exchange factors (GEFs), which promote exchange of guanosine diphosphate (GDP) for guanosine triphosphate (GTP) in the nucleotide binding site, leads to association with cell membranes. GTPase activating proteins (GAPs) enhance GTP hydrolysis resulting in cycling between the active, GTP-bound state, and the inactive, GDP-bound state (**Fig. 1-5**). These proteins drive actin polymerization through interactions with downstream effectors, such as Wiskott-Alrich Syndrome Protein (WASP/N-WASP) or WASP-family verprolin-homologous protein (Scar/WAVE), in a GTPase specific manner (128). This is followed by activation of the Arp2/3 complex, which directly mediates actin nucleation and branching (129).

The role of Rho-family GTPases appears to differ based which surface receptor is engaged (**Fig. 1-4**) (125). Active Cdc42 is found at the rim of the phagocytic cup and at the tip of the reaching membrane, where it promotes the extension of local polymerized actin (130-132). Rac1 is activated later during uptake and is associated with phagosome closure (133). Some analysis indicates that like Cdc42, Rac1 also contributes to local actin polymerization (134). However, disruption of WAVE2 in macrophages does not impair phagocytosis despite effectively disrupting Rac1-mediated actin polymerization. This suggests that Rac1 contributes to phagocytosis in another manner (135). In macrophages, Rac2 also localizes to the base of the phagocytic cup during uptake (133). Although Rac2-deficient cells display attenuated phagocytosis, actin polymerization is

maintained, indicating a yet undefined function for this protein (136). Furthermore, the disassembly of actin does not correlate with a loss of GTPase activity, suggesting that these proteins remain associated with the phagosome to perform additional functions independent of actin polymerization during particle uptake (137, 138). Prior to particle attachment, Rac also promotes the formation of membrane protrusions that probe the extracellular space, thereby facilitating contact with microbes (127). Indeed, the precise roles of Rac1 versus Rac2 in phagocytosis in macrophages remain to be further refined. In contrast, RhoA is thought predominantly contribute to microtubule dynamics and actin polymerization in CR-mediated phagocytosis (139, 140). Several GEFs have been implicated in activating Rho-family GTPases to drive phagocytosis. In the context of FcγR-mediated uptake, notable examples include Vav proteins and engulfment and cell motility protein-1 (ELMO1)-Dock180 (141-143).

The process of phagocytosis and phagosome maturation requires complex membrane remodeling and trafficking events. Particle internalization involves the extension and subsequent uptake of a significant portion of membrane, which is supported by trafficking events that provide an additional source thereof. This process involves membrane fusion events from the recycling endosomal compartment (144, 145). Cdc42 and Arf6 both contribute to membrane delivery during phagocytosis (146, 147)(148). Rab GTPases are another family of proteins that perform critical membrane and vesicular trafficking events in the cell, as such this family contributes to both phagocytosis and phagosome maturation (149). Rab11 in particular has been associated with rapid membrane delivery during FcγR-driven internalization (144). The coordinated and cumulative actions of actin cytoskeleton rearrangement, membrane delivery, and

membrane extension allow for the containment of extracellular microbes in an intracellular compartment for further processing.

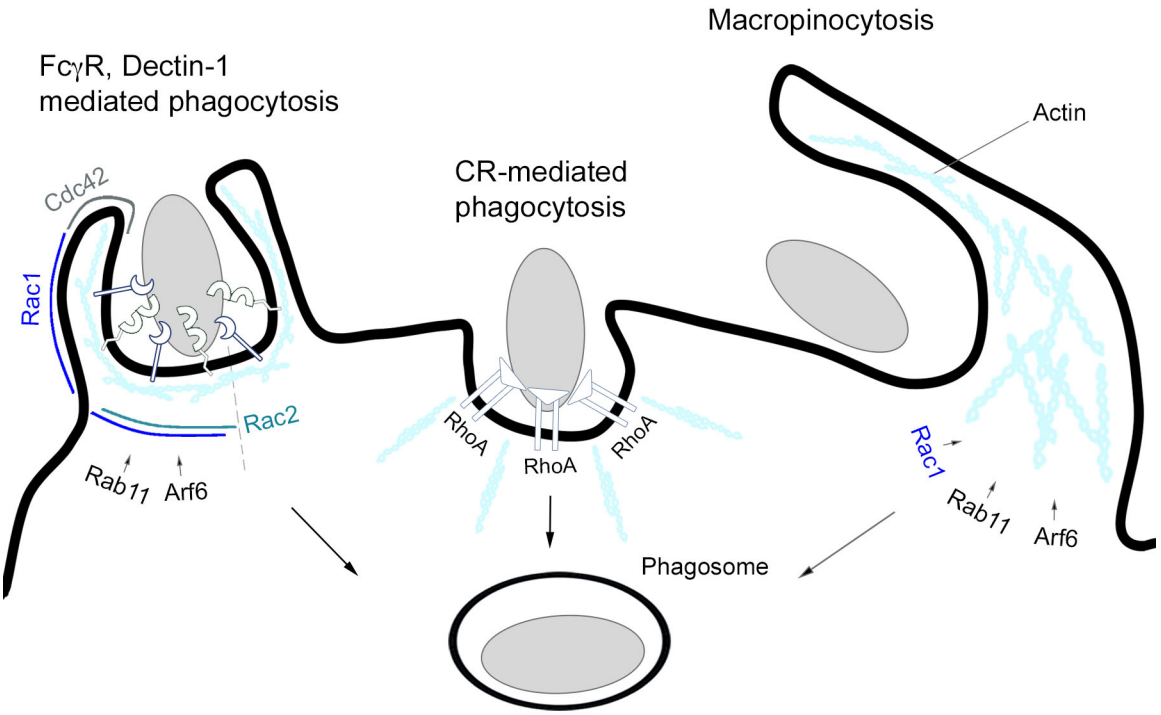
Macropinocytosis
FcγR, Dectin-1
mediated phagocytosis
Actin
CR-mediated
phagocytosis
Cdc42
Rac1
Rac2
Rab11
Arf6
RhoA
RhoA
RhoA
Rac1
Rab11
Arf6
Phagosome

Figure 1-4. Mechanisms of microbe internalization in macrophages

The internalization of large particles (> 0.5 um) requires actin cytoskeleton and membrane rearrangement (117, 125, 126). Phenotypically, phagocytosis occurs via extension of membrane out and around an attached particle (e.g. "reaching phagocytosis," FcγR, Dectin-1). This process requires activation of GTPases: Cdc42, Rac1, and Rac2 (133). Activation of Rab and Arf family GTPases also contribute to particle internalization (144, 148). CR mediated phagocytosis proceeds via "sinking phagocytosis," with limited membrane extension in a RhoA-dependent manner (139, 140). Macropinocytosis mediates the internalization of cell-associated particles in a non-specific or receptor-independent manner. Rac, Arf, and Rab11 GTPases contribute to actin rearrangement in this context (150, 151). (Adapted from Underhill and Goodridge 2012 (117))

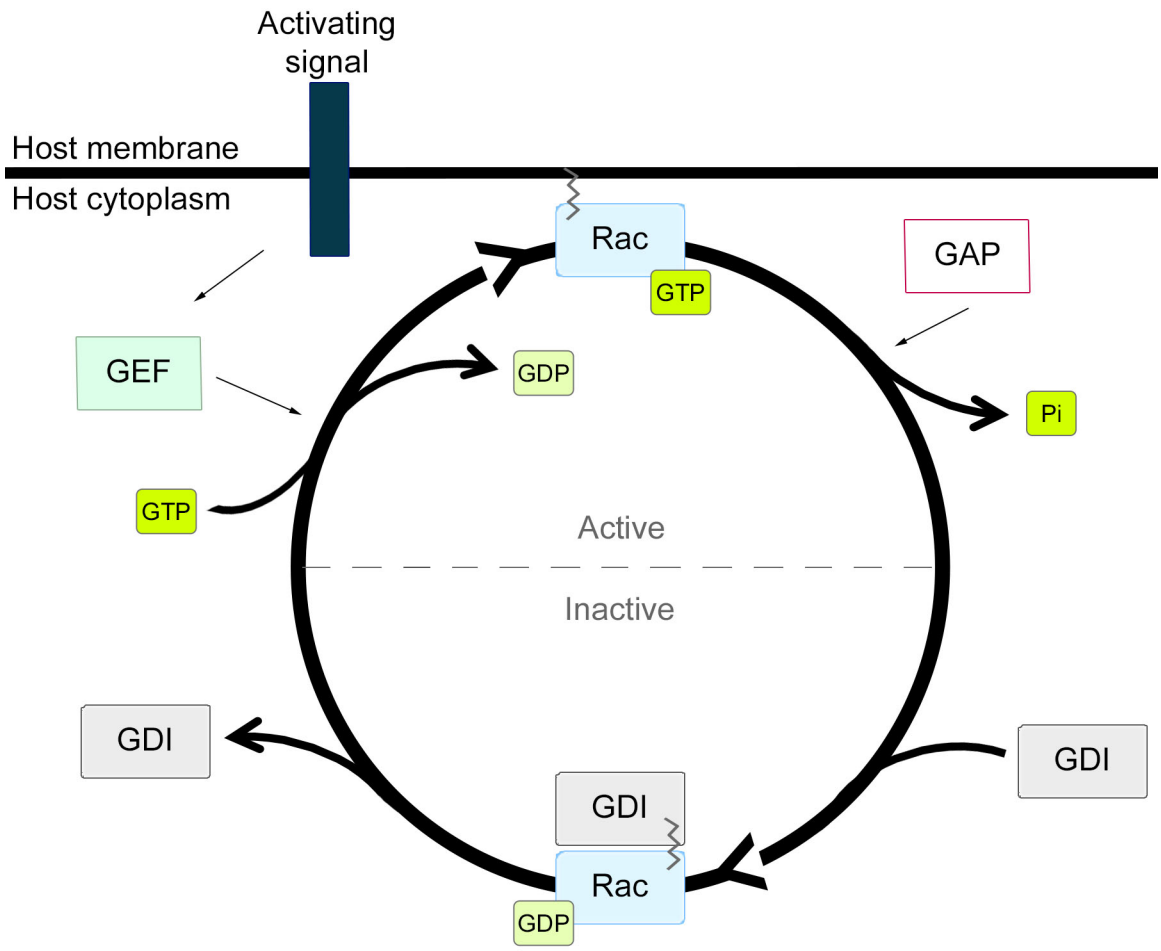
Activating
signal
Host membrane
Host cytoplasm
Rac
GTP
GAP
GEF
GDP
Pi
GTP
Active
Inactive
GDI
GDI
GDI
Rac
GDP

Figure 1-5. Regulation of small GTPases via GDP-GTP exchange cycle

Small GTPases cycle between a GTP-bound, active state and a GDP-bound, inactive state (138, 152). Nucleotide exchange by a GEF promotes the turnover of GDP molecules and re-activates the GTPase, while GTP hydrolysis is facilitated by GAPs. GTP loading leads to conformational changes in the switch I and switch II regions, allowing for altered subcellular distribution and interactions with downstream effector molecules and regulatory proteins (153). Guanosine-nucleotide dissociation inhibitors (GDIs) bind GDP-bound GTPases, thereby preventing GTP loading. These proteins sequester GTPases in the cytosol by shielding their C-terminal lipid anchors, thereby preventing GTPase activation. (Figure adapted from Kawano et al 2014 (152))

Microbicidal activity in phagocytes

The phagocytosis of microbes leads to bacterial killing, and thus is a critical component of the innate immune response to infection. Phagocytes, including resident macrophages, monocytes, and neutrophils are particularly suited to respond to infection via the induction of inflammatory responses and microbicidal activity. Importantly, several studies have suggested a relationship between the sensing of microbial products through PRRs and the activation and enhancement of bactericidal machinery (121, 154-158). These cells utilize a number of processes and tools to mediate bacterial killing including: phagosome acidification and maturation, antimicrobial peptides, autophagy machinery, the production of reactive oxygen and nitrogen species, and nutrient scavenging (159-161) (**Fig. 1-6**). The relative importance and the kinetics of each of these mechanisms can differ in distinct cells subsets, thereby providing a form of specialization during host-microbe interactions (162). Phagosome maturation proceeds quickly through a series of membrane fusion events that result in the delivery of vacuolar adenosine triphosphate hydrolases (V-ATPase), facilitating phagosome acidification, and the delivery of degradative enzymes (e.g. cathepsins, hydrolases) (161, 163-165). Similar to phagosome maturation, autophagy (or xenophagy) proceeds after recognition of cytosolic exposed MAMPs, leading to the formation of a membrane bound compartment that eventually fuses with lysosomes to drive microbicidal activity (166). Oxidative killing through the production of reactive oxygen species (ROS) occurs rapidly after detection of microbes (167), while reactive nitrogen species (RNS) production requires a priming step leading to the upregulated expression of nitric oxide synthase 2 (NOS2, iNOS) to catalyze the production of nitric oxide radicals (160, 168). Accordingly, the

bactericidal activity dependent on RNS occurs later. Macrophages also utilize nutrient deprivation to sequester divalent cations and iron, thereby delaying growth and promoting passive bactericidal activity (169). Although some pathogens have achieved the means to evade, manipulate, and alter cellular microbicidal responses, these processes generally mediate the destruction and clearance of cell-associated or internalized microbes.

The maintenance and the relationship between the routes of bacterial killing are not well understood (170). Evidence suggests that the duration of the ROS response and phagosome acidification are intimately tied (162, 170, 171). Several papers have linked autophagy machinery with ROS responses (157, 172, 173). Moreover, PRR signaling and the route of cell entry impacts the fate of the ingested particle (117, 164, 174). Accordingly, phagosomes within a single cell may differ in their functional properties and result in distinct downstream outcomes (175, 176).

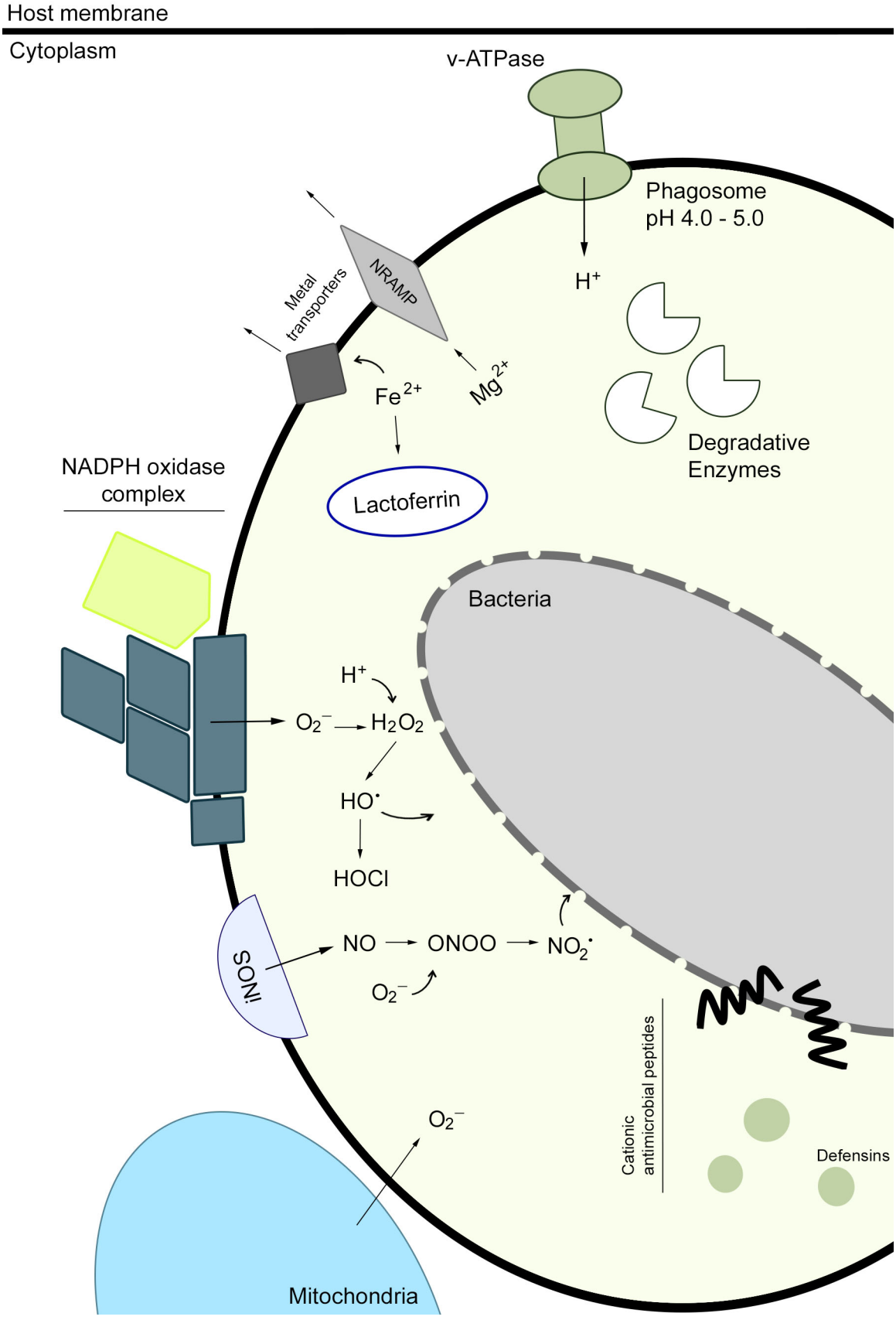
Host membrane
Cytoplasm
v-ATPase
Phagosome
pH 4.0 - 5.0
H+
NRAMP
Metal transporters
Fe2+
Mg2+
Degradative Enzymes
NADPH oxidase complex
Lactoferrin
Bacteria
H+
O2−
H2O2
HO•
HOCl
NO
ONOO
NO2•
O2−
SONi
Cationic antimicrobial peptides
Defensins
O2−
Mitochondria

Figure 1-6. The many mechanisms of microbicidal activity in macrophages

Phagocytes drive intracellular bactericidal activity through several mechanisms (159). Phagosome maturation proceeds through a series of membrane trafficking events, resulting in the exchange of proteins and content (161, 177). This process is complete upon fusion with lysosomes, a highly degradative and microbicidal compartment within the cell (126). The delivery of V-ATPase, a hydrogen ion pump, results in phagosome acidification leading to optimal enzymatic activity within this compartment. Degradative enzymes, including proteases (e.g. cathepsins) and antimicrobial peptides (e.g. defensins) directly mediate microbicidal activity (161, 163-165). The delivery and activation of the phagocyte NADPH oxidase complex and mitochondrial superoxide contribute to oxidative killing (156, 167), while iNOS produces reactive nitrogen species (160, 168). Several reactive oxygen and nitrogen species are formed within this compartment to facilitate bacterial killing. Metal transporters (e.g. natural resistance-associated macrophage protein 1 (NRAMP1)) and iron scavengers (e.g. lactoferrin) limit nutrient availability (169). (Adapted from Flannagan et al 2009 (159))

Oxidative killing in the macrophage microbicidal response

The generation of reactive oxygen and nitrogen species is a critical component of antimicrobial mechanisms available to phagocytes. Nicotinamide adenine dinucleotide phosphate (NADPH) oxidases (NOX) are a family of multimeric protein complexes with cytosolic and membrane associated components (170, 178-181) (**Fig. 1-7**). Six homologs of the catalytic subunit of these protein complexes exist in mammals including: NOX1, NOX2 (also named gp91phox), NOX3, NOX4, NOX5, Dual oxidase (DUOX) 1, and DUOX2. Collectively referred to as the NOX family of NADPH oxidases, these protein complexes function to generate superoxide in cell and stimuli-specific manner. In phagocytes, gp91phox and p22phox are membrane bound, while p40phox, p47phox, and p67phox form a separate complex in the cytosol at steady state (170, 182). The distribution of p47phox is determined by accessibility of a PxxP motif that mediates interaction with p22phox and a PX box that has affinity for phospholipids. The precise function of p40phox is less understood, but appears to play a regulatory role like p47phox. This protein has a PX domain that promotes association with phosphatidlyinositol 3-phosphate (PI(3)P) after activation, and in neutrophils has been associated with targeting ROS responses to the phagosomal compartment instead of the cell surface (183-185). Upstream signaling from an activating receptor (e.g. TLRs) leads to the phosphorylation of p47phox, providing a conformational change that promotes the redistribution of the cytosolic subunits to the phagosomal membrane with the catalytic subunits (see **Fig. 1-7** for further details on signaling driving phosphorylation of p47phox) (158, 186). Finally, Rac GTPases are also required to complete the activation of the phagocyte NADPH oxidase complex by facilitating assembly with the

transmembrane catalytic subunit gp91phox and activation of the cytosolic regulatory subunits (138, 170, 182). All macrophage lineages express gp91phox (NOX2), while evidence suggests that other NOX family members (e.g. NOX4) are also present (179). In addition to NADPH oxidases, macrophages also utilize mitochondrial ROS to mediate oxidative antimicrobial activity (156, 187).

The activation of ROS and phagocytosis are closely tied. NADPH oxidase activation occurs rapidly downstream of phagocytic receptor engagement. This process has been primarily characterized downstream of the opsonic phagocytic receptors FcγR and CR, but its activation in response to non-opsonized, Gram-negative bacteria is less defined. FcγRs signal through ITAMs to drive the activation of Syk kinase and Vav family GEFs to promote Rac activation. In this context, ITAMs also signal to PLCγ to activate protein kinase C (PKC), leading to the phosphorylation of p47phox. Collectively, this leads to the activation of the cytoplasmic components of the NADPH oxidase complex as described above (170, 188). The induction of NADPH oxidase ROS responses occurs within minutes (167). Accordingly, components of the NADPH oxidase machinery are recruited to sites of internalization early, even before phagocytosis is complete (189-192). Rab11 has been shown to mediate the delivery of gp91phox and p22phox to phagosomes (193). Rab27a has also been associated with assembly of NADPH oxidase machinery on phagosomes (194). Some of the machinery mediating uptake and the NADPH oxidase complex, such as the Rac GTPases (e.g. Rac1 and Rac2) and Rab11, are shared. This perhaps facilitates the formation of a local environment where the necessary anti-microbial machinery is concentrated in time and space.

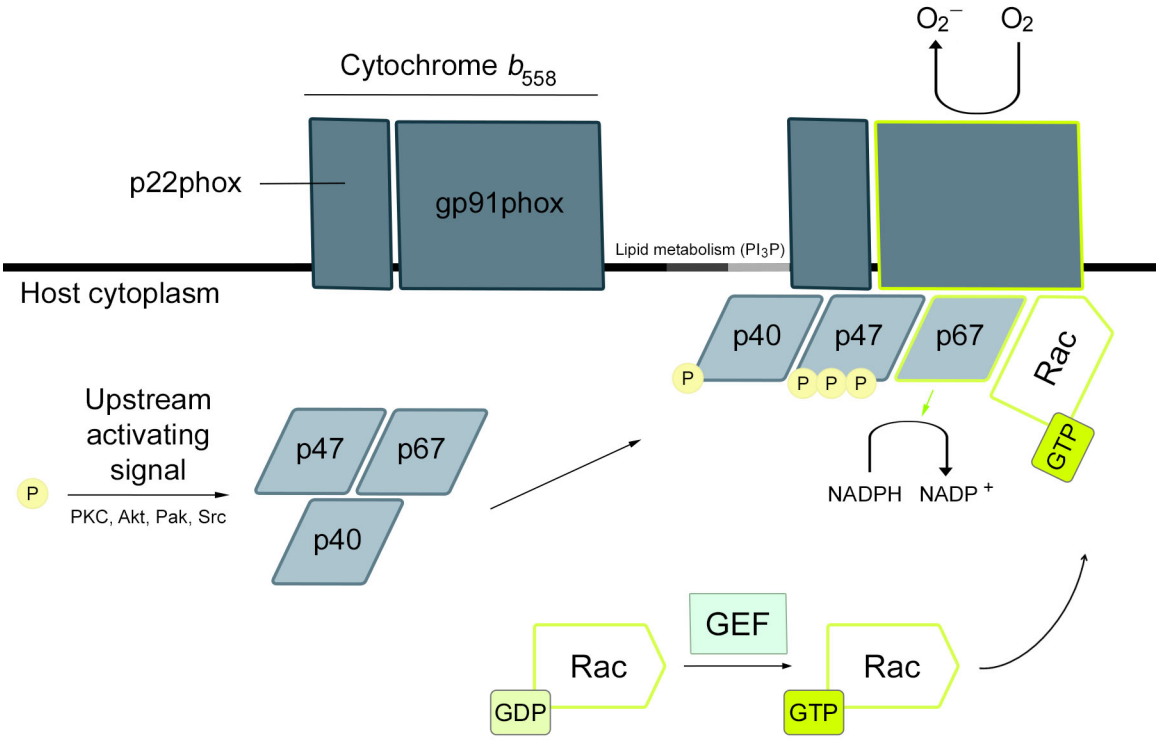
O_2^-
O_2
Cytochrome b_{558}
p22phox
gp91phox
Lipid metabolism (PI_3P)
Host cytoplasm
p40
p47
p67
Rac
P
P P P
GTP
Upstream activating signal
P
PKC, Akt, Pak, Src
p47
p67
p40
NADPH
$NADP^+$
GEF
Rac
GDP
Rac
GTP

Figure 1-7. Assembly and activation of the NADPH oxidase complex

Activation of the phagocyte NADPH oxidase complex is tightly regulated to prevent unwarranted oxidative damage (178, 195). The constitutively membrane bound Flavocytochrome *b*558 is composed of two subunits, p22phox and gp91phox. Gp91phox (NOX2) is the catalytic subunit of the complex, which drives electron transfer and the generation of superoxide. Recognition of Gram-negative bacteria triggers signaling to drive the assembly and activation of NADPH oxidase at the membrane. Activation of protein kinases (e.g. PKC, Akt, Pak, Src) through upstream receptors triggers the phosphorylation of the regulatory subunit p47phox, which exists in complex with p40phox and p67phox in the cytoplasm at resting state (158, 186). p47phox phosphorylation results in a conformational change exposing a SH3 domain that binds the proline rich region of p22phox and a PX domain that associates with phosphoinositides. p40phox has also been implicated in mediating the localization of regulatory subunits upon stimulation through its PX domain (196). Activation of lipid-modifying enzymes (e.g. PI3K, phospholipases) generates local changes in the lipid environment that facilitates the recruitment of the cytosolic regulatory subunits. Activation of Rho GTPase, Rac, results in relocalization to the membrane associated NADPH oxidase complex. Rac participates in p67phox translocation and activation. Collectively, these signaling responses target the cytoplasmic regulatory subunits and Rac to the catalytic subunit, where p67phox with p22phox and gp91phox, facilitates electron transfer from an NADPH substrate molecule to generate superoxide within the phagosome. (Adapted from Lambeth 2004 (178))

Adhesion G-protein coupled receptors

Adhesion-type heterotrimeric guanine nucleotide-binding protein-coupled receptors (GPCRs) are a unique class of the GPCR family consisting of 33 receptors divided into 9 sub-families (197, 198). Functionally, this family participates in transducing upstream signals into downstream cellular responses and, unlike other families within the GPCR superfamily, also displays diverse roles in protein-protein interactions and adhesion. This evolutionarily ancient family of proteins performs critical functions in diverse contexts including development, tumorigenesis, and immunity. A large extracellular region linked via a GPCR proteolytic site (GPS) to seven transmembrane-spanning domains and an intracellular cytoplasmic region define the structural composition of this sub-family of proteins (198). The extracellular regions of these proteins contain distinct functional domains: these include epidermal growth factor (EGF)-like domains, type-I thrombospondin repeats (TSRs), LRRs, lectin-like domains, immunoglobulin domains, and cadherin domains, which impart adhesion and protein-protein interaction activity.

A feature of the adhesion GPCRs is the GPS motif. The GPS contains a cleavage site within a larger domain defined as the GPCR autoproteolysis-inducing (GAIN) domain, which is conserved across all members of this group (199). Cleavage is thought to occur constitutively in the endoplasmic reticulum during synthesis, after which the extracellular domain remains non-covalently physically associated with the transmembrane region through hydrogen bonds and hydrophobic interactions (200-202). However, this appears to be cell and tissue dependent (202, 203), and does not have the same function and significance across all members of this sub-family (197, 202, 204-

206). For example, the GAIN domains within latrophilin 1 and EGF-like module containing mucin-like hormone receptor 2 (EMR2) are cleaved in heterologous cell lines (201, 206), while brain angiogenesis inhibitor (BAI) 3 is not (202). In depth structural analysis indicates that this discrepancy may be due to minor differences in amino acid sequence and structure among GAIN domains that influences the folding and chemical environment surrounding the consensus site of cleavage (199, 202).

The cytoplasmic region couples extracellular interactions to intracellular signaling responses. Signaling through members of the adhesion-type GPCRs occurs through G protein-dependent and independent mechanisms (207-210). Heterotrimeric G proteins include Gα, Gβ, and Gγ subunits (210, 211). In an inactivated state the GDP-bound Gα subunit exists in complex with the Gβ and Gγ subunits. GPCR receptor activation induces the exchange of GDP for GTP, thereby activating the Gα subunit, which is liberated from Gβ and Gγ. Both the Gα and Gβγ subcomplex exert downstream signaling responses. A limited number of adhesion-type GPCRs have been demonstrated to couple to classical G protein signaling pathways (212-214), indicating similarities in the form and function of this family of proteins relative to other GPCRs. However, many of these proteins also possess cytoplasmic modules or motifs (e.g. PSD-95/Disc-large/ZO-1 homology (PDZ) binding motif) that suggest competency for signaling through alternative means (215, 216). The functional importance of receptor cleavage and signaling is discussed further below pertaining to its relevance for the BAI family of adhesion GPCRs.

The BAI subfamily of adhesion GPCRs

Domain architecture and expression in vivo

BAI1 (adhesion G protein-coupled receptor B1, ADGRB1), BAI2 (B2, ADGRB2), and BAI3 (B3, ADGRB3) comprise subgroup VII of the adhesion-type GPCRs (208, 217). These proteins share ~50% sequence homology at the amino acid level. Members of the BAI sub-family contain a large extracellular region with distinct functional domains that contribute to interactions in the extracellular space, typical of adhesion GPCRs (**Fig. 1-8A**). These proteins share a series of type-I TSRs, a hormone binding domain (HBD), and a GAIN domain, including the GPS motif, in their extracellular regions. However, BAI1 also uniquely expresses a membrane distal N-terminal RGD integrin-binding motif, suggestive of a role in adhesion and cell-cell interactions. BAI2 and BAI3 express four TSR domains, compared to BAI1, which contains five. TSRs are a widely conserved domain found in several mammalian proteins, consisting of approximately 60 amino acids each, implicated in cell-cell communication and interactions with the extracellular matrix (218-220). The extracellular region is coupled to the cytoplasmic domain through 7 transmembrane spanning repeats. The intracellular regions of BAI1-3 contain conserved protein interaction modules, presumably facilitating protein-protein interactions in signaling responses. These include: a positively charged alpha helical region (RKR) and a C-terminal PDZ-binding motif (e.g. QTEV). Unlike BAI2 and BAI3, BAI1 also possesses a proline rich region (**Fig. 1-8**) (198, 208, 217).

All members of this sub-family are highly expressed in the brain, but display distinct expression patterns. Analysis of mRNA expression suggests that BAI1 is most abundant in the brain, while BAI2 and BAI3 are more widely expressed during development (221). BAI1 is found in neurons, astrocytes, and microglia in the brain (222-

224). However, BAI1 is also expressed outside of the brain in myeloid lineage cells, including macrophages and monocytes (225, 226), myoblasts (227), and epithelial cells (Lee et al, *in press*). In contrast, BAI2 expression is largely limited to the brain after birth (228). BAI3 has been specifically identified in hippocampal neurons and in myoblasts outside of the central nervous system (229, 230). The particular expression patterns of BAI2 and BAI3 in the brain and in other tissues remain to be defined. The distinct distributions observed for each member of this sub-family suggests unique functionality dependent on cell and tissue-specific contexts (208).

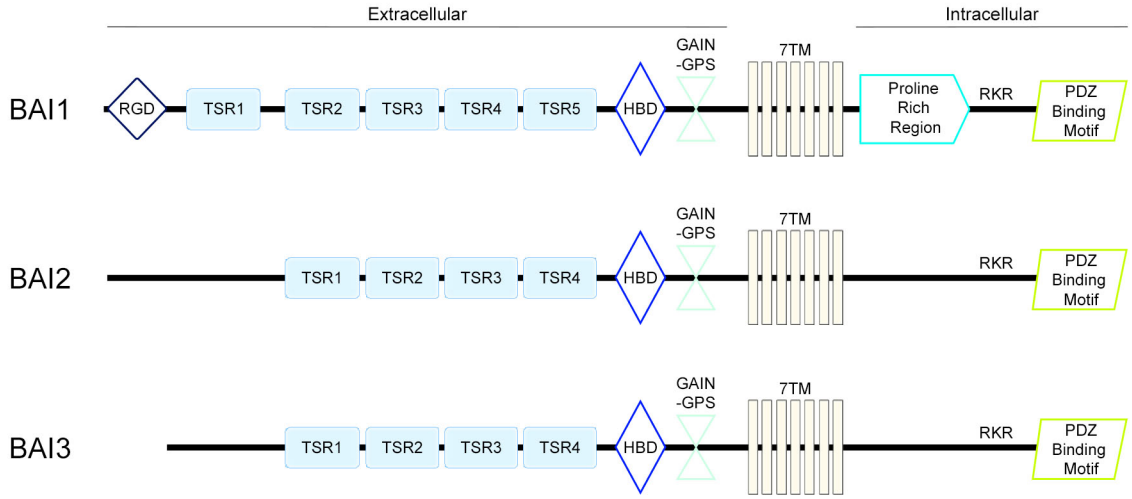
Extracellular
Intracellular
BAI1
RGD
TSR1
TSR2
TSR3
TSR4
TSR5
HBD
GAIN
-GPS
7TM
Proline
Rich
Region
RKR
PDZ
Binding
Motif
BAI2
TSR1
TSR2
TSR3
TSR4
HBD
GAIN
-GPS
7TM
RKR
PDZ
Binding
Motif
BAI3
TSR1
TSR2
TSR3
TSR4
HBD
GAIN
-GPS
7TM
RKR
PDZ
Binding
Motif

Figure 1-8. Schematic of the BAI subfamily of adhesion GPCRs

Figure 1-8 depicts schematics of BAI1-3 noting regions of structural and functional importance. All family members share TSRs, a HBD, and a GAIN domain in the extracellular region. BAI1 expresses an N-terminal RGD integrin-binding motif. The intracellular domains of BAI1-3 share a positively charged alpha helical region (RKR) and a C-terminal PDZ-binding motif, while BAI1 uniquely possesses a proline rich region.

BAI1-dependent signaling responses and roles

The following section highlights what is currently known on the function, the regulation, and the signaling responses of BAI1 in distinct tissues and cell types (**Fig. 1-9**). The relevance of the known functions and signaling responses discussed in detail below may be important in other cell types, such as macrophages, and in the context of the innate immune response.

Inhibition of angiogenesis

BAI1 was first identified as a protective negative regulator of angiogenesis in the development of glioma and glioblastoma (231-233). The initial identification and characterization of BAI1 determined that it was significantly reduced or absent in several glioblastoma cell lines, indicating that it was negatively regulated in that disease state. BAI1 RNA expression has also been correlated with colorectal cancers and pulmonary adenocarcinomas (234, 235). Recombinant protein comprising the extracellular region of BAI1, including the five TSR domains, inhibits neovascularization in vivo, thus demonstrating that BAI1 negatively regulates angiogenesis. Other groups have also confirmed the angiostatic effects of the extracellular region of BAI1 in in vivo models (236-238).

The extracellular region of BAI1 was determined to be cleaved at the GPS proteolytic cleavage site to generate a 120kDa protein fragment, defined as vasculostatin120, that is secreted in the extracellular space. Two mechanisms have been proposed for the angiostatic effect mediated by BAI1. First, Koh et al determined that BAI1 was cleaved to generate a soluble product that inhibited human umbilical vein endothelial cell proliferation through an interaction between the cleaved BAI1-TSR

domains and $\alpha_v\beta_5$ integrins (239). Alternatively, Kaur et al showed that the extracellular region of BAI1 cleaved at the GPS (e.g. vasculostatin120) inhibited growth of malignant gliomas and suppressed tumor vascularization. They proposed this was due to BAI1-TSR interactions with CD36 on vascular endothelial cells (237, 240). More recently, Cork et al discovered that BAI1 is also cleaved after the first TSR to generate a 40kDa protein (vasculostatin40) that exhibits angio-static effects (241). These studies provide intriguing areas of investigation on the role and regulation of BAI1 cleavage on function.

Regulation of signaling and function in the brain

BAI1 has also been associated with regulating neuronal functions. The presence of signaling modules in the cytoplasmic region of BAI1 is indicative of a function for the cell-associated form of the protein independent of its angiostatic effects. Early work centered on the identification and characterization of proteins interacting with BAI1, largely through the use of yeast 2-hybrid systems. BAI1 was initially found to associate with four proteins: BAI1 associated proteins (BAIAP or BAP) 1-4. Functionally, these protein-protein interactions suggested various roles for BAI1 in neuronal processes (223). Shiratsuchi et al determined that BAP1 (or membrane associated guanylate kinase, WW and PDZ domain containing protein (MAGI)-1) association was mediated through its multiple PDZ domains and the C-terminal PDZ binding motif (e.g. QTEV) of BAI1 . BAP1 is a membrane associated guanylate kinase family member, which is known to regulate synaptic transmission and proliferation (242). BAIAP2, an IRSp53 homolog, was instead shown to associate with the proline rich region of BAI1 through its Src homolog 3 (SH3) domain (243). Interestingly, BAIAP2 is also found to be a downstream effector of RhoA through a direct interaction with mDia, which is functionally relevant

for stress fiber formation and cytokinesis (244). Functionally, Oda et al proposed that this interaction contributes to growth cone guidance through modulating adhesion and cytoskeletal changes during neuronal growth. Similarly, interaction with BAP3, a C2 domain containing protein with homology to Munc13 and synaptotagmin, suggested a role for BAI1 in neurotransmitter release (245). Finally, BAI1 was shown to interact with phyatanoyl-CoA alpha-hydroxylase (or BAP4), again indicating a role in neurological development and function (246). Many aspects of the precise roles of these protein-protein interactions on neuronal health and disease remain to be fully explored.

The functional significance of BAI1 protein-protein interactions in the brain has been further explored in a select number of publications. The early observations placing BAI1 with scaffold proteins known to be enriched at post-synaptic densities indicated a role for BAI1 in the physiology and form of these structures (247). Stephenson et al further defined "the interactome" of BAI1 (203). The recombinant C-terminal cytoplasmic region of BAI1 containing the PDZ binding motif was used to screen a proteomic array of several PDZ domains to identify novel protein-protein interactions mediated by this region of BAI1. Similar to previous studies, all of the positive hits identified from the array were proteins enriched at the synaptosomal or post-synaptic density. Moreover, BAI1 physically associated with post-synaptic density (PSD)-95 by immunoprecipitation from homogenates of mouse brain tissue and was enriched in PSD fractions and synaptosomes. These interactions had functional significance on downstream signaling responses of BAI1. For example, association with MAGI-3 lead to increased ERK activation dependent on the PDZ binding motif of BAI1. This data in combination with signaling data discussed below, indicates that BAI1 may in fact be

critical for migration, synapse formation, PSD structure and spine morphogenesis, and plasticity.

Indeed, others have shown that BAI1 directly regulates synaptogenesis (248). Duman et al showed that BAI1 was required for spinogenesis and synaptogenesis. In this capacity, BAI1 contributed to maintaining cell polarity necessary for functional synaptogenesis. BAI1 was required for the recruitment of Par3 and Tiam1, a Rac GEF, to the synapse, leading to the activation of a local pool of Rac1. This interaction was likely driven through BAI1-integrin interactions mediated through the RGD motif in the extracellular region. Collectively, this spatial activation of Rac1 was required for the modulation of actin dynamics in synapses and spines of hippocampal neurons.

Receptor cleavage and signaling through heterotrimeric G proteins

The ability to couple to classical G-protein mediated signaling cascades and the impact of receptor cleavage on intracellular signaling responses have been further explored in the context of BAI1 in heterologous cell culture systems. While the cleavage of BAI1 has been identified in the brain, the role and prevalence of cleavage in other contexts is less understood. When expressed in heterologous cell systems such as 293T cells, BAI1 and BAI3 are not cleaved (202, 203, 249, 250), and the detection of cleaved forms of BAI1 in macrophages has not been observed (data not shown). However, exogenous expression of the N-terminal and C-terminal fragments shows that the extracellular and membrane associated proteins can remain physically associated after cleavage at the GPS motif. This cleavage event is critical for potentiating select BAI1-dependent signaling events. Stephenson et al showed that both full length and cleaved BAI1 couple to $G\alpha_{12/13}$ to mediate activation of RhoA in a manner dependent on the PDZ

binding motif of BAI1 (203). This signaling pathway is enhanced in the context of the cleaved protein suggesting a role for cleavage in the regulation of signal transduction. Similarly, the cleaved protein, but not the full-length protein, interacts with β-arrestin2. This appeared to be negatively regulated by QTEV-dependent protein-protein interactions, as the association between β-arrestin2 and BAI1 was increased when the PDZ motif was altered.

Studies on the role of receptor cleavage in the context of other members of the adhesion GPCR family suggest that it contributes to receptor function in two possible ways: (1) by acting as a direct antagonist inhibiting signaling until fully disengaging from the membrane bound cleavage product or (2) by shielding or sequestering an internal agonist, that upon loss of association with the cleaved N-terminal fragment potentiates signaling through the membrane bound cleaved product. This second mechanism is based on the fact that cleavage reveals or generates a stalk-like structure at the newly formed N-termini of the adhesion GPCR (251-253). Follow up studies by Kishore et al examined the role of the stalk component of the extracellular region of BAI1 that remains at the N-terminus after receptor cleavage (250). Consistent with previous results, receptor cleavage was not required for signaling to $G\alpha_{12/13}$ proteins. To test the importance of the stalk region on signaling responses, a BAI1 mutant truncated to lack this region was analyzed in several functional assays. In all cases, signaling was unaffected or enhanced in the absence of the stalk region. Interestingly, the authors observed that cleaved BAI1 with and without the stalk region physically associated with $G\alpha_{13}$, but full-length protein did not. Additionally, Kishore et al also showed that BAI1-dependent activation of Gβγ subunits exert downstream signaling effects by measuring signaling outputs in the

presence of gallein, a Gβγ inhibitor. The authors proposed a model by which conformational changes in a cleavage-dependent and independent manner impact the signaling transduction through the 7 transmembrane repeats leading to classical heterotrimeric G protein signaling responses. Notably, the physiological importance of these signaling pathways in vivo and in the context of relevant ligands is currently unknown.

Apoptotic cell recognition and clearance

The clearance of dead or dying cells from the body is critical for maintaining homeostasis and resolving infection. It is also particularly important during development, where there is an abundance of cell turnover. Receptor engagement triggers the activation of distinct signaling pathways that drive actin cytoskeletal rearrangement and uptake of apoptotic corpses. Early work on the mechanisms leading to apoptotic cell clearance was largely done in *C. elegans* (254, 255). One key signaling pathway involves CED2 (mammalian homologue, CrkII), CED5 (Dock180), and CED12 (ELMO) promoting the activation of CED10 (Rac1). In this capacity, ELMO1 and Dock180 together act as an atypical bipartite Rac-GEF (256), mediating Rac-driven actin cytoskeleton rearrangement and particle ingestion. The DOCK superfamily is comprised of 11 proteins that utilize a "Docker" domain to mediate nucleotide exchange, which differs from that of other conventional GEFs, while ELMO proteins (e.g. ELMO1, ELMO2, and ELMO3) act as master regulators of Dock GEF activity (143). The upstream signal triggering ELMO1 activation is not well understood. Moreover, the means through which ELMO modulates Dock-mediated Rac activation are not fully defined. However, several possible mechanisms exist: (1) ELMO stabilizes the Dock180-Rac ternary complex, (2) ELMO

associates with Dock180 in a manner that relieves inhibition of GEF activity, and (3) ELMO facilitates the redistribution of the ternary complex to the membrane through armadillo repeats present in the N-terminus of the protein (143, 257). Several interactions between ELMO and Dock have been mapped to account for these models. First, the N-terminal PH domain of ELMO1 is thought to mediate interaction with Dock180 and Rac to form a complex (258). Additionally, association between the PH domain of ELMO and a region adjacent to the SH3 domain of Dock180 or the association of C-terminal proline rich region of ELMO with the SH3 domain of Dock180 are thought to contribute to complex form and function (257, 259).

While ELMO1 and Dock180 are absolutely critical for apoptotic cell clearance, an upstream signal coupling the extracellular recognition of altered self ligands or apoptotic cells is necessary to activate this signaling module. Park et al identified BAI1 as a phagocytic receptor that mediates this function by driving the attachment and subsequent internalization of apoptotic cells (225). The interaction between BAI1 and ELMO-Dock-Rac was first identified through a yeast two-hybrid screen against the N-terminus of ELMO1. BAI1 has been demonstrated to be critical for the recognition and internalization of apoptotic cells (225). Exogenous expression of BAI1 in macrophage cell lines and non-phagocytic cells increased the binding and uptake of apoptotic corpses, while loss of BAI1 or its signaling partners, ELMO1 and Dock180, reduced apoptotic cell internalization. The interaction between BAI1 and the ELMO-Dock signaling module resulted in enhanced Rac activation in response to apoptotic cells and required a positively charged helix in the cytoplasmic region of BAI1. Furthermore, it was determined that the TSR domains were specifically required for recognition of

phosphatidyl serine exposed on apoptotic cells. Several other studies have since confirmed the importance of BAI1 as a phagocytic receptor in apoptotic cell clearance in the brain, the gastric epithelia, and the intestinal epithelia (224, 225, 260)(Lee et al, *in press*). Notably, this highlights the importance of BAI1 in mediating phagocytosis in non-professional phagocytes, as well as macrophage and monocyte lineage cells.

The implications of the interaction between the BAI1-TSR domains and phosphatidyl serine extend beyond phagocytosis. During apoptotic cell clearance, the viable cell must contend with a massive increase in lipid and cholesterol content. BAI1-dependent signaling through ELMO-Dock-Rac increased the expression of ABCA1, an ABC membrane transporter, to facilitate and contend with cholesterol fluxes accompanying this event (261). Additionally, Hochreiter-Hufford et al showed that BAI1 contributes to myoblast fusion and is required for fully competent muscle regeneration and repair (227). In this process, BAI1-mediated recognition of phosphatidyl serine on apoptotic myoblasts allowed for fusion and formation of myotubes. Collectively, BAI1 recognition of phosphatidyl serine leading to the activation of Rac GTPase through ELMO-Dock is critical for several physiological processes.

A novel phagocytic receptor for Gram-negative bacteria

Several PRRs implicated in apoptotic cell recognition are also highly important for the detection and internalization of microbes and microbial products (262, 263). The presence of five TSRs in the extracellular region of BAI1 and its relevance as a phagocytic receptor in other contexts (e.g. apoptotic cells) triggered the investigation of BAI1 as a PRR for bacterial ligands. TSRs are widely conserved domain found in several mammalian proteins, consisting of approximately 60 amino acids each. In other contexts,

these domains are implicated in cell-cell communication and interactions with the extracellular matrix (218-220). Several studies have found a role for TSR domains in bacterial recognition. For example, Rennemeier et al showed that Thrombospondin-1 (TSP-1) binds the peptidoglycan of several Gram-positive bacterial species, promoting adherence to host cells (264). He et al characterized mindin, an extracellular matrix protein, as a PRR for both Gram-positive and Gram-negative species that functions in bacterial clearance and inflammatory responses (265). Each TSR is composed of a three, anti-parallel strands—two β- sheets and one "rippled" strand (266). **Fig. 1-10** shows a model of a BAI1-TSR domain generated by threading the sequence of BAI1 onto the known structure of TSP-1 (**Fig. 1-10, A and B**). The three anti-parallel strands interact through the stacking of charged side chains, which allows for the formation of a positively charged groove. The TSR structure contains distinct post-translational modifications, which are important for function and structural stability in certain contexts, although their importance in bacterial recognition is unknown (267, 268) (**Fig. 1-10C**). It has been proposed that this positively charged groove forms the recognition face of the molecule (266, 267, 269). Interestingly, each of the five TSRs in BAI1 display distinct isoelectric points and positive charge, indicating that they may differentially interact with ligands (**Fig. 1-10, D and E**).

Given the presence of the TSR domains and their functionality in the recognition of apoptotic cells, Das et al examined the role of BAI1 in bacterial recognition. BAI1 selectively enhanced the attachment of several Gram-negative bacterial species, but not Gram-positive bacteria, to the host cell surface, indicating that it contributed to bacterial recognition (226). Importantly, this interaction was mediated through the TSR domains

and was independent of the integrin binding motif, similar to the recognition and binding pathway observed in the context of apoptotic cells. Consistent with this, bacterial internalization in primary macrophages was also dependent on BAI1. Moreover, expression of BAI1 in heterologous cell lines enhanced phagocytic function, indicating that BAI1 can directly promote phagocytosis of Gram-negative bacteria. Das et al also determined that the signaling pathway coupling recognition to bacterial uptake was driven through the known ELMO-Dock-Rac signaling module, as described above.

The function of BAI1 in bacterial attachment and the specificity of BAI1 for Gram-negative bacterial species indicated that TSR recognition was mediated through a surface-exposed component of the Gram-negative bacterial membrane. Das et al determined that BAI1 specifically recognized the LPS of the Gram-negative bacterial outer membrane (226). Moreover, the recognition of LPS by BAI1 was specific to the core oligosaccharide region, distinct from the specificity observed for TLR4-MD2 and caspase-11 (270-273). Interestingly, other PRRs have been shown to recognize the core oligosaccharide, indicating this is a conserved mechanism of microbial recognition and response (274, 275).

Phagocytic receptors appear to play a critical role in modulating TLR responses either by promoting ligand delivery, accessibility, and presentation or by regulating cell signaling. The impact of BAI1 on the inflammatory response of macrophages was preliminarily examined by Das et al (226). In this study, BAI1-depleted macrophages showed reduced TNF-α production in response to both Gram-negative bacteria and soluble LPS. This indicates that in addition to mediating bacterial internalization, BAI1

also modulates TLR4-driven inflammatory responses, suggesting a broader role for BAI1 in innate immunity.

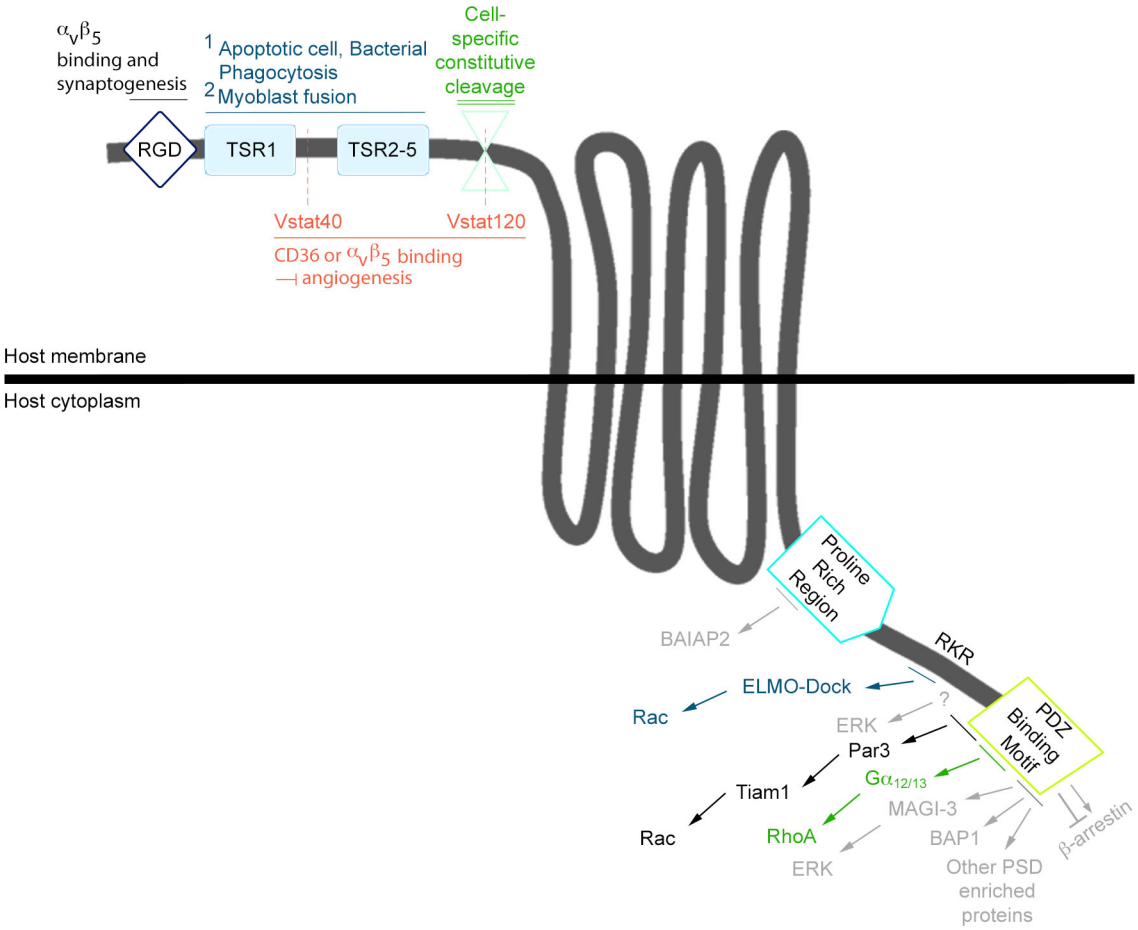
αvβ5
binding and
synaptogenesis
1 Apoptotic cell, Bacterial
Phagocytosis
2 Myoblast fusion
Cell-
specific
constitutive
cleavage
RGD
TSR1
TSR2-5
Vstat40
Vstat120
CD36 or αvβ5 binding
⊣ angiogenesis
Host membrane
Host cytoplasm
Proline
Rich
Region
BAIAP2
RKR
ELMO-Dock
Rac
?
ERK
PDZ
Binding
Motif
Par3
Gα12/13
Tiam1
MAGI-3
Rac
RhoA
BAP1
β-arrestin
ERK
Other PSD
enriched
proteins

Figure 1-9. BAI1 functional and signaling responses

Figure 1-9 shows identified functions, protein-protein interactions, and downstream signaling responses of BAI1. BAI1 is cleaved at the GPS-GAIN domain (e.g. vstat120), which inhibits angiogenesis through interactions with either $\alpha_v\beta_5$ integrins or CD36 (236-239). BAI1 is also cleaved after the first TSR domain, resulting in the release of vstat40 that also exhibits angio-static effects (241). The RGD integrin-binding motif mediates interactions with $\alpha_v\beta_5$ integrins promoting BAI1-PDZ motif-dependent recruitment of Par3 and Tiam1 and localized Rac activation during synaptogenesis (248). The TSR domains bind phosphatidyl serine and LPS to promote Rac activation leading to phagocytosis of attached particles through an interaction with ELMO-Dock, a bipartite Rac-GEF, that requires the positively charged RKR sequence in the cytoplasmic region of BAI1 (224-226). This interaction also promotes myoblast fusion (227). The C-terminal PDZ-binding motif associates with several proteins enriched in the PSD, including MAGI-3 (203) and BAP1 (MAGI-1) (242). This region facilitates signaling through $G\alpha_{12/13}$, leading to the activation of RhoA, which is enriched upon cleavage at the GPS. The cleaved protein also promotes ERK signaling. BAI1 interacts with β-arrestin2, which is negatively regulated by a functional PDZ interacting motif (203). The proline rich region interacts with BAI2AP (IRSp53) through a cognate SH3 domain (243). Signaling pathways are color coded to match functional responses from the extracellular domain. The color grey indicates that ligand interactions or cleavage have not been mechanistically determined to regulate the respective signaling response.

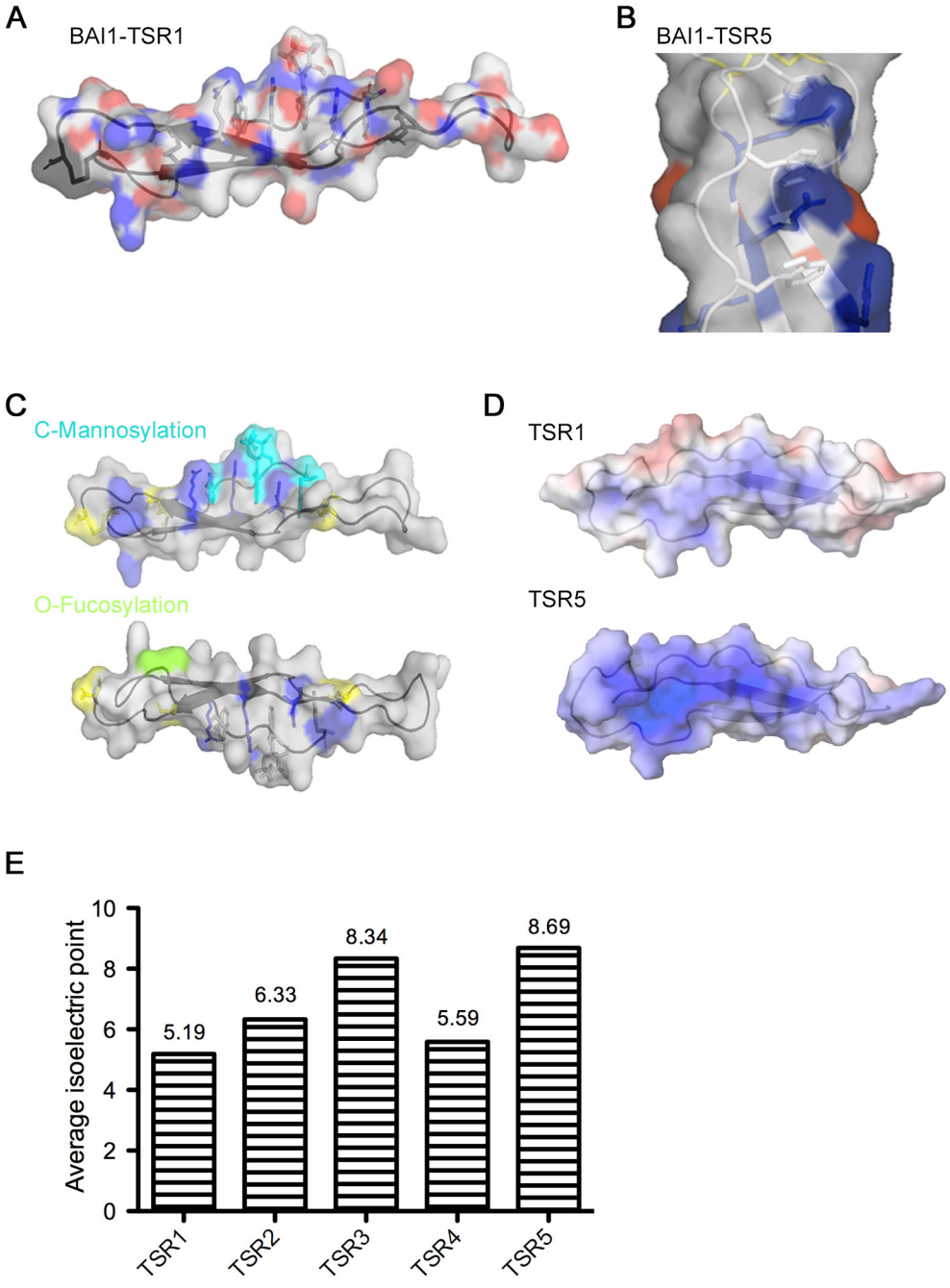
A
BAI1-TSR1
B
BAI1-TSR5
C
C-Mannosylation
O-Fucosylation
D
TSR1
TSR5
E
Average isoelectric point
10
8
6
4
2
0
5.19
6.33
8.34
5.59
8.69
TSR1
TSR2
TSR3
TSR4
TSR5

Figure 1-10. Structure and properties of BAI1 TSR domains

(**A**) The amino acid sequence of the BAI1-TSR1 domain was threaded onto the known crystal structure of the TSR domains in TSP-1 (266). (From Linda Columbus) (**B**) Fig. 1-10B highlights the ladder region of the TSR structure, where tryptophan and arginine side chains interlace to form a positively charged face predicted to be the binding site. (**C**) The TSR protein contains several structural features of note. Disulfide bonds that cap the end of the TSR structure are highlighted in yellow. Two types of post-translational modifications have been observed in other TSR domains. C-mannosylation occurs on the tryptophan residues within WXXW sequences (276, 277). The mannosylation of the first tryptophan in this sequence is most common, however other residues can be modified. The CSVTCG sequence motif is O-fucosylated at the threonine residue (277). The predicted post-translational modifications on the TSRs of BAI1 have not been confirmed. (**D**) The surface charge based on amino acid sequence is displayed for TSR1 and TSR5 emphasizing the variation in the surface charge displayed by the BAI1-TSR domains. (From Linda Columbus) (**E**) The five TSRs of BAI1 display distinct charge properties, with some displaying greater positive charge than others. Fig. 1-10D shows the average calculated isoelectric points for each TSR.

Summary

Here we show that BAI1 is a phagocytic pattern recognition receptor for Gram-negative bacteria that also modulates early inflammatory responses. The impact of BAI1 on the global innate immune response in macrophages and in vivo is unknown. Macrophages are critical for driving bacterial clearance through phagocytosis and microbicidal activity and for mounting and mediating inflammatory responses. After recognition of the core oligosaccharide of LPS, BAI1 drives the internalization of microbes from the extracellular space (226). The route of internalization can markedly effect microbe survival and innate immune responses (117, 164). The impact of BAI1-mediated internalization on bacterial killing and host susceptibility to bacterial challenge is analyzed in Chapter 2. Phagocytic receptors have been shown to interact with TLR recognition, signaling, and compartmentalization, resulting in either positive or negative regulation of TLR-dependent inflammatory responses. The role of co-receptors or accessory proteins in modulating TLR-driven inflammatory signaling is becoming better appreciated. However, the mechanisms through which BAI1 may regulate the innate response to Gram-negative bacteria are largely unknown. The impact of BAI1 on early innate responses in macrophages and possible interactions with other PRRs is assessed in Chapter 3. In Chapter 4, we investigate the specificity of the TSR domains for bacterial recognition, which provides insight into the relevance and breadth of the importance of BAI1 in response to bacterial ligands. Collectively, determining novel pathways by which the innate immune response is regulated provides greater understanding to the complexity of microbe recognition and innate immunity, and may allow for targeted approaches to upregulate or downregulate innate responses.

Chapter 2:

The adhesion G protein-coupled receptor BAI1 enhances macrophage ROS response and microbicidal activity against Gram-negative bacteria

The following work has been published:
Billings, E. A., C. S. Lee, K. A. Owen, R. S. D'Souza, K. S. Ravichandran, and J. E. Casanova. 2016. The adhesion GPCR BAI1 mediates macrophage ROS production and microbicidal activity against Gram-negative bacteria. *Sci. Signal.* 9: ra14

Billings, E. A. performed all experiments and analysis shown in Chapter 2 and wrote and revised the publication. Lee, C.S. provided critical reagents required for the completion of this publication. Owen, K.A. and D'Souza, R.S. advised on the design and methods for the animal model and microscopy, respectively. Ravichandran, K.S. provided critical reagents required for the completion of this publication and reviewed and advised on the manuscript. Casanova, J. E. provided intellectual guidance and reviewed and revised the manuscript.

Chapter 2 The adhesion G protein-coupled receptor BAI1 enhances macrophage ROS response and microbicidal activity against Gram-negative bacteria

Abstract

The detection of microbes and initiation of an innate immune response occurs through PRRs, which are critical for the production of inflammatory cytokines and activation of the cellular microbicidal machinery. In particular, the production of ROS by the NADPH oxidase complex is a critical component of the macrophage bactericidal machinery. We previously characterized BAI1 as a PRR that mediates the selective phagocytic uptake of Gram-negative bacteria by macrophages. Here, we showed that BAI1 promoted phagosomal ROS production through activation of the Rho-family GTPase Rac1, thereby stimulating NADPH oxidase activity. We found that primary macrophages deficient in BAI1 exhibited attenuated Rac activation and reduced ROS production in response to several Gram-negative bacteria, resulting in impaired microbicidal activity. Furthermore, BAI1-deficient mice exhibited increased susceptibility to bacterial challenge in a peritoneal infection model because of impaired bacterial clearance. Together, these findings suggest that BAI1 mediates the clearance of Gram-negative bacteria by stimulating both phagocytosis and NADPH oxidase activation, thereby coupling bacterial detection to the cellular microbicidal machinery. These results highlight a mechanism through which phagocytes can initiate ROS production and subsequent microbe clearance, which is relevant for the response to both pathogenic and commensal microbes and the maintenance of the local inflammatory milieu at sites of recognition.

Introduction

The innate immune system relies upon the ability of the host to detect and respond to both pathogenic and non-pathogenic microbes. Detection occurs through a limited set of germ line–encoded receptors called PRRs (15, 278). The coordinated actions of these innate receptors drive the activity and specificity of the host response, and loss of individual receptors can have devastating consequences on innate immunity (279-281). Macrophages and monocytes interpret the signals from PRRs to couple microbial detection to phagocytic, microbicidal, and cell signaling machinery, which results in local inflammatory responses and bacterial clearance (282, 283). Phagocytic receptors, such as the C-type lectin receptors (118) mannose receptor (119) and Dectin-1 (120) and the scavenger receptors (20) CD36 (121) and MARCO (122), mediate the internalization of microbes from the extracellular space, and their delivery to highly degradative compartments within the cell, resulting in bacterial killing and antigen-processing for the generation of an adaptive immune response (117). These phagocytic receptors are also crucial for innate bactericidal activity and for the compartmentalization and presentation of bacterial ligands to other PRRs, such as Toll-like receptors (TLRs) (46, 67, 117).

BAI1 is a member of subgroup VII of the adhesion-type G protein–coupled receptors (GPCRs), which was originally identified for a role in inhibiting angiogenesis in brain tumor models (221). BAI1 was also recognized as a phagocytic receptor for apoptotic cells, mediating apoptotic cell clearance by several cell types, including neurons, myoblasts, epithelial cells, and myeloid lineage cells (224, 225, 227, 260). We and others reported that, in addition to recognizing apoptotic cells, BAI1 also recognizes Gram-negative bacteria (224, 226). In this context, BAI1 recognizes the core

oligosaccharide of bacterial lipopolysaccharide (LPS) through a series of five type-1 thrombospondin repeats (TSRs) in the extracellular domain (226). Binding of either apoptotic cells or Gram-negative bacteria to the extracellular domain of BAI1 stimulates the rapid rearrangement of the actin cytoskeleton, which culminates in phagocytosis of the bound particle. In this mechanism, the cytoplasmic domain of BAI1 interacts directly with ELMO and Dock180, which together function as a bipartite guanine nucleotide exchange factor (GEF) that activates the Rho-family GTPase Rac1 (225, 226).

In addition to its role in phagocytosis (134, 284), Rac is also a critical part of the NADPH oxidase complex, a key component of the antimicrobial ROS response (178-180). Active, GTP-bound Rac is required for the assembly of the cytosolic regulatory subunits with the transmembrane catalytic subunit gp91phox (138, 170, 182). The activation of NADPH oxidase was characterized downstream of the opsonic phagocytic receptors, FcγR and CR, but its activation in response to non-opsonized Gram-negative bacteria is poorly understood. Here, we show that BAI1 not only mediates the capture and internalization of several species of Gram-negative bacteria by macrophages, but also enhances oxidative killing in a Rac-dependent manner. We also demonstrate that BAI1 mediates bacterial clearance in vivo, in a mouse model of peritoneal challenge. Together, these results suggest that BAI1 functions as a critical phagocytic PRR in the host response to Gram-negative bacteria.

Results

BAI1 mediates binding and uptake of Gram-negative bacteria in primary macrophages

We previously showed that BAI1 mediates the binding and uptake of Gram-negative bacteria in several cell culture model systems (226). Consistent with our earlier

studies, we found that fibroblasts (LR73 Chinese hamster ovary (CHO) cells) expressing exogenous BAI internalized *Escherichia coli* strain DH5α more efficiently than did control, non-BAI1-expressing cells (**Fig. 2-1A**). To test the function of endogenous BAI1 in bacterial recognition, we compared primary bone marrow-derived macrophages (BMDMs) from wild type C57BL/6 mice to cells derived from BAI1-deficient mice (227). For this purpose, bacteria were centrifuged onto monolayers of macrophages at 4°C for 5 min to enable binding, and then the cells were warmed to 37°C for an additional 30 min to enable internalization. We used an immunofluorescence-based assay to distinguish extracellular from intracellular bacteria by specifically labeling extracellular bacteria before cell permeabilization (**Fig. 2-1B**). In this assay, the total number of *E. coli* associated with BAI1-deficient BMDMs was reduced by approximately 30% relative to that associated with BAI1-expressing control macrophages (**Fig. 2-1, C and D**). We found that although the surface binding of *E. coli* DH5α was not statistically significantly different between wild type and BAI1-deficient macrophages (**Fig. 2-1, C and D**, white arrowheads), internalization was reduced by ~50% in the absence of BAI1 (**Fig. 2.1C**, white arrows). This observation suggests that BAI1-mediated uptake contributes substantially to bacterial phagocytosis in primary macrophages.

A

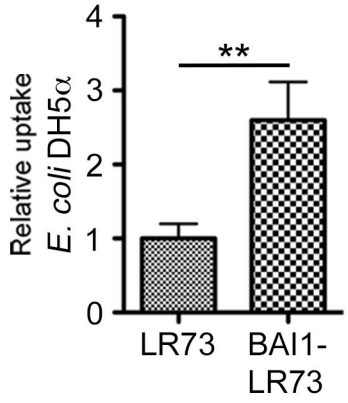

B

Location	Biotinylated *E. coli*			Symbol
	dsRed	SA-488	Example	
Extracellular (EC)	+	+		◁
Intracellular (IC)	+	-		◁

C

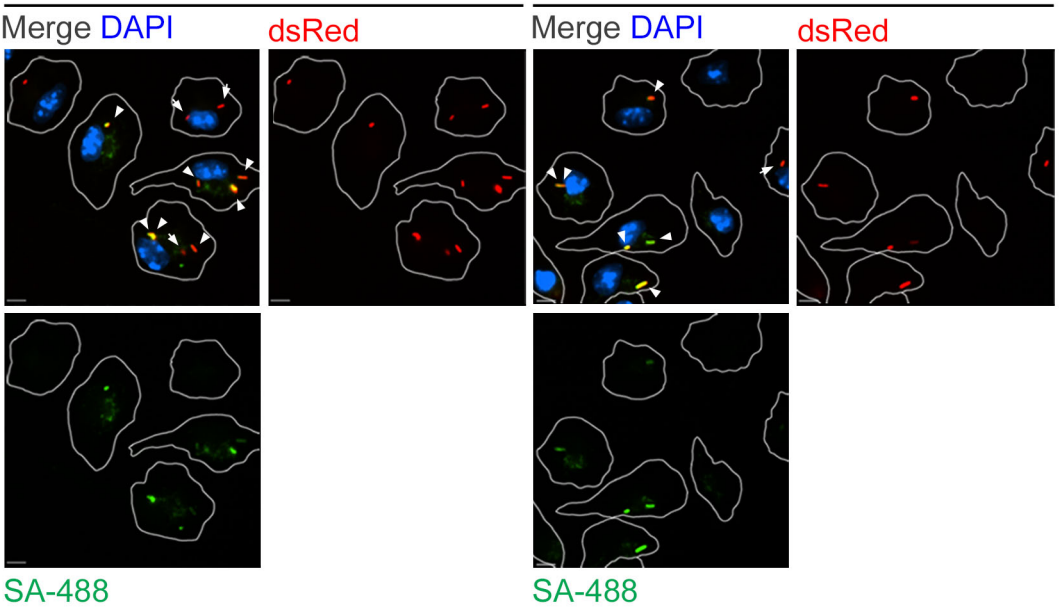

D

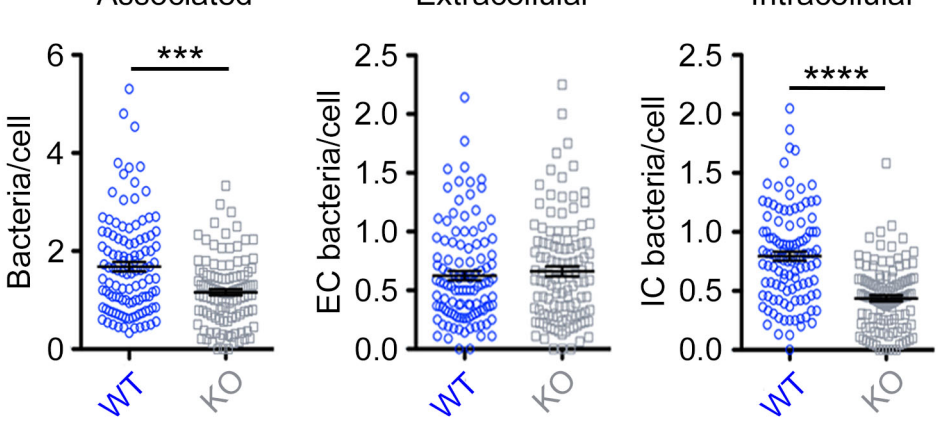

Figure. 2-1. BAI1 mediates the binding and uptake of Gram-negative bacteria by primary macrophages

(**A**) The internalization of *E. coli*-DH5α was measured in parental LR73 cells and cells stably expressing exogenous BAI1 using the gentamicin protection assay as described in Materials and Methods. Data are the mean fold internalization ± SEM of 10 experiments. $^{**}P < 0.01$ by Mann Whitney test. (**B**) Schematic of the immunofluorescence-based internalization assay. Wild type (WT) and BAI1 knockout (BAI1-KO) BMDMs were incubated with biotinylated *E. coli*-DH5α expressing dsRed at an MOI of 10 for 30 min. Cells were washed and fixed, but not permeabilized, and extracellular bacteria were labeled with Alexa Fluor 488-conjugated streptavidin (SA, green). Nuclei were labeled with DAPI (blue). In this assay, intracellular bacteria appear red (and are indicated by arrows), whereas extracellular bacteria appear yellow (and are marked by arrowheads). (**C**) Representative images of WT and BAI1-KO BMDMs from the immunofluorescence-based internalization assay. Scale bar, 5 μm. (**D**) Quantification of total cell-associated bacteria (left), extracellular bacteria (center), and intracellular bacteria (right) per cell from the experiments shown in (C). At least 125 cells per experiment were imaged and five experiments were performed. Plots show the numbers of bacteria per cell per frame ± SEM. $^{***}P < 0.001$, $^{****}P < 0.0001$ by Mann Whitney test.

BAI1 is recruited to sites of bacterial internalization in macrophages

We next analyzed the cellular localization of BAI1 during bacterial recognition by confocal microscopy and live-cell imaging. Because of the poor quality of existing anti-BAI1 antibodies, we used BMDMs derived from transgenic mice expressing a BAI1 construct containing an N-terminal extracellular hemagglutinin (HA) tag (261)(Lee et al, *in press*). In uninfected macrophages, BAI1 was present on the plasma membrane and in the perinuclear region in a punctate distribution, consistent with previous reports (**Fig. 2-2A**) (222, 225). Macrophages incubated with the Gram-positive pathogen *Staphylococcus aureus* showed very little association or enrichment with BAI1, whereas incubation with *E. coli* for 30 min resulted in substantial clustering of BAI1 around associated bacteria (**Fig. 2-2, B and C**, white arrows).

The extent of the association of BAI1 with *S. aureus* or *E. coli* was quantified in two ways. First, we determined the mean fluorescence intensity (MFI) of BAI1 at sites of bacterial association. The MFI of BAI1 associated with *E. coli* was statistically significantly higher than that with *S. aureus* (**Fig. 2-2D**) Similarly, the percentage of bacteria enriched for BAI1 was 10-fold higher for *E. coli* than for *S. aureus* (**Fig. 2-2E**). Although the overall cellular distribution of BAI1 did not change in response to infection (**Fig. 2-2, F and G**), these results indicate a preferential recruitment of BAI1 to sites of interaction with Gram-negative *E. coli* relative to sites of interaction with the Gram-positive *S. aureus*. Consistent with this observation, live-cell imaging indicated that BAI1 was concentrated at sites of bacterial attachment (**Fig. 2-3, A and B**, and **Movie 2-1**), and that it remained associated with bacteria during internalization. Together, these findings

suggest that BAI1 preferentially recognizes Gram-negative bacteria at the macrophage plasma membrane.

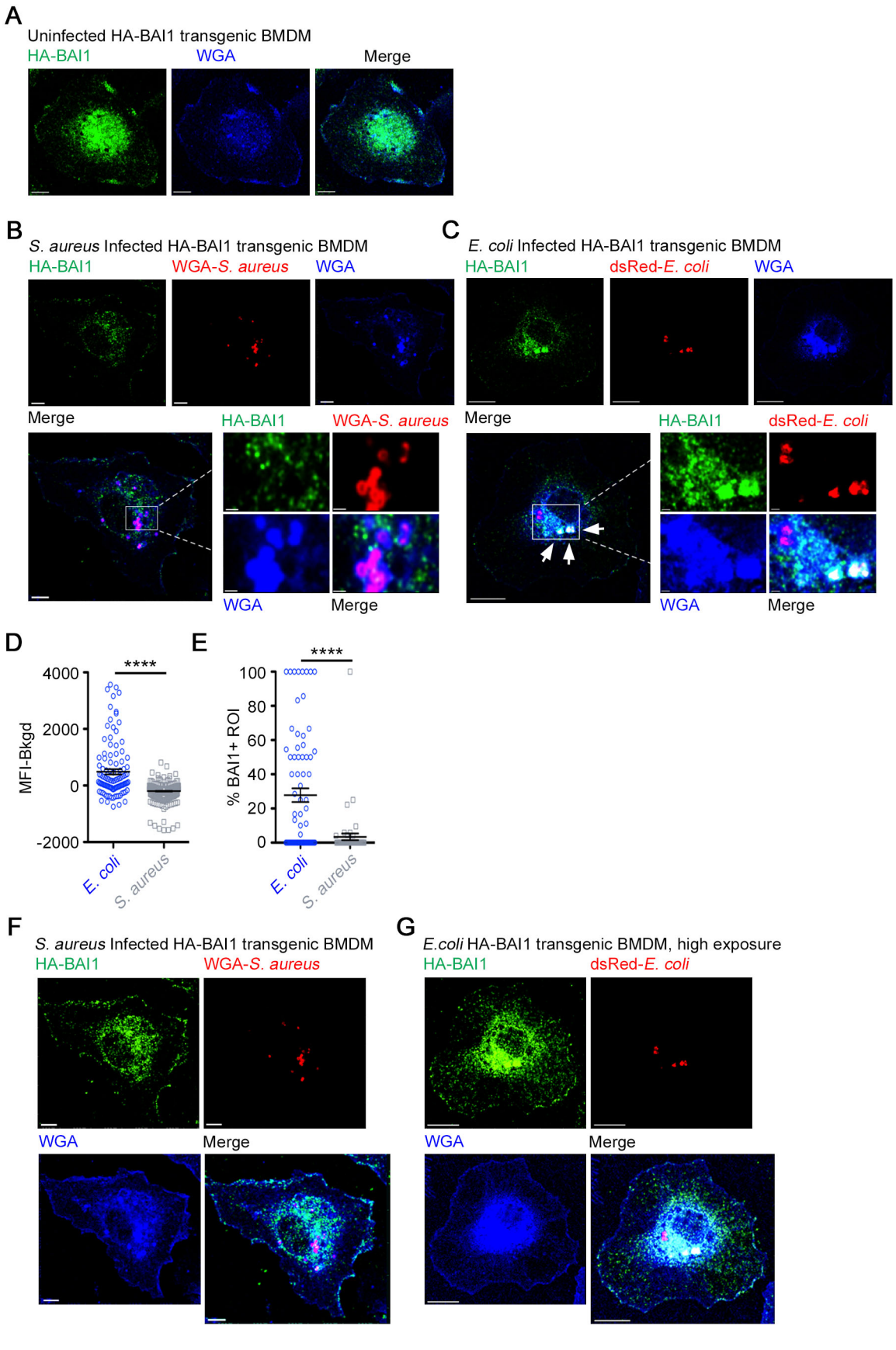
A
Uninfected HA-BAI1 transgenic BMDM
HA-BAI1
WGA
Merge
B
S. aureus Infected HA-BAI1 transgenic BMDM
HA-BAI1
WGA-S. aureus
WGA
Merge
HA-BAI1
WGA-S. aureus
WGA
Merge
C
E. coli Infected HA-BAI1 transgenic BMDM
HA-BAI1
dsRed-E. coli
WGA
Merge
HA-BAI1
dsRed-E. coli
WGA
Merge
D
****
MFI-Bkgd
4000
2000
0
-2000
E. coli
S. aureus
E
****
% BAI1+ ROI
100
80
60
40
20
0
E. coli
S. aureus
F
S. aureus Infected HA-BAI1 transgenic BMDM
HA-BAI1
WGA-S. aureus
WGA
Merge
G
E.coli HA-BAI1 transgenic BMDM, high exposure
HA-BAI1
dsRed-E. coli
WGA
Merge

Figure. 2-2. BAI1 is recruited to sites of bacterial association

(**A**) Transgenic BMDMs expressing HA-BAI1 were fixed and stained with anti-HA antibody (green). The plasma membrane was labeled with wheat germ agglutinin (WGA, blue), and cells were imaged by confocal microscopy. The representative image shows a single confocal section. Scale bar, 5μm. (**B** and **C**) BMDMs expressing transgenic HA-BAI1 were infected for 30 min with either *S. aureus* (B) or *E. coli* (C) at an MOI of 10. The image shows a single confocal section. The boxed areas of the merged images are magnified. White arrows indicate BAI1-positive bacteria. Scale bar, 5μm, Inset scale bar, 1μm. (**D**) Quantification of the mean fluorescence intensity (MFI) of HA-BAI1 associated with bacteria. At least 7 cells per condition per experiment were analyzed from a total of three experiments. A region of interest (ROI) was drawn around each bacterium and the MFI was measured within the ROI (for details see Materials and Methods). Plot shows the MFI ± SEM of HA-BAI1 per ROI after subtraction of background MFI (Bkgd). ****$P < 0.0001$ by Mann Whitney test. (**E**) Percentage of bacteria enriched for HA-BAI1. At least 7 cells per condition were imaged. Plot shows the percentage of bacteria with a HA-BAI1 signal that was more than two-fold greater than that of the background per cell ± SEM from three experiments. ****$P < 0.0001$ by Mann Whitney test. (**F** and **G**) The gain was increased in the single confocal sections from (A) and (B) to show the global cellular distribution of BAI1 after infection with either (F) *S. aureus* or (G) *E. coli*. Scale bar, 5 μm.

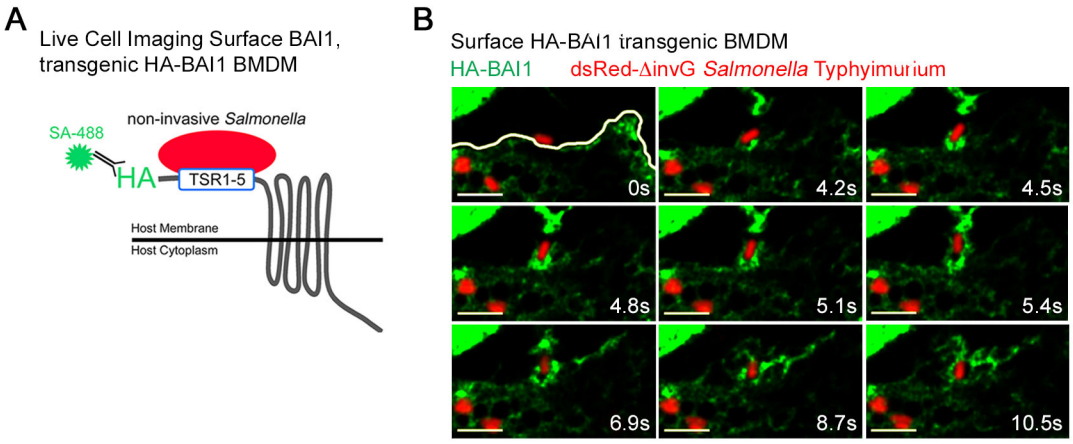
A
Live Cell Imaging Surface BAI1, transgenic HA-BAI1 BMDM
non-invasive Salmonella
SA-488
HA
TSR1-5
Host Membrane
Host Cytoplasm
B
Surface HA-BAI1 transgenic BMDM
HA-BAI1
dsRed-ΔinvG Salmonella Typhyimurium
0s
4.2s
4.5s
4.8s
5.1s
5.4s
6.9s
8.7s
10.5s

Figure. 2-3. BAI1 is recruited to sites of bacterial engulfment

(**A**) Schematic of the protocol for live-cell imaging analysis of BAI1 distribution. BMDMs expressing transgenic HA-BAI1 were incubated with fluorescently conjugated anti-HA antibody (green) to label extracellular receptors and then were incubated with non-invasive *S.* Typhimurium (ΔinvG) expressing dsRed. (**B**) Images from representative Movie 2-1A are shown as a time-lapse series. The white line indicates the cell periphery. Movies were generated for at least two cells from two separate experiments. Scale bar, 5 μm.

Movie 2-1. BAI1 is enriched at the phagocytic cup

BMDMs expressing transgenic HA-BAI1 were incubated with fluorescently conjugated anti-HA antibody (green) to label extracellular receptors and then were incubated with noninvasive *Salmonella* Typhimurium (ΔinvG) expressing dsRed. Note the concentration of BAI1 in the phagocytic cup and in the nascent phagosome during bacterial uptake. Scale bar, 5 μm.

BAI1 ligation stimulates cellular microbicidal activity

The route of cellular entry can markedly affect microbe survival, immune responses, and antigen processing (117, 164). Indeed, several bacterial pathogens target specific receptors during infection to alter downstream cellular responses and compartmentalization within macrophages (285-288). Although somewhat controversial, a large body of evidence suggests that the specific subset of innate immune receptors, such as TLRs, engaged during recognition and uptake can affect phagosome maturation and particle fate (154, 155, 283). To determine whether the recognition and internalization of Gram-negative bacteria by BAI1 affected their survival, we examined intracellular microbicidal activity in primary macrophages and cell lines with a standard gentamicin protection assay. In this assay, cells were allowed to internalize bacteria for 30 min and then were chased for up to seven hours in the presence of gentamicin, which kills extracellular, but not intracellular, bacteria. We found that BAI1-deficient BMDMs were attenuated in their ability to kill two different strains of *E. coli* (**Fig. 2-4, A and B**) and two Gram-negative bacterial pathogens, *Salmonella* Typhimurium and *Pseudomonas aeruginosa* (**Fig. 2-4, C and D**). Consistent with our earlier data (**Fig. 2-2**), loss of BAI1 did not affect bactericidal activity against *S. aureus* (**Fig. 2-4E**). Similar results were observed in peritoneal macrophages (PEMs) from wild type and BAI1-deficient mice (**Fig. 2-4, F and G**) and BAI1-depleted J774 cells, a macrophage cell line (**Fig. 2-5, A to C**). Although the magnitude and kinetics of bacterial killing at earlier time points was affected by the loss of BAI1, differences at later time points were not as pronounced. This presumably reflects the activity of other bactericidal machinery, including antimicrobial peptides or nitric oxide. Together, these observations suggest that BAI1 not

only mediates bacterial internalization, but also selectively promotes microbicidal activity against Gram-negative bacteria in infected macrophages.

BAI1-mediated internalization of Gram-negative bacteria occurred rapidly after infection. Because the difference in bacterial survival between wild type and BAI1-deficient cells was reduced at later time points, we hypothesized that BAI1-mediated bactericidal activity occurred earlier. To test this hypothesis, we examined microbicidal activity over a short time course in which bacteria were internalized for 15 min, then washed, and chased to 30 or 60 min. Viable cell-associated bacteria were then quantified by colony-forming assays. BAI1-deficient BMDMs displayed statistically significantly attenuated bactericidal activity at both 30 and 60 min against non-pathogenic *E. coli* (**Fig. 2-6A).** Similarly, decreased microbicidal activity in BMDMs lacking BAI1 was also observed against the pathogens *P. aeruginosa* and two strains of *Burkholderia cenocepacia* (**Fig. 2-6, B to D**). Bactericidal activity against cell-associated *S. aureus* at early time points was minimal and did not differ between wild type and BAI1-deficient cells (**Fig. 2-6E**).

We previously showed that BAI1 mediates the internalization of Gram-negative bacteria by signaling through the ELMO-Dock complex, which leads to activation of the Rho-family GTPase Rac1. Macrophages depleted of either BAI1 or ELMO1 are similarly impaired in their ability to internalize non-invasive *S.* Typhimurium (ΔinvG), and CHO cells expressing a BAI1 mutant, BAI1-R^{1489}KR-AAA, which is unable to couple to the ELMO-Dock complex, show impaired internalization of bacteria relative to that by cells expressing wild type BAI1 (225, 226). To determine whether BAI1-mediated Rac1 activation contributed to the difference in bactericidal activity observed in wild type

macrophages compared to that in BAI1-deficient macrophages, we isolated BMDMs from knock-in mice expressing an HA-tagged form of this BAI1 mutant (HA-BAI1-R^{1489}KR-AAA) (261)(Lee et al, *in press*). These cells exhibited attenuated microbicidal activity that was quantitatively similar to that of cells deficient in BAI1 (compare **Fig. 2-6F to Fig. 2-6A**). These results suggest that BAI1-dependent bactericidal activity is dependent upon the ELMO-Dock-mediated activation of Rac1.

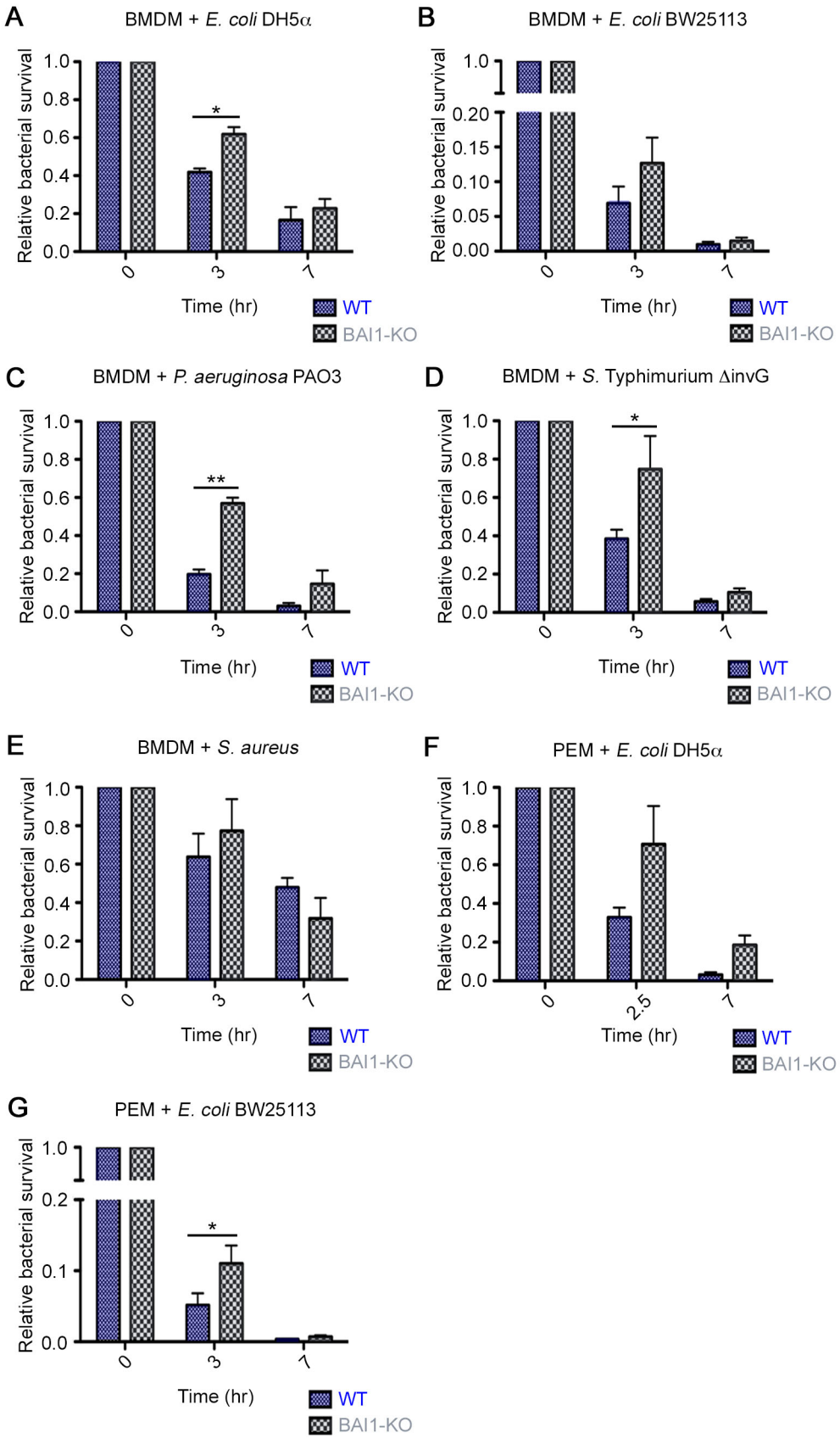
A
BMDM + E. coli DH5α
Relative bacterial survival
1.0
0.8
0.6
0.4
0.2
0.0
*
0
3
7
Time (hr)
WT
BAI1-KO
B
BMDM + E. coli BW25113
Relative bacterial survival
1.0
0.20
0.15
0.10
0.05
0.00
0
3
7
Time (hr)
WT
BAI1-KO
C
BMDM + P. aeruginosa PAO3
Relative bacterial survival
1.0
0.8
0.6
0.4
0.2
0.0
**
0
3
7
Time (hr)
WT
BAI1-KO
D
BMDM + S. Typhimurium ΔinvG
Relative bacterial survival
1.0
0.8
0.6
0.4
0.2
0.0
*
0
3
7
Time (hr)
WT
BAI1-KO
E
BMDM + S. aureus
Relative bacterial survival
1.0
0.8
0.6
0.4
0.2
0.0
0
3
7
Time (hr)
WT
BAI1-KO
F
PEM + E. coli DH5α
Relative bacterial survival
1.0
0.8
0.6
0.4
0.2
0.0
0
2.5
7
Time (hr)
WT
BAI1-KO
G
PEM + E. coli BW25113
Relative bacterial survival
1.0
0.2
0.1
0.0
*
0
3
7
Time (hr)
WT
BAI1-KO

Figure. 2-4. Intracellular killing of Gram-negative bacteria is increased by BAI1-mediated bacterial recognition

(**A**) WT and BAI1-KO BMDMs were incubated for 30 min with *E. coli*-DH5α at an MOI of 25 (t=0), and then chased in the presence of gentamicin for the indicated times to kill extracellular bacteria. Lysates were then plated to count viable intracellular bacteria. Survival is shown relative to the bacterial counts at t=0. All graphs in Fig. 2-4 display relative mean ± SEM of at least three independent experiments. Data were analyzed by two-way ANOVA with Bonferroni post-hoc comparisons. A *P*-value is provided in the figure legend describing the source of variation in the data set (e.g. cell genotype, time, or an interaction between the cell genotype and time, which can also be considered as kinetics). Statistical information in the figure shows the results from the post-hoc comparison (Cell: $*P < 0.05$; Time: $***P < 0.001$, $N = 3$). (**B** to **E**) Intracellular bactericidal activity by BMDMs from the indicated mice against Gram-negative bacteria was measured as described in (A). These included (B) *E. coli*-BW25113 (Time: $**P < 0.01$, $N = 4$), (C) *P. aeruginosa* (Cell: $*P < 0.05$; Time: $***P < 0.001$, $N = 3$), (D) non-invasive *S.* Typhimurium (ΔinvG) (Time: $***P < 0.001$, $N = 3$), and (E) the Gram-positive *S. aureus* (Time: $*P < 0.05$, $N = 4$). (**F** and **G**) The survival of intracellular (F) *E. coli*-DH5α (Cell: $*P < 0.05$; Time: $**P < 0.01$, $N = 3$) and (G) *E. coli*-BW25113 (Time: $***P < 0.001$, $N = 4$) in peritoneal macrophages (PEMs) from the indicated mice was measured as described in (A).

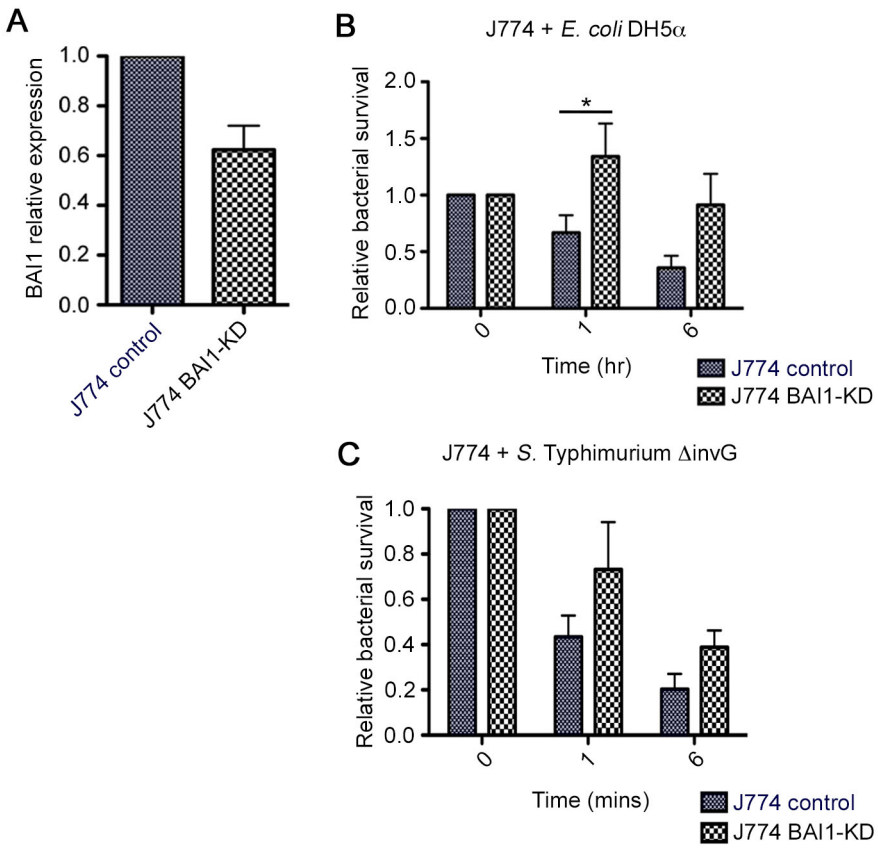
A
BAI1 relative expression
1.0
0.8
0.6
0.4
0.2
0.0
J774 control
J774 BAI1-KD
B
J774 + E. coli DH5α
Relative bacterial survival
2.0
1.5
1.0
0.5
0.0
*
0
1
6
Time (hr)
J774 control
J774 BAI1-KD
C
J774 + S. Typhimurium ΔinvG
Relative bacterial survival
1.0
0.8
0.6
0.4
0.2
0.0
0
1
6
Time (mins)
J774 control
J774 BAI1-KD

Figure. 2-5. BAI1 promotes cellular microbicidal activity in J774 macrophages

(**A**) Stable J774 macrophage cell lines were generated by transduction with lentivirus expressing BAI1-specific shRNA and subsequent selection with puromycin. Scrambled shRNA was used as a control. BAI1 knockdown was quantified by qRT-PCR analysis. Data are the mean ± SEM from three experiments of the relative expression of BAI1 compared to that of control cells, which was set at 1. (**B**) Control and BAI1-depleted J774s were infected with *E. coli*-DH5α at an MOI of 25 for 30 min. Bacterial killing was measured as described in Fig. 2-4A with the gentamicin protection assay. Data are mean relative survival ± SEM of three experiments. Data were analyzed by two-way ANOVA with Bonferroni post-hoc comparisons as discussed in Fig. 2-4A (Cell: $^{**}P < 0.01$). (**C**) Control and BAI1-depleted J774s were infected with non-invasive *S.* Typhimurium (ΔinvG) at an MOI of 25 for 30 min. Bacterial killing was measured as described in Fig. 2-4A with the gentamicin protection assay. Data are mean relative survival ± SEM of three experiments. Data were analyzed by two-way ANOVA with Bonferroni post-hoc comparisons (Time: $^{*}P < 0.05$).

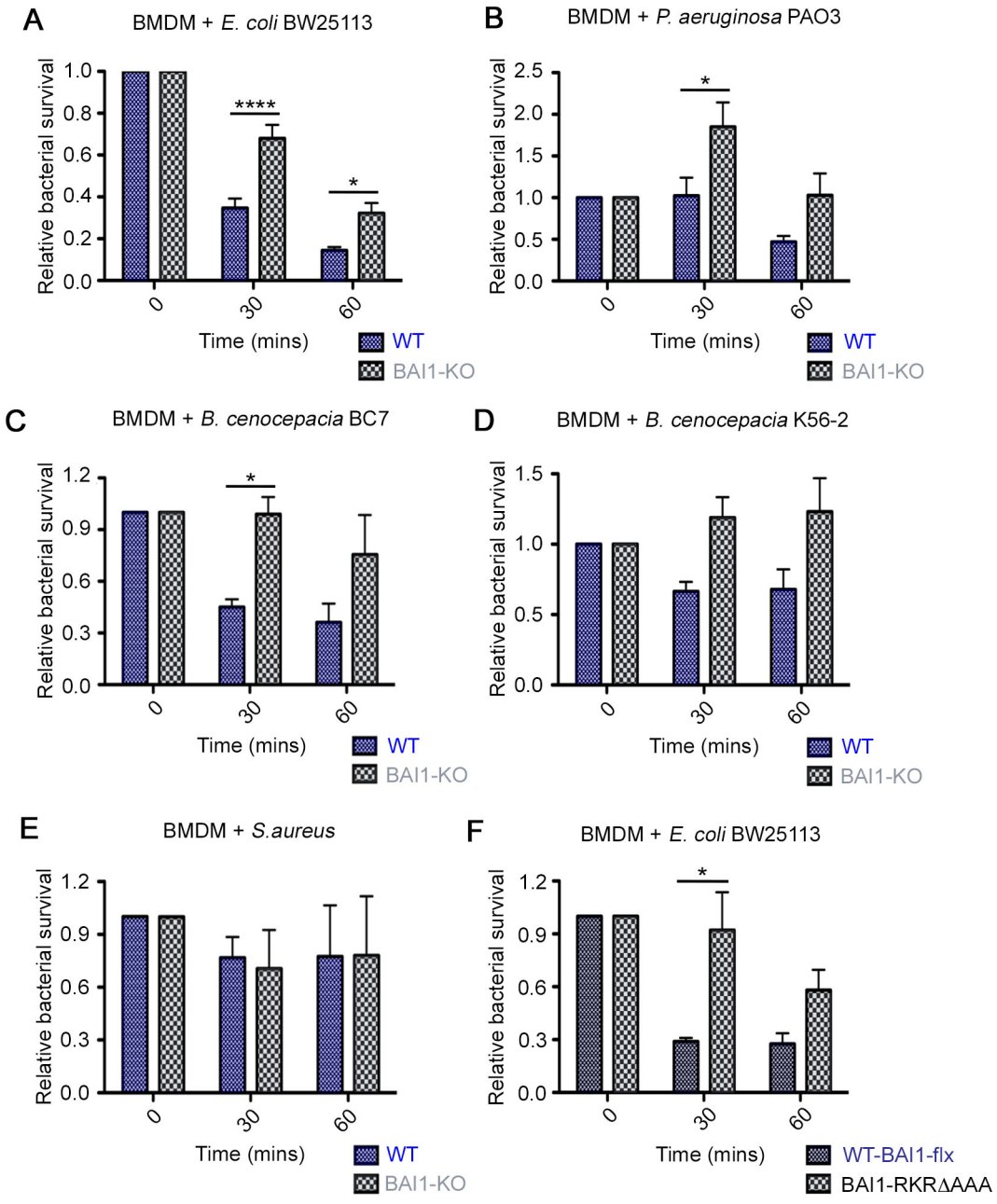
A
BMDM + E. coli BW25113
Relative bacterial survival
1.0
0.8
0.6
0.4
0.2
0.0
****
*
0
30
60
Time (mins)
WT
BAI1-KO
B
BMDM + P. aeruginosa PAO3
Relative bacterial survival
2.5
2.0
1.5
1.0
0.5
0.0
*
0
30
60
Time (mins)
WT
BAI1-KO
C
BMDM + B. cenocepacia BC7
Relative bacterial survival
1.2
0.9
0.6
0.3
0.0
*
0
30
60
Time (mins)
WT
BAI1-KO
D
BMDM + B. cenocepacia K56-2
Relative bacterial survival
1.5
1.0
0.5
0.0
0
30
60
Time (mins)
WT
BAI1-KO
E
BMDM + S.aureus
Relative bacterial survival
1.2
0.9
0.6
0.3
0.0
0
30
60
Time (mins)
WT
BAI1-KO
F
BMDM + E. coli BW25113
Relative bacterial survival
1.2
0.9
0.6
0.3
0.0
*
0
30
60
Time (mins)
WT-BAI1-flx
BAI1-RKRΔAAA

Figure. 2-6. Early microbicidal activity against Gram-negative bacteria is enhanced by BAI1 in macrophages

(**A**) WT and BAI1-KO BMDMs were incubated for 15 min with *E. coli*-BW25113 at an MOI of 25. After extensive washing, cells were either lysed immediately (t=0) or were chased in complete medium for 30 or 60 min. For each time point, lysates were plated on LB agar to enumerate viable bacteria. Survival is shown relative to total cell-associated bacteria at t=0. All graphs display relative means ± SEM. Data were analyzed by two-way ANOVA with Bonferroni post-hoc comparisons (Cell: ****$P < 0.0001$; Time: ****$P < 0.0001$, $N = 8$). (**B** to **E**) Cell-associated bactericidal activity of BMDMs from the indicated mice against (B) *P. aeruginosa* PAO3 (Cell: **$P < 0.01$; Time: **$P < 0.01$, $N = 5$), (C) *B. cenocepacia* BC7 (Cell: **$P < 0.01$, $N = 4$), (D) *B. cenocepacia* K56-2 (Cell: **$P < 0.01$, $N = 5$), and (E) *S. aureus* ($N = 5$) was measured as described in (A). (**F**) WT-Flx and transgenic BAI1-RKR-AAA BMDMs were incubated with *E. coli*-BW251113 at an MOI of 25. Bacterial killing was measured as described in (A) (Cell: **$P < 0.01$, $N = 3$).

BAI1-mediated Rac activation is enhanced in macrophages in response to bacterial infection

We previously showed that cells over-expressing BAI1 exhibit increased Rac activity in response to the Gram-negative pathogen *S.* Typhimurium, and that altering the ability of BAI1 to interact with the ELMO-Dock GEF complex inhibits Rac activation and phagocytosis (225, 226), as described earlier. To confirm that endogenous BAI1 was required for Rac activation in response to Gram-negative bacteria, we measured Rac activity in BMDMs with a well-characterized pull-down assay (289). Incubation of wild type BMDMs with *E. coli* led to robust activation of Rac1 within 30 min (**Fig. 2-7, A and B**). In contrast, no detectable increase in Rac1 activation was observed in BMDMs lacking BAI1. Similar results were obtained with BMDMs that had been primed with IFN-γ (**Fig. 2-7, C and D**). BAI1-deficient macrophages were not inherently defective in priming, because signaling in response to IFN-γ as determined by measuring the phosphorylation of signal transducer and activator of transcription 1 (STAT1), was comparable between wild type and BAI1-deficient cells (**Fig. 2-8**). These results suggest that endogenous BAI1 is required for the activation of Rac in response to Gram-negative bacteria.

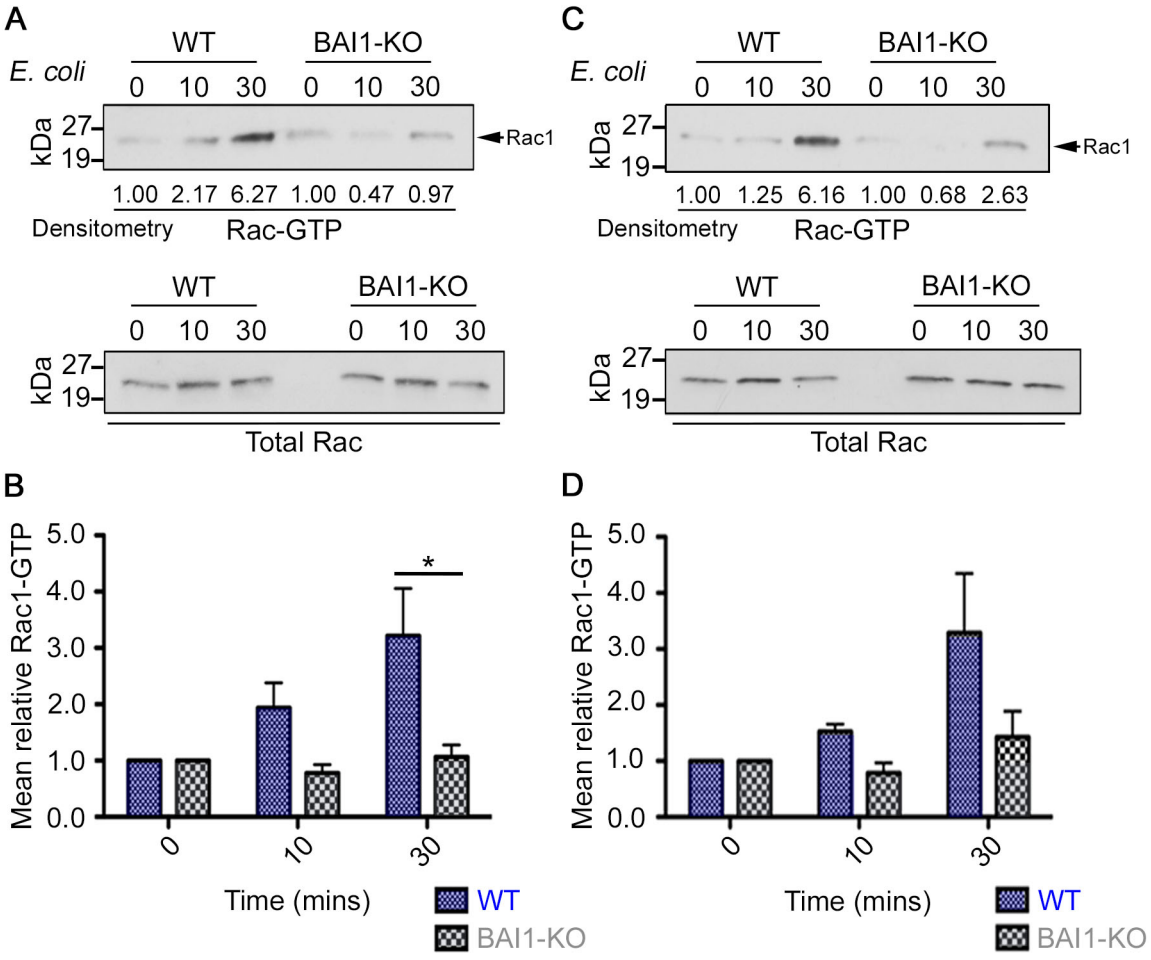
A
WT
BAI1-KO
E. coli
0 10 30 0 10 30
kDa
27
19
Rac1
1.00 2.17 6.27 1.00 0.47 0.97
Densitometry
Rac-GTP
WT
BAI1-KO
0 10 30 0 10 30
kDa
27
19
Total Rac
C
WT
BAI1-KO
E. coli
0 10 30 0 10 30
kDa
27
19
Rac1
1.00 1.25 6.16 1.00 0.68 2.63
Densitometry
Rac-GTP
WT
BAI1-KO
0 10 30 0 10 30
kDa
27
19
Total Rac
B
Mean relative Rac1-GTP
5.0
4.0
3.0
2.0
1.0
0.0
*
0
10
30
Time (mins)
WT
BAI1-KO
D
Mean relative Rac1-GTP
5.0
4.0
3.0
2.0
1.0
0.0
0
10
30
Time (mins)
WT
BAI1-KO

Figure. 2-7. Loss of BAI1 impairs Rac activation in response to *E. coli*

(**A** and **B**) Rac1 activation was measured by a standard pull-down assay. Unprimed BMDMs were incubated with *E. coli*-BW25113 for 10 or 30 min. Cells were then lysed and GTP-bound Rac was precipitated with GST-PBD beads as described in Materials and Methods. Precipitates were then analyzed by Western blotting to detect Rac1. Band intensities were quantified by densitometry. Aliquots of each cell lysate were analyzed by Western blotting for total Rac1 (bottom) to demonstrate equal total Rac1 protein in control and BAI1-KO lysates. (B) Quantitation of Western blotting data from six separate experiments. Data are mean fold-changes in Rac1-GTP abundance ± SEM. Two-way ANOVA with Bonferroni post-hoc comparison was used for analysis (Cell: $*P < 0.05$). (**C**) IFN-γ-primed BMDMs were incubated with *E. coli*-BW25113 for 10 or 30 min and then Rac activation was measured as described in (A). Western blots are representative of four experiments. (**D**) Quantitation of the extent of Rac1 activation in IFN-γ-primed cells relative to that in uninfected cells. Data are the mean fold-increase ± SEM in Rac1-GTP activity of four experiments. Two-way ANOVA with Bonferroni post-hoc comparison was used for analysis (Cell: $*P < 0.05$).

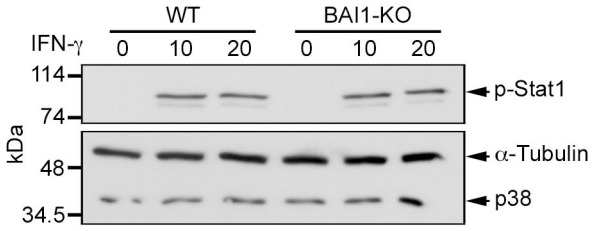
WT
BAI1-KO
IFN-γ
0
10
20
0
10
20
114
74
48
34.5
kDa
p-Stat1
α-Tubulin
p38

Figure. 2-8. Loss of BAI1 does not affect IFN-γ priming

Analysis of IFN-γ signaling. WT and BAI1-KO BMDMs were left untreated or were treated with IFN-γ (20 ng/ml) for the indicated times and then were analyzed by Western blotting with antibodies specific for the indicated proteins. Western blots are representative of three independent experiments.

ROS production in response to Gram-negative bacteria is regulated by BAI1

As professional phagocytes, macrophages use multiple mechanisms to kill bacteria, including the production of ROS and RNS (159). Macrophages use two primary systems to generate ROS for oxidative killing: mitochondria and the phagocyte NADPH oxidase (156, 178, 179, 290, 291). In the case of NADPH oxidase, upstream signaling initiates phosphorylation of the cytoplasmic regulatory subunit p47phox, which associates with two other cytosolic proteins, p67phox and p40phox (182). Assembly of this cytosolic complex on the phagosomal membrane and activation of the membrane-associated catalytic subunits gp91phox and p22phox requires the activation of Rac1, Rac2, or both (138, 292). Whereas Rac2 is the predominant activating form of Rac in neutrophils (293), Rac1 is critical for ROS responses in macrophages (136, 294, 295). Our observations that BAI1 is required for Rac activation in response to Gram-negative bacteria and that microbicidal activity is reduced in BAI1-deficient cells suggested that BAI1 may stimulate ROS production upon binding to Gram-negative bacteria.

To test this hypothesis, we measured ROS production in IFN-γ-primed wild type and BAI1-deficient BMDMs in a luminol-dependent chemiluminescence (LDCL) assay. We found that incubation of wild type macrophages with *E. coli* induced the rapid and robust production of ROS, which was completely blocked by the pharmacological NADPH oxidase inhibitor diphenyleneiodonium (DPI) (**Fig. 2-9, A and B**). In contrast, ROS production was attenuated in cells lacking BAI1. Although the kinetics of activation were different, the ROS responses to two other Gram-negative bacterial pathogens, *P. aeruginosa* and *B. cenocepacia*, were reduced in BAI1-deficient cells (**Fig. 2-9, C to F**). For comparison, no defect in ROS production was observed when macrophages were

incubated with the Gram-positive bacterium *S. aureus* (**Fig. 2-9, G and H**) or the phorbol ester, phorbol myristate acetate (PMA) (**Fig. 2-9, I and J**). Furthermore, macrophages derived from gp91phox-deficient mice, which are completely defective in phagocyte NADPH oxidase activity, showed no detectable ROS generation in response to *E. coli* (**Fig. 2-9, K and L**). Similar results were observed in an in situ fluorescence assay with CellRox Green, a fluorescent ROS reporter (**Fig. 2-10A**). ROS production in BAI1-deficient macrophages incubated with *E. coli* was reduced nearly to the level of that in gp91phox- knockout cells (**Fig. 2-10, B and C**). Whereas macrophage generation of ROS occurs within minutes of bacterial detection (167), generation of RNS requires the expression of iNOS, which occurs substantially later (296-298). We found that cellular iNOS protein was similarly induced in wild type and BAI1 knockout macrophages after 6 hours of exposure to *E. coli*, indicating that iNOS expression did not require BAI1 (**Fig. 2-11**).

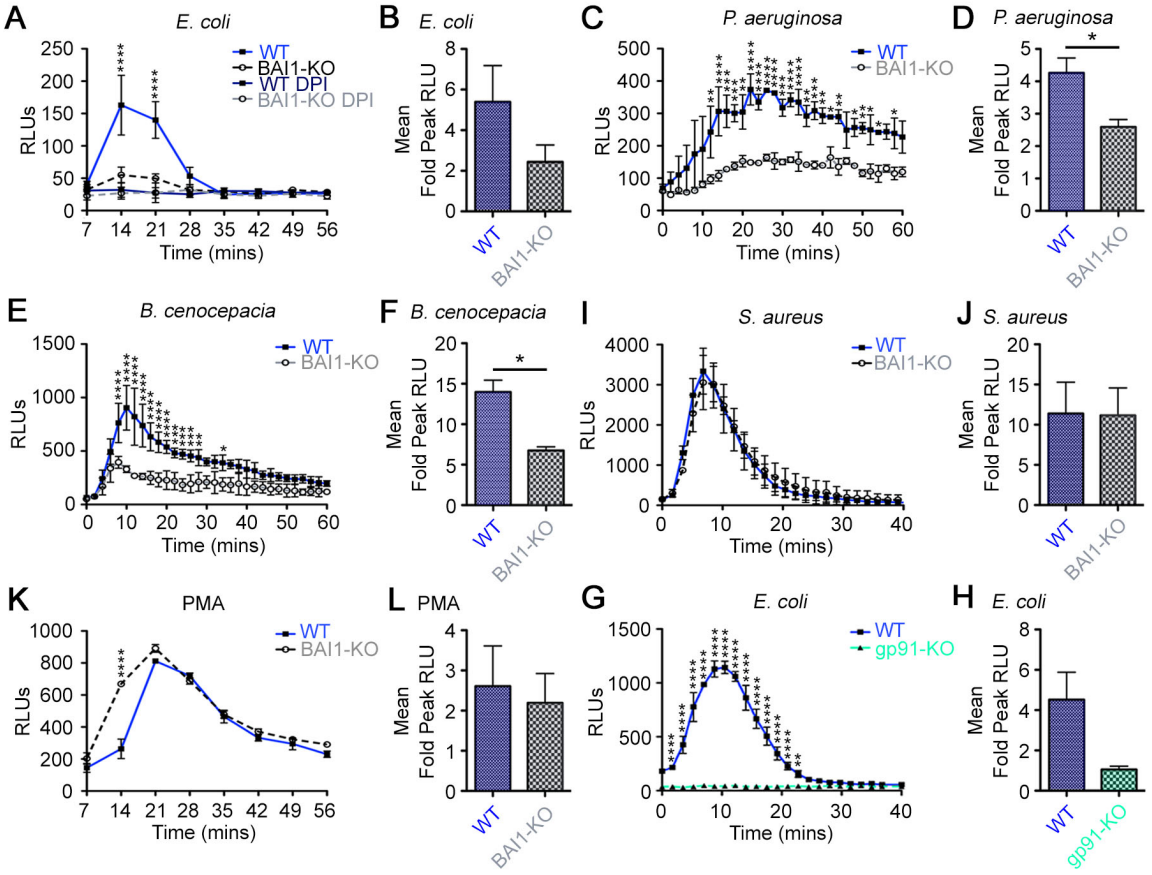
A
E. coli
WT
BAI1-KO
WT DPI
BAI1-KO DPI
RLUs
Time (mins)
B
E. coli
Mean Fold Peak RLU
WT
BAI1-KO
C
P. aeruginosa
WT
BAI1-KO
RLUs
Time (mins)
D
P. aeruginosa
Mean Fold Peak RLU
WT
BAI1-KO
E
B. cenocepacia
WT
BAI1-KO
RLUs
Time (mins)
F
B. cenocepacia
Mean Fold Peak RLU
WT
BAI1-KO
I
S. aureus
WT
BAI1-KO
RLUs
Time (mins)
J
S. aureus
Mean Fold Peak RLU
WT
BAI1-KO
K
PMA
WT
BAI1-KO
RLUs
Time (mins)
L
PMA
Mean Fold Peak RLU
WT
BAI1-KO
G
E. coli
WT
gp91-KO
RLUs
Time (mins)
H
E. coli
Mean Fold Peak RLU
WT
gp91-KO

Figure. 2-9. BAI1-deficient macrophages exhibit attenuated ROS production in response to Gram-negative bacteria.

(**A**) LDCL assays were performed to measure ROS production by WT and BAI1-KO BMDMs after incubation with *E. coli*-BW25113. 10 μM DPI was added to replicate wells to inhibit NADPH oxidase activity. Graph shows a representative example of ROS activity and kinetics as mean relative light units (RLUs) ± SEM. Repeated-measures two-way ANOVA with Bonferroni post-hoc comparison was used for analysis (Interaction: ****$P < 0.0001$; Cell: ****$P < 0.0001$; Time ****$P < 0.0001$). (**B**) The mean fold-change in peak ROS production ± SEM of WT or BAI1-KO BMDMs treated with *E. coli*-BW25113 from 8 separate experiments is analyzed by Students t-test. (**C** to **J**) BMDMs from the WT or BAI1-KO mice were treated with inflammatory stimuli as indicated and analyzed as in (A) and (B). The stimuli are listed, followed by the corresponding analysis of a representative experiment and the mean fold-change in peak ROS production. (**C**) *P. aeruginosa,* Interaction: **$P < 0.01$; Cell: **$P < 0.01$; Time: ****$P < 0.0001$ (**D**) * $P < 0.05$, $N = 5$ (**E**) *B. cenocepacia,* Interaction: ****$P < 0.0001$; Cell: *$P < 0.05$; Time: ****$P < 0.0001$) (**F**) *$P < 0.05$, $N = 2$ (**G**) *S. aureus,* Time: ****$P < 0.0001$ (**H**) $N = 5$ (**I**) PMA, Interaction: ****$P < 0.0001$; Cell: **$P < 0.01$; Time: ****$P < 0.0001$ (**J**) $N = 4$ (**K**) ROS was measured in WT or gp91phox-KO BMDMs incubated with *E. coli*-BW25113 using LDCL and analyzed as described in (A) (Interaction: ****$P < 0.0001$; Cell: ****$P < 0.0001$; Time: ****$P < 0.0001$). (**L**) The mean fold-change in peak ROS production ± SEM from three experiments is shown for

WT and gp91phox-KO BMDMs treated with *E. coli*-BW25113. Data were analyzed by Students t-test.

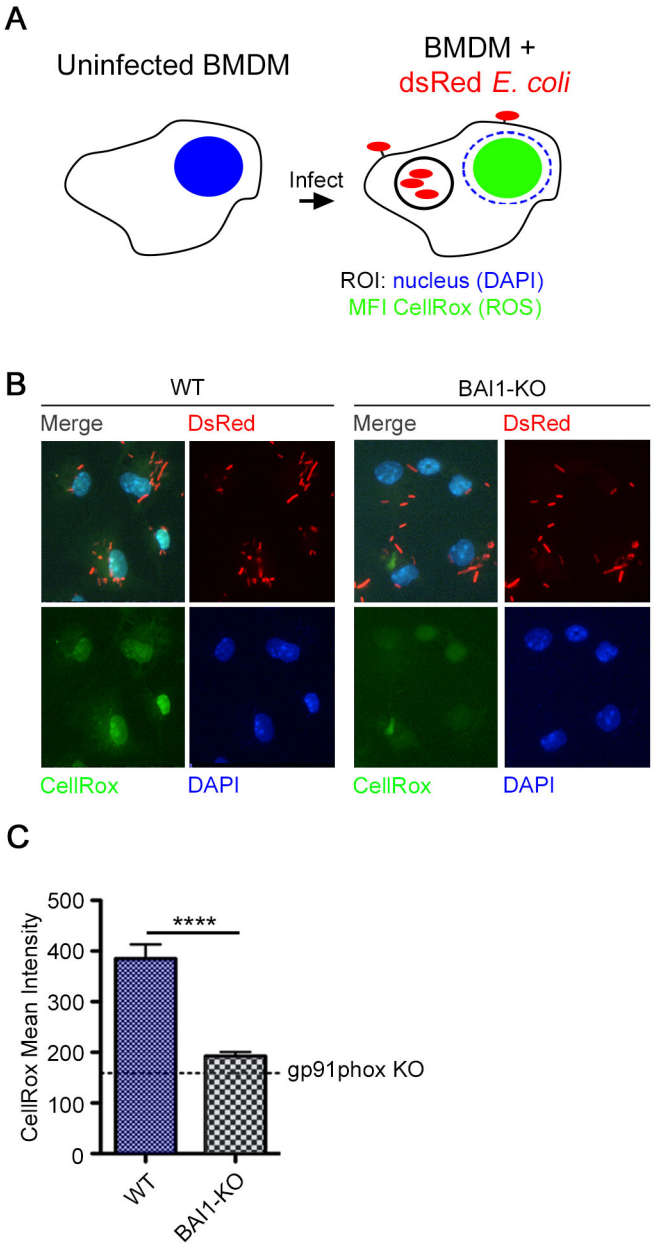
A
Uninfected BMDM
BMDM +
dsRed E. coli
Infect
ROI: nucleus (DAPI)
MFI CellRox (ROS)
B
WT
BAI1-KO
Merge
DsRed
Merge
DsRed
CellRox
DAPI
CellRox
DAPI
C
CellRox Mean Intensity
500
400
300
200
100
0
****
gp91phox KO
WT
BAI1-KO

Figure. 2-10. Loss of BAI1 impairs intracellular ROS responses

(**A**) Schematic of the CellRox analysis of ROS production in macrophages. WT and BAI1-KO BMDMs were incubated with *E. coli*-DH5α-dsRed. Cells were then incubated with 5 μM CellRox Green, fixed, permeabilized, and counterstained with DAPI. Cells were imaged by wide-field fluorescence microscopy. The nuclear DAPI signal defined the regions of interest (ROIs) in which to measure CellRox mean intensity. (**B**) Representative images of WT and BAI1-KO BMDMs after treatment with *E. coli*-DH5α and CellRox. Scale bar, 5 μm. (**C**) Graph shows the mean fluorescence intensity ± SEM from four experiments of the nuclear CellRox signal. This was measured from at least 300 cells per experiment after infection. Dashed horizontal line indicates CellRox fluorescence in gp91phox KO macrophages. Data were analyzed with a Mann Whitney test. ****$P < 0.0001$.

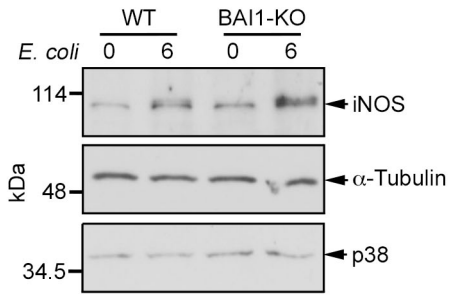
WT
BAI1-KO
E. coli
0
6
0
6
114
iNOS
kDa
48
α-Tubulin
34.5
p38

Figure. 2-11. Loss of BAI1 does not affect iNOS induction by *E. coli*

iNOS abundance was determined by Western blotting analysis of lysates from WT and BAI1-KO BMDMs that were incubated with *E. coli*-BW25113 for 6 hours. Images are representative of two independent experiments.

BAI1-mediated ROS responses result in the enhanced microbicidal activity of macrophages

To determine the extent to which BAI1-mediated bactericidal activity depended on ROS, we treated control and BAI1-deficient macrophages with the ROS scavenger N-acetylcysteine (NAC) and measured bacterial survival. Treatment of infected wild type macrophages with NAC increased bacterial survival to an extent observed in cells lacking BAI1 (**Fig. 2-12A**). Moreover, treatment of BAI1-deficient cells with NAC did not further improve bacterial survival, confirming that the extent of ROS-derived killing at this time point in the absence of BAI1 was negligible. Similar results were observed with gp91phox-deficient macrophages, which showed defects in early microbicidal activity, but no change in bacterial killing in the presence of NAC (**Fig. 2-12, B and C**). In contrast, treatment of cells with the mitochondrial ROS inhibitor MitoTempo (299) had no statistically significant effect on bactericidal activity (**Fig. 2-13**), indicating that most early microbicidal ROS was derived from the phagosomal NADPH oxidase complex.

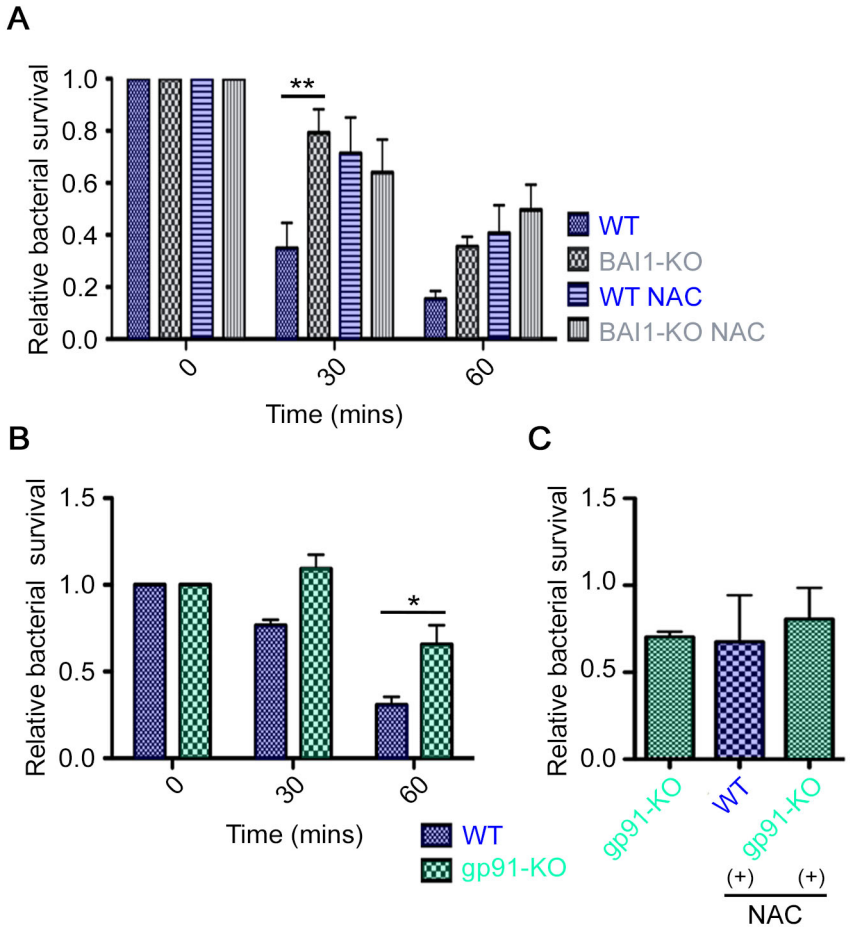
A
Relative bacterial survival
1.0
0.8
0.6
0.4
0.2
0.0
**
0
30
60
Time (mins)
WT
BAI1-KO
WT NAC
BAI1-KO NAC
B
Relative bacterial survival
1.5
1.0
0.5
0.0
*
0
30
60
Time (mins)
WT
gp91-KO
C
Relative bacterial survival
1.5
1.0
0.5
0.0
gp91-KO
WT
gp91-KO
(+)
(+)
NAC

Figure. 2-12. ROS-mediated microbicidal activity in BAI1-expressing macrophages

(**A**) BMDMs were pre-treated with either vehicle or the ROS scavenger N-acetylcysteine (NAC) before being incubated with *E. coli*-BW25113 for the indicated times. Bacterial survival was measured as described in Fig. 2-6A. All graphs show mean survival ± SEM from four separate experiments. Data were analyzed by two-way ANOVA with Bonferroni post-hoc comparisons, WT vs. BAI1-KO: (Cell: ***$P < 0.001$; Time: ***$P < 0.001$) WT vs. WT-NAC: Cell: (*$P < 0.05$; Time: * $p<0.05$). (**B**) WT and gp91phox-KO BMDMs were infected with *E. coli*-BW25113 for the indicated times and the survival of the associated bacteria was measured and analyzed as described in Fig. 2-6A (Cell: **$P < 0.01$; Time: ***$P < 0.001$). $N = 6$ experiments. (**C**) Incubation of WT cells with the ROS scavenger NAC reduces bacterial killing to the extent exhibited by gp91phox KO cells. WT and gp91phox KO BMDMs were incubated with *E. coli*-BW25113 for 60 min in the presence or absence of NAC. Bacterial survival was measured as described in Fig. 2-6A. One-way ANOVA with Bonferroni post-hoc comparison was used for analysis. $N = 2$ experiments.

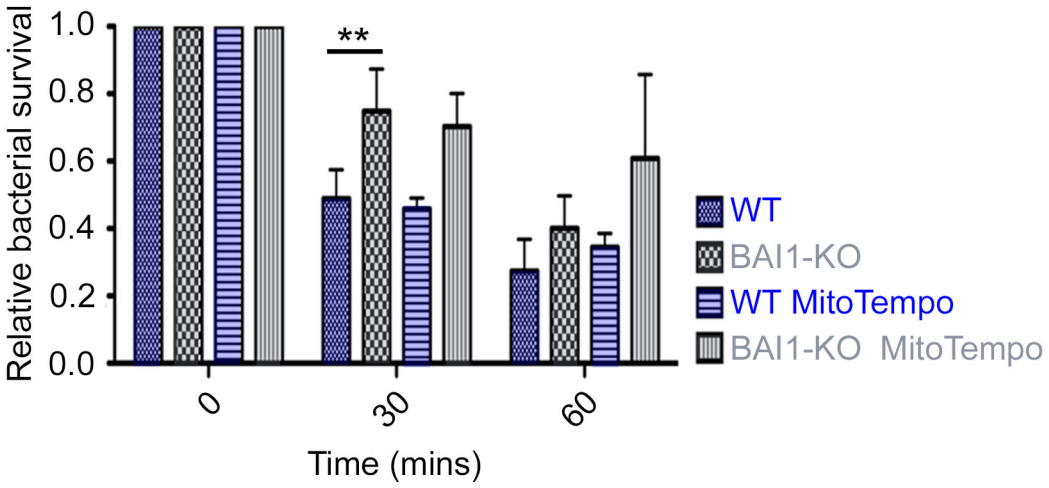
Relative bacterial survival
1.0
0.8
0.6
0.4
0.2
0.0
**
0
30
60
Time (mins)
WT
BAI1-KO
WT MitoTempo
BAI1-KO MitoTempo

Figure. 2-13. Mitochondrial ROS produced in response to Gram-negative bacteria is not dependent on BAI1-mediated recognition and signaling

Macrophages from the indicated mice were pre-treated with either vehicle or the mitochondrial ROS inhibitor MitoTempo (350 μM), then were incubated with *E. coli*-BW25113 for the indicated times. Bactericidal activity was measured as described in Fig. 2-6A. Data are mean survival ± SEM of four experiments and were analyzed by two-way ANOVA with Bonferroni post-hoc comparisons, WT vs. BAI1-KO: (Time: $*P < 0.05$).

BAI1 promotes bacterial clearance in vivo

Given the defect in bacterial phagocytosis and killing in BAI1-deficient primary cells, we hypothesized that BAI1 knockout animals would exhibit impaired bacterial clearance and increased susceptibility to bacterial challenge (298, 300). To test this possibility, we used a well-characterized model of bacterial peritonitis in which we infected wild type, BAI1 knockout, and gp91phox knockout mice intraperitoneally with non-pathogenic *E. coli* and then analyzed several parameters of susceptibility (**Fig. 2-14A**). First, a disease score was determined for each animal based on macroscopic examination of their behavior, including posture, eye discharge, grooming, and movement at 4 hours after infection (**Fig. 2-15**). BAI1-deficient animals exhibited enhanced disease activity compared to that of wild type mice (**Fig. 2-14B**), which was comparable to that of mice lacking gp91phox. Second, BAI1 knockout animals succumbed to peritoneal infection more rapidly than did control wild type mice (**Fig. 2-14C**). Measurement of colony-forming units (CFUs) revealed statistically significantly greater bacterial burden in the peritoneum, liver, and spleen at 4 hours after infection in BAI1 knockout mice compared to wild type mice (**Fig. 2-14, D to F**). At 24 hours after infection, wild type mice had almost completely cleared bacteria from the liver and spleen. In contrast, both the BAI1 knockout and gp91phox knockout animals showed persistent, viable CFUs in these tissues (**Fig. 2-14, G to I**). Furthermore, bacterial counts in the BAI1 knockout animals were similar to those in the gp91phox knockout animals, suggesting that defective ROS production contributes to increased susceptibility to bacterial infection.

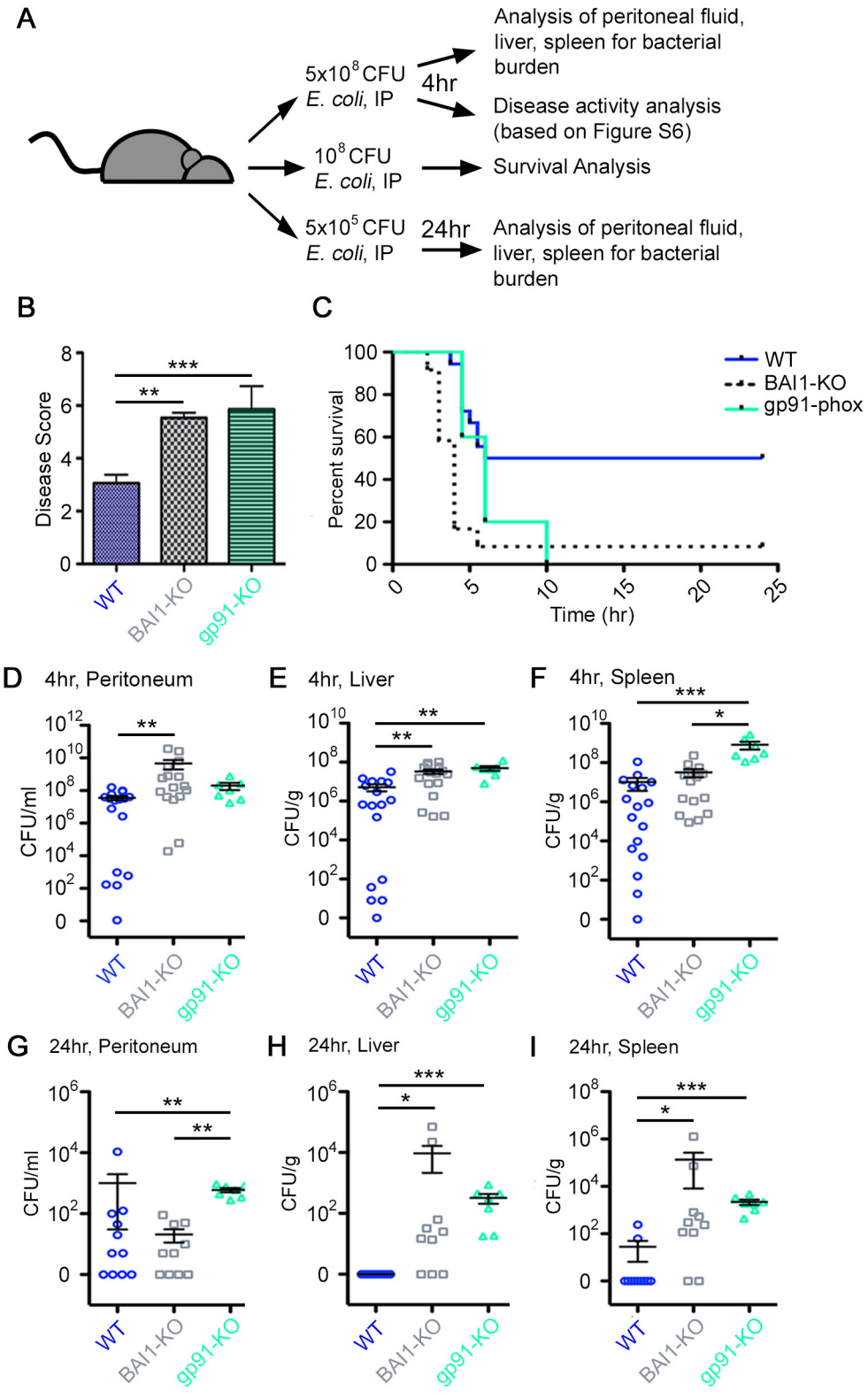
A
5x10^8 CFU
E. coli, IP
4hr
Analysis of peritoneal fluid, liver, spleen for bacterial burden
Disease activity analysis (based on Figure S6)
10^8 CFU
E. coli, IP
Survival Analysis
5x10^5 CFU
E. coli, IP
24hr
Analysis of peritoneal fluid, liver, spleen for bacterial burden
B
Disease Score
WT
BAI1-KO
gp91-KO
C
Percent survival
Time (hr)
WT
BAI1-KO
gp91-phox
D 4hr, Peritoneum
CFU/ml
E 4hr, Liver
CFU/g
F 4hr, Spleen
CFU/g
G 24hr, Peritoneum
CFU/ml
H 24hr, Liver
CFU/g
I 24hr, Spleen
CFU/g

Figure. 2-14. BAI1 mediates bacterial clearance in vivo

(**A**) WT, BAI1-KO, and gp91phox-KO mice were infected intraperitoneally with *E. coli*-BW25113 and analyzed based on several parameters of susceptibility to bacterial challenge. Bacterial dose, length of infection, and type of analysis are shown in schematic form. (**B**) WT, BAI1-KO, and gp91phox-KO mice were infected intraperitoneally with 5 x 10^8 CFU *E. coli* and disease severity was analyzed 4 hours later. Graph displays mean score ± SEM of three experiments. ***$P < 0.001$, **$P < 0.01$ by one-way ANOVA Kruskal-Wallis test with Dunn's post-hoc comparisons. (**C**) Survival was measured in WT and BAI1-KO mice after intraperitoneal infection with 10^8 CFU *E. coli.* Survival was blindly scored based on the criteria in (B). Mantel Cox log rank was used to compare survival. **$P < 0.01$. $N = 2$ experiments. (**D** to **F**) Bacterial burden 4 hours post-infection: CFUs were measured in the peritoneum (D) liver (E), and spleen (F) of the indicated mice 4 hours after challenge with 5 x 10^8 CFU *E. coli*. Each data point is representative of a single animal. Data are mean CFUs per tissue ± SEM of four experiments. Analysis was performed by one-way ANOVA Kruskal-Wallis test with Dunn's post-hoc comparison. *** $p<0.001$, ** $p<0.01$, * $p<0.05$. (**G** to **I**) Bacterial burden at 24 hours post-infection: CFUs were measured in the peritoneum (G), liver (H), and spleen (I) 24 hours after challenge with $5x10^5$ CFU *E. coli*. Data are mean CFUs per tissue ± SEM of three experiments. Analysis was performed by one-way ANOVA Kruskal-Wallis test with Dunn's post-hoc comparison. *** $p<0.001$, ** $p<0.01$, * $p<0.05$.

Disease activity analysis

Score	Posture	Activity	Haircoat	Eyes
0	Normal	Normal	Normal	Normal
1	Hunched	Slight decrease, movement after slight stimluation	Rough	Squinted or closed
2	Hunched, Head on floor	Inactive, movement after moderate stimulation	Ungroomed, hairloss	Squinted or closed with discharge
3	Prone on floor	Immobile	n/a	n/a

Animals with a cummulative score above (7.5) or a (3) in two categories were euthanized

Figure. 2-15. Measurement of disease activity analysis

Description of disease activity analysis based on the macroscopic observation of behavior.

Discussion

Innate immune cells express an array of PRRs that function in bacterial detection and phagocytosis (15, 17, 117, 301). We previously showed that BAI1 acts as a PRR for Gram-negative bacteria and that it specifically binds to the relatively invariant core oligosaccharides of bacterial LPS (226). Furthermore, this recognition mechanism is distinct from that used by TLR4, which binds to the acyl chains of LPS (302). Binding of bacteria to BAI1 stimulates their phagocytic uptake through the direct activation of the ELMO-Dock complex, which acts as a GEF for Rac (226). Here, we extend these observations to show that BAI1-mediated Rac activation not only stimulates bacterial internalization by macrophages, but is also necessary for robust activation of the phagocyte NADPH-oxidase complex. In vitro, primary macrophages lacking BAI1 exhibited substantially reduced bactericidal activity because of attenuated induction of ROS in response to both non-pathogenic and pathogenic Gram-negative bacteria.

The importance of the NADPH oxidase complex in the innate immune response to bacterial infection is highlighted in patients with chronic granulomatous disease (CGD), who have deficiencies in specific components of the NADPH oxidase machinery (179, 180). Patients with CGD are particularly susceptible to select bacterial pathogens, including *B. cenocepacia* (303, 304). Consistent with the presentation of CGD in humans, mice deficient in gp91phox, the catalytic subunit of phagocyte NADPH oxidase, are highly susceptible to bacterial infections (298, 300, 305, 306). Here, we showed that BAI1-deficient macrophages were similarly impaired in their ability to generate ROS in response to *B. cenocepacia* and several other Gram-negative pathogens, including *P.*

aeruginosa, which resulted in inefficient killing. Together, these data suggest that BAI1 broadly contributes to defense against Gram-negative bacteria. Although we cannot rule out other defects in the early inflammatory response to *E. coli*, such as defects in inflammatory signaling and cytokine production, we showed that the loss of BAI1 had an effect on susceptibility to bacterial challenge in vivo that was similar to that caused by loss of gp91phox, which suggests that BAI1-dependent ROS activity is a critical factor in early innate immunity and bacterial clearance.

The cellular mechanisms that couple non-opsonic, phagocytic receptors to cellular bactericidal machinery are not well understood (170). It is well-established that Rac1 and Rac2 are critical components of the NADPH oxidase machinery in macrophages and neutrophils, respectively (136, 294, 295, 307). The recruitment and activation of Rac proteins occurs through GEFs that catalyze the exchange of GDP for GTP (308). In neutrophils, the Rac-GEF P-Rex1 is implicated in the activation of Rac2 and NADPH oxidase by the bacterial formyl peptide fMetLeuPhe (309), whereas in both macrophages and neutrophils, the Vav family of Rho-GEFs is linked to ROS and inflammatory cytokine responses downstream of TLRs (158) and FcγRs (310). One study showed that deletion of the three Vav family proteins (Vav1, Vav2, and Vav3) attenuated macrophage ROS production in response to high concentrations of LPS, and that the activation of Vav was dependent on the TLR adaptor protein MyD88 (158). In that study, Vav family members mediated the activation of Rac2; however, Rac1 was not examined. In contrast, here we observed almost complete abrogation of Rac1 activity in BAI1-deficient cells and a corresponding reduction in ROS production, suggesting that BAI1-mediated activation of these responses occurs independently of the Vav signaling pathway. Note

that BAI1 does not appear to be required for phagocytosis or ROS production in response to Gram-positive bacteria, because no differences were observed between wild type and BAI1-deficient macrophages infected with *S. aureus*.

BAI1 signals through several pathways that lead to Rac1 activation. These include direct binding and activation of the bipartite ELMO-Dock Rac GEF complex in response to both apoptotic cells and Gram-negative bacteria (225, 226), as well as the recruitment and activation of the Par3-Tiam1 complex during synaptogenesis (248). Rac activation during synaptogenesis requires its interaction with the Par3-Tiam1 complex, but not ELMO-Dock180 (69). Here, we showed that macrophages expressing a BAI1 mutant that cannot interact with ELMO-Dock were as attenuated in bacterial killing, as were cells that lacked BAI1. Although we cannot rule out an interaction between BAI1 and Tiam1 in this context, this observation suggests that the ELMO-Dock complex is the primary mediator of Rac activation in response to Gram-negative bacteria.

In addition to NADPH oxidase, mitochondrial ROS has been implicated in oxidative killing in a pathway dependent on both TLR4 and MyD88 (156). Here, we found that MitoTempo, which selectively scavenges mitochondrial superoxide (299), had no effect on BAI1-dependent bactericidal activity, indicating that BAI1-mediated bacterial killing occurs independently of mitochondrial ROS. Moreover, in our hands, the ROS response to *E. coli* was completely absent in cells lacking the NADPH oxidase subunit gp91phox, which suggests that at the time points examined, ROS production occurred primarily through the phagocyte NADPH oxidase. The reduced microbicidal activity of BAI1-deficient macrophages in vitro was comparable to that of gp91phox-

deficient cells, and similar defects in bacterial clearance were observed in vivo in a mouse model of peritoneal infection.

Together, these results suggest that BAI1 is an innate phagocytic receptor that couples bacterial detection to the induction of oxidative killing by stimulating Rac activation in phagocytes. There are many innate immune receptors that initiate ROS production, but they do so in response to distinct stimuli. The specificity of BAI1 for non-opsonized, Gram-negative bacteria represents a previously uncharacterized mechanism for the regulation of ROS production in macrophages. This study reveals a potentially broader role for BAI1 in modulating cellular immune responses, ROS production, and inflammation not only during infection by bacterial pathogens, but also under homeostatic conditions through the recognition of resident microbes at mucosal sites.

Materials and Methods

Ethics statement

All experiments were performed in accordance with the recommendations in the Guide for the Care and Use of Laboratory Animals of the National institutes of Health. Protocols were approved by the Institutional Animal Care and Use Committee at the University of Virginia (Protocol number 3488).

Mice

Age- and sex-matched C57BL/6 mice between 6 and 10 weeks of age were used for the harvesting of primary macrophages and for peritoneal challenge experiments. BAI1 knockout mice have been described previously (227). Mice expressing transgenic wild type BAI1 or BAI1-AAA coding sequences were generated by knocking the coding

sequence for human BAI1 or its mutant into the non-essential *Rosa26* locus of C57BL/6 embryonic stem cells, and generating mice with these targeted embryonic stem cells (Lee et al, *in press*, (261)). Gp91phox knockout mice were a kind gift from Dr. Borna Mehrad, University of Virginia, Charlottesville, VA. Mice were housed in pathogen-free conditions.

Isolation and culture of cells

Stable BAI1-depleted J774 macrophage cell lines were generated by transduction with lentiviruses encoding short hairpin RNA (shRNA) against murine BAI1 (hairpin sequence V3LHS_322807, catalog number RHS4531-NM_174991, Open Biosystems) and selection with puromycin. J774 cells were cultured in Dulbecco's modified Eagle medium (DMEM, 4.5 g/L glucose, Gibco) supplemented with 10% fetal bovine serum (FBS) and 1% penicillin-streptomycin (pen-strep). Knockdown was confirmed by quantitative real-time polymerase chain reaction (qRT-PCR) analysis. LR73 CHO cell lines have been described previously (225) and were cultured in α minimal essential medium (αMem, Gibco) containing 10% FBS and 1% pen-strep. PEMs were isolated from mouse peritoneal lavage with sterile phosphate-buffered saline (PBS). To generate BMDMs, cells were seeded onto non-tissue culture treated plastic plates and cultured in RPMI supplemented with 10% FBS, 10% L929-conditional medium (as a source of colony-stimulating factor-1 (CSF1)), and 1% pen-strep. BMDMs were cultured for 6 days ex vivo before use, and the culture medium was changed every 2 days. Macrophage differentiation was confirmed by flow cytometric analysis of the cell surface abundances of F4/80 (eBioscience, clone BM8) and CD11b (eBioscience, clone M1/70).

Bacterial strains and culture

All bacteria, including *Escherichia coli* DH5α (Invitrogen, 18265-017) or BW25113 (*E. coli* Genetic Stock Center Keio collection parent strain (311)), were cultured overnight in Luria-Bertani (LB) broth under aerobic conditions before use. Immunofluorescence microscopy was performed using either *E. coli* DH5α or non-invasive *Salmonella* Typhimurium expressing dsRed (312). Δspa *Staphylococcus aureus* Newman strain (313) was a gift from Dr. Alison Criss, University of Virginia, Charlottesville, VA. *Pseudomonas aeruginosa* PAO3 was a gift from Dr. Borna Mehrad, University of Virginia, Charlottesville VA. *Burkholderia cenocepacia* strains BC7 and 56-2 were gifts from Dr. Costi Sifri, University of Virginia, Charlottesville, VA.

Immunofluorescence-based internalization assay

E. coli DH5α-dsRed were surface-labeled with EZ-Link Sulfo-NHS-LC-Biotin (Life Technologies, 1 mg/ml) for 30 min at 4°C. BMDMs were plated on glass coverslips (Fisher) overnight before being infected for 30 min with biotinylated bacteria at an MOI of 25 in RPMI with 10% FBS. Cells were washed and then fixed with 4% paraformaldyhyde (PFA) without permeabilization and then were blocked in PBS containing 3% bovine serum albumin (BSA). Extracellular bacteria were labeled with Streptavidin-Alexa Fluor 488 conjugate (Life Technologies) for 30 min, after which cells were permeabilized with 0.1% Triton-X-100 in PBS with 3% BSA. Cells were counterstained with DAPI to label nuclei. Images were acquired with a Nikon Eclipse E800 microscope equipped with a QImaging Retiga camera and Nikon NIS Elements software. Test images determined optimal exposure gains, and this gain was subsequently used for all conditions within an experimental replicate. In this assay, intracellular

bacteria appear red, whereas extracellular bacteria are double-positive for dsRed and Alexa Fluor 488, and appear yellow. At least 125 cells per replicate were imaged.

Immunofluoresence microscopy

1×10^5 transgenic BMDMs expressing HA-BAI1 were plated on fibronectin-coated coverslips (Sigma). The following day, the cells were incubated with *E. coli* DH5α-dsRed at an MOI of 10 for 30 min at 37°C. Cells were then fixed with 4% PFA and labeled with Alexa Fluor 647-conjugated WGA (Life Technologies, 5 μg/ml) in Hanks' balanced salt solution (HBSS) for an additional 10 min to label the plasma membrane. After washing, the cells were permeabilized for 30 min in PBS containing 3% BSA, 1% normal goat serum (NGS), FcR blocking antibody (eBioscience, clone 93), and 0.1% Triton X-100. Cells were labeled with mouse anti-HA antibody (Covance, clone 16B12) followed by Alexa Fluor 488-conjugated anti-mouse secondary antibody. ROIs for *E. coli* DH5a-treated cells were determined by dsRed signal. WGA signal was used to define ROIs in *S. aureus* conditions, because the bacteria displayed substantially greater staining than did eukaryotic cell membranes. Images were captured with a Nikon C1 Plus confocal microscope with Z-stacks at 0.5-μm. Analysis and processing was performed with NIS-Elements software (Nikon).

Live-cell imaging

Cells were plated on fibronectin-coated Matek dishes (P35G-1.5-14c) 18 hours before imaging. Imaging was performed in phenol red-free RPMI containing 10 mM hepes (pH 7.4) and 10% heat-inactivated FBS. After blocking endogenous FcR as described earlier, surface-exposed HA-BAI1 was labeled for 30 min with Alexa Fluor 488-conjugated mouse anti-HA antibody (Life Technologies, 4 μg/ml). Cells were then infected with

non-invasive ΔinvG *Salmonella* Typhimurium SL1344 expressing dsRed and imaged with a 100X objective fitted to a Nikon TE 2000 microscope equipped with a Yokogawa CSU 10 spinning disc and a 512X512 Hamamatsu 9100c-13 EM-BT camera. Movies were captured at a frame rate of 300 ms.

Short-course bacterial association and killing assay

1×10^5 BMDMs were seeded onto 24-well plates 18 hours before infection with bacteria at an MOI of 25. To synchronize infections, bacteria were spun onto cells at 4°C as described earlier, and then were incubated for 10 min at 37°C to enable bacterial attachment and internalization. To measure bacterial killing, cells were washed extensively with RPMI and then were placed at 37°C for the times described in the figure legends. At each time point, cells were washed and lysed and viable bacteria were enumerated as described earlier.

Gentamicin protection and intracellular bactericidal assay

The longer-course gentamicin protection assay was performed as described previously (226). Briefly, 5 x 10^4 CHO cells/well or 1 x 10^5 BMDMs/well were seeded into 24-well plates 18 hours before infection. Cells were incubated with bacteria at an MOI of 50 for 30 min at 37°C in αMEM (CHO) or RPMI (BMDMs) containing 10% heat-inactivated FBS, after spinning bacteria onto the cells at 500 x g for 5 min at 4°C to synchronize uptake. After 30 min of internalization, cells were treated with gentamicin (500 mg/ml, Gibco) for 30 min to kill extracellular bacteria, but leave intracellular bacteria viable. To measure bacterial killing, cells were then washed and lysed immediately or incubated with gentamicin (10 mg/ml) for the remaining times indicated in the figure legends. Cells

were lysed in HBSS containing 0.5% saponin with calcium and magnesium, and viable intracellular CFUs were determined by plating cell lysates on LB agar.

Rac activation assay

The precipitation of active, GTP-bound Rac was performed as described previously (226). BMDMs were serum-starved for 2 hours in RPMI and then infected with *E. coli* K-12 BW25113 at an MOI of 100 for 10 or 30 min at 37°C. Cells were lysed in 50 mM Tris-HCl (pH 7.5), 10 mM $MgCl_2$, 100 mM NaCl, 10% glycerol, 0.5% NaDOC, and 1% Triton X-100. GTP-bound Rac was precipitated with a glutathione-*S*-transferase (GST) fusion containing the p-21-binding domain of PAK (PBD) immobilized on glutathione sepharose beads for 30 min. Precipitates were resolved by SDS-polyacrylamide gel electrophoresis (SDS-PAGE) and then analyzed by Western blotting with a Rac1-specific antibody (Millipore). Rac-GTP was quantified as a percentage of the total amount of Rac in cell lysates.

Detection of ROS

For LDCLs, 3.5 x 10^5 macrophages were plated in 96-well plates in 200 μl of phenol red-free RPMI (Gibco) containing 10% FBS, and then were primed overnight with IFN-γ (50 ng/ml, Peprotech). Cells were incubated with 20 μM luminol (Sigma) and treated with bacteria at 37°C in phenol red-free RPMI (Gibco). Luminescence was measured with a VICTOR3 Wallac luminometer (Perkin-Elmer). For in situ fluorescence assays, 1 x 10^5 BMDMs were plated on glass coverslips (Fisher) overnight before infection for 30 min with *E. coli* DH5α expressing dsRed at an MOI of 25 in phenol red-free RPMI containing 1% heat-inactivated FBS. Cells were then washed and incubated for 30 min with 5 μM CellRox Green (Molecular Probes C10444). The cells were then fixed with

4% PFA, followed by blocking and permeabilization in PBS containing 3% BSA and 0.1% Triton-X-100. Cells were counterstained with DAPI (Sigma) to mark nuclei, and mounted with Prolong Gold antifade (Life Technologies). Images were acquired and analyzed with a Nikon E-800 microscope as described earlier. Test images determined the optimal exposure gain, which was subsequently used for all conditions within an experimental replicate. DAPI was used to select nuclei as ROIs to measure the MFI of CellRox Green. At least 300 cells were imaged per replicate.

Peritoneal infection model

Age- and sex-matched mice between 6 and 8 weeks of age were infected by peritoneal injection with 5×10^5, 1×10^8, or 5×10^8 CFUs of *E. coli* K-12 BW25113 in 0.2 ml of sterile DPBS. Mice were monitored for disease state and severity. Disease state was determined for each animal based on macroscopic examination of behavior, including posture, eye discharge, grooming, and movement. Mice were euthanized at either 4 or 24 hours after infection. Bacterial loads in the peritoneum, liver, and spleen were determined by plating the lysates of homogenized tissues on LB agar.

Statistical analysis

Statistical analysis was performed with GraphPad Prism 5 software. Statistical significance was set at the 5% standard. Data that did not match the assumptions for parametric analysis (normality, equal variance, normalization), were analyzed with nonparametric analysis as indicated in the figure legends. All analysis was two-tailed. Graphs show means ± SEM. When appropriate, Two-way analysis of variance (ANOVA) with Bonferroni post-hoc comparisons was used for analysis. Information represented in the figure legend indicates the analysis regarding the two independent variables (e.g. time

and cell type) and whether there is an interaction between them. Statistical information represented on the graph refers to the post-hoc comparison. In all data sets, *$P < 0.05$, **$P < 0.01$, ***$P < 0.001$, ****$P < 0.0001$. The number of independent experimental replicates is indicated by N.

Chapter 3:

BAI1 selectively promotes intracellular TLR4 activity during early immune responses in macrophages

The following work represents unpublished work in progress.

Billings, E. A. performed all experiments and analysis shown in Chapter 3. D'Souza, R.S. advised on the design and methods for the microscopy. R.S. provided Ravichandran, K.S. and Lee, C.S. provided critical reagents required for this Chapter. Casanova, J. E. provided intellectual guidance.

Chapter 3 BAI1 selectively promotes intracellular TLR4 activity during early immune responses in macrophages

Abstract

The detection and initiation of the innate immune response occurs through the use of a limited set of germ-line encoded pattern recognition receptors, or PRRs. The coordinated actions of these proteins allows for a tailored immune response resulting in clearance and resolution of infection. During the recognition of Gram-negative bacteria, TLR4 functions as a key signaling receptor that leads to the induction of MyD88- and TRIF-dependent signaling to promote the expression of proinflammatory cytokine and chemokines or type-I IFN responses, respectively. BAI1 functions as a phagocytic PRR that drives the internalization of Gram-negative bacteria, thereby providing a distinct service to the cellular immune response relative to TLR4, which is not inherently phagocytic. The role of BAI1 in the context of early innate signaling and transcriptional responses to Gram-negative bacteria is largely unknown. Here, we show that BAI1 selectively promotes the intracellular signaling response of TLR4. BAI1-deficient macrophages have attenuated TLR4-dependent activation of TBK1 and IRF3 and diminished induction of TRIF-dependent genes. In contrast, the activation of NF-κB and MAPKs and the downstream transcription of MyD88-dependent inflammatory cytokines and chemokines is unaffected by the loss of BAI1. Moreover, these two PRRs spatially and physically interact, and the expression of BAI1 promotes TLR4 association with cell-associated Gram-negative bacteria. Functionally, this implicates BAI1 as a critical

accessory protein enhancing intracellular, perhaps phagosome-specific, TLR4 activity during the early inflammatory response to Gram-negative bacteria.

Introduction

The innate immune system is the host's first line of defense against microbial insult. As such, the recognition of pathogenic and non-pathogenic microbes is a critical step for the host response. This occurs through a limited set of germ-line encoded receptors, termed PRRs, which recognize conserved microbial signatures now defined as MAMPs present on and within microbes (5, 17, 18). Immune cells like macrophages and monocytes interpret the signals from PRRs to induce inflammatory signaling leading to the local induction of cytokines, chemokines, and type I-IFNs. TLRs are type-I integral membrane proteins expressed on the cell surface and within endosomal networks that are particularly critical in this response (17). TLR4, in complex with MD2, recognizes the lipid A region of LPS in the outer membrane of the Gram-negative bacterial cell wall (270, 302). The importance of TLR4-MD2 in host defense and inflammatory responses to Gram-negative bacteria is exemplified by the greatly increased susceptibility to bacterial infection and enhanced protection against endotoxin (or LPS) in animals lacking functional TLR4. Moreover, humans with polymorphisms in the TLR4 pathway display increased sensitivity to infection with select Gram-negative bacterial pathogens and altered inflammatory states in the gut, where host-microbe interactions contribute to homeostasis (54).

It is now appreciated that the coordinated actions of several receptors drive the specificity and magnitude of the early cellular immune response. Therefore, direct or indirect PRR interaction is used to modulate both the recognition of bacterial products

and the downstream inflammatory responses initiated by innate immune cells. TLR4 recognition of LPS at the cell surface occurs through the sequential interaction with several accessory proteins including LBP and CD14, a soluble or GPI-anchored protein, which function together to isolate and deliver LPS to the TLR4-MD2 complex, thereby promoting recognition (97-101). TLR4 activation at the cell surface is initiated after dimerization and trafficking to lipid rafts (98, 314). There, signaling though adaptor proteins TIRAP and MyD88 lead to the recruitment of the IL-1 receptor associated kinase (IRAK) proteins and TRAF6, forming a signaling complex or scaffold (8, 315). Recruitment of TAK1 binding protein 1 (TAB1), TAB2, TAB3, and transforming growth factor β-activated kinase 1 (TAK1) leads to the activation of IKKs to activate NF-κB and MAPKs and the induction of pro-inflammatory cytokines. Upon receptor internalization, TLR4 signals through the adaptors TRAM and TRIF to recruit TRAF3, TRAF family member-associated NF-κB activator (TANK), and the non-canonical IKK-related kinases, TBK1 and IKKε, to directly phosphorylate IRF3 and induce type-I-IFNs and TRIF-dependent cytokines and chemokines (37, 79, 85, 86, 316, 317). Alternatively, TRIF couples to RIP1 and TRAF6 to mediate a secondary wave of NF-κB and MAPK activity (81, 83).

PRRs commonly engage in signaling crosstalk to modulate inflammatory responses. For example, DC-SIGN (SIGNR1) enhances transcriptional activity of NF-κB downstream of TLRs by promoting acetylation of the p65 subunit (106, 318). The activation of SR-A has been shown to synergize with TLR4-dependent LPS responses, but has also been shown to negatively regulate inflammatory signaling (107-109, 319).

The trafficking of TLR4 within the cell is also critical for defining functional outputs of TLR4 signaling. CD14 promotes endocytosis of TLR4 complexes, thereby regulating TRIF-dependent signaling. Other proteins including CD36, a class B scavenger receptor, have been shown to mediate the internalization of TLR4-TLR6 complexes during sterile inflammation (112). This complex interplay between innate receptors during the early immune response to Gram-negative bacteria provides a method for context-specific fine-tuning of the host response.

Phagocytic receptors modulate inflammatory responses, drive microbicidal activity, promote adaptive immunity, and aid in resolution of the inflammatory response (46, 67, 117, 320). TLRs are not inherently phagocytic, emphasizing the unique importance of these proteins in the innate immune response. While the response to soluble LPS is important for the inflammatory response to Gram-negative bacteria, phagocytic receptors play a critical role in the clearance of microbes.

BA1I is a subgroup VII adhesion-type G protein-coupled receptor first defined for its role in inhibiting angiogenesis in brain tumor models (221). BAI1 has also been recognized as a phagocytic receptor for apoptotic cells, mediating apoptotic cell clearance by several cell types including neurons, myoblasts, epithelial cells, and myeloid lineage cells (224, 225, 227, 260). Park et al determined that BAI1 recognizes exposed phosphatidyl serine to mediate the internalization of apoptotic cells. We and others have reported that, in addition to apoptotic cells, BAI1 also recognizes Gram-negative bacteria (224, 226). In this context, the five TSRs present in the extracellular region recognize the core oligosaccharide of bacterial LPS (226), thus BAI1 and TLR4 recognize distinct components of the LPS structure. The recognition and binding of apoptotic cells or

Gram-negative bacteria results in activation of ELMO and Dock180 (or perhaps Dock2 in macrophages), which together act as a bipartite GEF. Collectively, this drives the activation of Rho family GTPase Rac1 to promote actin cytoskeleton remodeling and internalization of the attached particle (225, 226).

The mechanism through which BAI1 may regulate innate inflammatory responses to Gram-negative bacteria is largely unknown. We previously showed that the inflammatory cytokine response to non-invasive *S.* Typhimurium and soluble LPS was attenuated in primary macrophages depleted of endogenous BAI1 (226). This indicated that BAI1 generally enhanced the inflammatory phenotype of macrophages in response to Gram-negative bacteria. As a phagocytic receptor, it is possible that BAI1 promotes the delivery or presentation of bacterial products to other PRRs, including TLR4. Alternatively, BAI1 is itself capable of initiating signal transduction, which may modulate inflammatory responses by signaling crosstalk. Recognition of apoptotic cells and bacteria leads to activation of the ELMO-Dock-Rac signaling module (225-227). Rac has been shown to directly modulate TLR signaling in other contexts (49, 321). As an adhesion GPCR, BAI1 also activates RhoA via a $G\alpha_{12/13}$-dependent mechanism and ERK via an interaction with MAGI-3 (203), indicating that BAI1 may intersect with inflammatory signaling through other pathways. Thus, many mechanisms of crosstalk and interaction between BAI1 and innate inflammatory responses may exist.

While the initiation of an immune response is critical to fight infection, overly robust or unchecked inflammation can be detrimental to the host. As such, the magnitude and kinetics of the early inflammatory response are tightly regulated by the coordinated actions of several receptors and accessory proteins. BAI1, similar to other defined

scavenger receptors, recognizes both apoptotic cells and bacterial products. Whether and how BAI1 coordinates a response specific to each stimulus is not known, but may provide context for the initiation of protective immune responses and deleterious immune disorders. Here, we determined that BAI1 modulates the TLR4-driven inflammatory response to Gram-negative bacteria. We found that BAI1 selectively promotes the activation of IRF3 and TRIF-dependent transcriptional responses, indicating that the interaction between BAI1 and TLR4 is specific to the intracellular signaling response of TLR4-MD2. TLR4 and BAI1 physically interact and this interaction promoted the association of TLR4 with cell-associated Gram-negative bacteria. Although the mechanism through which BAI1 impacts the intracellular TLR4 response was not determined, our data suggest that both the compartmentalization of TLR4-ligand within the cell and BAI1-mediated signaling contribute. Determining novel pathways by which these responses are regulated provides greater understanding to the complexity of microbe recognition, innate immunity, and inflammation, and may allow for targeted approaches to upregulate or downregulate innate responses.

Results

NF-κB and MAPK signaling in response to Gram-negative bacteria is independent of BAI1

We hypothesized that BAI1 could regulate the macrophage innate cellular response via several mechanisms. To better understand how BAI1 alters the innate immune response to Gram-negative bacteria we first examined inflammatory signaling in primary macrophages derived from wild type C57BL/6 mice and BAI1-deficient animals (227). TLR4 is activated in response to LPS and is required for robust pro-inflammatory

cytokine production (e.g. TNF-α), by triggering the activation of NF-κB and MAPKs. For this purpose, we stimulated wild type and BAI1-deficient BMDMs with three representative Gram-negative bacterial species (*E. coli* DH5α, *E. coli* BW25113, or non-invasive and non-pathogenic ΔSPI1ΔSPI2 *Salmonella enterica* serovar Typhimurium) over a time course from 0-90 min. Cell lysates were probed for markers of activation of NF-κB and MAPKs by immunoblotting. To assess activation of NF-κB we analyzed lysates for the degradation of IκBα, a negative regulator that retains the transcription factor in the cytoplasm in an inactive state. Surprisingly, BAI1-deficient macrophages showed no apparent defect in the activation of NF-κB compared to the wild type cells (**Fig. 3-1, A to F**). Similarly, MAPK signaling, including ERK, p38, and c-Jun N-terminal kinase (JNK) activation, was not affected by the loss of BAI1 at any time point examined (**Fig. 3-2, A to F**). Interestingly, the phosphorylation and activation of p38 and JNK appeared to be bi-phasic in response to *E. coli* BW25113, but not in response to *E. coli* DH5α. This perhaps suggests that the engagement of PRRs in response these two strains of bacteria differs slightly. These results indicate that MyD88-dependent signaling is not attenuated in macrophages lacking BAI1.

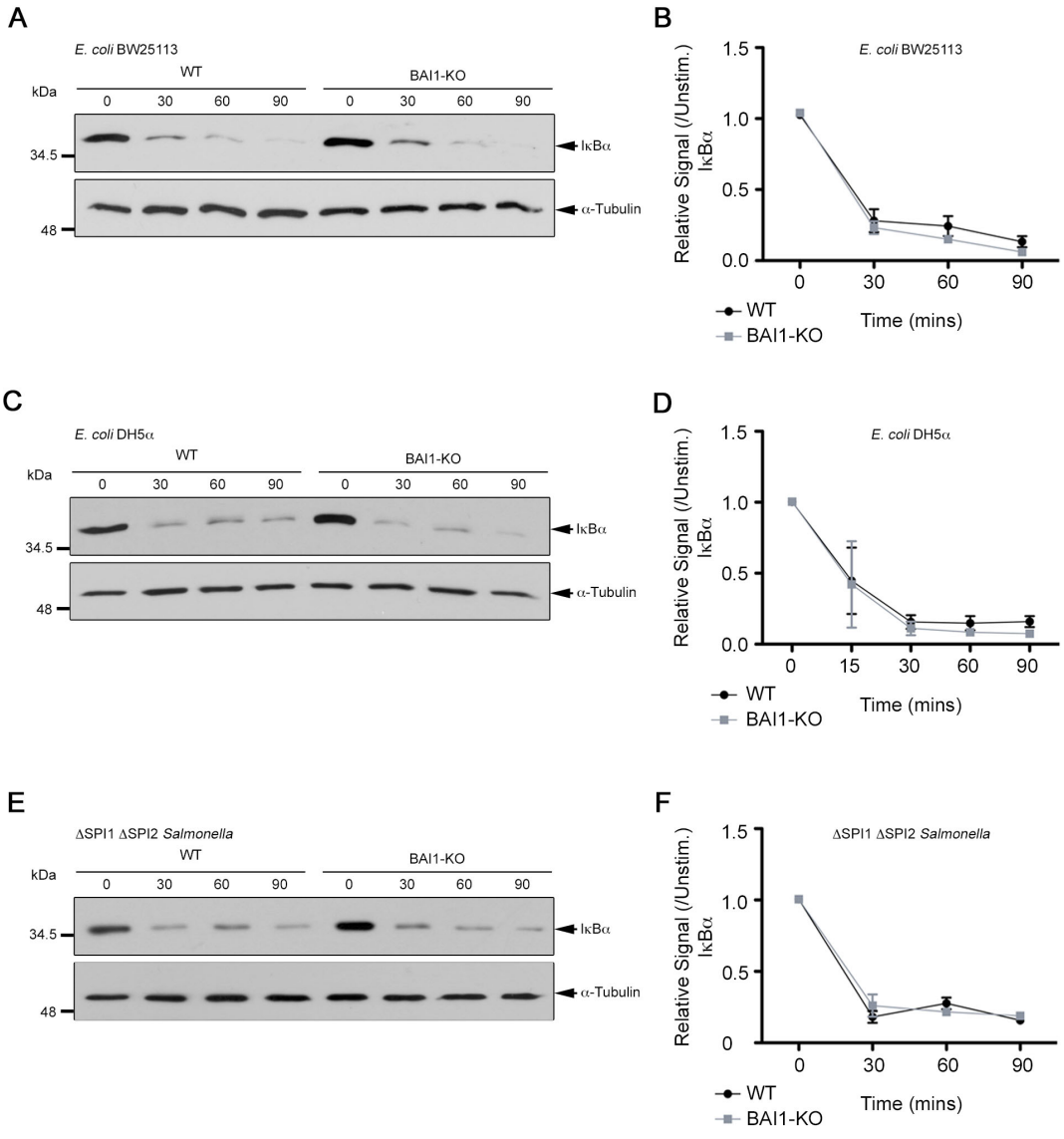
A
E. coli BW25113
WT
BAI1-KO
kDa
0
30
60
90
34.5
48
IκBα
α-Tubulin
B
E. coli BW25113
Relative Signal (/Unstim.) IκBα
1.5
1.0
0.5
0.0
Time (mins)
WT
BAI1-KO
C
E. coli DH5α
D
E. coli DH5α
15
E
ΔSPI1 ΔSPI2 Salmonella
F
ΔSPI1 ΔSPI2 Salmonella

Figure 3-1. Innate signaling leading to NF-κB activation is not attenuated in BAI1-deficient macrophages

(**A**) BMDMs from WT and BAI1-KO animals were treated with *E. coli* BW25113 (MOI 25) at 37° over the indicated time course. Cells were lysed and signaling was analyzed using immunoblotting. α-Tubulin was used an internal control. Fig. 3-1A shows a representative blot. **(B**) Quantitation of (A) shows mean fold change ± SEM in the integrated density of IκBα normalized to total signal (α-Tubulin) from five separate experiments. Data were analyzed by two-way ANOVA with Bonferroni post-hoc comparisons. A *P*-value is provided in the figure legend describing the source of variation in the data set (e.g. cell genotype, time, or an interaction between the cell genotype and time, which can also be considered as kinetics) (Time: ***$P < 0.001$). (**C**) Representative blot of cell lysates from WT and BAI1-KO BMDMs treated with *E. coli* DH5α as in (A). (**D**) Quantification is shown in (D) (Time: ****$P < 0.0001$, $N = 4$). (**E**) Signaling was analyzed as in (A) with cells treated with ΔSPI1ΔSPI2 *Salmonella* (MOI 25). (**F**) Data is shown and statistical analysis was performed as above (Time: ****$P < 0.0001$, $N = 2$).

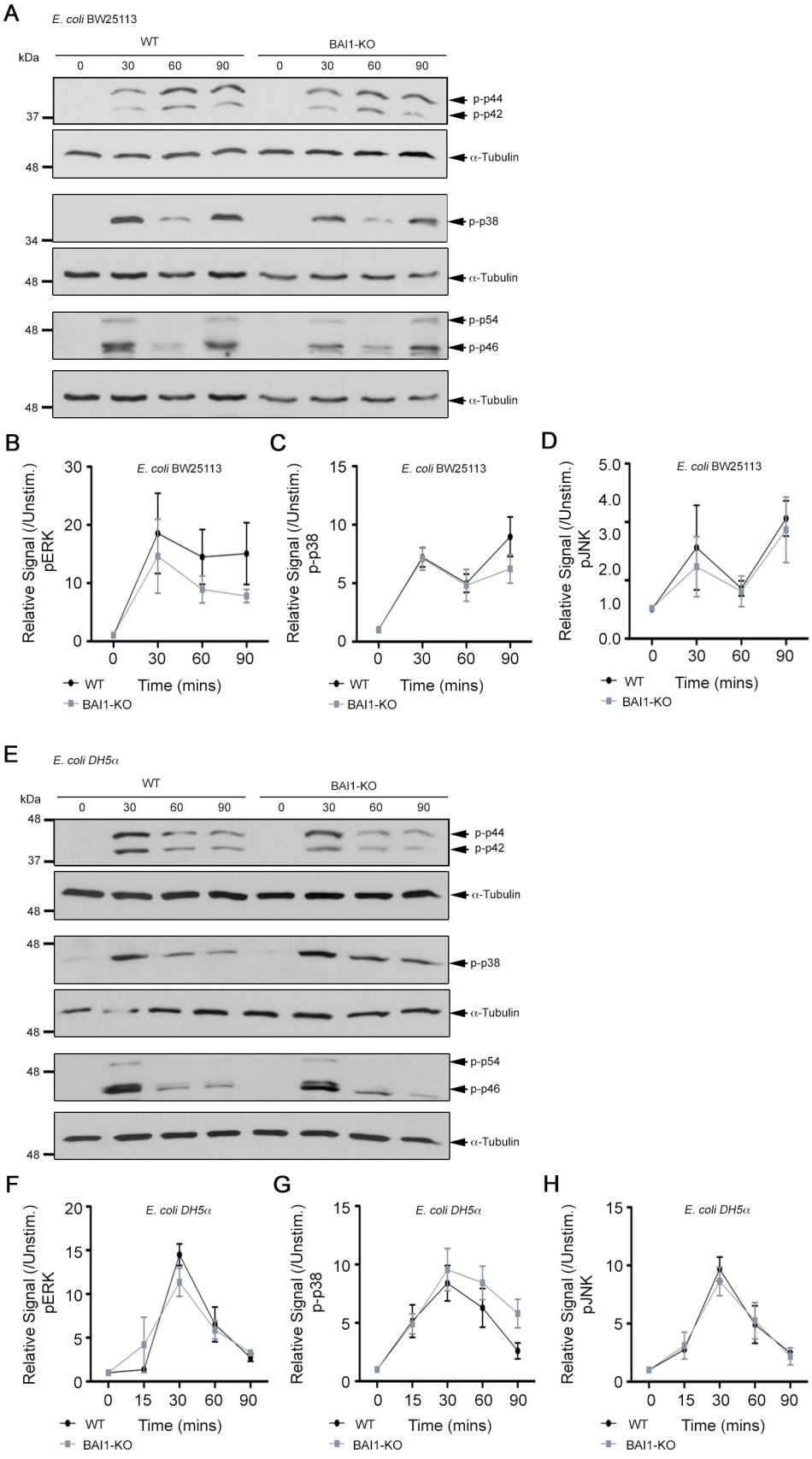
A
E. coli BW25113
WT
BAI1-KO
kDa
0 30 60 90 0 30 60 90
37
48
p-p44
p-p42
α-Tubulin
34
p-p38
p-p54
p-p46
B
C
D
Relative Signal (/Unstim.) pERK
Relative Signal (/Unstim.) p-p38
Relative Signal (/Unstim.) pJNK
Time (mins)
WT
BAI1-KO
E
E. coli DH5α
F
G
H
0 15 30 60 90

Figure 3-2. BAI1 is not required for MAPK signaling in macrophages after treatment with Gram-negative bacteria

(**A**) BMDMs from WT and BAI1-KO animals were treated with *E. coli* BW25113 over a time course. Cells were lysed and signaling was analyzed using immunoblotting with antibodies specific to the active form of the signaling molecule. α-Tubulin was used an internal control. Fig. 3-1A shows representative blots of phosphorylated- ERK (Thr202/Tyr204), p38 MAPK (Thr180/Tyr182), or JNK1/2 (Thr183/Tyr185), which indicates kinase activation. In (B) to (D), quantitation of the abundance of activated (**B**) ERK (Time: $^{**}P < 0.01$, $N = 5$), (**C**) p38 (Time: $^{****}P < 0.0001$, $N = 5$), and (**D**) JNK1/2 (Time: $^{*}P < 0.05$, $N = 3$) is displayed as the mean fold change ± SEM of the integrated density of each protein, normalized to the internal control. Data was analyzed using 2-way ANOVA with Bonferroni post-hoc comparison, as in Fig. 3-1. (**E**) WT and BAI1-KO BMDMs were treated with *E. coli* DH5α and analyzed using immunoblotting, with the respective representative western blots for each condition shown, while (F) to (H) include the quantitation of the activation of (**F**) phospho-ERK (Time: $^{****}P < 0.0001$, $N = 4$), (**G**) phospho-p38 (Time: $^{****}P < 0.0001$, $N = 6$), and (**H**) phospho-JNK1/2 (Time: $^{****}P < 0.0001$, $N = 4$), similar to (B) to (D).

BAI1 selectively regulates the activation of TBK1 and IRF3 signaling in macrophages

Inflammatory signaling in response to Gram-negative bacteria also induces a robust type-I-IFN response. After endocytosis TLR4 signals through the adaptors TRAM and TRIF to activate a separate signaling response leading to the phosphorylation and activation of IRF3 and the induction of TRIF-dependent transcriptional responses. In contrast to NF-κB and MAPK signaling, we observed a significant reduction in phosphorylated IRF3 signal in cells lacking BAI1, indicating attenuated activation of IRF3 in response to all Gram-negative bacteria assessed (**Fig. 3-3, A to F**). To further examine the TRIF-dependent signaling response we assessed the activation of TBK1, which is recruited to TLR4 signaling complexes to directly phosphorylate IRF3, in wild type and BAI1-deficient cells. TBK1 activity, as measured by phosphorylation of serine 172 in the activation loop of the protein, was also significantly decreased in response to *E. coli* BW25113 and ΔSPI1ΔSPI2 double mutant *Salmonella* (**Fig. 3-3, A and B, E and F**). This suggested that the TLR4-TRIF signaling response is attenuated upstream of TBK1 activation. However, attenuation of TBK phosphorylation was not observed in all contexts. There was no difference and considerable variability in the phosphorylation of TBK in response to *E. coli* DH5α (**Fig. 3-3, C to D**). This discrepancy was surprising, as it would indicate that the activation of IRF3 may differ between *E. coli* strains, similar to the discrepancy observed in the biphasic activation of MAPKs in **Fig. 3-2**.

In summary, the activation of NF-κB and MAPKs in response to Gram-negative bacteria was not affected by the loss of BAI1, indicating that early MyD88-dependent inflammatory signaling and late TRIF-dependent signaling through RIP1 and TRAF6 are not regulated by BAI1. However, IRF3 phosphorylation was significantly reduced in

BAI1-deficient cells compared to control BMDMs. This correlated with decreased activating phosphorylation of TBK1 in most cases, indicating a defect in TLR4-TRIF signaling when BAI1 is lost.

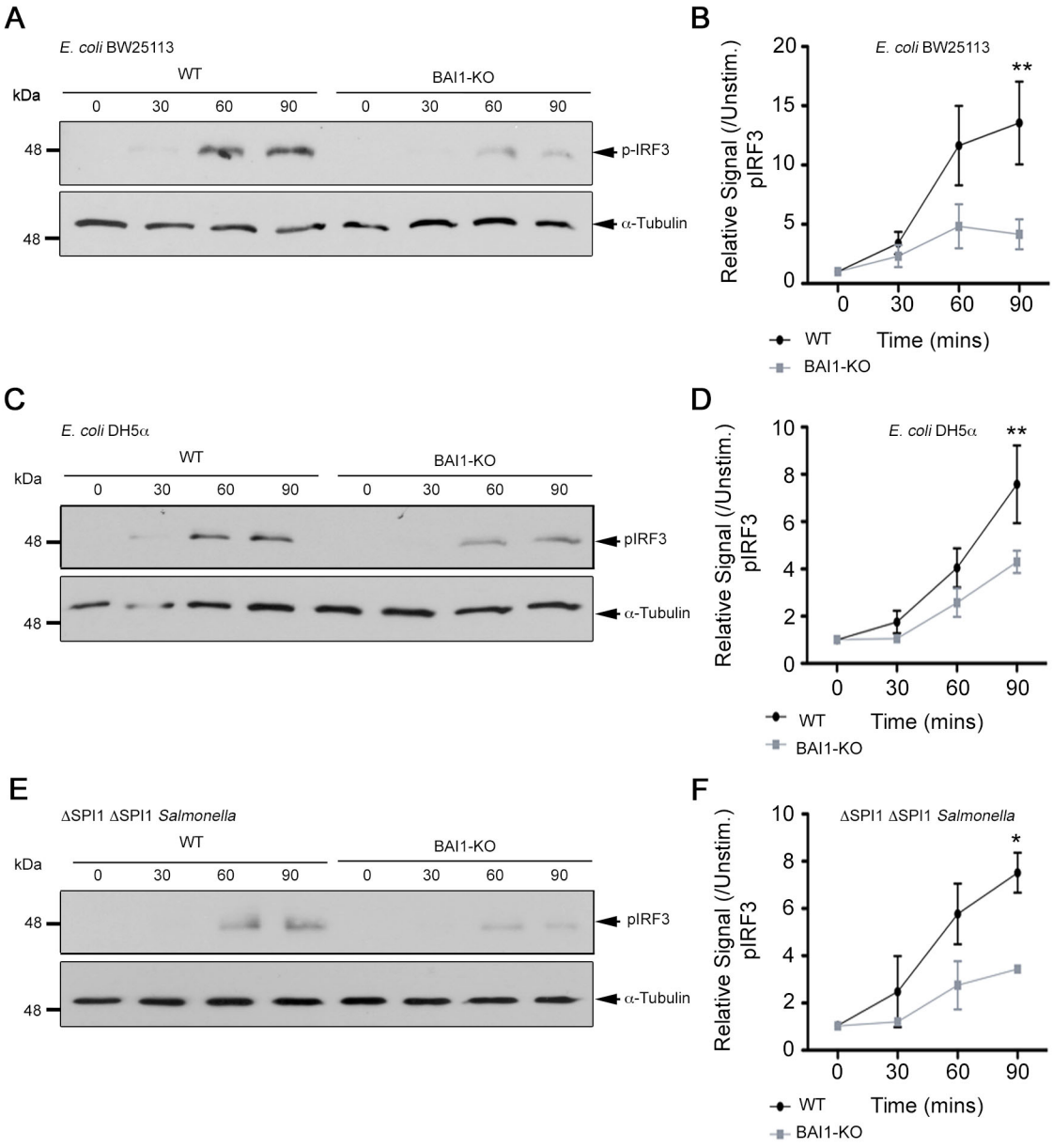
A
E. coli BW25113
WT
BAI1-KO
kDa
0
30
60
90
0
30
60
90
48
p-IRF3
48
α-Tubulin
B
E. coli BW25113
**
Relative Signal (/Unstim.) pIRF3
20
15
10
5
0
0
30
60
90
Time (mins)
WT
BAI1-KO
C
E. coli DH5α
WT
BAI1-KO
kDa
0
30
60
90
0
30
60
90
48
pIRF3
48
α-Tubulin
D
E. coli DH5α
**
Relative Signal (/Unstim.) pIRF3
10
8
6
4
2
0
0
30
60
90
Time (mins)
WT
BAI1-KO
E
ΔSPI1 ΔSPI1 Salmonella
WT
BAI1-KO
kDa
0
30
60
90
0
30
60
90
48
pIRF3
48
α-Tubulin
F
ΔSPI1 ΔSPI1 Salmonella
*
Relative Signal (/Unstim.) pIRF3
10
8
6
4
2
0
0
30
60
90
Time (mins)
WT
BAI1-KO

Figure 3-3. Phosphorylation of IRF3 upon treatment with Gram-negative bacteria is impaired in macrophages deficient in BAI1

BMDMs from WT and BAI1-KO mice were treated with three representative Gram-negative bacterial species, *E. coli* BW25113 (A and B), *E. coli* DH5α (C and D), and ΔSPI1ΔSPI2 *Salmonella* (E and F) over a time course. Immunoblotting was used to measure phospho-IRF3 (Ser396) levels in cell lysates. A representative blot of lysates from cells treated with *E. coli* BW25113 is shown in (**A**), while the mean fold abundance ± SEM of phospho-IRF3 relative to α-Tubulin is displayed in (**B**). Data was analyzed as in Figure 3-1 using 2-way ANOVA with Bonferroni post-test (Cell: $^{**}P < 0.01$, Time: $^{***}P < 0.001$, $N = 5$). In (**C**), the representative blot shows phospho-IRF3 abundance in cells treated with *E. coli* DH5α, while the quantification of separate experiments is shown as analyzed above (**D**) (Cell: $^{**}P < 0.01$, Time: $^{****}P < 0.0001$, $N = 7$). Phosphorylation of IRF3 in WT and BAI1-KO BMDMs, after treatment with ΔSPI1ΔSPI2 *Salmonella,* is represented in (**E**) and was analyzed as described previously (**F**) (Cell: $^{**}P < 0.01$, Time: $^{**}P < 0.01$, $N = 2$).

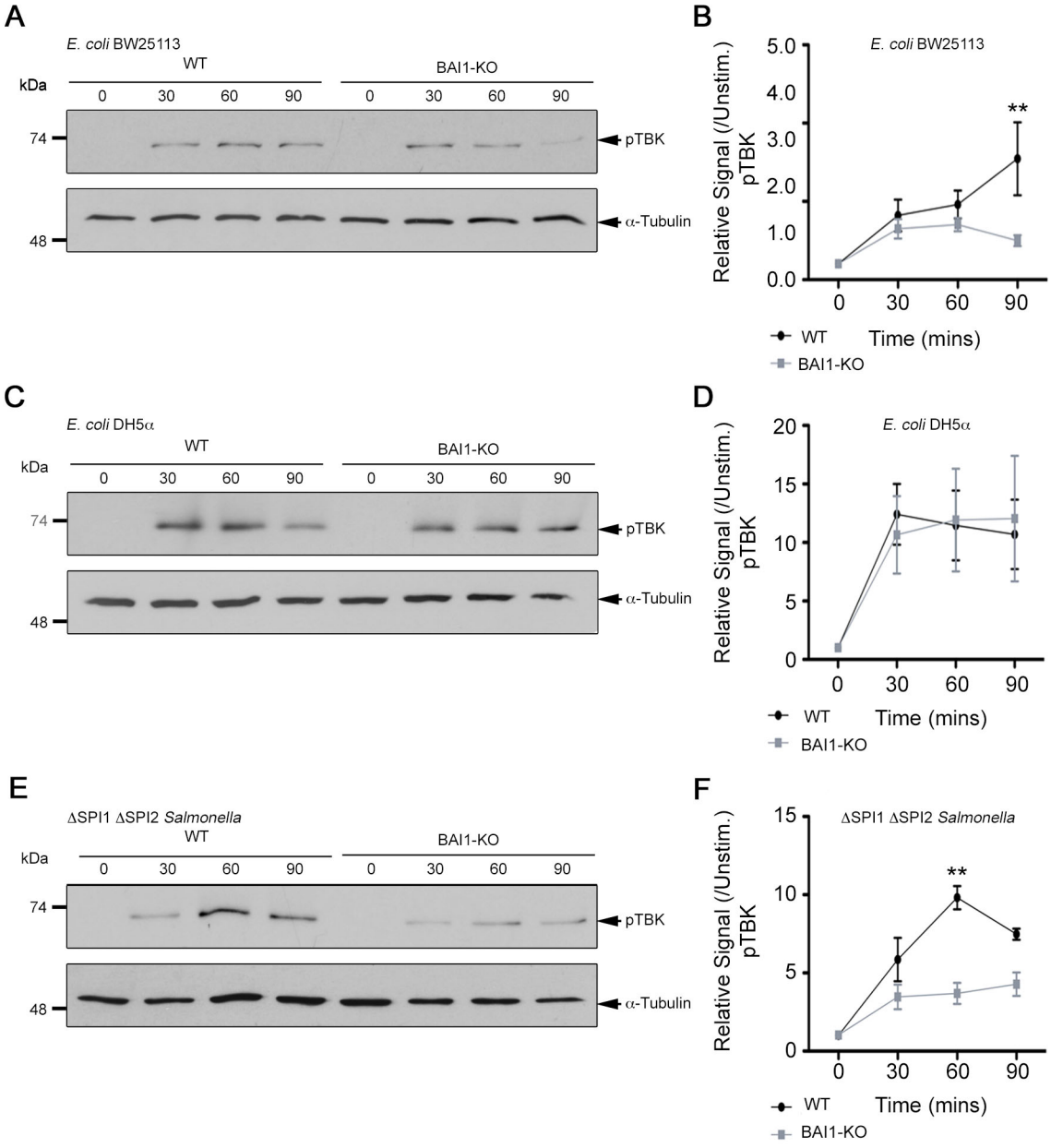
A
E. coli BW25113
WT
BAI1-KO
kDa
0 30 60 90 0 30 60 90
74
48
pTBK
α-Tubulin
B
E. coli BW25113
Relative Signal (/Unstim.) pTBK
5.0
4.0
3.0
2.0
1.0
0.0
**
0 30 60 90
Time (mins)
WT
BAI1-KO
C
E. coli DH5α
WT
BAI1-KO
kDa
0 30 60 90 0 30 60 90
74
48
pTBK
α-Tubulin
D
E. coli DH5α
Relative Signal (/Unstim.) pTBK
20
15
10
5
0
0 30 60 90
Time (mins)
WT
BAI1-KO
E
ΔSPI1 ΔSPI2 Salmonella
WT
BAI1-KO
kDa
0 30 60 90 0 30 60 90
74
48
pTBK
α-Tubulin
F
ΔSPI1 ΔSPI2 Salmonella
Relative Signal (/Unstim.) pTBK
15
10
5
0
**
0 30 60 90
Time (mins)
WT
BAI1-KO

Figure 3-4. Attenuated TBK1 phosphorylation in response to Gram-negative bacteria is observed in macrophages lacking BAI1 in a context-dependent manner

(**A**) WT and BAI1-KO BMDMs were stimulated with *E. coli* BW25113 (MOI 25). The abundance of phospho-TBK1 (Ser172) was measured in cell lysates using western blotting. A representative example is shown, while in (**B**), the quantitation shows the mean fold change in phospho-signal ± SEM normalized to an internal control. Analysis was performed as in Fig. 3-1 (Cell: $*P < 0.05$, Time: $**P < 0.01$, $N = 5$). (**C**) and (**D**) show similar data, except cells were instead treated with *E. coli* DH5α (Time: $**P < 0.01$). BMDMs were treated with ΔSPI1ΔSPI2 *Salmonella* and analyzed as in (A). (**E**) shows a representative blot, while (**F**) shows the statistical results from a Two-way ANOVA with Bonferroni post-hoc comparison (Cell: $***P < 0.001$, Time: $***P < 0.001$, Interaction: $*P < 0.05$, $N = 2$).

TRIF-associated transcriptional responses are attenuated in BAI1-deficient macrophages

Analysis of transcriptional responses in MyD88-deficient and TRIF-deficient macrophages have identified genes selectively regulated or co-regulated by each adaptor protein in response to both LPS and Gram-negative bacteria. MyD88 is required for robust activation of pro-inflammatory cytokines and chemokines, such as Tumor necrosis factor-α (TNF-α), and C-X-C motif ligand 1 (CXCL1). Alternatively, the production of IFN-β and C-C motif ligand 5 (CCL5) is mediated in a TRIF-dependent manner. To determine if the decreased phosphorylation of IRF3 correlates with attenuated transcriptional responses, we analyzed the induction of MyD88-dependent and TRIF-dependent genes in control and BAI1-knockout BMDMs. Cells were incubated with *E. coli* BW25113 and the transcriptional response was assessed with qRT-PCR. Consistent with the signaling data, we observed no significant differences in the induction of MyD88-dependent TNF-α, CXCL1, or IL-6 between wild type and BAI1-deficient cells (**Fig. 3-5, A to C**). However, wild type macrophages produced significantly higher amounts of CCL5 and IFN-β in response to Gram-negative bacteria compared to BAI1-knockout BMDMs (**Fig. 3-5, D and E**). Interestingly, we also observed a significant reduction in the amount of IL-10, an anti-inflammatory cytokine critical for controlling an overly robust inflammatory response to LPS (**Fig. 3-5F**). This is consistent with the observation that BAI1-deficient macrophages have attenuated TRIF-dependent responses, as IL-10 expression is first regulated by IRF3 and potentiated by autocrine and paracrine signaling via IL-10 receptor and type-I IFN receptors (79, 316, 322, 323). Interestingly, BAI1 expression increases 2.0-fold ± 0.31 (SEM) relative to untreated BMDMs after four hours of stimulation with *E. coli* (data not shown), suggesting that it is also induced in

response to bacterial challenge. Together, these findings indicate an important and selective role for BAI1 in promoting the activation of IRF3 and TRIF-dependent transcriptional responses.

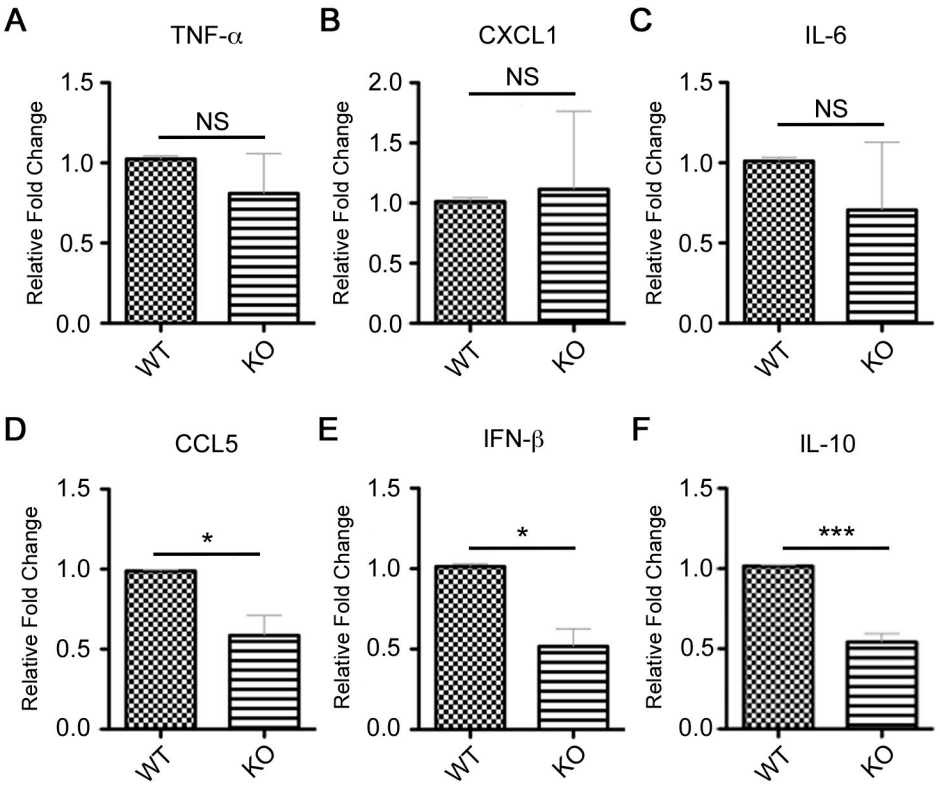
A
TNF-α
Relative Fold Change
1.5
1.0
0.5
0.0
NS
WT
KO
B
CXCL1
2.0
1.5
1.0
0.5
0.0
NS
C
IL-6
NS
D
CCL5
*
E
IFN-β
*
F
IL-10
***

Figure 3-5. The TLR4-TRIF driven transcriptional response is selectively attenuated in BAI1-deficient macrophages

BMDMs from WT and BAI1-KO animals were incubated with *E. coli* BW25113 (MOI 25) at 37° for 30 minutes. Cells were then washed and extracellular bacteria were killed with gentamicin. RNA was isolated and analyzed using qPCR after 4 hours. In (A) to (F), the graph shows the relative fold change of transcript normalized to the WT sample. Data were analyzed using Student's t-test with Welch's correction when appropriate. (**A**), (**B**), and (**C**) display the induction of TNF-α ($N = 5$), CXCL1 ($N = 3$), and IL-6 ($N = 4$), respectively. (**D**), (**E**), and (**F**), show the relative fold change of CCL5 ($^{*}P < 0.05$, $N = 5$), IFN-β ($^{*}P < 0.05$, $N = 5$), or IL-10 ($^{***}P < 0.001$, $N = 5$) transcript levels in response to *E. coli* as analyzed above.

BAI1 requires functional TLR4 for innate signaling and is specific to Gram-negative bacteria

Despite the critical role for TLR4 in the activation of inflammatory signaling and cytokine production to Gram-negative bacteria, macrophages utilize other PRRs to initiate immune responses. TLR3 and TLR9 recognize microbial nucleic acid signatures, while cytosolic receptors like the NLR and RLR family also contribute to innate immune responses to bacteria. To determine if the attenuated IRF3 and transcriptional response observed in BAI1-deficient macrophages is dependent on direct or indirect interaction with TLR4 or another PRR, we examined inflammatory signaling in response to purified *S.* Typhimurium LPS. Again, we observed no defect in the activation of NF-κB in cells lacking BAI1 relative to wild type macrophages (**Fig. 3-6, A and B**). In contrast, and consistent with the response to live bacteria, there was significantly reduced abundance of phospho-IRF3 after treatment with LPS in BAI1-deficient cells compared to control macrophages (**Fig. 3-6, C and D**). The kinetics of activation of all signaling pathways examined were similar to those observed in response to live *E. coli* and *Salmonella* suggesting that TLR4 dominates the early signaling and transcriptional response to Gram-negative bacteria.

To further examine whether the innate signaling phenotypes observed were due to an interaction with TLR4-dependent responses we analyzed signaling in TLR4-deficient cells. BMDMs from TLR4-knockout mice had little to no observable phospho-IRF3 signal after stimulating with *E. coli* BW25113 (**Fig. 3-6, G and H**). The phosphorylation of TBK1 was also reduced in TLR4-deficient cells compared to control BMDMs (**Fig. 3-6, I and J**). Interestingly, despite a nearly complete loss of IRF3 phosphorylation,

residual TBK1 activation was observable without TLR4 expression. This indicates a TLR4-independent mechanism of TBK1 activation in response to Gram-negative bacteria. As expected, the NF-κB signaling pathway was also markedly higher in wild type macrophages compared to TLR4-deficient cells (**Fig. 3-6, E and F**). Interestingly, the relative defect in the signaling responses leading to either NF-κB or IRF3 activation in TLR4-deficient cells indicated a particularly strong reliance upon TLR4 for the activation of IRF3 in response to Gram-negative bacteria. Although other PRRs are activated in response to Gram-negative bacteria, BAI1 likely interacts with TLR4 early in the innate inflammatory signaling and cytokine responses.

To further probe the specificity of BAI1 on TLR4-driven inflammatory signaling, we examined the activation of NF-κB, MAPKs, and IRF3 in wild type and BAI1-deficient macrophages incubated with the Gram-positive bacterial pathogen, *S. aureus*. This did not reveal any differences in the inflammatory signaling response between control and BAI1-knockout BMDMs (**Fig. 3-7, A to H**). Interestingly, we observed that TBK1 and IRF3 were similarly activated in response to *S. aureus* in both cell types suggesting that TLR2 heterocomplexes or other PRRs mediate this pathway (**Fig. 3-7, E to H**). Collectively, these results suggest that the attenuated IRF3 activation and TRIF-dependent responses observed in BAI1-knockout macrophages are due to altered or modulated TLR4-dependent cellular responses.

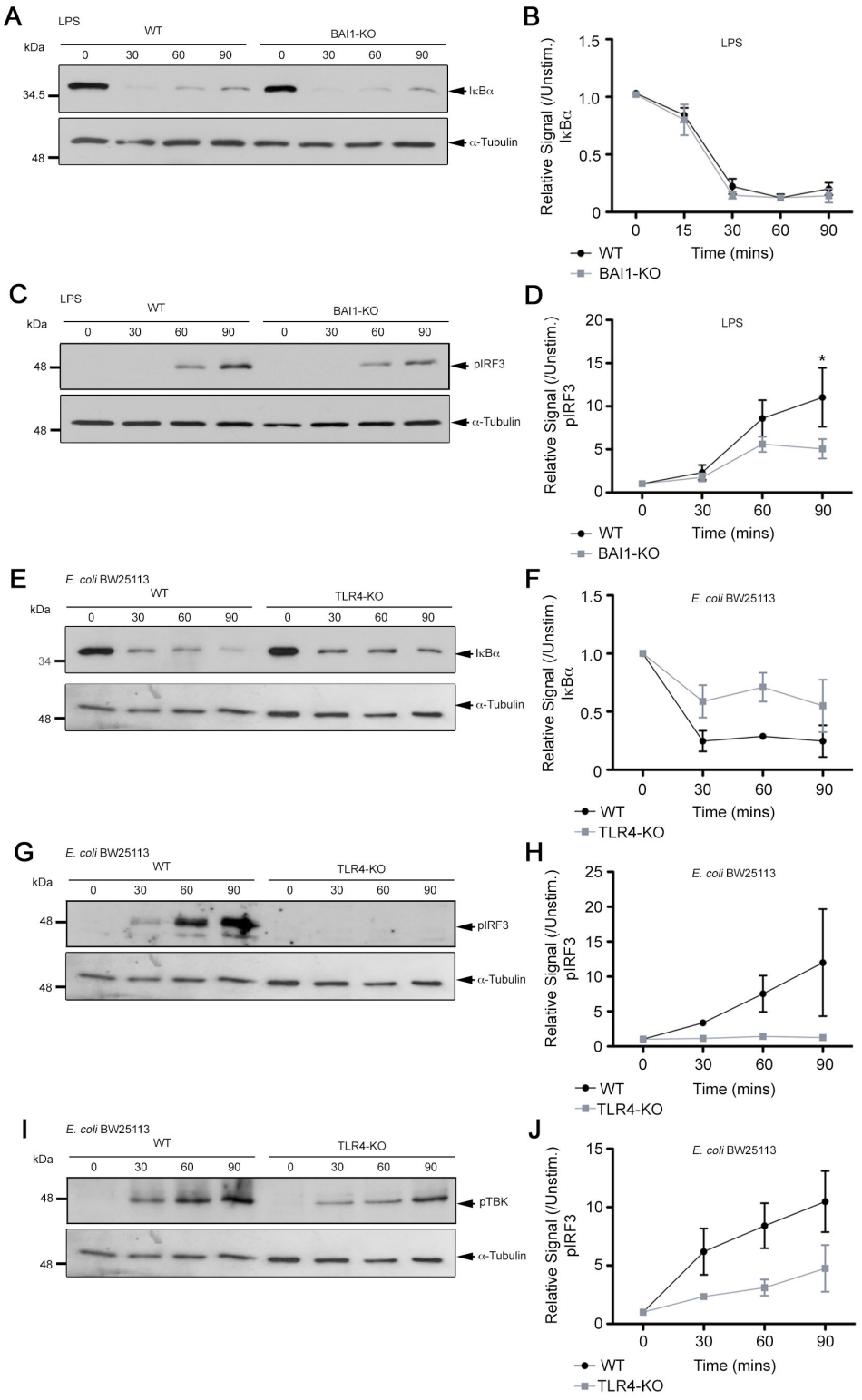
A
LPS
WT
BAI1-KO
kDa
0 30 60 90 0 30 60 90
34.5
48
IκBα
α-Tubulin
B
LPS
Relative Signal (/Unstim.) IκBα
1.5
1.0
0.5
0
0 15 30 60 90
Time (mins)
WT
BAI1-KO
C
LPS
WT
BAI1-KO
kDa
0 30 60 90 0 30 60 90
48
48
pIRF3
α-Tubulin
D
LPS
Relative Signal (/Unstim.) pIRF3
20
15
10
5
0
*
0 30 60 90
Time (mins)
WT
BAI1-KO
E
E. coli BW25113
WT
TLR4-KO
kDa
0 30 60 90 0 30 60 90
34
48
IκBα
α-Tubulin
F
E. coli BW25113
Relative Signal (/Unstim.) IκBα
1.5
1.0
0.5
0
0 30 60 90
Time (mins)
WT
TLR4-KO
G
E. coli BW25113
WT
TLR4-KO
kDa
0 30 60 90 0 30 60 90
48
48
pIRF3
α-Tubulin
H
E. coli BW25113
Relative Signal (/Unstim.) pIRF3
25
20
15
10
5
0
0 30 60 90
Time (mins)
WT
TLR4-KO
I
E. coli BW25113
WT
TLR4-KO
kDa
0 30 60 90 0 30 60 90
48
48
pTBK
α-Tubulin
J
E. coli BW25113
Relative Signal (/Unstim.) pIRF3
15
10
5
0
0 30 60 90
Time (mins)
WT
TLR4-KO

Figure 3-6. The attenuated activation of IRF3 is mediated by BAI1-TLR4 interactions

(**A**) BMDMs from WT and BAI1-KO animals were incubated with LPS (100ng/ml) over a time course. Cells were lysed and signaling was analyzed using immunoblotting. α-Tubulin was used an internal control. Fig. 3-6A shows a representative blot. (**B**) Quantitation of (A) shows the mean fold change in integrated density of IκBα normalized to total signal (α-Tubulin) ± SEM from seven experiments. Data were analyzed by two-way ANOVA with Bonferroni post-hoc comparisons (Time: ****P < 0.0001, $N = 7$). Fig. 3-6 (**C**) and (**D**) show the representative western blot and the quantitation of the phosphorylation of IRF3 (Ser396) in WT and BAI1-deficient BMDMs in response to LPS, respectively (Cell: *$P < 0.05$, Time: ****$P < 0.0001$, $N = 7$). (**E**) BMDMs from WT and TLR4-KO animals were infected with *E. coli* BW25113 (MOI 25) over a time course. Cells were lysed and the relative abundance of IκBα over time from a single experiment is shown. The quantitation of separate experiments, as performed in (B), is shown in (**F**) (Cell: *$P < 0.05$, Time: **$P < 0.01$, $N = 2$). The abundance of (**G**) phospho-TBK1 or (**I**) phospho-IRF3 in TLR4-deficient and control BMDMs after incubation with E. coli BW25113 was analyzed as in (A) and (B). (G) and (I) show representative immunoblots, while (**H**) and (**J**) display the quantitation and statistical analysis of the relative abundance of phospho-TBK1 (Cell: **$P < 0.01$, Time: *$P < 0.05$, $N = 2$) or phospho-IRF3 (Cell: *$P < 0.05$, $N = 2$) normalized to an internal control over time.

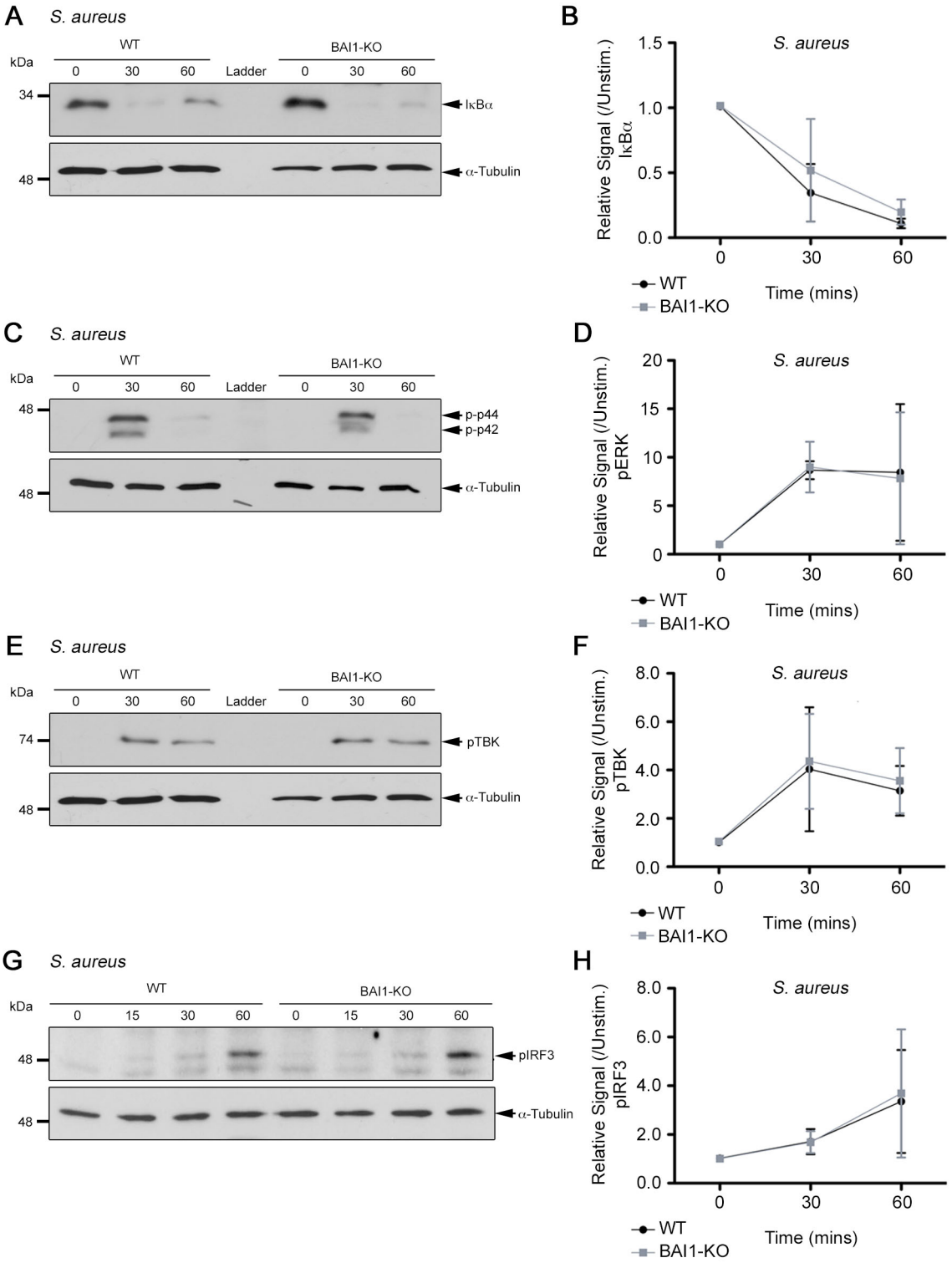
A
S. aureus
WT
BAI1-KO
kDa
0
30
60
Ladder
0
30
60
34
48
IκBα
α-Tubulin
B
S. aureus
Relative Signal (/Unstim.) IκBα
1.5
1.0
0.5
0.0
0
30
60
Time (mins)
WT
BAI1-KO
C
S. aureus
48
p-p44
p-p42
α-Tubulin
D
S. aureus
Relative Signal (/Unstim.) pERK
20
15
10
5
0
E
S. aureus
74
pTBK
F
S. aureus
Relative Signal (/Unstim.) pTBK
8.0
6.0
4.0
2.0
0.0
G
S. aureus
0
15
30
60
pIRF3
H
S. aureus
Relative Signal (/Unstim.) pIRF3

Figure 3-7. BAI1 expression does not affect innate signaling responses to Gram-positive bacteria

BMDMs from WT and BAI1-KO animals were incubated with *S. aureus* (MOI 25) at 37° over a time course. Cells were lysed and signaling was analyzed using immunoblotting. α-Tubulin was used an internal control. Antibodies against proteins associated with protein activation, such as a phospho-specific epitope were used as described in previous figures. (**A**), (**C**), (**E**), and (**G**) show representative examples of IκBα, phospho-ERK (Thr202/Tyr204), phospho-TBK (Ser172), and phospho-IRF3 (Ser396), respectively. Quantitation of separate experiments, as described in the previous figures, is also shown. Two-way ANOVA with Bonferroni post-hoc comparison was used for analysis. (**B**) shows the mean fold decrease ± SEM in relative abundance of IκBα (Time: $*P < 0.05$, $N = 2$). (D), (F), and (H) include the mean fold increase ± SEM in the integrated density of either (**D**) phospho-ERK ($N = 2$), (**F**) phospho-TBK ($N = 2$), or (**H**) phospho-IRF3 ($N = 2$) normalized to α-Tubulin.

TLR4 and BAI1 physically interact in a stimulus-enhanced manner in heterologous cell culture models

Several PRRs physically interact with TLRs to regulate innate immune responses by promoting ligand delivery and accessibility, signaling crosstalk, and subcellular localization. For example, CD36 co-immunoprecipitates with a TLR4-TLR6 heterocomplex in response to β-amyloid and oxidized LDL to mediate internalization and sterile inflammatory signaling (112). To determine if BAI1 acts a co-receptor for TLR4, we first assessed whether BAI1 physically interacted with TLR4. For this purpose, FLAG-tagged BAI1 and the TLR4 signaling complex, including TLR4, MD2, and CD14 were exogenously co-expressed in heterologous cell lines. 293T cells were then incubated with either *E. coli* DH5α or ΔinvG *Salmonella*, and BAI1 was immunoprecipitated from cell lysates using anti-Flag M2-coupled sepharose. As shown in **Fig. 3-8**, TLR4 and MD2 co-immunoprecipitated with BAI1 both at steady state and after stimulation with Gram-negative bacteria when expressed in 293T cells (**Fig. 3-8, A and C**).

MD2 associates with TLR4 in the Golgi complex and is required for surface expression and stability. Latz et al showed that mature TLR4 and MD2 are glycosylated (66). The co-association with MD2 and the molecular weight of both TLR4 and MD2 indicated that a substantial portion of the TLR4-MD2 complex associated with BAI1 was mature. Moreover, the addition of Gram-negative bacteria augmented the association between BAI1 and TLR4-MD2 (**Fig. 3-8, B and D**). Similar results were observed in CHO cells infected with *E. coli* DH5α (**Fig. 3-8, E and F**). For comparison, we also examined the association between BAI1 and TLR2, a surface expressed PRR critical for the recognition of Gram-positive bacteria. BAI1 and TLR2 were co-expressed in 293T

cells and stimulated with either *S. aureus* or *E. coli* DH5α. TLR2 did not co-immunoprecipitate with BAI1 in untreated cells or in response to either Gram-positive or Gram-negative bacteria (**Fig. 3-9**). This indicates that BAI1 specifically associates with TLR4, and that the association between BAI1 and TLR4 is responsive to stimulation with Gram-negative bacteria.

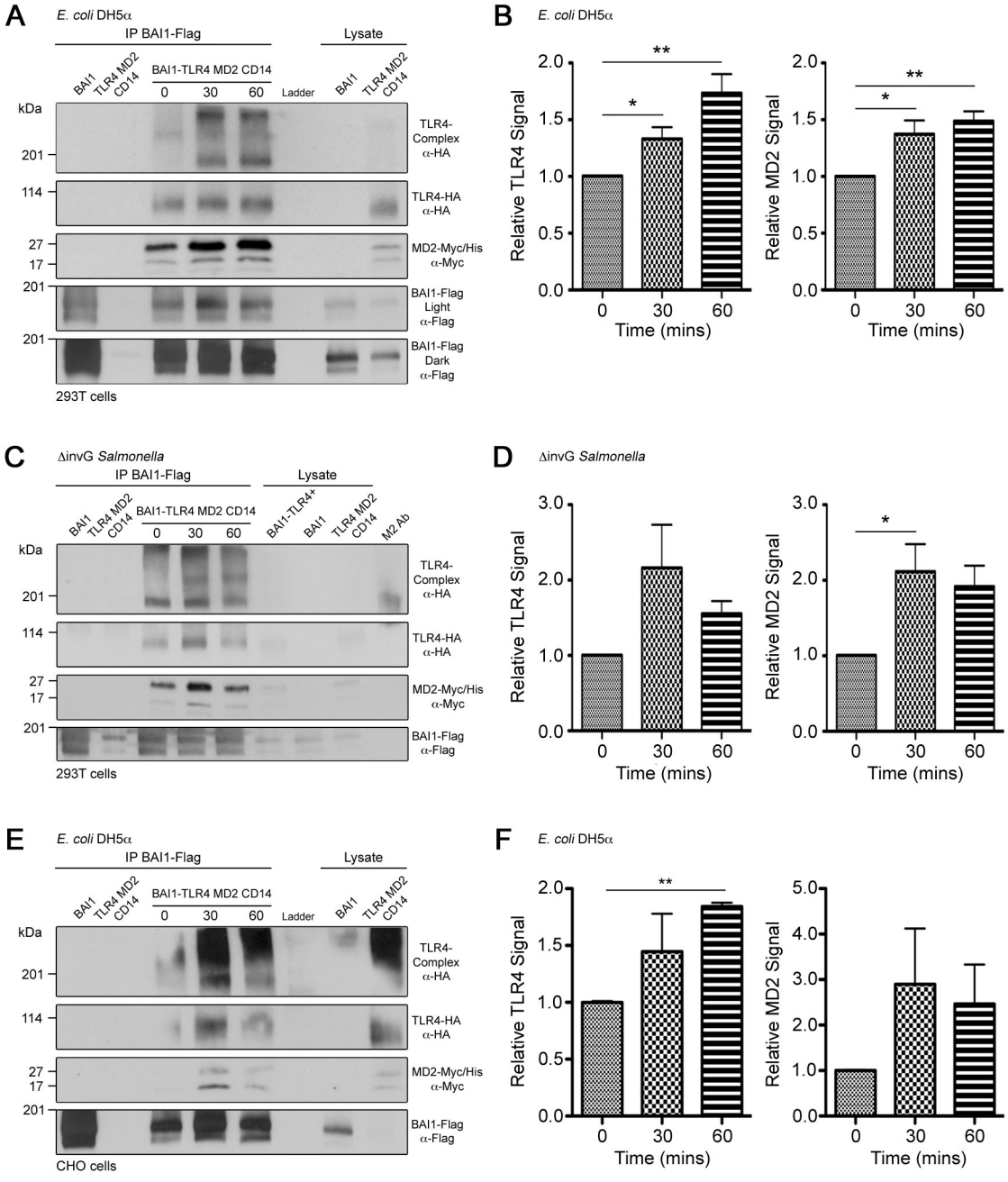
A
E. coli DH5α
IP BAI1-Flag
Lysate
BAI1
TLR4 MD2 CD14
BAI1-TLR4 MD2 CD14
0 30 60
Ladder
kDa
201
114
27
17
TLR4-Complex α-HA
TLR4-HA α-HA
MD2-Myc/His α-Myc
BAI1-Flag Light α-Flag
BAI1-Flag Dark α-Flag
293T cells
B
E. coli DH5α
Relative TLR4 Signal
Relative MD2 Signal
Time (mins)
C
ΔinvG Salmonella
BAI1-TLR4+
M2 Ab
D
ΔinvG Salmonella
E
E. coli DH5α
CHO cells
F
E. coli DH5α

Figure 3-8. TLR4-MD2 physically associates with BAI1

(**A**) 293T cells were transfected with BAI1 and TLR4-signaling complex (including TLR4, MD2, and CD14), then stimulated with *E. coli* DH5α at an MOI of 150 for 30 or 60 minutes. Cells were lysed and BAI1-Flag was immunoprecipitated using anti-Flag M2-affinity gel (Sigma) and analyzed using western blotting. Samples were prepped under non-reducing conditions. Image shows representative example of BAI1 immunoprecipitation. (**B**) Band intensities were quantified by densitometry. Graph shows the mean fold integrated density ± SEM of either TLR4-HA (30 min: $*P < 0.05$, $N = 5$, 60 min: $*P < 0.01$, $N = 6$) or MD2-Myc-His6 (30 min: $*P < 0.05$, $N = 5$, 60 min: $*P < 0.01$, $N = 6$) after treatment with bacteria, normalized to the total amount of BAI1 protein immunoprecipitated. Student's standard T-test with Welch's correction was used for analysis. (**C**) 293T cells were transfected with BAI1 and TLR4-signaling complex, then incubated with ΔinvG *S.* Typhimurium at an MOI of 100 for 30 or 60 mins. Cells were lysed and BAI1-Flag was immunoprecipitated using anti-Flag M2-affinity gel (Sigma) and analyzed using as in (A). Samples were prepped under non-reducing conditions. (**D**) Graph shows the relative mean integrated density of either TLR4-HA (30 min: $N = 4$, 60 min: $N = 2$) or MD2-Myc-His6 (30 min: $*P < 0.05$, $N = 4$, 60 min: $N = 2$) as analyzed above. (**E**) CHO cells were transfected with BAI1 and TLR4-signaling complex, then infected with *E. coli* DH5α at an MOI of 150 for 30 or 60 minutes. Immunoprecipitation was done as described in (A). (**F**) Graph shows normalized mean signal of either TLR4-HA (30 min: $N = 2$, 60 min: $**P < 0.01$, $N = 2$) or MD2-Myc-His6 (30 min: $N = 2$, 60 min: $N = 2$) as analyzed above.

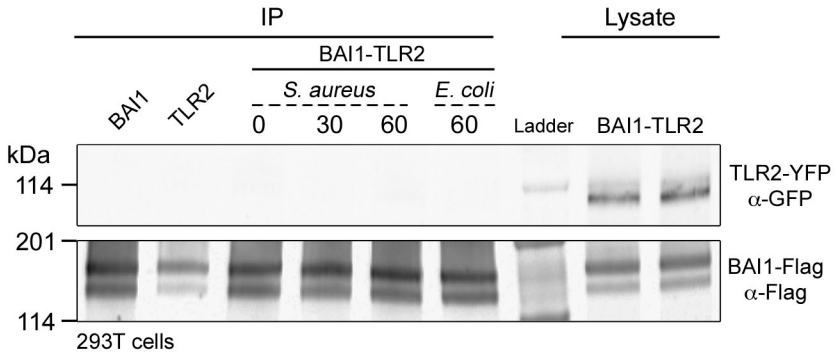
IP
Lysate
BAI1-TLR2
BAI1
TLR2
S. aureus
E. coli
0
30
60
60
Ladder
BAI1-TLR2
kDa
114
201
114
TLR2-YFP
α-GFP
BAI1-Flag
α-Flag
293T cells

Figure 3-9. TLR2 does not associate with BAI1

293T cells were transfected with BAI1 and TLR2 then incubated with *S. aureus* or *E. coli* DH5α at an MOI of 100 for 30 and 60 minutes. Cells were lysed and BAI1-Flag was immunoprecipitated using anti-Flag M2-affinity gel (Sigma) and analyzed using western blotting. Samples were prepped under non-reducing conditions. Image shows representative example. ($N = 3$)

Formation of high molecular weight signaling complexes containing TLR4 requires stimulation with Gram-negative bacteria

After stimulation with LPS, TLR4 membrane mobility and trafficking dynamics are altered. This translates to the formation of multi-protein signaling complexes containing CD14, TLR4-MD2, and LPS, perhaps representative of active signaling complexes (62, 69). The co-immunoprecipitation of higher molecular weight products containing TLR4-HA was observed only in the presence of Gram-negative bacteria (**Fig. 3-8, A, C, and E**). We hypothesized that the higher molecular weight products were composed of signaling complexes of BAI1 and TLR4-MD2. To further characterize this observation, immunoprecipitation assays were performed in 293T cells exogenously expressing both BAI1 and TLR4, MD2, and CD14. Samples were prepared under reducing and non-reducing conditions to better disassociate the higher molecular weight products. Under reducing conditions, we observed a noticeable increase in the MD2 and TLR4 signal at their predicted molecular weights suggesting that the higher molecular weight bands contained TLR4 and MD2 protein (**Fig. 3-10A**). Although some of the higher molecular weight complexes were lost upon treatment with β-mercaptoethanol, some remained, indicating that the components of the higher molecular weight products were partially resistant to reduction. Again, the association between BAI1 and TLR4-MD2 increased upon stimulation with Gram-negative bacteria under reducing conditions (**Fig. 3-10B**).

CD14 has been directly implicated in regulating the mobility of BAI1 on the plasma membrane and within intracellular compartments, and directly mediates the internalization of TLR4-MD2 from the cell surface (63, 69, 74). To determine whether

expression of CD14 impacted the interaction between BAI1 and TLR4-MD2, we analyzed the association of BAI1 and TLR4 with and without CD14 co-expressed using the immunoprecipitation assay described above. TLR4-MD2 co-immunoprecipitated with BAI1 in the absence of CD14 indicating that the association did not require CD14 (**Fig. 3-10C**). Although some higher molecular weight bands were observed without CD14, others were selectively found in the context of CD14 expression, indicating that the higher molecular weight products may represent LPS responsive signaling complexes (**Fig. 3-10C**). We still observed an increase in the association between BAI1 and TLR4-MD2 without CD14 expression, indicating that CD14 is not required for this interaction **(Fig. 3-10D**). Collectively, this again supports the hypothesis that BAI1 associates with TLR4 signaling complexes in a manner that is responsive to stimulation with Gram-negative bacteria.

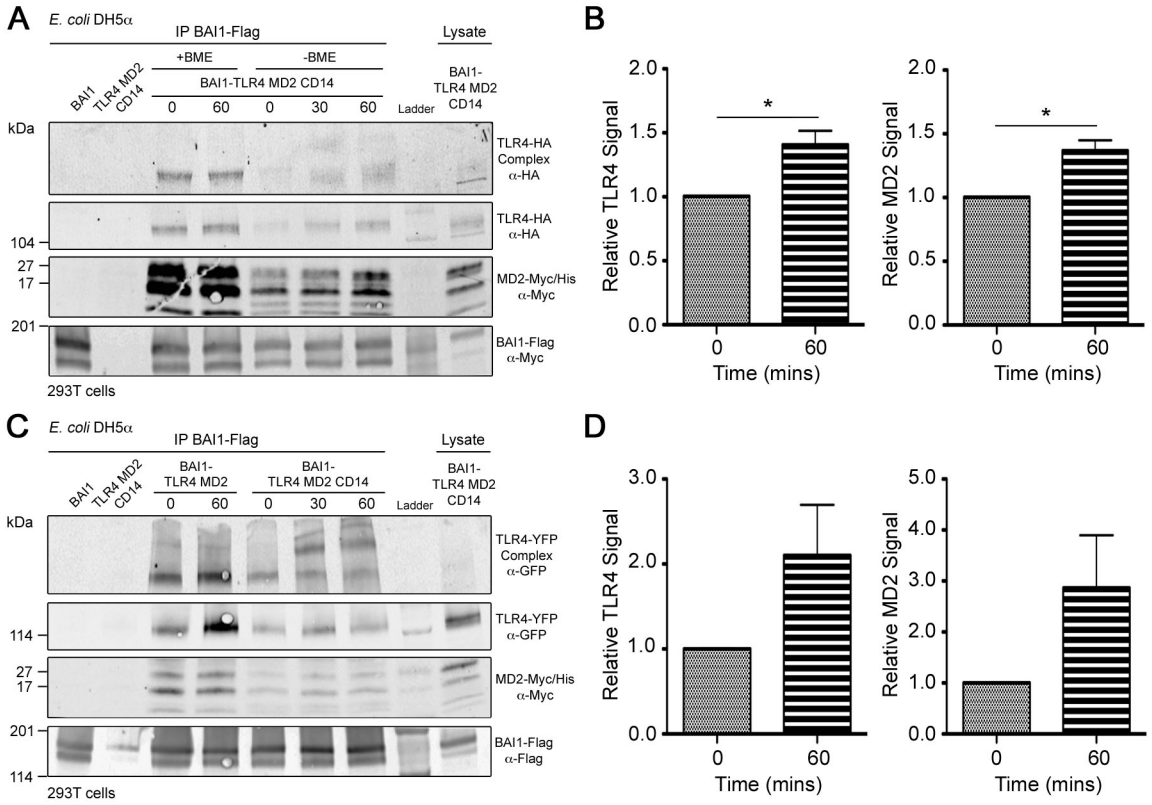
A
E. coli DH5α
IP BAI1-Flag
Lysate
+BME
-BME
BAI1
TLR4 MD2 CD14
BAI1-TLR4 MD2 CD14
0 60 0 30 60
Ladder
BAI1-TLR4 MD2 CD14
kDa
TLR4-HA Complex α-HA
TLR4-HA α-HA
104
27
17
MD2-Myc/His α-Myc
201
BAI1-Flag α-Myc
293T cells
B
Relative TLR4 Signal
Relative MD2 Signal
2.0
1.5
1.0
0.5
0.0
*
0 60
Time (mins)
C
E. coli DH5α
IP BAI1-Flag
Lysate
BAI1
TLR4 MD2 CD14
BAI1-TLR4 MD2
BAI1-TLR4 MD2 CD14
0 60 0 30 60
Ladder
BAI1-TLR4 MD2 CD14
kDa
TLR4-YFP Complex α-GFP
TLR4-YFP α-GFP
114
27
17
MD2-Myc/His α-Myc
201
114
BAI1-Flag α-Flag
293T cells
D
Relative TLR4 Signal
Relative MD2 Signal
3.0
2.0
1.0
0.0
5.0
4.0
3.0
2.0
1.0
0.0
0 60
Time (mins)

Figure 3-10. The association between BAI1 and high molecular weight complexes containing TLR4 is enriched after infection with Gram-negative bacteria

(**A**) 293T cells were transfected with BAI1 and TLR4-signaling complex (including TLR4, MD2, and CD14), then incubated with *E. coli* DH5α at an MOI of 150 for 30 or 60 mins. Cells were lysed and BAI1-Flag was immunoprecipitated using anti-Flag M2-affinity gel (Sigma) and analyzed using westerns. Samples were prepared under non-reducing and reducing conditions. Image shows representative example. (**B**) Graph shows the mean integrated density ± SEM of either TLR4-HA (**P* < 0.05, *N* = 5) or MD2-Myc-His6 (**P* < 0.05, *N* = 4) normalized to the total BAI1 protein immunoprecipitated and run under reducing conditions. Data is presented relative to the unstimulated sample. Student's standard T-test with Welch's correction was used for analysis. In (C) and (D), 293T cells were transfected with BAI1 and TLR4-signaling complex (including TLR4 and MD2) with and without CD14, then treated with *E. coli* DH5α at an MOI of 150 for 30 or 60 mins. (**C**) shows a representative example of the immunoprecipitation of BAI1 as described in (A). (**D**) Band intensities for TLR4 or MD2 at the predicted molecular weights in immunoprecipitates from 293T cells not expressing CD14 were quantified by densitometry. Graph shows mean fold intensity ± SEM of either TLR4-HA (*N* = 2) or MD2-Myc-His6 (*N* = 2), normalized to the amount of BAI1 immunoprecipitated. Samples were prepared under non-reducing conditions. Student's standard T-test with Welch's correction was used for analysis.

BAI1 does not regulate the internalization of TLR4-MD2 complexes from the plasma membrane

Since BAI1 physically associates with TLR4 in heterologous cell systems and selectively regulates the intracellular signaling response of TLR4 in primary macrophages, we hypothesized that BAI1 may mediate this effect by driving the delivery of functional TLR4-MD2 and ligand to a phagosomal compartment. In this role, BAI1 and TLR4 associate at the cell surface via recognition of distinct components of the LPS structure. Then, BAI1 functions to drive the internalization of the TLR4 complex and attached Gram-negative bacteria, thereby promoting intracellular, TRIF-dependent signaling responses. To determine if BAI1 affects the internalization of TLR4 during recognition of Gram-negative bacteria, we measured the loss of the TLR4-MD2 signal from the cell surface of macrophages after incubation with bacteria over a time course using flow cytometry. **Fig. 3-11, A and B** show histograms of surface TLR4-MD2 over time after treatment with *E. coli* BW25113 in wild type and BAI1-deficient BMDMs from a representative experiment. There was no difference in TLR4-MD2 uptake in control or BAI1-knockout cells, indicating that the internalization of TLR4 from the cell surface is unimpaired (**Fig. 3-11, C and D**).

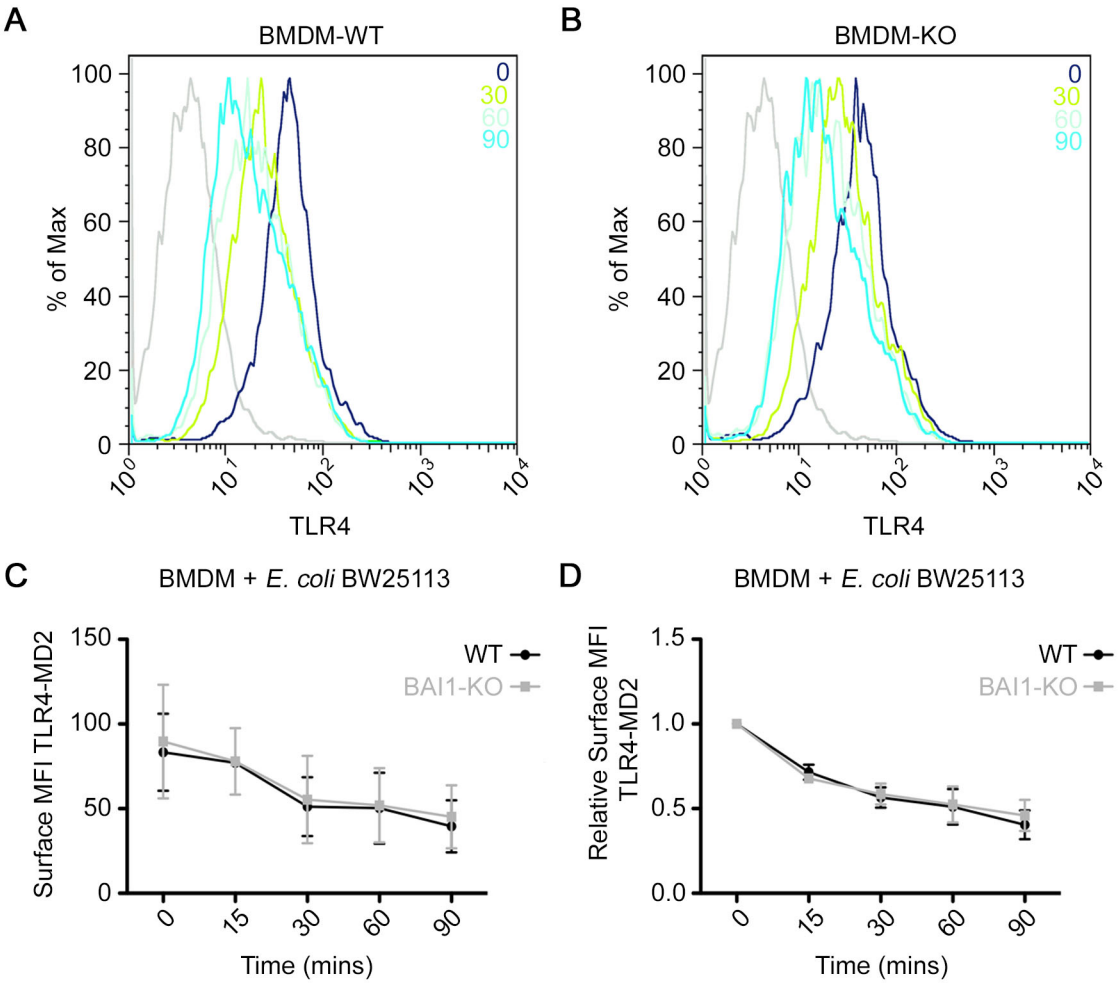
A
BMDM-WT
% of Max
TLR4
0
30
60
90
B
BMDM-KO
% of Max
TLR4
0
30
60
90
C
BMDM + E. coli BW25113
Surface MFI TLR4-MD2
Time (mins)
WT
BAI1-KO
D
BMDM + E. coli BW25113
Relative Surface MFI TLR4-MD2
Time (mins)
WT
BAI1-KO

Figure 3-11. Internalization of surface TLR-MD2 after treatment with Gram-negative bacteria is not regulated by BAI1

BMDMs from WT and BAI1-KO animals were incubated with *E. coli* BW25113 (MOI25) at 37° over the indicated time course. Cells were then put on ice and stained for surface levels of TLR4-MD2 using a biotin labeled antibody (clone SA15-21) and analyzed using FACS. Histograms display WT (**A**) and BAI1-KO macrophages (**B**) from a representative experimental repeat. (**C**) Graph displays the decrease in mean fluorescence intensity (MFI) of surface TLR4-MD2 over the time course, while (**D**) shows the decrease of surface TLR4-MD2 relative to the unstimulated cells in WT or BAI1-KO BMDMs ($N = 3$).

BAI1 promotes intracellular TLR4 signaling by driving the internalization and compartmentalization of ligand

We also examined the role of BAI1-mediated internalization of Gram-negative bacteria in promoting TLR4 intracellular signaling responses in macrophages. We hypothesized that BAI1-driven phagocytosis promotes TRIF-dependent responses by compartmentalizing and sequestering LPS within an intracellular compartment, thereby promoting intracellular signaling. To assess this, we pre-treated wild type and BAI1-deficient macrophages with Cytochalasin D to inhibit actin reorganization and phagocytosis. We found that Cytochalasin D significantly attenuated the phosphorylation of IRF3 in wild type BMDMs in response to *E. coli* BW25113, while only slightly decreasing phospho-IRF3 abundance in BAI1-deficient cells (**Fig. 3-12, A and B**). These results suggest that delivery of *E. coli* to phagosomes potentiates TLR4-TRIF-dependent signaling.

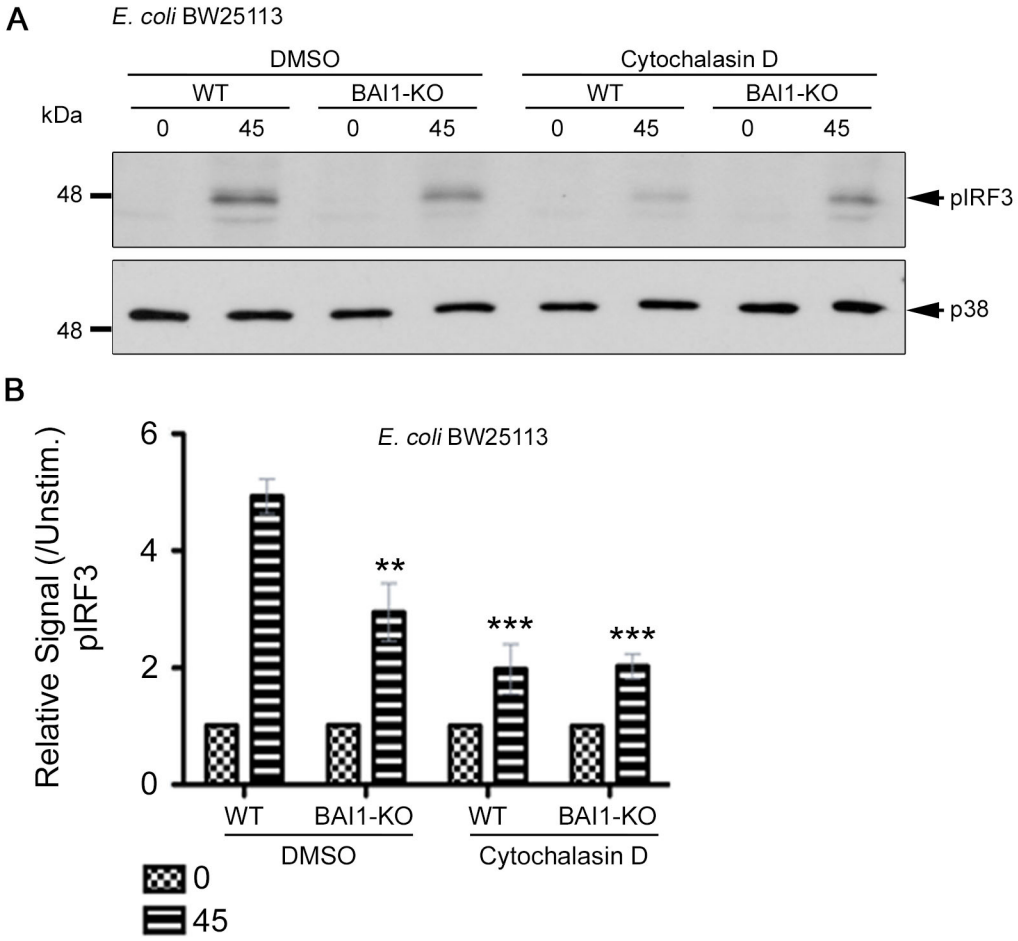
A
E. coli BW25113
DMSO
Cytochalasin D
WT
BAI1-KO
WT
BAI1-KO
kDa
0
45
0
45
0
45
0
45
48
pIRF3
48
p38
B
E. coli BW25113
Relative Signal (/Unstim.) pIRF3
6
4
2
0
**
***
***
WT
BAI1-KO
WT
BAI1-KO
DMSO
Cytochalasin D
0
45

Figure 3-12. BAI1-mediated phagocytosis promotes enhanced activation of IRF3 signaling

BMDMs from WT and BAI1-KO animals were pre-treated with Cytochalasin D at 1μg/ml followed by stimulation with *E. coli* BW25113 (MOI 25) for 45 minutes. Cells were lysed and signaling was analyzed using immunoblotting with antibodies specific to the active form of the signaling molecule. p38 MAPK was used an internal control. (A) shows a representative example of the phosphorylation of (**A**) phospho-IRF3 (Ser396). Quantitation of separate experimental repeats is shown in (B). Graph shows mean fold integrated density ± SEM of (**B**) phospho-IRF3 (Ser396) (**$P < 0.01$, ***$P < 0.001$, $N = 4$). Data is normalized to the total signal (p38) and relative to the unstimulated cells. One-way ANOVA with Bonferroni post-hoc comparison was used for analysis.

Association between BAI1 and TLR4 requires the cytoplasmic domain of BAI1

Biochemical analysis indicated that BAI1 and TLR4 interact at steady state, and that upon stimulation with Gram-negative bacteria, the association between BAI1 and TLR4 is enhanced. Although BAI1 does not regulate TLR4 internalization from the cell surface, we hypothesized that the physical interaction between BAI1 and TLR4 was, at least in part, mediated by the shared recognition of LPS or Gram-negative bacteria. In this regard, an attached microbe would bridge BAI1 and TLR4, facilitating complex formation. It is not known how BAI1 and TLR4-MD2 interact or what the precise region of BAI1 is that mediates this interaction. We further analyzed the relationship between BAI1 and TLR4 by assessing which region of BAI1 was required for this association. A series of truncated or mutated BAI1 constructs described in **Figure 3-13A** were compared for association with TLR4 using immunoprecipitation. We originally hypothesized that the extracellular domain would be critical for the association between BAI1 and TLR4 by cross-linking BAI1 and TLR4 in the context of membrane associated bacteria. Surprisingly, we found that TLR4 co-immunoprecipitated only when the intracellular cytoplasmic region of BAI1 was expressed, as there was no detectable signal after immunoprecipitating a truncated form of BAI1 containing only the N-terminal extracellular region and seven transmembrane repeats in 293T cells (**Fig. 3-13, B and C**). Similar results were obtained in CHO cells assayed under the same conditions. TLR4 associated with full length BAI1, BAI1 lacking the TSRs, and the intracellular domain of BAI1, but not with the extracellular domain plus the seven transmembrane region (**Fig. 3-13, D and E**). This provided further evidence that in addition to promoting bacterial

phagocytosis, BAI1 modulates TLR4 responses by another mechanism, perhaps through signaling crosstalk.

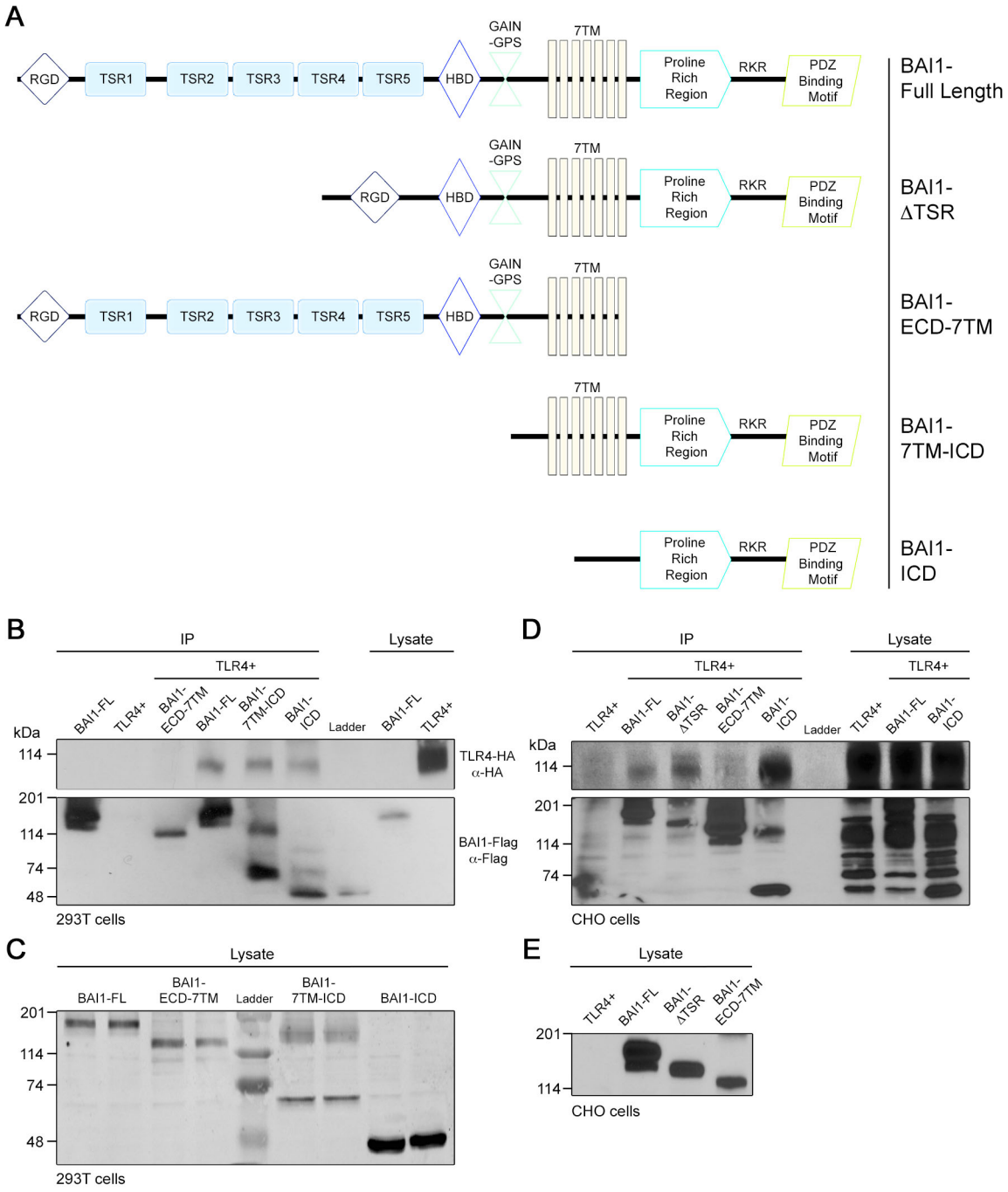
A
RGD
TSR1
TSR2
TSR3
TSR4
TSR5
HBD
GAIN -GPS
7TM
Proline Rich Region
RKR
PDZ Binding Motif
BAI1- Full Length
BAI1- ΔTSR
BAI1- ECD-7TM
BAI1- 7TM-ICD
BAI1- ICD
B
IP
Lysate
TLR4+
BAI1-FL
TLR4+
BAI1- ECD-7TM
BAI1-FL
BAI1- 7TM-ICD
BAI1- ICD
Ladder
BAI1-FL
TLR4+
kDa
114
201
114
74
48
TLR4-HA α-HA
BAI1-Flag α-Flag
293T cells
C
Lysate
BAI1-FL
BAI1- ECD-7TM
Ladder
BAI1- 7TM-ICD
BAI1-ICD
201
114
74
48
293T cells
D
IP
Lysate
TLR4+
TLR4+
TLR4+
BAI1-FL
BAI1- ΔTSR
BAI1- ECD-7TM
BAI1- ICD
Ladder
TLR4+
BAI1-FL
BAI1- ICD
kDa
114
201
114
74
CHO cells
E
Lysate
TLR4+
BAI1-FL
BAI1- ΔTSR
BAI1- ECD-7TM
201
114
CHO cells

Figure 3-13. The cytoplasmic region of BAI1 is required for the association with TLR4 signaling complexes

(**A**) Cartoon schematics of WT, modified, or truncated BAI1 proteins used to define the region of BAI1 critical for the association with TLR4 signaling complexes. (**B**) 293T cells were transfected with full-length BAI1 or the modified BAI1 constructs and TLR4-signaling complex (including TLR4, MD2, and CD14). Cells were lysed and BAI1-Flag was immunoprecipitated using anti-Flag M2-affinity gel (Sigma) and analyzed using western blotting. The image shows a representative example ($N = 3$). (**C**) shows a representative blot of cell lysates transfected with the BAI1 constructs used for immunoprecipitation in (B). (**D**) CHO cells were transfected with full-length BAI1 or the modified BAI1 constructs and TLR4-signaling complex, as in (A). Cells were lysed and BAI1-Flag was immunoprecipitated using anti-Flag M2-affinity gel (Sigma) and analyzed using western blotting. (**E**) Image shows representative example ($N = 5$). Cell lysates show the corresponding molecular weight and expression of the BAI1 constructs used for immunoprecipitation in (D).

BAI1 selectively promotes the association of TLR4 with cell-associated Gram-negative bacteria

The interplay between the recognition of soluble LPS versus intact *E. coli* is considerably complex. Some evidence suggests that TLR4 delivery to the phagosome is required for complete activation of IRF3 and induction of IFN-β in response to Gram-negative bacteria, indicating that the process of phagocytosis plays a crucial role in activating TLR4-TRIF responses (67). However, Zanoni et al showed that CD14 was required for TLR4-TRIF responses by mediating receptor endocytosis, even in the context of whole bacteria (74). In both contexts, the cellular distribution of TLR4 was the critical factor in defining the downstream outcomes. TLR4 is found at the cell surface and within endosomal and phagosomal compartments (66-69). We wanted to further explore where BAI1 and TLR4 interact to understand how BAI1 impacts TLR4-dependent signaling. For this purpose, we expressed BAI1 and TLR4, with MD2 and CD14, in Cos7 cells and examined their cellular distribution using confocal microscopy. Consistent with its expression in primary macrophages, BAI1-GFP was found on the plasma membrane and in the perinuclear region at steady state (**Fig. 3-14**) (222, 225). In 293T cells, TLR4 is found at the cell surface, in the ERC, and in the Golgi, while monocytes primarily express TLR4 within intracellular compartments, particularly in the ERC (66, 67). In Cos7 cells, TLR4 displayed a similar distribution as when expressed in 293T cells. It was visible in the cell periphery, in punctate structures within the cells (presumably early endosomes), and in the ERC (**Fig. 3-14**). Interestingly, BAI1 and TLR4 displayed similar cellular distribution in the absence of bacteria.

We next observed the distribution of TLR4 and BAI1 in cells infected with either *E. coli* DH5α or *S. aureus.* The global distribution of BAI1 and TLR4 did not obviously change upon infection (**Fig. 3-15, A to F**). When expressed alone, BAI1 and TLR4 were found clustered around *E. coli*, but not Gram-positive bacteria (**Fig. 3-15, A and B**). Importantly, we observed a substantial enrichment of both BAI1 and TLR4 when expressed together around cell-associated and internalized *E. coli*, but not around *S. aureus* (**Fig. 3-15C**). To quantify the association of BAI1 or TLR4 with bacteria, we measured the Pearson's coefficient of BAI1 or TLR4 with either *E. coli* or *S. aureus*, with each microbe defined as a ROI. The extent of colocalization between BAI1 and Gram-negative bacteria was significantly higher than with Gram-positive bacteria, irrespective of co-expression with TLR4 (**Fig. 3-15D**). Perhaps not surprisingly, TLR4 also showed a significantly higher association with *E. coli* than *S. aureus* (**Fig. 3-15E**). Moreover, the extent of the association between TLR4 and *E. coli,* but not *S. aureus*, was significantly increased when BAI1 was co-expressed (**Fig. 3-15, E and F**). Finally, TLR4 colocalization with BAI1 was also significantly higher when cells were infected with Gram-negative bacteria, compared to Gram-positive microbes (**Fig. 3-15F**). Collectively, this showed that BAI1 and TLR4 are expressed in similar compartments at steady state and after infection, and that the association between BAI1 and TLR4 is significantly higher at phagosomes containing *E. coli*, as opposed to *S. aureus*.

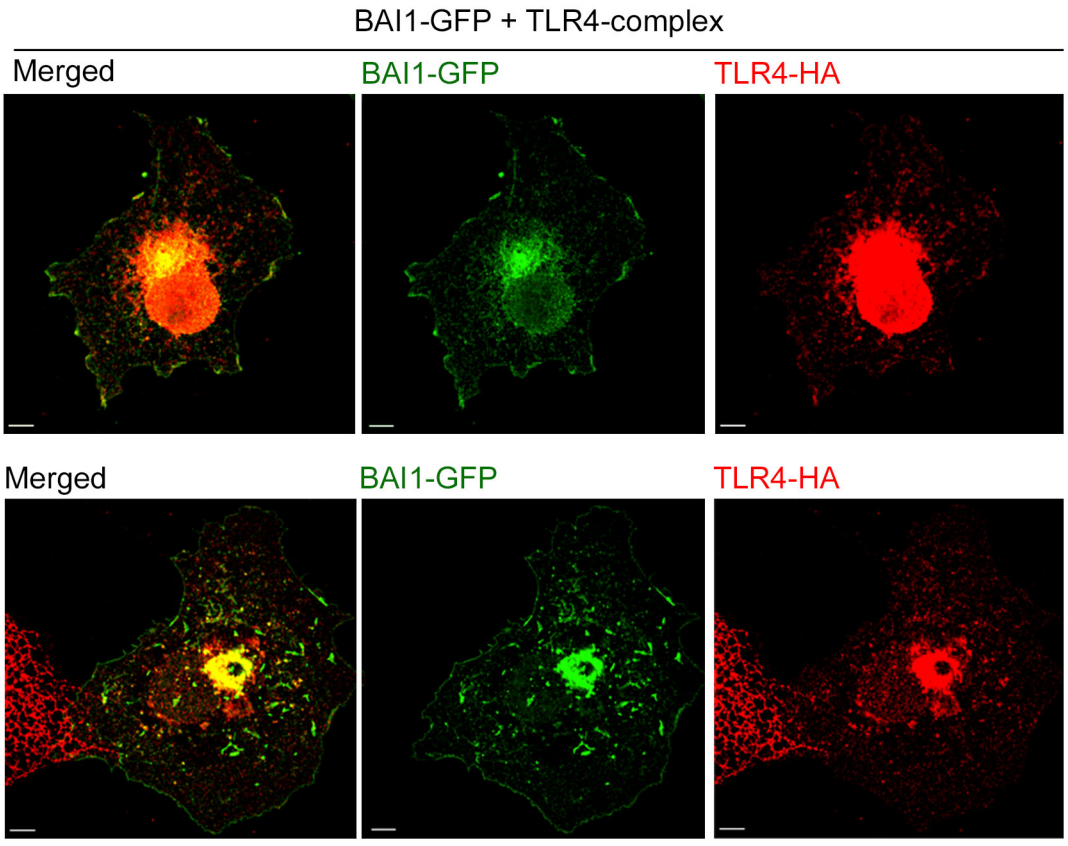
BAI1-GFP + TLR4-complex
Merged
BAI1-GFP
TLR4-HA
Merged
BAI1-GFP
TLR4-HA

Figure. 3-14. BAI1 and TLR4 are found at the cell periphery and the perinuclear region when exogenously expressed in Cos7 cells

Cos7 cells were transfected with BAI1-GFP and TLR4 signaling complex (TLR4-HA, MD2-Myc-His6, and CD14), then fixed and stained with an anti-HA antibody (red). GFP fluorescence (green) was used to detect BAI1. The representative images show a single confocal section of two cells expressing both BAI1 and TLR4-HA. Scale bar, 5 μm.

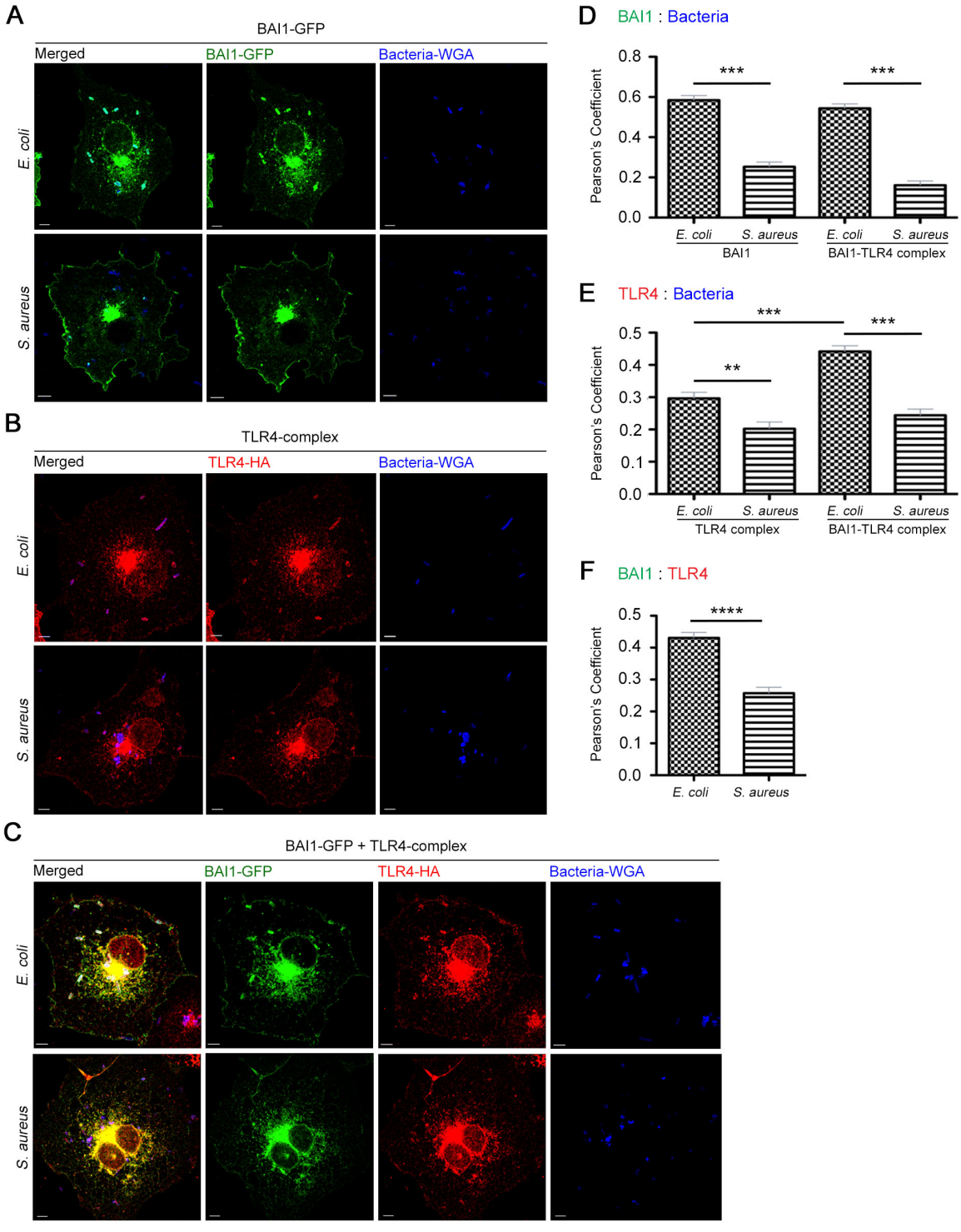
A
BAI1-GFP
Merged
BAI1-GFP
Bacteria-WGA
E. coli
S. aureus
B
TLR4-complex
Merged
TLR4-HA
Bacteria-WGA
E. coli
S. aureus
C
BAI1-GFP + TLR4-complex
Merged
BAI1-GFP
TLR4-HA
Bacteria-WGA
E. coli
S. aureus
D
BAI1 : Bacteria
Pearson's Coefficient
0.8
0.6
0.4
0.2
0.0
***
***
E. coli
S. aureus
E. coli
S. aureus
BAI1
BAI1-TLR4 complex
E
TLR4 : Bacteria
Pearson's Coefficient
0.5
0.4
0.3
0.2
0.1
0.0
***
***
**
E. coli
S. aureus
E. coli
S. aureus
TLR4 complex
BAI1-TLR4 complex
F
BAI1 : TLR4
Pearson's Coefficient
0.5
0.4
0.3
0.2
0.1
0.0
****
E. coli
S. aureus

Figure 3-15. BAI1 and TLR4 colocalize during recognition of Gram-negative bacteria

Cos7 cells were transfected with BAI1-GFP or TLR4 signaling complex (TLR4-HA, MD2-Myc-His6, and CD14) alone or in combination. Bacteria were labeled by pre-incubation with WGA (blue). Cells were incubated with either *E. coli* or *S. aureus* for 45 min, then were fixed and stained with an anti-HA antibody to detect TLR4 (red). GFP fluorescence (green) was used to detect BAI1 when appropriate. The cells were imaged by confocal microscopy. The representative images show a single confocal section of cells expressing (**A**) BAI1, (**B**) TLR4-complex, and (**C**) BAI1 and TLR4-complex. Scale bar, 5μm. The association between BAI1, TLR4, or bacteria was quantified based on the Pearson's coefficient at sites of cell-associated bacteria defined as regions of interest (ROIs). At least 6 Cos7 cells per condition per experiment were analyzed from a total of two experiments. The *n* value below indicates the total number of ROIs assessed. Statistical analysis was performed using 1-way ANOVA with Tukey's multiple comparison post-test. (**D**) Graph shows the mean Pearson's coefficient ± SEM between BAI1 and either *E. coli* or *S. aureus* in cells expressing BAI1 alone or in combination with TLR4-complex (***$P < 0.001$, $n = 344$). (**E**) shows the Pearson's coefficient ± SEM between TLR4 and either *E. coli* or *S. aureus*, as described in (D) (**$P < 0.01$, ***$P < 0.001$, $n = 286$). (**F**) Shows the Pearson's coefficient between BAI1 and TLR4 at ROIs, defined as cell associated *E. coli* and *S. aureus*. Data was analyzed using a Student's T-test (****$P < 0.0001$, $n = 290$).

Discussion

PRRs perform a critical function by initiating and modulating inflammatory responses, promoting microbicidal activity and pathogen clearance, and generating adaptive immunity. TLR4 is required for initiating inflammatory signaling and cytokine responses to LPS. However, the ability of TLR4 and other PRRs to act together in a coordinated and collaborative manner provides an additional level of specificity and control for the magnitude and type of immune responses generated to microbial stimuli. BAI1 is a phagocytic PRR that recognizes the core oligosaccharide of LPS, thereby displaying distinct specificity and functionality relative to TLR4, which recognizes lipid A and cannot directly mediate phagocytosis.

Little is known about how BAI1 impacts the innate immune response to Gram-negative bacteria. Here, we expand upon early work by showing that BAI1 acts together with TLR4 in the response to Gram-negative bacteria. In this capacity, BAI1 selectively enhances intracellular TLR4 signaling by promoting the activation of IRF3 and the induction of IRF3-dependent cytokines. We found that BAI1-deficient macrophages exhibit attenuated TRIF-dependent signaling based on two distinct criteria: 1) decreased phosphorylation of TBK1 and IRF3 and 2) reduced expression of IRF3-dependent genes (IFN-β, CCL5, and IL-10) in response to Gram-negative bacteria.

The non-canonical IKK kinase, TBK1, mediates activating phosphorylation of IRF3 in the context of TLR4 signaling. We found that TBK1 phosphorylation was reduced in BAI1-deficient macrophages in response to Gram-negative bacteria, but this was not observed in all contexts. How TBK1 and the related kinase, IKKε, are activated

is poorly understood, and both the kinase activity and subcellular distribution can impact the potency of TBK1 activity (324). Structural and biochemical analysis indicates a role for a currently unknown activating kinase and the transactivation by other TBK1 molecules. Some evidence suggests that downstream kinase activity of TBK1 is controlled by an as-yet undefined feedback mechanism (325-327). For example, the use of pharmacological inhibitors of IKK-related kinases that suppress IRF3 phosphorylation is associated with increased abundance of phosphorylated TBK and IKKε in LPS stimulated macrophages (325). A closer analysis of the kinase activity of TBK1, the recruitment and formation of signaling complexes, and the distribution of TLR4 signaling components in wild type and BAI1-knockout macrophages may resolve this discrepancy and better reveal where BAI1 intersects with TLR4 signaling.

We previously showed that BAI1 mediates bacterial attachment to and internalization by host cells through the recognition of the core oligosaccharide of LPS. This is distinct from TLR4, which recognizes the lipid A region of LPS, suggesting that BAI1 may function as a co-receptor. In support of this hypothesis, we found that TLR4-MD2 complexes specifically co-immunoprecipitate with BAI1 in a manner that is enhanced after incubation with Gram-negative bacteria (*E. coli* and non-invasive *Salmonella*). Surprisingly, however, the rate of TLR4 internalization from the cell surface was unaffected by the absence of BAI1, suggesting that BAI1 is not required for the delivery of TLR4 from the plasma membrane to the phagosomal compartment. Instead, BAI1 and TLR4 strongly colocalized with bacteria in what are likely phagocytic cups or phagosomes, suggesting that BAI1 interacts with and promotes TLR4-dependent signaling from within the phagosomal compartment. We were also surprised to discover

that the cytoplasmic domain of BAI1, rather than the extracellular domain which directly binds bacteria and LPS, mediates the interaction between BAI1 and TLR4. While a direct interaction between the cytoplasmic regions is unlikely, it is possible that BAI1 and TLR4 are scaffolded together by a currently unidentified linker protein. Alternatively, the cytoplasmic domain may be necessary for the appropriate subcellular localization of BAI1 required for interactions with TLR4-MD2.

The cytoplasmic domain of BAI1 is critical for mediating several signaling cascades. Accordingly, it is possible that BAI1 and TLR4 interact through signaling crosstalk. In response to Gram-negative bacteria and apoptotic cells, BAI1 mediates the activation of Rac1 GTPase by coupling to the bipartite Rac-GEF, ELMO-Dock (225, 226, 328). Additionally, during synaptogenesis BAI1 interacts with Par3 and Tiam1 to regulate local Rac activity (329). Rac has been associated with enhancing TLR2 and TLR7/TLR9-dependent responses in other contexts (321, 330). For example, Dock2-dependent Rac1 signaling is required for the activation of IKKα and the induction of type-I IFNs downstream of TLR7 and TLR9 in response to nucleic acid ligands, perhaps indicating that BAI1 acts as an upstream signal triggering similar crosstalk events in the context of LPS (49). BAI1 has also been shown to mediate classical GPCR signaling responses. In this context, it promotes the activation of RhoA through $G\alpha_{12/13}$ (203). Although this response is potentiated upon receptor cleavage, signaling is detectable in the context of the full-length protein. In other contexts, $G\alpha_{12/13}$ signaling has been associated with the regulation of p120catenin (331), which together with RhoA regulates intracellular TLR4 responses (77), perhaps providing a direct mechanism through which BAI1 may modulate TRIF signaling in macrophages. BAI1 also associates with β-

arrestin2, which has been shown to modulate TLR4 signaling, providing another potential mechanism of crosstalk (332-334). Stephenson et al also showed that BAI1 promoted the activation of ERK via either an interaction with MAGI-3, a protein enriched in the PSD that associates with the C-terminal PDZ binding motif of BAI1, or through another as yet undefined mechanism (203). It is unlikely that this mechanism contributes to the phenotype described in this study given that MAPK activation was maintained in BAI1-deficient macrophages. Other protein-protein interactions associated with the C-terminus of BAI1, for example the association with BAP2 (IRSp53), are of unknown functional significance and require further exploration (243).

The compartmentalization and trafficking of TLR4 within the cell also plays a critical role in regulating immune responses. Signaling through TRIF-TRAM adaptor proteins is initiated from the early endosomal compartment after CD14-driven endocytosis (63, 68, 74). A recent study suggested that TLR4 is also delivered to the phagosomal compartment from the ERC in a Rab11a-dependent manner and that this pre-existing endosomal pool of TLR4 is required for the type-I IFN response to Gram-negative bacteria (67). Thus, it is possible that BAI1 mobilizes trafficking of TLR4 from the ERC via one or more signaling intermediates. Interestingly, Husebye et al showed that the actin depolymerizing agent Cytochalasin D impaired both bacterial internalization and delivery of TLR4 from the ERC to the phagosome. Consistent with this, we found that Cytochalasin D impaired activation of IRF3 in wild type macrophages, but not in BAI1-deficient cells. This suggests that BAI1-mediated uptake promotes delivery of ligand (e.g. bacteria) to an intracellular compartment, but may also indicate a role for BAI1 signaling in TLR4 recruitment. Although it has not been

observed, it is possible that classical GPCR signaling through the Gβγ subunit could also account for promoting the delivery of TLR4 from an intracellular compartment. For example, activation of lysophosphatidic acid (LPA) receptors regulates trafficking within the endosomal compartment through an interaction between $G\beta_1\gamma_2$ and Rab11a (335). The interaction between BAI1 and the ERC, including Rab11a, requires further exploration.

In addition to mediating IRF3 responses, TRIF-dependent signaling leads to the late activation of NF-κB and MAPKs through an interaction with RIP1 and TRAF6 (81-84). Accordingly, TRIF-deficient macrophages display attenuated late activation of NF-κB and MAPKs and reduced induction of NF-κB-dependent cytokines, such as TNF-α. We showed that BAI1-deficient macrophages do not completely phenocopy TRIF-deficient cells, as NF-κB and MAPK activation are fully functional in response to both Gram-negative bacteria and LPS. This suggested that BAI1 perhaps modulates signaling downstream of TRIF-TRAM. Alternatively, it may indicate that the endosomal and phagosomal compartments from which TLR4 signals are not homogenous and that they differ in their capacity to promote IRF3 signaling versus late NF-κB and MAPK signaling. Accordingly, BAI1 may help define the phagosomal compartment for selective TLR4 signaling.

Collectively, these results implicate BAI1 as a novel accessory protein that modulates TLR4 signaling responses. TLR4 and BAI1 form a complex that is enhanced after treatment with bacteria and is found associated with *E. coli*-containing phagosomes. TRIF-dependent responses play a critical, but variable, role in protective immunity to Gram-negative bacterial infection and LPS responsiveness (336-338). Autocrine and

paracrine signaling by IFN-β promotes local activation of macrophages and monocytes to enhance microbicidal activity (339). Moreover, the activation of IRF3 also prevents endotoxic shock by upregulating anti-inflammatory cytokines, including IL-10 (79, 316, 336, 340, 341). By regulating the activation of TBK1 and IRF3 and the TRIF-dependent transcriptional response, BAI1 may enhance protective immune responses associated with enhanced phagocytic and anti-microbial function and the anti-inflammatory resolution of overly robust innate responses. This study reveals the potential implications of a novel LPS receptor on the innate immune response to Gram-negative bacteria.

Materials and Methods

Ethics statement

All experiments were performed in accordance with the recommendations in the Guide for the Care and Use of Laboratory Animals of the National institutes of Health. Protocols were approved by the Institutional Animal Care and Use Committee at the University of Virginia (Protocol number 3488).

Plasmids

The BAI1 constructs used in this study were a gift from Dr. Kodi Ravichandran, University of Virginia (225). pEBB-hBAI1 with either Flag or GFP C-terminal tags were used for immunoprecipitation or imaging assays, respectively. The BAI1 mutants were expressed in pEBB vectors with C-terminal Flag tags. pUNO1-hTLR4-HA3x (Invivogen), pCMV-SPORT6 hCD14 (Thermo Scientific), and pEF6 hMD2-Myc-His (Invitrogen) comprised the TLR4 signaling complex. The TLR4 and CD14 vectors were a gift from Dr. Soumita Das, UCSD. The MD2 vector is from Dr. Michael F Smith,

GlaxoSmithKline. pcDNA3 hTLR4-YFP (plasmid 13018) and pcDNA3 TLR2-YFP (plasmid 13016) were purchased from Addgene.

Mice

Age- and sex-matched C57BL/6 mice between 6 and 10 weeks of age were used for the harvesting of primary macrophages. BAI1 knockout mice have been described previously (227). TLR4 knockout mice were purchased from Jackson Laboratories (stock # 007227). Mice were housed in pathogen-free conditions.

Isolation and culture of cells

293T and Cos7 cells were cultured in DMEM (4.5 g/L glucose, Gibco) supplemented with 10% FBS and 1% penicillin-streptomycin (pen-strep). CHO cells were cultured in αMem (Gibco) containing 10% FBS and 1% pen-strep. To generate BMDMs, cells were seeded onto non-tissue culture treated plastic plates and cultured in RPMI supplemented with 10% FBS, 10% L929-conditional medium (as a source of CSF1), and 1% pen-strep. BMDMs were cultured for 6 days ex vivo before use, and the culture medium was changed every 2 days. Macrophage differentiation was confirmed by flow cytometric analysis of the cell surface abundances of F4/80 (eBioscience, clone BM8) and CD11b (eBioscience, clone M1/70).

Bacterial strains and culture

All bacteria, including *E. coli* DH5α (Invitrogen, 18265-017), BW25113 (*E. coli* Genetic Stock Center Keio collection parent strain (311)), or *Salmonella* Typhimurium SL1344 ΔinvG were cultured overnight in LB broth under aerobic conditions before use. *Salmonella* Typhimurium SL1344 ΔorgA, ΔspiA (ΔSPIΔSPI2 double mutant) was a gift from Dr. Denise Monack, Stanford University. Immunofluoresence microscopy was

performed using WGA-labeled bacteria where indicated. Δspa *Staphylococcus aureus* Newman strain (313) was a gift from Dr. Alison Criss, University of Virginia, through Dr. Eric Skaar at Vanderbilt University.

Immunoblotting

2.5×10^5 wild type and BAI1-knockout BMDMs were plated in 12-well tissue culture treated dishes. The following day, cells were stimulated in RPMI + 10% heat inactivated FBS with bacteria at an MOI of 25 or 100ng/ml *S.* Typhimurium (Sigma). When indicated cells were pre-treated with Cytochalasin D (Sigma) at 1 μg/ml or DMSO vehicle control for 30 minutes, then treated with bacteria. Cells were lysed in RIPA buffer supplemented with protease inhibitors (1mM aprotinin, pepstatin, leupeptin, and PMSF), plus EDTA, sodium orthovanadate, and sodium fluoride. Cell lysates were separated by SDS PAGE, then transferred to PVDF membrane. Antibodies used include: phospho-Ser^{396} IRF3 (Cell Signaling, 4947), phospho-Ser^{172} TBK1 (Cell Signaling, 5483), IκBα (Cell Signaling, 4812), phospho-Thr^{180}/Tyr^{182} p38 (Cell Signaling, 4511), phospho-Thr^{183}/Tyr^{185} JNK (Cell Signaling, 9255), phospho-$Thr^{202}Tyr^{204}$ p44/42 ERK (Cell Signaling, 4370), and α-Tubulin (Sigma).

Immunoprecipitation

7.5×10^5 293T or LR73 CHO cells were plated in 60mm dishes overnight then infected with bacteria at an MOI 150. Cells were lysed in 50 mM Tris HCl, pH 7.4, 150mM NaCl, 1mM EDTA, and 1% Triton X-100 plus protease inhibitors. Lysates were pre-cleared with CL4B beads by spinning at 13,000 x *g,* and BAI1-Flag was immunoprecipitated using ANTI-FLAG M2 Affinity Gel (Sigma, A2220) rotating overnight at 4 degrees. After washing, samples were prepped using reducing conditions containing β-

mercaptoethanol or non-reducing conditions as indicated and analyzed using immunoblotting with the following antibodies: anti-HA tag (Covance), anti-Myc tag 91D10 (Cell Signaling), anti-GFP (Life Technologies, A11122), and anti-Flag (Sigma).

Quantitative RT-PCR

Macrophages from wild type and BAI1-knockout mice were infected with *E. coli* BW25113 at an MOI of 25 for 30 minutes at 37 degrees in RPMI containing 10% heat inactivated FBS to allow for internalization. After 30 min of uptake, cells were treated with gentamicin (500 μg/ml, Gibco) for 30 min to kill extracellular bacteria to prevent outgrowth of bacteria in the media. Media was then replaced with low gentamicin (10 μg/ml) for the remaining time. After four hours, total RNA was isolated using RNAeasy kit with DNAase treatment to remove genomic DNA contaminant, in accordance with manufacturer's instructions (Qiagen). Complementary DNA was generated with Superscript II (Invitrogen). TaqMan Real-Time PCR master mix was used for RT-PCR with according to the manufacturers protocol (ThermoFisher Scientific). The following primers were used for analysis: TNF-α (Mm00443258_m1), CXCL1 (Mm04207460_m1), IL-10 (Mm004439614_m1), IFN-β (Mm00439552_m1), CCL5 (Mm01202428_m1), and BAI1 (Mm001195143_m1).

TLR4 Internalization Assay

The internalization assay was modified from Kagan et al. BMDMs from control or BAI1-knockout animals in RPMI + 10% heat inactivated FBS were stimulated in suspension with *E. coli* BW25113 at an MOI of 25 over a time course. Cells were then placed on ice for the remainder of the experiment. Cells were blocked in DPBS with 10% FBS and 5% NGS with FcR blocking antibody (eBioscience, clone 93) for 10 minutes, then labeled

with Biotin-labeled anti-TLR4-MD2 (clone SA15-21), a gift from Dr. Jon Kagan, Harvard Medical School, for one hour. Cells were washed then labeled with Streptavidin-APC (Biolegend, 405027) and fixed prior to flow cytometric analysis of the cell surface TLR-MD2 signal.

Immunofluoresence microscopy

Cos7 cells were transfected by nucleofection using program W001 with pEBB-hBAI1-GFP, pUNO1-hTLR4a-HA3x, pEF6-hMD2-Myc-His, pCMV-SPORT6-hCD14. pcDNA3.1+ empty vector was used to normalize DNA quantity used for transfection. 1×10^5 cells were plated on fibronectin coated coverslips overnight then infected with either *S. aureus* or *E. coli* DH5α, pre-labeled with Alexa Fluor 647-conjugated WGA (Life Technologies, 5 μg/ml, in HBSS), at an MOI of 25. Images were captured with a Nikon C1 Plus confocal microscope with Z-stacks at 0.5-μm. Analysis and processing was performed with NIS-Elements software (Nikon). Cell-associated bacteria were defined as ROIs for analysis of the association between BAI1, TLR4, and bacterial stimuli.

Statistical analysis

Statistical analysis was performed with GraphPad Prism 5 software. Statistical significance was set at the 5% standard. All analysis was two-tailed. Graphs show means ± SEM. When appropriate, Two-way ANOVA with Bonferroni post-hoc comparisons was used for analysis. Information represented in the figure legend indicates the analysis regarding the two independent variables (e.g. time and cell type) and whether there is an interaction between them. Statistical information represented on the graph refers to the post-hoc comparison. In all data sets, $*P < 0.05$, $**P < 0.01$, $***P < 0.001$, $****P < 0.0001$. The number of independent experimental replicates is indicated by *N*. The

number of ROIs used for analysis in imaging quantification is denoted by *n*.

Chapter 4:

Recognition of Gram-negative bacterial LPS by BAI1

The following work represents unpublished work in progress.

Billings, E. A. performed all experiments and analysis shown in Chapter 4. Ravichandran, K.S. and Goldberg, J.B. provided critical reagents required for this Chapter. Casanova, J. E. provided intellectual guidance.

Chapter 4 Recognition of Gram-negative bacterial LPS by BAI1

Abstract

Recognition of bacterial LPS is critical for host defense against Gram-negative bacteria and the regulation of local inflammatory responses at sites of host-microbial interface. BAI1 is a phagocytic PRR that displays distinct specificity and function relative to the dominant LPS-receptor, TLR4, which recognizes the lipid A region of LPS and is not inherently phagocytic. Recognition and binding of Gram-negative bacteria by BAI1 occurs through five TSRs in the extracellular domain that selectively detect the core oligosaccharide of canonical enteric LPS structures. However, the exact moiety within the LPS structure being recognized was not known. This study expands upon previous observations by further defining the specificity of BAI1 for bacterial LPS. Using a heterologous cell system, we found that phosphorylation of the inner core L-glycero-d-manno-heptose moiety appears to be critical for uptake via BAI1-driven mechanisms. The phosphorylation of the inner core oligosaccharide of LPS is critical for membrane stability and function and is conserved across many microbes, indicating that BAI1 may play a broad role in the innate immune response to Gram-negative bacteria. The recognition of this conserved component of the Gram-negative bacterial cell wall strengthens the potential relevance of BAI1 in innate immunity, reveals which pathogens may be recognized by BAI1 in greater detail, and provides contextual evidence for the mechanisms behind the biophysical interactions between the TSR domains and their cognate ligands.

Introduction

PRRs have evolved to recognize conserved molecular features found on and in microbes to distinguish self from non-self. These molecular motifs, defined as MAMPs, are often highly conserved across the respective classes of microbes and are typically distinct from host structures. For example, exposed components of the microbial cell wall, including β-glycans and zymosan in fungi (342-344), peptidoglycan and lipotechoic acid in Gram-positive bacteria (95, 345), and LPS in Gram-negative bacteria (108, 346) are selectively recognized by PRRs. A notable exception to this is the detection of microbial nucleic acids, which share structural and biochemical features with the host. The recognition of microbes in the extracellular space by humoral or cell associated receptors is critical for neutralization, initiation of inflammatory responses, and phagocytosis. The importance of this interaction between host and microbe is further emphasized by the targeted modification of MAMPs by pathogens and commensals to evade and modulate the host immune system.

LPS, or endotoxin, is a vital component of the Gram-negative bacterial outer membrane that contributes to pathogenicity, membrane stability, expression and folding of outer membrane proteins, and vesicle shedding (347, 348). The canonical LPS structure is composed of three regions: a highly conserved lipid A region, a core oligosaccharide, and a highly variable terminal O-antigen (302, 349-351) (**Fig. 4-1**). LPS is synthesized sequentially by forming the lipid A region first, then covalently linking sugar molecules and units to extend into the core oligosaccharide and O-antigen regions (346, 348). Bacteria expressing the O-polysaccharide are phenotypically defined as expressing smooth LPS, while mutants lacking this structural feature are defined as rough

based early observations of colony morphology (352). Functionally, lipid A provides an anchor in the outer membrane and confers the majority of the immunostimulatory properties of endotoxin through an interaction with TLR4-MD2 (346, 349, 353-355). Crystallographic studies have shown that five lipid chains of LPS are bound by MD2 within a large hydrophobic pocket, allowing for the remaining acyl chain and the two phosphate groups from the lipid A backbone to be displayed on the surface of MD2 for presentation to TLR4 (270, 302). The phosphates play a critical role in forming charge and hydrogen bonds with MD2 and TLR4. In contrast, the core oligosaccharide makes minimal contact with the TLR4-MD2 complex, forming weak ionic and hydrogen bonds (270). Pathogens and gut resident microbes that modify the phosphate moieties and net negative charge of the lipid A molecule poorly stimulate TLR4 driven inflammatory responses (346, 356, 357).

The lipid A proximal, inner core oligosaccharide is also highly conserved, indicating its critical role in structural integrity. Accordingly, until very recently the inner most part of the core disaccharide backbone of lipid A consisting of two 3-deoxy-D-manno-otulosonic acid (KDO) moieties was considered the minimal structure necessary for bacterial viability (346). Deep rough mutants that lack the majority of the core oligosaccharide display altered membrane composition and susceptibility to cationic peptides, detergents, and bacterial killing (358, 359). The inner core oligosaccharide consists of two KDO molecules attached to three heptose residues (346, 360). The heptosyl backbone is covalently attached to the outer core, a trisaccharide backbone that displays more variability than the inner core (360). The highly variable O-antigen, composed of linked oligosaccharides that vary in length and composition, is attached to

the outer core oligosaccharide. This region serves as a critical virulence factor as it has been shown to inhibit phagocytosis and to promote escape from humoral and adaptive immunity (361, 362).

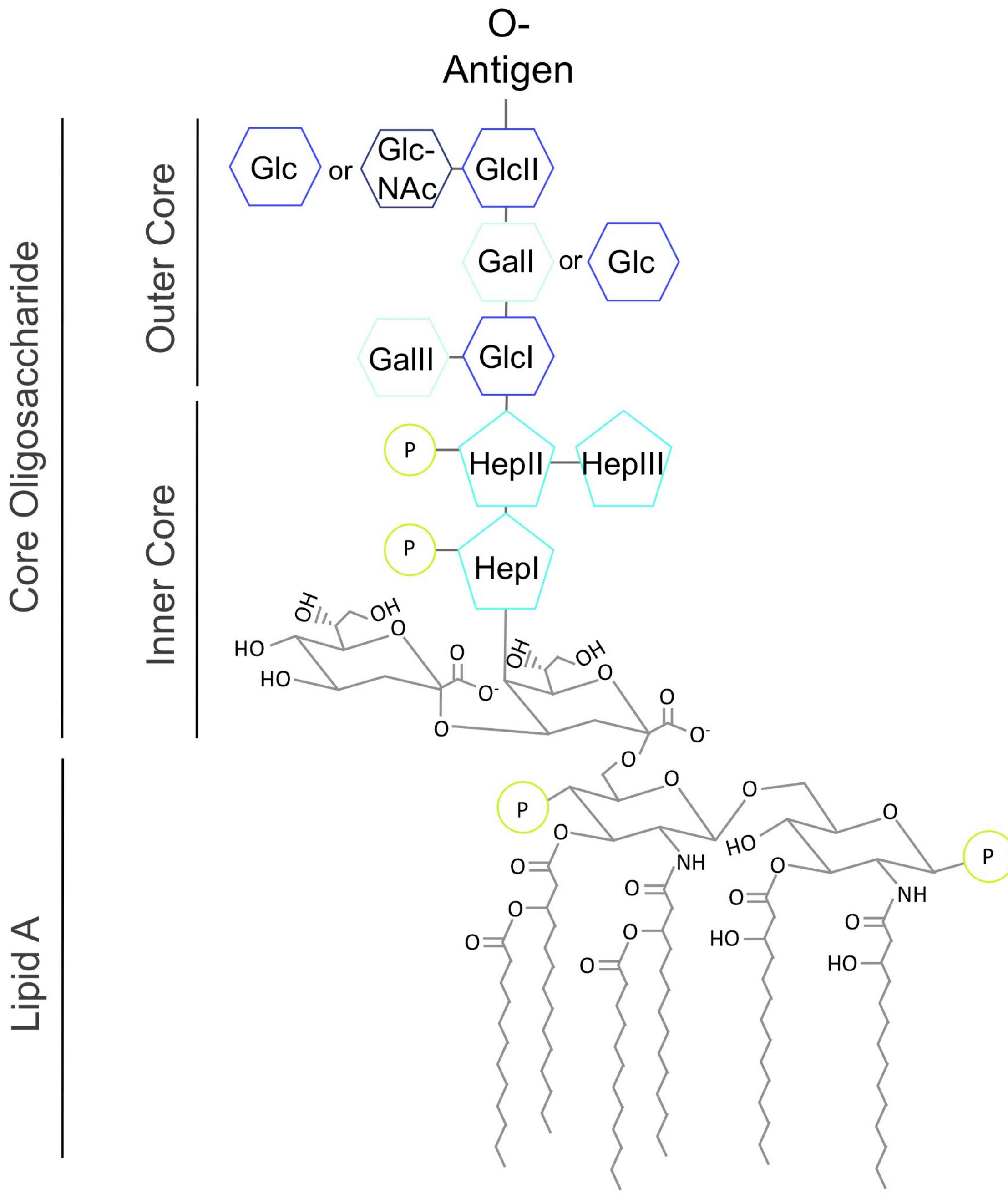
O-
Antigen
Core Oligosaccharide
Outer Core
Inner Core
Lipid A
Glc
or
Glc-
NAc
GlcII
GalI
or
Glc
GalII
GlcI
P
HepII
HepIII
P
HepI
HO
HO
O
O-
OH
OH
NH
NH
P
P

Figure 4-1. Structure and composition of canonical enteric lipopolysaccharide from *Salmonella*

LPS is composed of a lipid A region, a core oligosaccharide, and O-antigen. The core oligosaccharide is covalently linked with the polysaccharide O-antigen, forming the designated "smooth" phenotype. LPS lacking the O-antigen are designated as "rough" strains. Synthesis occurs through a series of coordinated biochemical steps starting with the production of lipid A (346, 348), composed of a diphosphorylated glucosamine dimer linked to several fatty acid chains (346, 349, 353). The inner core oligosaccharide consists of two KDO moieties attached to three heptosyl residues. The heptose sugars in the inner core undergo phosphorylation (346, 360). The heptosyl backbone is attached to the outer core, a trisaccharide backbone that displays more variability than the inner core (360). The highly variable O-antigen, composed of linked oligosaccharides that vary in length and composition, is attached to the outer core oligosaccharide.

Several PRRs have been shown to bind LPS, with diverse consequences on host responses. For example, Caspase-11, a cytosolic component of the non-canonical inflammasome, binds the lipid A region of LPS found in the cytoplasm of infected cells to induce inflammasome activity (271, 272, 363). Other host proteins have been shown to bind the core oligosaccharide. Surfactant protein D (SP-D) is a soluble CLR that recognizes the heptose moieties within the core oligosaccharide of LPS (274). Another CLR, DC-SIGN (SIGNR1), recognizes the outer core oligosaccharide of LPS (275). Extracellular matrix proteins, such as TSP-1, also function in bacterial attachment. TSP-1 recognizes peptidoglycan in the Gram-positive bacterial cell wall (264). The related protein mindin (spondin2) binds both Gram-positive and Gram-negative microbes via recognition of carbohydrate moieties in lipotechoic acid or LPS through a direct interaction with a single type I TSR (265, 267). Common features found in many mammalian proteins mediating microbial recognition include positive charge, hydrophobicity, and amphipathicity (356).

BAI1 is a member of subgroup VII of the adhesion-type GPCRs that acts as a phagocytic receptor for apoptotic cells and bacteria. Similar to mindin (spondin2) and TSP-1, which are soluble secreted proteins, BAI1 contains TSRs in its extracellular region (226). Consistent with the role of TSR domains in other contexts, work from our laboratory showed that the BAI1-TSRs were required for bacterial recognition and phagocytosis (226). However, unlike mindin (spondin2) and TSP-1, BAI1 specifically and selectively recognized Gram-negative bacteria through an interaction dependent on the core oligosaccharide of LPS. However, the importance of this interaction on the

innate immune response is not known. Moreover, the precise ligand recognized by BAI1 remains unidentified. Insight on the specificity of this interaction would provide greater understanding of the breadth and importance of BAI1 for immunity to Gram-negative bacteria and may shed light onto how BAI1 recognizes both apoptotic cells and LPS.

In this chapter, we determined that phosphorylation of the core oligosaccharide was critical for BAI1-mediated recognition, as bacterial mutants unable to phosphorylate the core heptose moieties were no longer phagocytosed in a BAI1-dependent manner. Consistent with our previous findings, BAI1 was able to recognize Ra-type LPS expressing bacteria that express the inner core oligosaccharides, but was unable to mediate the internalization of deep rough mutants (Re-type LPS). However, select deep rough mutants were internalized to a greater extent in BAI1-expressing cells relative to control fibroblasts, suggesting that the interaction between BAI1 and bacteria may be affected by global bacterial surface composition and structure in addition to LPS chemotype. The specificity of BAI1 for the phospho-heptose sugars in the inner core oligosaccharide suggests broad importance for recognition of Gram-negative bacteria, as this region is conserved across many resident and pathogenic bacteria alike.

Results

The outer core oligosaccharide of Salmonella is dispensable for BAI1 recognition

We previously determined that BAI1 mediates the binding and internalization *Salmonella enterica* serovar Typhimurium, a representative Gram-negative bacterial pathogen, in several cell culture model systems (226). Das et al showed that the recombinant BAI1 ectodomain (GST tagged BAI1-RGD-TSR) bound wild type, smooth LPS and rough (Ra chemotype) LPS, lacking the polysaccharide O-antigen in binding assays. However, LPS isolated from a deep rough mutant (Re chemotype) and peptidoglycan from Gram-positive bacteria were not recognized, indicating that BAI1 selectively recognizes a component of the core oligosaccharide in bacterial LPS. We established that fibroblasts (LR73 CHO cells) expressing exogenous BAI1 internalized *E. coli* strain DH5α more efficiently than did control, non-BAI1-expressing cells (**Fig. 2-1**). *E. coli* DH5α naturally expresses rough (Ra chemotype) LPS, indicating that the internalization assay recapitulated the preliminary findings of the solid phase binding assay performed by Das et al.

To further examine the specificity of BAI1-LPS interactions, we analyzed the ability of BAI1 to recognize and internalize a set of *Salmonella* mutants that lack components of the core oligosaccharide. These strains contained defects in the enzymes that synthesize the LPS core. Since synthesis of the LPS occurs sequentially, mutations result in a truncated LPS structure. **Figure 4-2A** lists the strains, LPS chemotypes, and descriptions used in this study, while **Figure 4-2B** shows a cartoon of the truncated core oligosaccharide expressed in each respective strain.

For this analysis we used fibroblasts stably expressing exogenous BAI1 and a standard gentamicin protection assay (**Fig. 4-3**). Consistent with previous observations that suggested BAI1 recognizes bacteria expressing smooth and rough variants of LPS, fibroblasts expressing BAI1 internalized significantly more wild type (SL3770) and rough strains of *Salmonella* Typhimurium LT2 (SL3749, SA1627) compared to control cells (**Fig. 4-4, A to C**). Similarly, LPS mutants expressing truncations in the outer core oligosaccharide were also recognized in a BAI1-dependent manner. This included *Salmonella* lacking N-acetyl glucosamine side chains (SL733), the terminal glucose moiety (SL3750) (**Fig. 4-4, D and E**), and galactose side chains (SL1306) (**Fig. 4-4F**). *Salmonella* expressing LPS truncated before the second hexose moiety in the outer core (SL3748) (**Fig. 4-4G**) or LPS lacking the outer core oligosaccharide entirely (SL3769) (**Fig. 4-4H**) were also phagocytosed at a higher rate in cells expressing exogenous BAI1.

Interestingly, truncations into the outer core oligosaccharide resulted in an increase in the fold difference between control and BAI1-expressing cells, suggesting that deletion of the outer core promoted BAI1-ligand interactions by further exposing a structural component required for binding to the TSRs (**Fig. 4-5**). Collectively, these results indicated that the composition of the outer core oligosaccharide of *Salmonella* does not impact BAI1 binding and internalization.

BAI1-mediated recognition of Salmonella requires the expression of phosphorylated heptoses in the inner core oligosaccharide

We next analyzed the internalization of inner core oligosaccharide mutants in wild type and BAI1-expressing fibroblasts. Similar to the outer core oligosaccharide mutants, *Salmonella* expressing LPS truncated before the terminal heptose moieties

(SL3789) were phagocytosed significantly more efficiently in BAI1 expressing cells (**Fig. 4-4I**). However, we observed a relative decrease in the amount of BAI1-dependent internalization between the inner core mutant and strains lacking components of the outer core oligosaccharide (**Fig. 4-5**).

Through deductive reasoning, this perhaps indicated that the first heptose sugar within the inner core oligosaccharide was critical for BAI1-dependent recognition. The LPS of many enteric Gram-negative bacteria is phosphorylated on the KDO-proximal heptose. This modification is critical for membrane integrity and susceptibility to detergents and cationic peptides. Interestingly, a mutant deficient in the phosphorylation of the inner core oligosaccharide (SH7770) was not recognized by BAI1 in the gentamicin protection assay (**Fig. 4-4J**), indicating that phospho-heptose may be critical for bacterial binding by the TSRs. BAI1-expressing fibroblasts did not internalize *Salmonella* that lacked the core oligosaccharide (Re chemotype) (SL1102, SA1377) more efficiently than control cells, consistent with solid phase binding assays (**Fig. 4-4, K and L**). Thus the recognition of LPS by BAI1 requires the presence of phospho-heptose structures within the core oligosaccharide.

A

Strain	Phenotype	Description
SL3770	WT	Smooth
SL3749	Ra	Rough, no O-Ag
SA1627	Ra	Rough, no O-Ag
SL733	-	No core GlcNAc
SL3750	Rb2	Lack 3rd Hexose
SL3748	Rb3	Lack 2nd Hexose
SL1306	Rc	Lack Galactose
SL3769	Rd1	Hexoseless
SH7770	-	Lack phospho-HepI
SL3789	Rd2	Lack HepII, HepIII
SL1102	Re	Heptoseless
SA1377	Re	Heptoseless

B

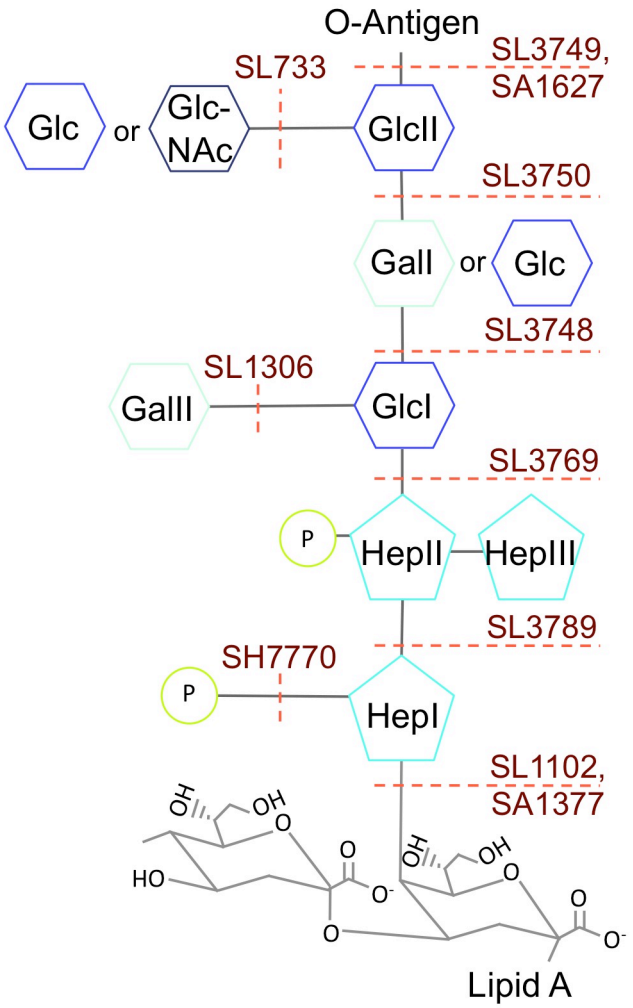

Figure 4-2. List and description of Salmonella LPS mutants used in this study

(**A**) Fig. 4-2A contains the list of Salmonella LPS mutants used in this study, the LPS chemotype or phenotype, and the description of the truncation in the LPS structure. (**B**) Schematic of the core oligosaccharide structure of respective LPS mutants described in (A).

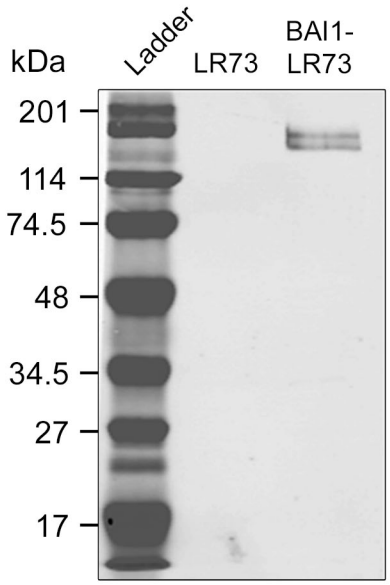
kDa
Ladder
LR73
BAI1-
LR73
201
114
74.5
48
34.5
27
17

Figure 4-3. Measurement of protein expression in LR73 control cells or cells stably expressing BAI1

LR73 control cells and cells exogenously expressing BAI1 are maintained under puromycin selection. Cell lysates were probed with an anti-BAI1 antibody (Allele Biotechnology, ABP-PAB-10421) to confirm maintenance of BAI1 expression. BAI1 is detected as two bands in LR73 cells, with no visible cleavage products at the predicted sites described in Chapter 1.

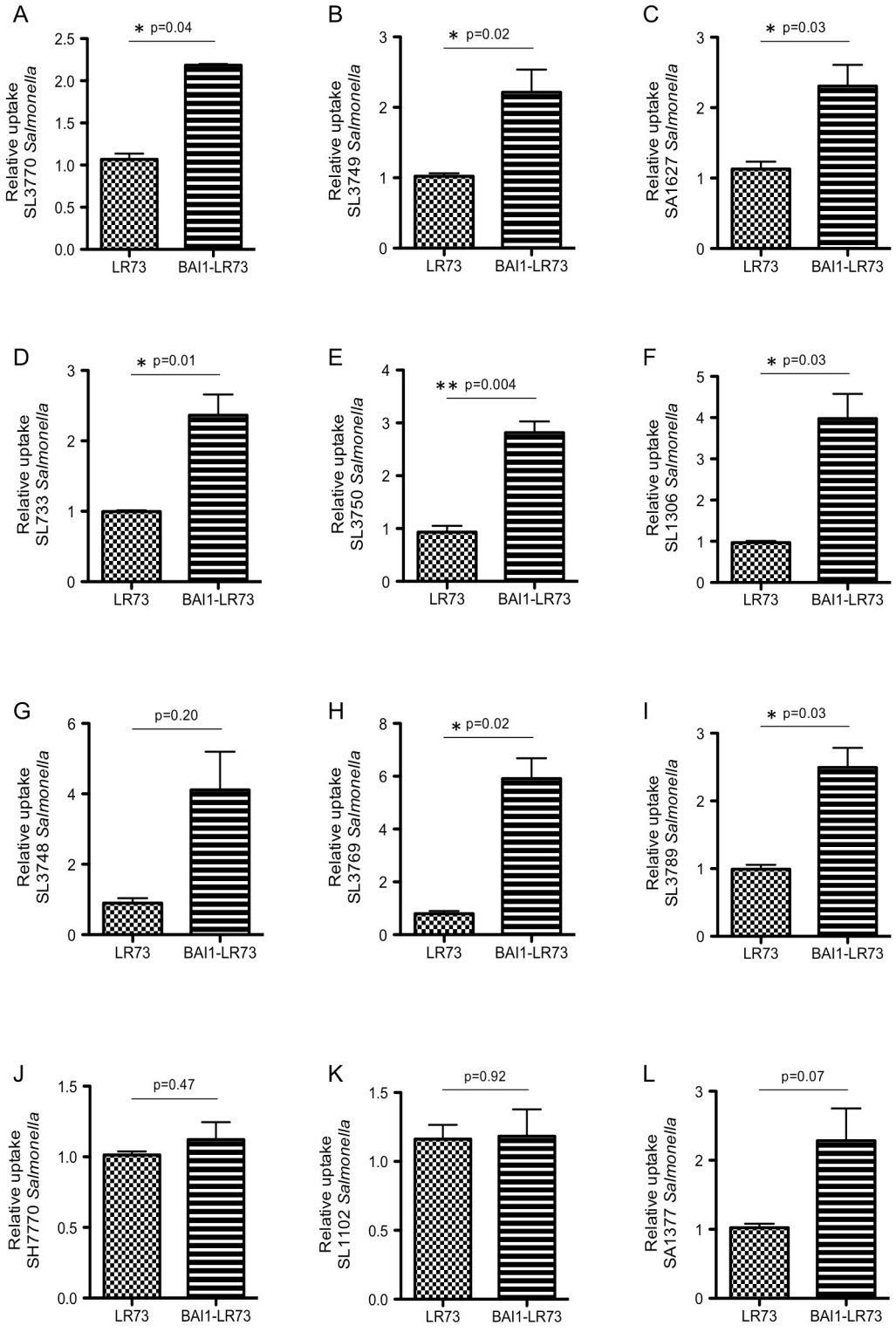
A
* p=0.04
Relative uptake SL3770 Salmonella
2.5
2.0
1.5
1.0
0.5
0.0
LR73
BAI1-LR73
B
* p=0.02
Relative uptake SL3749 Salmonella
3
2
1
0
LR73
BAI1-LR73
C
* p=0.03
Relative uptake SA1627 Salmonella
3
2
1
0
LR73
BAI1-LR73
D
* p=0.01
Relative uptake SL733 Salmonella
3
2
1
0
LR73
BAI1-LR73
E
** p=0.004
Relative uptake SL3750 Salmonella
4
3
2
1
0
LR73
BAI1-LR73
F
* p=0.03
Relative uptake SL1306 Salmonella
5
4
3
2
1
0
LR73
BAI1-LR73
G
p=0.20
Relative uptake SL3748 Salmonella
6
4
2
0
LR73
BAI1-LR73
H
* p=0.02
Relative uptake SL3769 Salmonella
8
6
4
2
0
LR73
BAI1-LR73
I
* p=0.03
Relative uptake SL3789 Salmonella
3
2
1
0
LR73
BAI1-LR73
J
p=0.47
Relative uptake SH7770 Salmonella
1.5
1.0
0.5
0.0
LR73
BAI1-LR73
K
p=0.92
Relative uptake SL1102 Salmonella
1.5
1.0
0.5
0.0
LR73
BAI1-LR73
L
p=0.07
Relative uptake SA1377 Salmonella
3
2
1
0
LR73
BAI1-LR73

Figure 4-4. BAI1-mediated internalization of *Salmonella* specifically requires phosphorylated heptose molecules in the inner core oligosaccharide

The internalization of the *Salmonella* LPS mutants listed in Fig. 4-1A were measured in Fig. 4-4 (A) to (L) in parental LR73 CHO cells and cells stably expressing exogenous BAI1 using the gentamicin protection assay as described in Materials and Methods. Data shown include the mean fold internalization ± SEM. Data were analyzed using the Student's t-test with Welch's correction to account for unequal variances. The strain used is listed below, followed by the *P* value, and the number of experimental repeats (*N*). (**A**) SL3770, **P* < 0.05, *N* = 2 (**B**) SL3749, **P* < 0.05, *N* = 5 (**C**) SA1627, **P* < 0.05, *N* =4 (**D**) SL733, **P* < 0.05, *N* = 4 (**E**) SL3750, ***P* < 0.01, *N* = 3 (**F**) SL1306, **P* < 0.05, *N* = 3 (**G**) SL3748, *N* = 2 (**H**) SL3769, **P* < 0.05, *N* = 3 (**I**) SL3789, **P* < 0.05, *N* = 3 (**J**) SH7770, *N* = 3 (**K**) SL1102, *N* = 5 (**L**) SA1377, *N* = 4

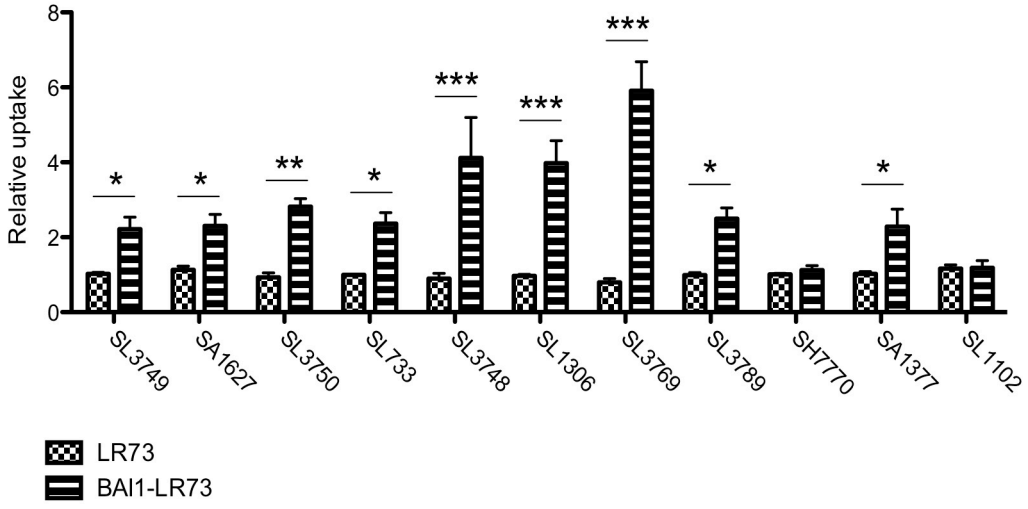
Relative uptake
8
6
4
2
0
*
*
**
*
***
***
***
*
*
SL3749
SA1627
SL3750
SL733
SL3748
SL1306
SL3769
SL3789
SH7770
SA1377
SL1102
LR73
BAI1-LR73

Figure 4-5. Relative internalization of Gram-negative bacteria with truncated LPS structures

The internalization of the *Salmonella* LPS mutants listed in Fig. 4-2A were measured in parental LR73 CHO cells and BAI1-CHO cells stably expressing exogenous BAI1 as described in Fig. 4-4. The data shown here reflects the relative BAI1-dependent internalization across all LPS mutants normalized to control cells. Here, data was analyzed with 2-way ANOVA with Bonferroni post-hoc comparison. *$P < 0.05$, **$P < 0.01$, ***$P < 0.001$

Soluble LPS competes with whole bacteria for BAI1 attachment

While the evidence above indicated that the interaction between BAI1 and LPS is mediated by the recognition of phospho-heptose moieties within the inner core oligosaccharide, the specific binding of LPS in the context of bacterial phagocytosis had not been directly measured. This is particularly important given that the surface structures present on the exposed outer leaflet of bacteria vary when LPS structures are altered. To confirm the specificity of BAI1 for LPS in a cell based assay, we used a modified gentamicin protection assay, where control and BAI1-expressing fibroblasts were pretreated with soluble LPS, then infected with non-invasive, ΔinvG *Salmonella.* Exposure to LPS prior to infection competitively inhibited the internalization of non-invasive *Salmonella*, indicating that BAI1 binds both soluble and bacteria-associated LPS structures (**Fig. 4-6A**). This confirmed the findings from the solid phase binding assays and suggested that BAI1 specifically and selectively recognized LPS, independent of other features exposed on the bacterial surface and independent of interactions with other PRRs.

BAI1 dependency on phospho-heptose moieties is not an off target effect due to altered invasiveness and motility

In addition to receptor driven internalization, *Salmonella* utilizes a type three secretion system (T3SS) to inject effector molecules into host cells to drive internalization or invasion. The *Salmonella* strains used in this study are invasive, but the expression of functional T3SS required for invasion is affected by truncation of LPS molecules. The expression of flagella, which contributes to motility and promotes host cell contact, has also been linked to LPS structure (364-368). To better control for altered

invasion and motility, we utilized a modified version of the competitive inhibition assay described above. Here, control and BAI1-expressing fibroblasts were pretreated with intact dead bacteria for 30 minutes, then treated with viable non-invasive *Salmonella.* Again, BAI1-expressing fibroblasts internalized significantly more bacteria compared to control cells. Pretreatment with either heat inactivated (HIA) or PFA-fixed *Salmonella* competitively inhibited the BAI1-dependent internalization of viable ΔinvG *Salmonella* (**Fig. 4-6B**). *Salmonella* expressing LPS without the O-antigen (Ra-chemotype, SL3749) or the outer core oligosaccharide (SL3769) inhibited the internalization of viable bacteria in BAI1-expressing cells, while *Salmonella* lacking phosphorylated heptose I or inner core oligosaccharide (Re-chemotype, SL1102) did not (**Fig. 4-6C**). This confirmed that the presence of phospho-heptose moieties within the inner core oligosaccharide was critical for BAI1-dependent recognition and internalization.

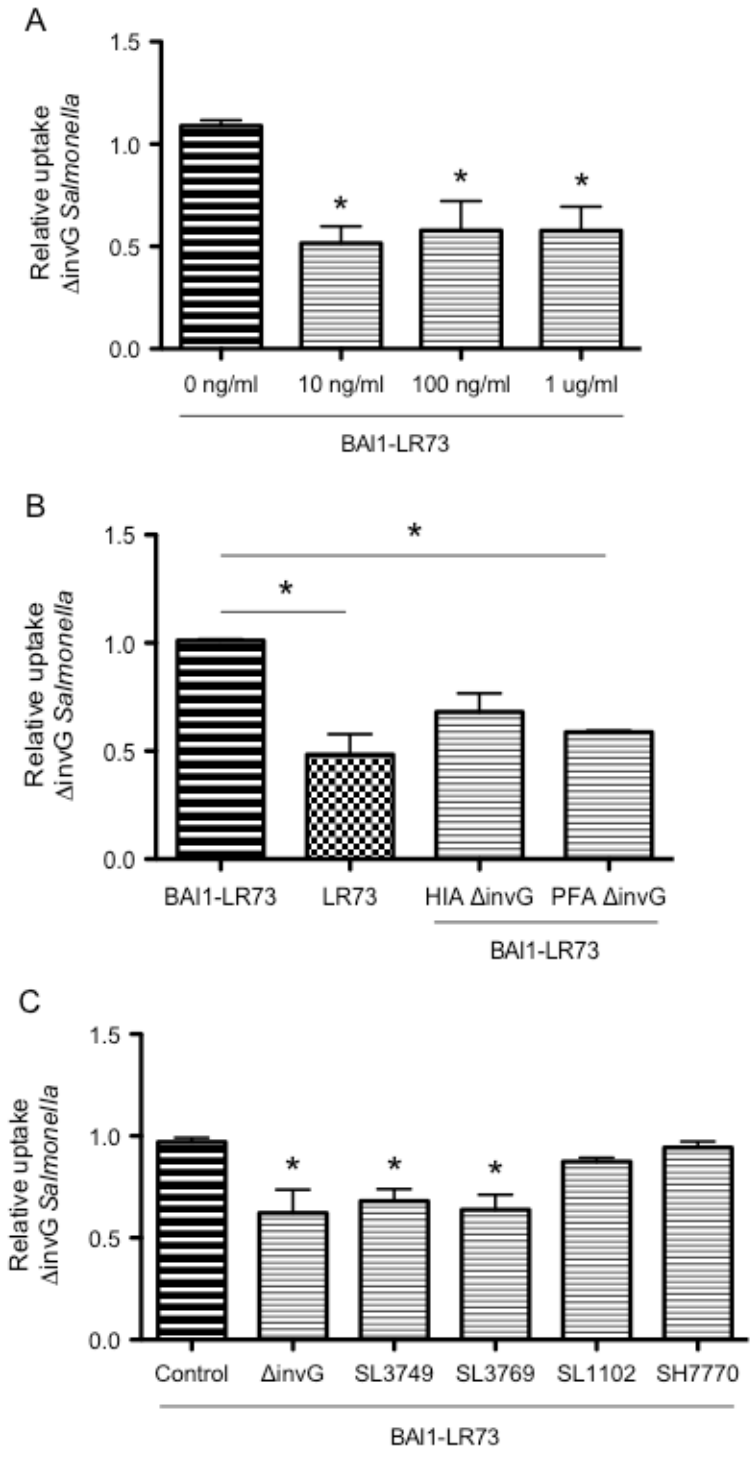
A
Relative uptake ΔinvG Salmonella
1.5
1.0
0.5
0.0
*
*
*
0 ng/ml
10 ng/ml
100 ng/ml
1 ug/ml
BAI1-LR73
B
Relative uptake ΔinvG Salmonella
1.5
1.0
0.5
0.0
*
*
BAI1-LR73
LR73
HIA ΔinvG
PFA ΔinvG
BAI1-LR73
C
Relative uptake ΔinvG Salmonella
1.5
1.0
0.5
0.0
*
*
*
Control
ΔinvG
SL3749
SL3769
SL1102
SH7770
BAI1-LR73

Figure 4-6. BAI1-dependent internalization of *Salmonella* does not require other surface structures present on the Gram-negative bacterial membrane and is not directly impacted by altered motility and invasion due to LPS defects

The internalization of non-invasive ΔinvG *Salmonella* was measured in LR73 fibroblasts using the gentamicin protection assay as described above with select modifications. (**A**) Cells stably expressing BAI1 were pre-treated with soluble LPS at the indicated concentrations for 30 minutes before addition of *Salmonella*. Data shown includes the mean fold internalization ± SEM, relative to the untreated cells. Statistical analysis was performed using one-way ANOVA with Tukey's multiple comparisons post-test. **P* < 0.05, *N* = 3 (**B**) Cells were treated as in (A), except that either HIA or PFA killed ΔinvG *Salmonella* (MOI of 25) were used to competitively inhibit uptake of viable bacteria in BAI1-expressing fibroblasts. One-way with Tukey's multiple comparisons post-test was used for statistical analysis. **P* < 0.05, *N* = 2 (**C**) Graph shows mean fold internalization of viable ΔinvG *Salmonella,* with and without pre-treatment with PFA fixed ΔinvG *Salmonella* or *Salmonella* LPS mutants (MOI 25). Statistical analysis was performed as in (A) and (B), **P* < 0.05, *N* = 3

Receptor specificity of the BAI1-TSR domains for phosphorylated heptose moieties in the inner core oligosaccharide of LPS is recapitulated in an isogenic E. coli K-12 mutant collection

Finally, although the *Salmonella* LPS mutants utilized in **Figure 4-4** and **Figure 4-6** are all derived from the parental strain *S.* Typhimurium LT2, they are not isogenic. For example, some carry additional mutations relative to the wild type strain (e.g. SA1627), which may alter their behavior and interaction with host cells independent of LPS structure. To expand upon the observations made with *Salmonella*, we instead used a set of isogenic *E. coli* K-12 BW25113 LPS mutants derived from the Keio collection, a publically available single-gene deletion mutant library (**Fig. 4-7, A and B**). As we observed for *Salmonella*, fibroblasts expressing BAI1 internalized significantly more bacteria expressing wild type, rough LPS and LPS lacking the outer core oligosaccharide (rfaG) (**Fig. 4-8, A and B, Fig. 4-9**). In contrast, mutants lacking either the inner core oligosaccharides (rfaF) or only the phosphate on heptose I (rfaP) were not recognized by BAI1, also similar to what we had observed with *Salmonella* (**Fig. 4-8, C to E**). Surprisingly, however, further truncation of LPS resulting in a loss of all heptoses (rfaC and rfaE) restored the ability of BAI1 to recognize and internalize the mutant bacteria, with the exception of a single LPS mutant (rfaD) (**Fig. 4-8, F to H**). We observed a similar phenomenon with *Salmonella*, in which one of the deep rough LPS mutants, although not statistically significant, was phagocytosed to a greater extent in the context of BAI1. Collectively, this indicated that the phosphorylation of the core oligosaccharide is critical for BAI1-mediated internalization, but a complete lack of inner core oligosaccharides allows BAI1 to recognize the mutant bacteria. Whether this is due to

recognition of lipid A or the KDO moieties appended to it, or some other feature of the mutant bacterial membrane will require further investigation.

A

Strain	Phenotype	Description
K-12 BW25113	Ra	Rough
waaG, rfaG	Rd1	Rough, Lack outer core
waaF, rfaF	Rd2	Lack HepII, HepIII
waaP, rfaP	-	Lack phospho-HepI
waaC, rfaC	Re	Heptoseless
waaD, rfaD	Re	Heptoseless
waaE, rfaE	Re	Heptoseless

B

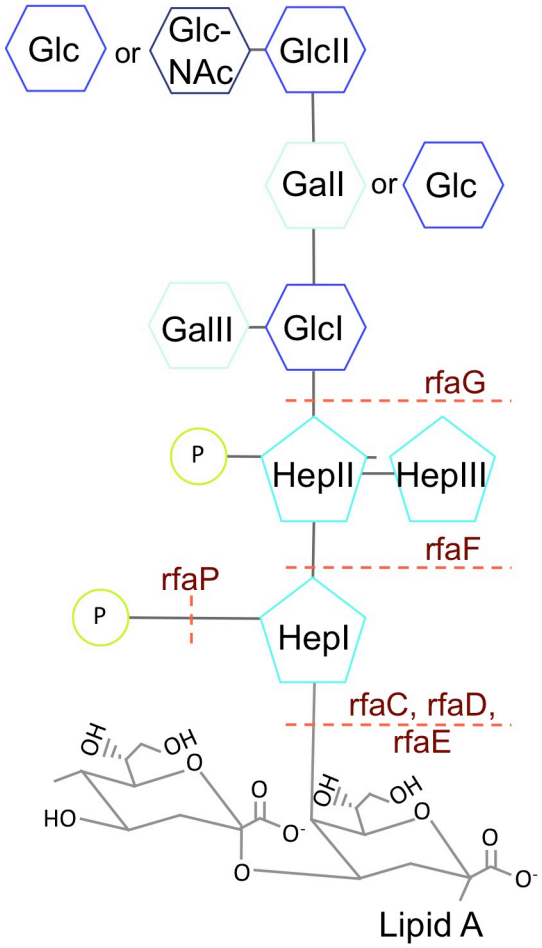

Figure 4-7. List and description of *E. coli* K-12 LPS mutants used in this study

(**A**) Fig. 4-7A contains the list of *E. coli* K-12 BW25113 LPS mutants used in this study, the LPS chemotype or phenotype, and the description of the truncation in the LPS structure. (**B**) Schematic of the core oligosaccharide structure of respective LPS mutants described in (A).

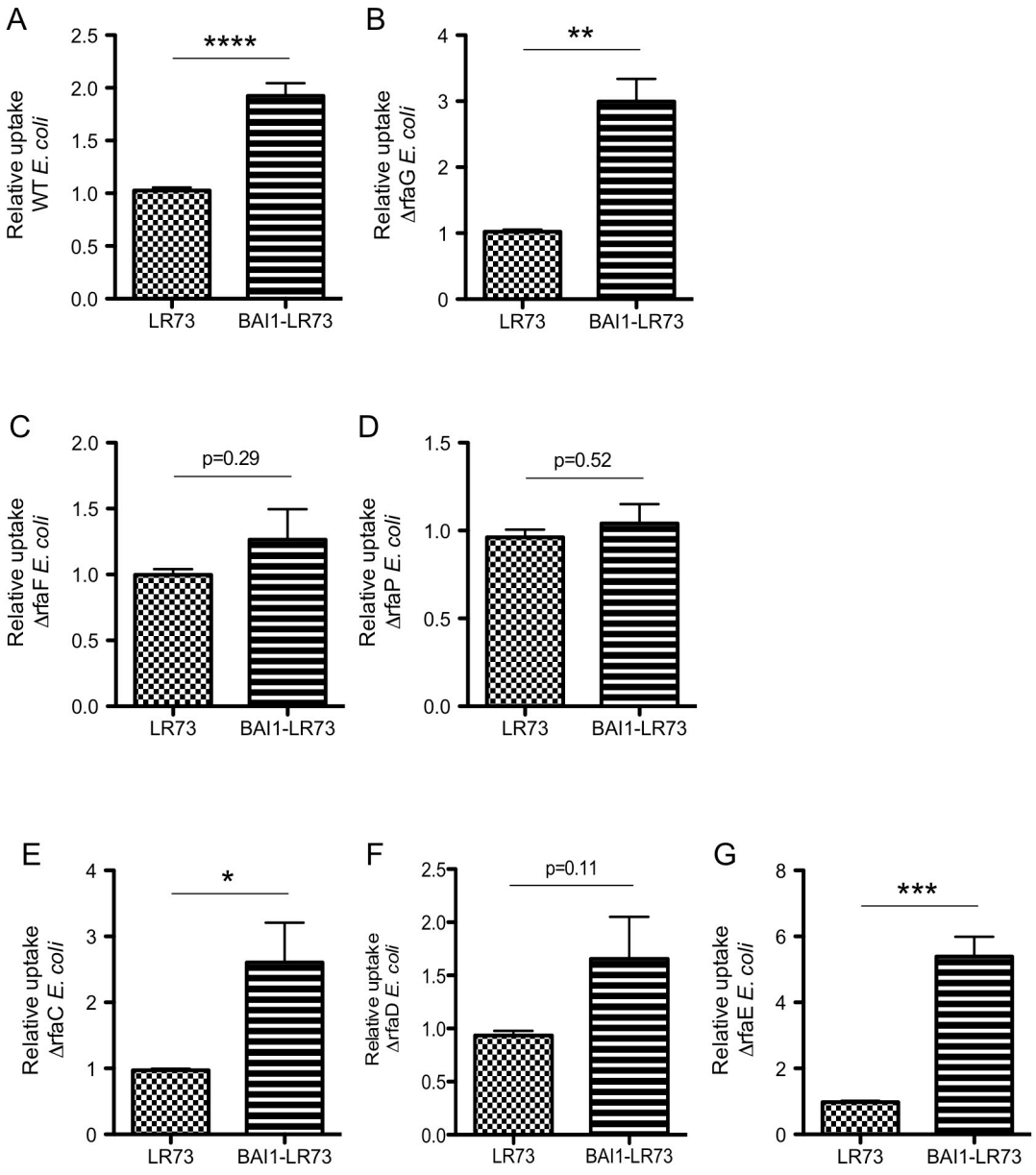
A
Relative uptake WT E. coli
****
LR73
BAI1-LR73
B
Relative uptake ΔrfaG E. coli
**
C
Relative uptake ΔrfaF E. coli
p=0.29
D
Relative uptake ΔrfaP E. coli
p=0.52
E
Relative uptake ΔrfaC E. coli
*
F
Relative uptake ΔrfaD E. coli
p=0.11
G
Relative uptake ΔrfaE E. coli
***

Figure 4-8. Phagocytosis of *E. coli* K-12 in a BAI1-dependent manner requires phosphorylated heptose sugars in the inner core oligosaccharide and can be compensated for in bacteria expressing deep rough mutant LPS

The uptake of the *E. coli* LPS mutants listed in Fig. 4-7A were measured in Fig. 4-8 (A) to (G) in BAI1-expressing LR73 CHO cells and control cells using the gentamicin protection assay as describe above. Data shown include the mean fold internalization ± SEM. Data were analyzed using the Student's t-test with Welch's correction to account for unequal variances. The strain used is listed below, followed by the *P* value, and the number of experimental repeats (*N*). (**A**) WT, ****$P < 0.0001$, $N = 14$ (**B**) ΔrfaG, **$P < 0.01$, $N = 6$ (**C**) ΔrfaF, $N = 7$ (**D**) ΔrfaP, $N = 13$ (**E**) ΔrfaC, *$P < 0.05$, $N = 6$ (**F**) ΔrfaD, $N = 8$ (**G**) ΔrfaE, ***$P < 0.001$, $N = 7$

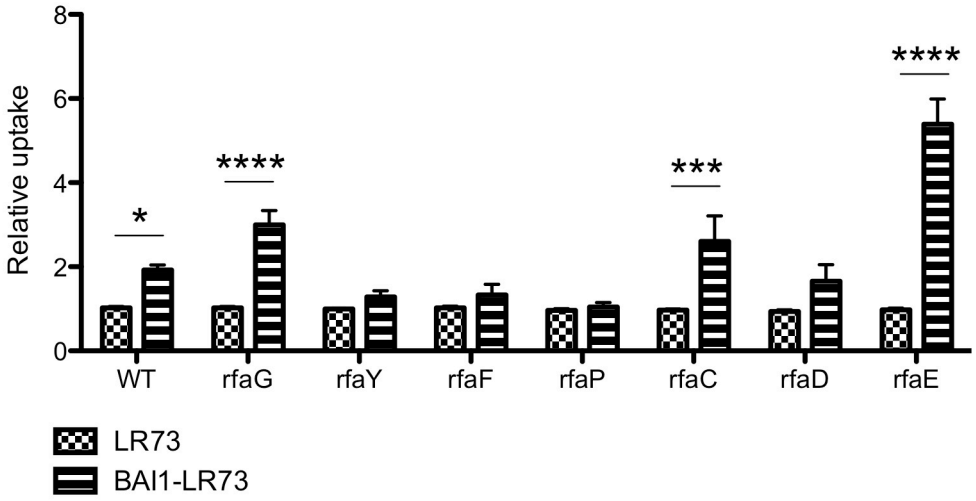
Relative uptake
8
6
4
2
0
*
****
***
****
WT
rfaG
rfaY
rfaF
rfaP
rfaC
rfaD
rfaE
LR73
BAI1-LR73

Figure 4-9. Relative internalization of Gram-negative bacteria with truncated LPS structures

Control and BAI1-expressing fibroblasts were analyzed for the internalization of the *E. coli* LPS mutants listed in Fig. 4-7A were measured as described in Fig. 4-8. Fig. 4-9 shows the comparative presentation across all LPS mutants normalized to control conditions. Data was analyzed with 2-way ANOVA with Bonferroni post-hoc comparison. $*P < 0.05$, $***P < 0.001$.

Discussion

The detection of bacteria occurs through the interaction of PRRs and conserved molecular motifs expressed on and within microbes, otherwise called MAMPs. We recently defined BAI1 as a novel PRR that directly binds and drives the internalization of Gram-negative bacteria (226). This interaction required the five TSRs in the extracellular domain of BAI1, which selectively bound Gram-negative bacteria. The interaction between BAI1 and LPS is direct and requires the core oligosaccharide region of LPS for binding. Importantly, this is distinct from the region of LPS recognized by TLR4, which binds to the acyl chains and diglucosamine backbone of LPS (302). In this study, we further defined the specificity of BAI1 by measuring the internalization of Gram-negative bacteria expressing truncated forms of LPS in a heterologous model system. Furthermore, we confirmed earlier in vitro findings in a cell-based system, which allowed for the analysis in the context of the functional consequences of BAI1 recognition (e.g. phagocytosis). BAI1 bound LPS in cell-based assays and mediated the internalization of bacteria expressing both smooth and rough LPS variants. Our results indicated that the presence of phosphorylated L-glycero-d-manno-heptose residues in the inner core oligosaccharide of LPS are required to mediate recognition of both *S.* Typhimurium and *E. coli,* two representative Gram-negative microbes.

The phosphorylation of the first heptose molecule within the inner core oligosaccharide was required for BAI1 mediated uptake in all cases. The dependency on secondary phosphorylation sites within the core differed between *Salmonella* and *E. coli*. Phosphorylation within the core oligosaccharide is less efficient in LPS molecules truncated above the second heptose molecule of the inner core oligosaccharide,

predominately at the second phosphorylation site (369, 370). Despite a reduced abundance of phosphorylation, we observed efficient BAI1-dependent internalization of Δ*waaG E. coli* and *Salmonella* lacking the second heptose moiety (SL3789), indicating that the remaining phosphorylation on the KDO-proximal heptose was sufficient for BAI1 recognition. Collectively, these results suggest that the exposure of the phospho-heptose moiety impacts TSR binding.

Although this analysis indicated that BAI1 recognizes phospho-heptose moieties in LPS, the results are not conclusive. We found that despite expressing the same canonical LPS structures, select deep rough mutants (Re-chemotype) were also recognized by BAI1. The Re LPS structure terminates after two KDO units attached to the lipid A region. In both *E. coli* and *Salmonella* spp. three genes are required for LPS synthesis (371): waaC (rfaC), a heptosyl transferase required for addition of the first heptose molecule (372), waaD (rfaD), an epimerase which converts the precursor molecule (373), and waaE (rfaE), the enzyme responsible for the synthesis of the donor molecule (374-376). This perhaps indicates that BAI1 does not specifically recognize the phosphorylated heptose structure, but instead relies on the net negative charge of the core oligosaccharide. Alternatively, this may indicate a difference in the global surface composition between LPS core oligosaccharide mutants that influences a specific or non-specific interaction with BAI1. In addition to enhanced susceptibility to cationic peptides and antimicrobials, deep rough mutants display altered membrane composition, including decreased expression of membrane proteins, a loss of lipid asymmetry in the outer leaflet of the membrane (377), and altered and increased phospholipid content (347, 348, 378, 379). These compensatory changes may alter interactions with BAI1. Consistent with this

hypothesis, others have observed that mutations in the genes that regulate the formation of Re-type LPS described above differentially affect interactions with PRRs, irrespective of having the same LPS structure (380).

The five TSRs in the BAI1 extracellular domain are the recognition site for both LPS and exposed phosphatidyl serine on apoptotic cells (225-227, 260). The highly conserved TSR domains consist of ~60 amino acids, which form three anti-parallel strands that interact by interlacing and stacking arginine and tryptophan side chains (266, 277). The front face of the TSR contains a positively charged groove that likely mediates protein interactions as the recognition face of the molecule (266, 267). Like phosphatidylserine, BAI1-mediated recognition of LPS appeared to require the presence of a negatively charged core oligosaccharide, consistent with electrostatic or charge interactions contributing to the specificity and function of this receptor.

The importance of LPS as a structural component of Gram-negative bacteria is exemplified the strikingly small number of Gram-negative bacteria lacking LPS (381) and the requirement of lipid A for viability (382). Accordingly, bacteria expressing extremely truncated forms of LPS display viability defects and physiological changes (383, 384). Some bacterial pathogens and commensal microbes are capable of modifying the net negative charge of LPS and the core oligosaccharide in response to environmental signals, perhaps making this interaction more complex (357, 360, 385). Importantly, the phosphorylation of the inner core is highly conserved in LPS structures of Gram-negative bacteria. Mutants lacking phosphoryl substituents in the inner core show defects similar to those observed with deep rough mutants, which is thought to be due to impaired membrane stability due to a loss of crosslinking within the lipid membrane (386).

Specifically, mutants show increased susceptibility to detergents and antimicrobial peptides (368), and display attenuated virulence in vivo (387). Collectively, these findings strengthen the potential of BAI1 for recognizing a relatively invariant motif found in many Gram-negative bacteria.

Materials and Methods

Isolation and culture of cells

LR73 CHO cell lines have been described previously (225) and were cultured in αMem, (Gibco) containing 10% FBS and 1% pen-strep under selection with puromycin to maintain BAI1 expression (Invitrogen).

Bacterial strains and culture

All bacteria were cultured overnight in LB broth under aerobic conditions before use. *E. coli* BW25113 parent strain and LPS mutants are listed in Figure 4-5 (A) and (B) were from the *E. coli* Genetic Stock Center Keio collection (311). The *Salmonella enterica* serovar Typhimurium LT2 wild type and LPS mutants, originally from the *Salmonella spp.* Genetic Stock Center, were a gift from Dr. Joanna Goldberg at Emory University. ΔinvG *Salmonella* Typhimurium SL1344 was used in gentamicin protection assays as a control when appropriate.

Gentamicin protection assay

The gentamicin protection assay was performed as described previously (226). Briefly, 5 x 10^4 LR73 cells/well were seeded into 24-well plates 18 hours before infection. Cells were incubated with bacteria at an MOI of 50 for 30 min at 37°C in αMEM containing 10% heat-inactivated FBS, after spinning bacteria onto the cells at 500 x g for 5 min at

4°C to synchronize uptake. After 30 min of internalization, cells were treated with gentamicin (500 μg/ml, Gibco) for 60 min to kill extracellular bacteria, but leave intracellular bacteria viable. For soluble competition assays, LR73 cells were pretreated with *S.* Typhimurium LPS at 100 ng/ml or with non-viable *Salmonella* spp. at an MOI of 50. Heat inactivation by incubation at 56 degrees Celsius for 30 min or fixation with 4% paraformaldehyde for 15 minutes was used to kill bacteria for competition assays with whole microbes.

Binding assay

Bacterial attachment was measured using colony forming assay. Fibroblasts were plated overnight. The following day cells were treated with Cytochalasin D at 1 μg/ml for 30 mins in αMEM containing 10% heat-inactivated FBS, then infected with ΔinvG *Salmonella* at an MOI of 50 for 30 min.

Chapter 5:

Conclusions and future perspectives

Chapter 5 Conclusions

BAI1-TSR receptor specificity

Conclusions and future directions

The research presented in Chapter 4 investigated the specificity of the TSRs of BAI1 for Gram-negative bacteria. Prior to this study, there was limited knowledge on the interaction between BAI1 and bacterial LPS. We had previously shown that BAI1 selectively recognized Gram-negative bacteria, and that this event was dependent on the core oligosaccharide of LPS. Here, we confirmed this finding. We show that BAI1 mediates the internalization of both *E. coli* and *Salmonella* spp. expressing smooth and rough variants of LPS. Furthermore, we determined that BAI1-mediated recognition and subsequent internalization of Gram-negative bacteria requires the expression of phospho-heptose moieties in the inner core oligosaccharide of LPS. Lack of the inner core phosphorylation epitope results in a loss of BAI1-mediated internalization of both *Salmonella* spp. and *E. coli*, indicating that this result is generalizable across bacteria with canonical enteric LPS structures (**Fig. 4-1**).

However, we observed some discrepancies with bacteria expressing deep rough mutants of LPS that completely lack the core oligosaccharide. Loss of the entire core oligosaccharide has been shown to result in enhanced susceptibility to detergents and antimicrobials, as well as altered membrane architecture and form. Changes in the composition of the outer membrane may compensate for the loss of BAI1-specific epitopes in a specific or non-specific manner. In particular, expression of the Re-chemotype of LPS has been associated with increased phospholipids in the outer leaflet and a loss of lipid asymmetry in the outer membrane of Gram-negative bacteria. Park et

al showed that recombinant BAI1-TSRs recognize the phospholipid phosphatidylserine to mediate the attachment and internalization of apoptotic cells (225) (**Fig. 1-9**). Analysis of the specificity of the ectodomain of BAI1 for phospholipid species in that study indicated that BAI1 binds other charged phospholipids, including phosphatidic acid, phosphatidylinositol-4 phosphate (PI(4)P), sulphatide and cardiolipin. Perhaps the enrichment and exposure of novel phospholipid species in the bacterial outer leaflet promotes interactions with the BAI1-TSR domain, despite lacking phospho-heptose moieties within the inner core. Alternatively, a change in the surface features of the bacteria may promote attachment and internalization through other means.

Several mammalian proteins distinguish bacterial membranes from host membranes on the basis of enriched negative charge. The TSR domain is known to bind bacterial products in other contexts. TSP-1 binds the peptidoglycan in the Gram-positive bacterial cell wall, while mindin (spondin2) recognizes sugar moieties present in LPS and lipotechoic acid. The structure of this conserved protein domain contains a positively charged groove, which is thought to be the recognition face. The properties of this region vary based on the strength of the positive charge and the placement of post-translational modifications, including C-mannosylation (**Fig. 1-10**). Accordingly, the five TSRs present in the extracellular region of BAI1 have varied charge properties, with TSR3 and TSR5 containing the most overall positive charge and a positively charged binding face (**Fig. 1-10**). The lipid A region of LPS was not required for BAI1-TSR binding in solid phase assays. It would be interesting to determine if loss of the phosphorylation motifs on the di-glucosamine backbone would affect BAI1-mediated recognition in a similar capacity to the loss of phospho-epitopes in the core oligosaccharide.

As noted above, the loss of the phospho-heptose moieties in the core region has deleterious effects on the bacterial membrane, resulting in the introduction of multiple variables that may impact host-microbe interactions. Instead, analysis of the specificity of the TSR domains for the core oligosaccharide and the phospho-heptose moieties in isolation may be better for assessing receptor specificity. This could be done using cell-based assays with LPS purified from wild type and core oligosaccharide mutant strains of *E. coli* BW25113. The use of purified LPS would avoid any defects in bacterial physiology due to LPS structure, such as altered motility and fimbrae expression, which would impact interactions with host cells. This approach would also account for the complex compensatory changes in the architecture and composition of the outer leaflet of the Gram-negative bacterial outer membrane that may vary across the LPS mutants analyzed in this study (387). Synthetic core oligosaccharide could be used in a similar manner (274, 388). Binding to purified LPS could be assessed using solid phase assays with the recombinant ectodomain of BAI1, effectively removing the impact of BAI1-independent interactions with Gram-negative bacteria. Collectively, this may provide further context for the enhanced phagocytosis of deep rough *Salmonella* spp. and *E. coli* mutants observed in BAI1-expressing fibroblasts compared to control cells. Further analysis of the interaction between BAI1 and the phospho-heptose molecules in the inner core oligosaccharide using such simplified model systems should therefore be pursued.

The conservation of phosphorylated inner core structures in Gram-negative bacterial pathogens

The inner core oligosaccharide of LPS is conserved across many bacterial species and plays a critical role in the structure and function of the outer membrane of Gram-

negative bacteria. Bacteria lacking phosphorylation within the core oligosaccharide display similar phenotypes to mutants expressing deep rough variants of LPS. This includes a loss of membrane integrity due to impaired crosslinking across the membrane and greater susceptibility to detergents and antimicrobial compounds (368, 386). As such, bacterial pathogens that lack the necessary phosphorylation machinery are vastly attenuated for survival in vivo (387). In addition to *E. coli* and *S. enterica* serovar Typhimurium, which have canonical enteric LPS structures, several other bacterial pathogens express phosphorylated sugars in the inner core oligosaccharide. The core oligosaccharide of *Pseudomonas* spp. is highly phosphorylated and contributes to virulence (389, 390). Unlike *E. coli* and *Salmonella,* phosphorylation is required for viability. Evidence suggests that *B. cenocepacia* also requires the inner core phospho-sugars for survival in animal models (391). As shown in Chapter 2, BAI1 mediates the activation of ROS responses and bactericidal activity against both *P. aeruginosa* and *B. cenocepacia*, indicating that BAI1-dependent recognition is relevant for those bacterial species. According to the results provided in Chapter 4, this is likely to be through detection of the conserved phospho-heptose moieties in the core oligosaccharide.

Some bacterial pathogens are able to modify the negative charge of the inner core oligosaccharide or express other negatively charged structures within this region. For example, *Klebsiella pneumoniae*, *Neisseria meningitidis*, and *Haemophilus influenzae* express heptose molecules modified with phosphoethanolamine, pyro-phosphoethanolamine, or galacturonic acid (360, 392-394). *Vibrio* spp. and *Haemophilus* spp. may also contain a phosphorylated KDO molecule that can replace or account for the necessary negative charge in the LPS structure (394, 395). It is unknown whether those

modifications alter interactions with BAI1, so further analysis of representative Gram-negative bacteria with distinct core oligosaccharide components and modifications may provide further context for the specificity and relevance of BAI1-mediated recognition across many Gram-negative bacterial pathogens. The importance of phosphorylation in the core oligosaccharide for bacterial fitness and pathogenicity for many bacterial pathogens (e.g. *Pseudomonas* spp., *B. cenocepacia, Salmonella* spp., and *E. coli*) indicates that the interaction between BAI1 and Gram-negative bacteria may be generally important in the context of many pathogens.

Distinguishing between bacterial and host molecular patterns

This study provided insight into the specificity of the TSR domains for the bacterial LPS, but many outstanding questions remain. Although the downstream cellular responses during the detection of apoptotic cells and Gram-negative bacteria differ, BAI1 interacts with both using the TSR domains as the recognition face. Phosphatidyl serine displays a negatively charged head group adjacent to a lipid domain, indicating that certain properties of the recognition of apoptotic cells and Gram-negative bacterial LPS are shared. Consistent with this, several receptors recognize both altered self ligands and bacterial products, and antibodies targeting LPS cross react with apoptotic cells (103, 262, 263, 396). Comparative biophysical analysis of the interaction between the TSR domains and phosphatidyl serine or LPS would provide insight into whether and how BAI1-ligand interactions differ depending on context. For example, it is not known whether all five TSRs interact with LPS, if there is cooperativity among the TSR domains, or if TSRs function separately in distinct contexts. The CLESH domain, which mediates the interaction between TSR domains and CD36, varies slightly from the

consensus sequence across the TSR domains in BAI1. Additionally, the linker region between the first and second TSR domains is considerably longer than the other linker regions and is cleaved in certain contexts, perhaps suggesting distinct functionality. Probably most important for the interaction between BAI1 and bacterial and apoptotic cell ligands is that each of the TSR domains express unique total and surface charge at the predicted binding face. It is possible that the relative amount of positive charge and any post-translational modifications alter the interactions of individual TSR domains with apoptotic cells versus bacteria based on the relative negative charge of phosphatidylserine or LPS.

There is also relatively little known on how BAI1 transduces the extracellular recognition event to the cytoplasmic domain to couple to phagocytic signaling. Receptor cleavage at the GPS site within the GAIN domain is thought to impact receptor signaling in other members of the adhesion GPCR sub-family (**Fig. 1-8**). However, cleavage of BAI1 in macrophages has not been observed and it is remains unknown whether cleavage occurs in a context-dependent manner and whether it impacts downstream signaling responses in this cell subset. The signaling response required for the phagocytosis of apoptotic cells and Gram-negative bacteria is known. The engagement of the TSRs in the context of both stimuli results in the activation of the bipartite GEF, ELMO-Dock (possibly Dock2 in macrophages), leading to Rac activation and cytoskeletal rearrangement. It would be interesting to determine if the interaction between BAI1 and apoptotic cells or Gram-negative bacteria triggers differences in the signaling response that could account for the distinct outcomes associated with each recognition event. For example, the selective use of individual TSRs or the relative strength of the interaction

between the TSRs and their respective ligands may influence the relative strength and duration of Rac activation downstream of binding. Alternatively, it may impact the complete suite of signaling responses mediated by BAI1, which has the potential to couple to other proteins in addition to the ELMO-Dock-Rac signaling pathway. In particular, signaling to $G\alpha_{12/13,}$ signaling dependent on the C-terminal PDZ-motif of BAI1, such as the activation of RhoA GTPase, or signaling mediated through interactions with the cytoplasmic proline-rich region of BAI1, which associates with BAP2 (IRSp53), may be activated in a manner dependent on the TSRs engaged and the strength of those interactions. Much remains to be determined regarding the specificity and parameters of the interaction of the TSR domains with its respective ligands, although the importance of negatively charged epitopes in the core oligosaccharide and the presence of negatively charged head groups on phosphatidyl serine suggests that electrostatic charge interactions are a critical factor. Perhaps our altered selves have more in common with our microbial selves than previously appreciated.

<u>BAI1 as a phagocytic receptor</u>

Conclusions and future directions

Relatively little is known on how BAI1 impacts the activity and immune response of primary macrophages. Chapter 2 addressed this gap first by further characterizing the interaction between BAI1 and Gram-negative bacteria during phagocytosis, then by analyzing the impact of BAI1-mediated recognition on bacterial killing. As discussed previously, BAI1 acts as a phagocytic receptor specific for Gram-negative bacteria through signaling to the ELMO-Dock-Rac signaling module (226) (**Fig. 1-9**). Here, we extended those observations to show that BAI1 mediated the uptake of *E. coli* DH5α, in

addition to non-invasive *S.* Typhimurium, in heterologous cell systems. Furthermore, we confirmed the importance of BAI1 as a phagocytic receptor for Gram-negative bacteria in primary BMDMs (227). In this context, BAI1 was required for maximal internalization of *E. coli* DH5α, consistent with preliminary work.

We further expanded these observations by analyzing the cellular distribution of BAI1 during bacterial recognition (**Fig. 5-1**). BAI1 was found in the perinuclear region, on the plasma membrane, and within the cytoplasm in a punctate distribution. Importantly, BAI1 was selectively enriched at sites of bacterial association with *E. coli*, but not the Gram-positive pathogen *S. aureus.* BAI1 concentrated at sites of bacterial attachment and phagocytosis in live-cell movies, consistent with the role of BAI1 as a phagocytic receptor. These results indicated that BAI1 preferentially recognizes Gram-negative bacteria at the plasma membrane.

Phagocytosis in macrophages proceeds rapidly. Although analysis of the early events of bacterial recognition and phagocytosis provide additional evidence for a role of BAI1 in the process of phagocytosis, the role and distribution of BAI1 after uptake is unknown. The distribution of BAI1 at the plasma membrane is consistent with its role in activating a local pool of Rac to facilitate internalization. Interestingly, it is not known whether BAI1 is able to mediate the activation of Rac2 in macrophages. Moreover, the trafficking dynamics of BAI1 throughout the process of phagocytosis and phagosome maturation have not been assessed (**Fig. 5-1**). For example, in many cases phagocytic receptors remain associated with the phagosome after internalization for a period of time, perhaps influencing the local compartment through signaling and interactions with trafficking proteins and other PRRs. The scavenger receptor Dectin-1 is internalized and

maintained on the phagosomal compartment in the context of larger particles, and recycles to the cell surface in the context of low molecular weight ligands (397). In contrast, FcγRs are not enriched within endosomal networks and localize to the plasma membrane (193). Labeling with compartment-specific markers may reveal where and for how long BAI1 associates with bacteria, and where BAI1 resides under steady state conditions. Further analysis of the localization and duration of BAI1 with the bacterial phagosome may provide insight into additional roles BAI1 plays downstream of phagocytosis, which is particularly relevant for the modulation innate immune signaling as discussed below and in Chapter 3.

A better understanding of the kinetics and trafficking of BAI1 during infection would reveal insight into the when and for how long BAI1 modulates phagocytosis and immune responses. Analysis of the kinetics of BAI1 accumulation and disassociation from the phagosome could be performed using live cell imaging microscopy. Dectin-1 is degraded after internalization of large particles. Surface expression is renewed by de-novo synthesis, resulting in a longer period of turnover (397). It would be interesting to assess whether BAI1 recycles from the phagosomal compartment back to the cell surface, and whether the trafficking of BAI1 differs in the context of whole microbes versus soluble LPS. Collectively, this would reveal the overall kinetics and dynamics involved in BAI1-dependent immune responses, thereby providing insight into when and where BAI1 may be most important in the context of innate immune and bacterial clearance in vivo.

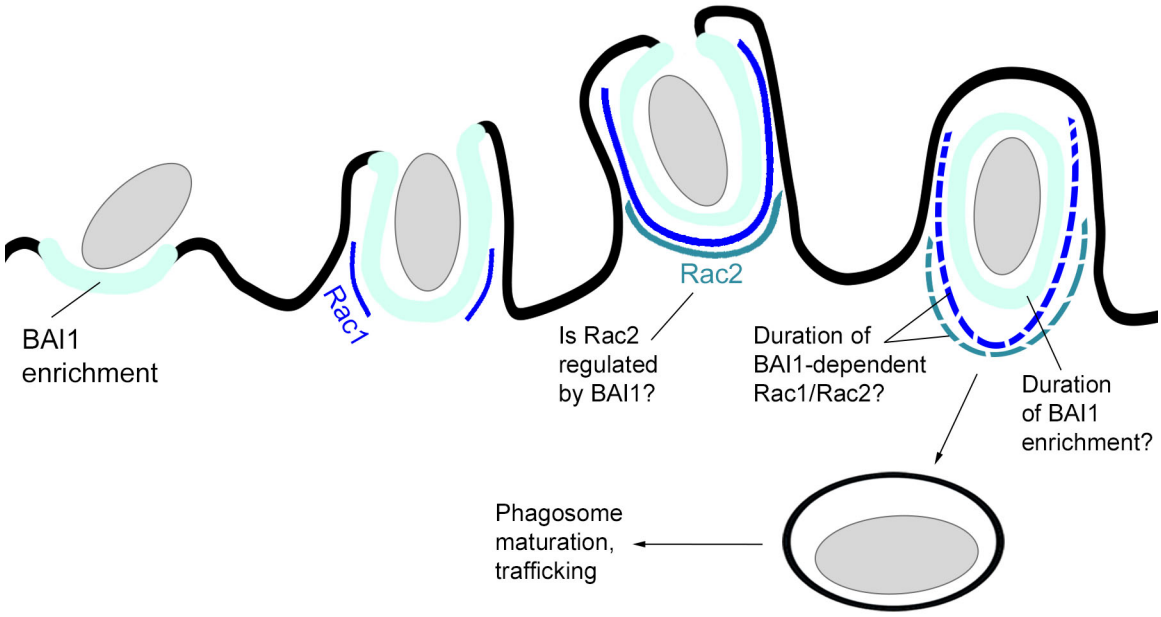
BAI1
enrichment
Rac1
Rac2
Is Rac2
regulated
by BAI1?
Duration of
BAI1-dependent
Rac1/Rac2?
Duration
of BAI1
enrichment?
Phagosome
maturation,
trafficking

Figure 5-1. Model of BAI1 enrichment at sites of bacterial phagocytosis

BAI1 is observed at sites of bacterial attachment with the formation of the phagocytic cup and remains in contact, extending to the tips and site of phagosome closer as internalization progresses. BAI1 remains enriched upon internalization for an undefined short period of time after phagosome closer. Rac2 is also found associated with the phagocytic cup and nascent phagosome, but it is not known whether Rac2 is regulated by BAI1. Moreover, the duration of the association of BAI1 with the bacterial phagosome, which may serve as a site of innate inflammatory signaling as described in Chapter 3, has not been assessed. We also observed that BAI1 is found on membrane ruffles, perhaps facilitating bacteria contact and attachment, and on the phagosome for an undefined period of time (data not shown).

Enhancing microbicidal activity through the ROS response in macrophages

Conclusions and future directions

Phagocytic receptors play a critical role in immunity by facilitating the killing and clearance of microbes from the extracellular space and educating the adaptive immune response. The route of cellular entry can markedly affect these downstream effects (117, 164). In fact, several bacterial pathogens target specific receptor-driven routes of cell entry to alter downstream responses and compartmentalization within macrophages (285-288). For example, internalization by CR3 or FcγR results in decreased phagosomal escape and intracellular replication of *Francisella tularensis* compared to entry via mannose receptor and SR-A (285). Alternatively, other bacterial pathogens target CR3-mediated entry in pathogenesis, indicating that this is a pathogen and cell-specific mechanism of manipulating host responses (288). In Chapter 2, we expand on the role of BAI1 as a phagocytic receptor for Gram-negative bacteria by examining the fate of microbes internalized in the context of BAI1 (**Fig. 5-2**). We defined a novel role for BAI1 in coupling phagocytosis with the activation of the phagocyte NADPH oxidase machinery and ROS production to promote oxidative killing of Gram-negative bacteria. BAI1-deficient macrophages exhibited decreased microbicidal activity against a range of Gram-negative bacterial species. This defect was due to reduced Rac1 activation in the absence of BAI1 and resulted in enhanced susceptibility to bacterial challenge. Although BAI1 can couple to Rac activation through Tiam1 during synaptogenesis (248), we found that signaling through ELMO-Dock is critical for the enhanced microbicidal activity observed. Given that the cellular mechanisms that couple upstream non-opsonic

phagocytic receptors with microbicidal machinery are poorly defined (170), this study provided novel mechanistic insight into how these cellular processes are coordinated.

The importance of the NADPH oxidase complex in host protection against bacterial infection is highlighted by the increased susceptibility to bacterial infection in patients with chronic granulomatous disease (CGD), who have deficiencies in specific components of the NADPH oxidase machinery (179, 180). Similar to humans, mice deficient in gp91phox, the catalytic subunit of phagocyte NADPH oxidase, are also highly susceptible to bacterial infections (298, 300, 305, 306). The attenuated microbicidal activity observed against Gram-negative bacterial pathogens *S.* Typhimurium, *P. aeruginosa,* and *B. cenocepacia* indicated that BAI1 broadly contributes to innate immune responses during infection. Future directions should investigate the role of BAI1 in other disease models to better define how BAI1 contributes to bacterial killing in those contexts.

Several aspects of the mechanistic interaction between BAI1 and the NADPH oxidase machinery have not been assessed. Despite the observed defect in ROS production that was dependent on BAI1-mediated Rac activation and the complete loss of ROS activity in gp91phox-deficient cells, we did not directly examine the activity the phagocyte NADPH oxidase complex in the context of BAI1 expression. The use of siRNA knockdown of components of the phagocyte NADPH oxidase complex would confirm the interaction with BAI1. Alternatively, the use of double knockout animals lacking both BAI1 and gp91phox would further emphasize whether the increased susceptibility to bacterial challenge observed in the BAI1 knockout animals was due to

defective ROS production or to additional effects on the innate immune response to LPS, discussed further below and in Chapter 3.

The process of internalization and activation of NADPH oxidase machinery has been investigated downstream of opsonic phagocytic receptors, including FcγR (**Fig. 1-7**). In addition to signaling responses, the subcellular distribution and local recruitment of NADPH oxidase regulatory subunits is critical for mounting ROS responses. This is in part dependent on lipid composition. Rac, p47phox, and p40phox express domains that promote association with phospholipid species (138, 185, 292, 295, 398, 399). Inflammatory stimuli trigger the trafficking and recruitment of the membrane bound components of the NADPH oxidase machinery as well. Specifically, LPS induces the redistribution of p22phox and gp91phox to intracellular compartments (194). In macrophages and heterologous cell lines these subunits are found on the plasma membrane, in the vicinity of the nascent phagosome, and enriched at the phagocytic cup during uptake. Rab11a is thought to participate in the trafficking and delivery of these subunits to the membrane during phagocytosis (193). Accordingly, in macrophages these proteins are also found within Rab11-positive recycling compartment and in the Rab5-postive early endosomal compartment. Rab27a has also been implicated in the delivery of NAPDH oxidase complexes to phagocytic cups and phagosomes (189, 194, 400). Finally, the autophagy adaptor protein Rubicon participates in NADPH oxidase delivery in response to TLR2 ligands, although the precise mechanism is unknown (172). While the role of Rubicon in promoting ROS responses in macrophages was selectively relevant for Gram-positive bacteria, Yang et al showed that it was required for optimal TLR4-NOX4-dependent ROS responses in certain cell types. This indicated that the role of Rubicon

may be generally relevant in TLR-NADPH oxidase pathways. Regardless, this highlights a complex network of crosstalk between autophagy machinery, phagocytosis, and ROS responses (172, 173).

It is clear that the processes of phagocytosis and the NADPH oxidase machinery are intimately tied. As such, it would be of interest to define the trafficking and distribution of these proteins in the context of BAI1 (**Fig. 1-7, Fig. 5-2**). Future analysis of the recruitment of the individual subunits of the NADPH oxidase machinery to sites of BAI1 enrichment, particularly at either the phagocytic cup or phagosome, would provide insight into the subcellular environment in which BAI1 interacts with the NADPH oxidase machinery. In addition to the cellular distribution and recruitment of the components of the holocomplex, upstream signaling from an activating receptor (e.g. TLRs) leads to the activation of protein kinases like PKC or Akt (158, 186) to mediate phosphorylation of regulatory subunits p47phox and p40phox. This event serves as the first signal mediating the formation and activation of the NADPH oxidase complex, with Rac activation as a necessary second signal. Analysis of the activation of the regulatory subunits of the NADPH oxidase complex should be assessed to confirm that Rac is the specific and dominant factor facilitating activation of NADPH oxidase machinery downstream of BAI1. For example, phosphorylation of p47phox and p40phox can be determined using immunoblotting. We propose that the upstream BAI1-dependent Rac activation and lipid composition changes accompanying phagocytosis provide a local enrichment of Rac1 and NADPH oxidase subunits priming the cell for downstream ROS responses.

The phagocytic NAPDH oxidase complex as described in Chapter 1 and Chapter 2 is expressed in phagocytes and is critical for host defense, however other NADPH oxidase complexes also produce ROS. In addition to the phagocyte NADPH oxidase (NOX2), macrophages also express NOX4 (401, 402). ROS production through NOX4 is poorly understood. Some studies indicate that it is dependent on Rac and p47phox, while others indicate that it is constitutively active when associated with p22phox, independent of cytosolic regulatory subunits (181, 403-406). Upon LPS stimulation, NOX4 directly interacts with the TIR domain of TLR4 to promote ROS responses and alter inflammatory signaling (402, 407). We think this pathway is not critical for the observed defect in ROS production in BAI1-deficient cells given the similarities between the gp91phox-knockout and BAI1-knockout cells and the complete loss of detectable ROS in gp91phox-deficient macrophages. Moreover, we do not observe defects in p38 MAPK activation in response to LPS, which occurs downstream of NOX4-TLR4-dependent signaling (Chapter 3). Direct analysis of the NOX4 pathway should be examined to confirm this assertion.

A role for BAI1 defined by cell and tissue-specific expression

Reactive oxygen species are derived from several cellular sources, including mitochondria or NADPH oxidase complexes. While other sources of ROS are often produced as by-products, the NADPH oxidase machinery is specifically dedicated to making ROS. Many cell subsets maintain the ability to produce reactive oxygen species through the use of NADPH oxidase complexes, and although the precise roles of this machinery in other contexts are largely unknown, it has been associated with redox signaling, ion channel function, proliferation, tissue repair, and cell death (178, 195, 406).

Other NOX isoforms, expressed in a cell and tissue specific manner play a role in host immunity (178, 408, 409). For example, the DUOX proteins maintain homeostasis and prevent barrier disruption by regulating ROS production and local inflammatory responses in the gut (409, 410). In Drosophila, loss of dDUOX, the fly homologue of mammalian DUOX, results in increased susceptibility and death due to infection with commensal and pathogenic microbes (411). The components and mechanisms of activation of other NADPH oxidase complexes vary from the phagocyte NADPH oxidase machinery. Rac has been implicated in the activation of NOX1, NOX3, and NOX4, while the activation of DUOX in mucosal epithelial cells is driven by GPCR-mediated calcium signaling independent of Rac activation in response to a currently undefined stimulus (179, 409). Perhaps BAI1 signaling contributes to the activation of other NADPH oxidase complexes in response to microbial stimuli and in the absence of phagocyte NADPH oxidase complex. Furthermore, given that BAI1 is expressed in cell subsets (e.g. intestinal macrophages and epithelial cells) in direct contact and constant communication with commensal resident microbes, it would be of interest to determine whether BAI1 facilitates gut homeostasis and immunological barrier control at this site. This could be either through intestinal phagocyte driven clearance of invading microbes, or through the sensing of and response to luminal bacteria by epithelial cells. Lee et al recently showed that expression of BAI1 in intestinal epithelial cells contributes to the clearance of dead or apoptotic cells during colitis, a process critical for physical barrier control (Lee et al, *in press*). In this case, BAI1 seems to act independent of an interaction with the resident microbiome. However, the role of the BAI1 at the interface between commensal

microbes and the host in either epithelial cells or intestinal phagocytes during homeostasis remains to be further explored.

BAI1 is expressed in several cell subsets including myeloid lineage cells (e.g. macrophages and monocytes), astrocytes, neurons, myoblasts, and epithelial cells (222-227, 260)(Lee et al, *in press*). Analysis of the loss of BAI1 in conditional knockouts, such as the CSF1-receptor-cre mice or LysM-cre mice for depletion in the monocyte and macrophage lineage cells would provide more detailed evidence on the importance of BAI1-mediated uptake and killing in this cell subset in vivo (412, 413). Determination of the cell-specific expression of BAI1 in macrophage subsets present in different tissues should also be done. For example, BAI1 is expressed in intestinal and gastric macrophages, perhaps indicating a role in clearance of enteric pathogens (226, 260). Although the use of conditional knockouts is imperfect in the heterogeneous and plastic myeloid compartment, the tissue specific expression and importance of macrophage subsets at critical sites of infection and host-pathogen interaction would provide context for the role of BAI1 in bacterial recognition and regulation of the host response, including the activation of ROS responses contributing to bacterial clearance.

Defining the impact of BAI1-dependent Rac activation in a stimulus-selective manner

The ROS burst accompanying phagocytosis of bacteria or fungi occurs in an inflammatory state and must be tightly regulated to avoid tissue damage and aberrant inflammatory processes (398, 414). Macrophage clearance of apoptotic cells is dominated by uptake in a highly degradative phagolysosome and lacks robust ROS responses. In fact, ROS production is minimal upon treatment of bone marrow macrophages with apoptotic thymocytes (data not shown). Thus, how and whether BAI1 acts distinctly in

the context of apoptotic cells versus Gram-negative bacteria in driving the activation of NADPH oxidase machinery and the production of ROS is an open question. In both contexts, BAI1 couples to ELMO-Dock to activate Rac and drive phagocytosis, indicating that additional factors are at play. This could in part be explained by the tight regulatory controls placed on the activation of the multi-component NADPH oxidase complex. In addition to Rac GTP-loading, the regulatory subunits: p47phox, p67phox, and p40phox, must be activated through upstream signaling activity. If the engagement of other necessary signaling cascades is absent in the context of apoptotic cells, this may prevent functional activation of the NADPH oxidase machinery. Comparative analysis of the distribution of BAI1 and the NADPH oxidase subunits in the context of apoptotic cells and Gram-negative bacteria, as described above, may also provide insight in the mechanistic role BAI1 plays in each context. Importantly, other inflammatory PRRs are engaged selectively in the context of bacteria ligands, including TLRs. This perhaps provides a second signal for the cell to mount an inflammatory response to bacteria, including ROS production, rather than an anti-inflammatory response, as observed with apoptotic cells.

The implications of this distinct activity on the immune response are quite intriguing. Of note, in select cell subsets ROS responses are associated with altered kinetics of phagosome-lysosome fusion and degradative capacity, thereby altering the potential for antigen processing and presentation (415, 416). Some evidence suggests that in the context of apoptotic cells degradation is increased and antigen processing is reduced, allowing for the avoidance of auto-reactive immune responses. It would be interesting to assess the expression of co-stimulatory molecules and the antigen

presentation potential in control and BAI1-deficient cells. Preliminary work suggests that BAI1 promotes protective immune responses in diverse inflammatory contexts. Further examination of the distribution and activation of BAI1 and the phagocyte NADPH oxidase complex would provide insight into the mechanism through which BAI1 and this evolutionarily ancient microbicidal machinery intersect, and may reveal how the activation of this response differs in a context-dependent manner.

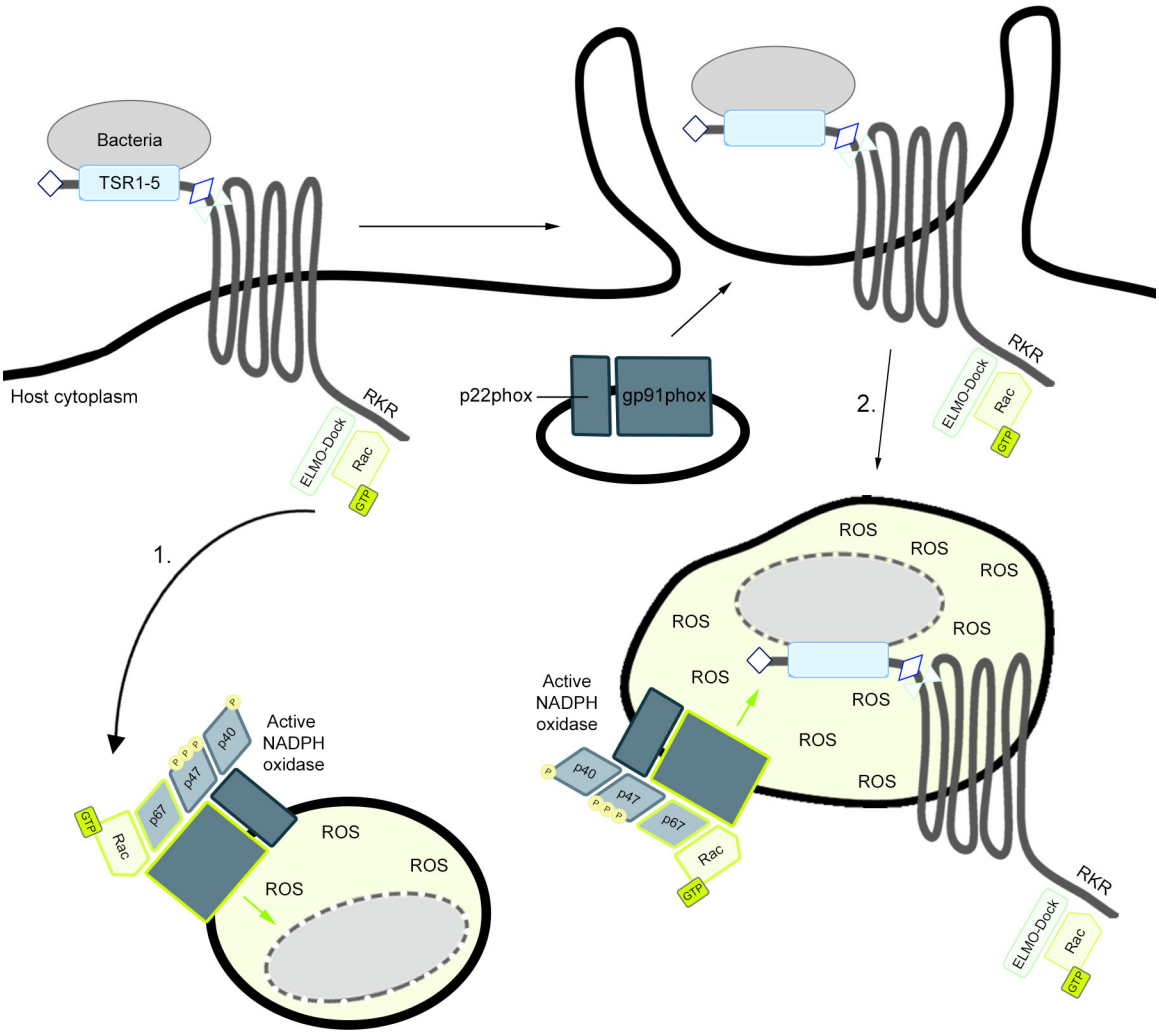
Bacteria
TSR1-5
Host cytoplasm
RKR
ELMO-Dock
Rac
GTP
p22phox
gp91phox
2.
1.
Active
NADPH
oxidase
p40
p47
p67
ROS

Figure 5-2. Model of the localized activation of phagocyte NADPH oxidase complex enhanced by BAI1-mediated bacterial recognition

After bacterial recognition, BAI1 promotes the activation of ELMO-Dock, a bipartite Rac GEF. This allows for the localized activation of Rac and actin cytoskeletal rearrangement driving internalization of the bound particle. The membrane bound components of the phagocyte NADPH oxidase complex are recruited to the phagocytic cup, nascent phagosomes, and the phagosomal compartment. First, receptor-mediated signaling triggers the phosphorylation and subsequent translocation of the regulatory subunits (p47phox, p67phox, and p40phox) to the membrane associated components of the NAPDH oxidase complex. A second signal mediates the activation and translocation of Rac GTPases, culminating in a functional NADPH oxidase complex. Here, we propose two models through which BAI1 promotes NAPDH oxidase activity and ROS responses. (1) BAI1 drives the upstream activation of Rac resulting in redistribution and association with the NADPH oxidase complex downstream. (2) Alternatively, the localized activation of Rac and the recruitment of NADPH oxidase subunits to sites of BAI1-bacterial attachment poise the macrophage ROS response at the early phagosome.

A selective role for the modulation of TLR4-dependent inflammatory signaling and cytokine responses by BAI1

Conclusions and future directions

Microbial recognition through PRRs triggers signaling pathways that promote the production of pro-inflammatory cytokines, chemokines, and type-I-IFNs (5, 10, 17, 18). This drives the local activation of innate immune cells and mediates the recruitment of additional responder cells to contend with infection. TLR4 in particular is the key receptor engaged in early inflammatory signaling to LPS (**Fig. 1-3**). However, it is not the only receptor activated in response Gram-negative bacteria. Defining the interactions of PRRs resulting in the refinement of the cellular innate immune response has become of great interest because of its potential for therapeutic targeting. As a phagocytic receptor, BAI1 plays a distinct role relative to TLRs, which do not directly mediate the internalization of microbes. The role of BAI1 in the innate inflammatory response to Gram-negative bacteria is entirely undefined. We address this gap with the work presented in Chapter 3. Here, we characterize the impact of BAI1 expression on inflammatory signaling and transcriptional responses in macrophages and provide insight into how BAI1 acts in the context of global cellular inflammatory signaling.

In Chapter 3, we showed that TRIF-dependent signaling leading to the activation of IRF3 was reduced in BAI1-deficient cells compared to control macrophages. This occurred in the context of several Gram-negative bacterial species and soluble LPS. Accordingly, we observed a defect in TLR4-TRIF-dependent transcriptional responses. BAI1-deficient cells had significantly impaired induction of IFN-β, CCL5, and IL-10, which are all dependent on IRF3 activation (**Fig. 1-3, Fig. 5-3**). The defect in

macrophage innate responses was selective, as we observed no defects in NF-κB or MAPK signaling and transcriptional responses. This suggested that BAI1 selectively modulates the intracellular signaling response of TLR4 (**Fig. 1-3, Fig. 5-3**).

The interaction between BAI1 and TLR4 is currently undefined. PRR crosstalk occurs through several means. Some receptors promote the delivery of ligand, form signaling complexes contributing to local inflammatory signaling, potentiate downstream signaling responses, modulate positive or negative regulators, or alter the cellular distribution of receptors. Since BAI1 and TLR4 share a common microbial ligand, LPS, we first examined whether or not a physical interaction between BAI1 and TLR4 existed. In heterologous cell lines, TLR4 and MD2 physically associate with BAI1, and that interaction is dependent on the cytoplasmic region of BAI1 and is enhanced upon incubation with Gram-negative bacteria. Additionally, higher molecular weight products selectively immunoprecipitated after stimulation. Although the precise identity of those higher molecular products is unknown, it is possible that they are LPS-sensitive signaling complexes.

Receptor internalization is a critical step in modulating TLR4-dependent responses (**Fig. 1-3**). However, expression of BAI1 did not impact the internalization of TLR4-MD2 complexes in primary macrophages. Loss of effective TLR4-MD2 internalization has been shown to result in aberrant and excessive inflammatory signaling from the cell surface (75, 76, 417). This was consistent with the observation that the MyD88-dependent responses were similarly induced in wild type and BAI1-deficient macrophages. Collectively, this indicates that BAI1 regulates TLR4 through signaling

crosstalk or through alteration of the intracellular distribution of functional signaling complexes rather than direct modulation of TLR4 internalization.

PRR trafficking and cellular compartmentalization is becoming increasingly appreciated as an important means of regulation for innate immune responses, and the localization of TLR4 and LPS determines the outcome of inflammatory signaling. While the trafficking of newly synthesized receptors is better understood, the regulation of the localization of TLR4-MD2 within the cell is less well-defined. While BAI1 did not appear to regulate receptor internalization from the cell surface, TLR4 and its signaling molecules are also recruited to bacterial phagosomes from the ERC. Thus, an intracellular source of TLR4 may be mobilized in a BAI1-dependent manner. We examined the distribution of exogenous BAI1 and TLR4 in Cos7 cells. Both were found at the plasma membrane and enriched in the perinuclear region, consistent with previous observations (66, 80, 222, 225). However, BAI1 and TLR4 were also selectively enriched around cell associated *E. coli,* and the association between TLR4 and bacteria was significantly augmented when BAI1 was co-expressed. Although this analysis did not differentiate between internalized and surface associated bacteria, the distribution of protein around the microbes indicated that they localized at the phagocytic cup or phagosome (**Fig. 5-3**). Collectively, this places BAI1 and TLR4 in a similar compartment, indicating that BAI1 may drive the recruitment of TLR4 to phagosome or may enhance local signaling events from this compartment.

The compartmentalization of bacterial ligands can also impact innate cellular responses. For example, SR-A down regulates TLR4-dependent signaling by receptor-mediated internalization of LPS (108, 109). BAI1 as a phagocytic receptor promotes the

uptake of bacteria, an enriched source of LPS, from the extracellular space to an intracellular compartment, thereby potentially priming intracellular TLR4-signaling. Accordingly, pharmacological inhibition of phagocytosis reduced the impact of BAI1 on IRF3 activation, indicating that BAI1 promoted IRF3 activation, in part, by targeting bacteria to an intracellular compartment. However, cells treated with soluble LPS also had impaired IRF3 activation further supporting the hypothesis that BAI1 signaling is also critical. A caveat to this interpretation is that the trafficking and internalization of BAI1 after exposure to soluble LPS is uncharacterized. Additionally, Cytochalasin D treatment impairs the recruitment of TLR4 to bacteria-containing phagosomes, making it difficult to uncouple internalization and ligand delivery from the intracellular signaling responses (67).

A detailed examination of TLR4-TRIF signaling

Chapter 3 addressed the impact of BAI1 on TLR4-dependent responses. Several of the observations derived from this study emphasize the importance of BAI1 on modulating intracellular TLR4 signaling pathways, while imaging and biochemical analysis suggests that the two proteins physically and spatially interact. To better confirm the previous results and to define the mechanism through which BAI1 alters TLR4 biology, a closer examination of the TLR4-TRIF-dependent signaling response is in order (**Fig 1-2, Fig. 1-3**). Specifically, further analysis of the recruitment and activation of distinct players in the signaling pathway would indicate where and how BAI1 intersects with TLR4 function.

First, during the endosomal or phagosomal TLR4 responses, a multi-protein complex is formed that serves as a scaffolding structure to facilitate downstream

signaling (62). TRAM is recruited to the PI(3)P and PI(3,4,5)P_3 enriched intracellular membrane. TRAM localization is determined by a bipartite localization motif, consisting of a myristate group and a polybasic sequence. The myristoylation of TRAM is particularly crucial for its recruitment to endosomal membranes (78, 92). This protein acts a bridge, required for the recruitment of the signaling adaptor TRIF (418). The TIR domains of TLR4, TRIF, and TRAM mediate homotypic and heterotypic interactions to form a signaling platform (62, 73, 82, 419) (**Fig. 1-2, Fig. 1-3**). Other proteins implicated in TRIF recruitment include the WD repeat and FYVE-domain-containing 1 protein (WDFY1). Hu et al showed that WDFY1 potentiates TLR4 endosomal signaling by associating with TRIF and promoting its recruitment to TLR3 and TLR4 signaling complexes upon stimulation with LPS, but the mechanism initiating this recruitment is unknown (420). The activity of TRAM and TRIF can also be modified by post-translational modifications (82, 421). For example, phosphorylation of TRAM by PKCε is associated with complete activation of IRF3 and induction of CCL5. The recruitment and oligomerization of TRIF and TRAM at the TLR4 interface is required for potentiating downstream signaling, as disrupting this interaction with mutations or small peptide inhibitors ablates branches of this pathway (82, 419).

TLR4 signaling proceeds through recruitment and activation of downstream E3 ubiquitin ligases and protein kinases (**Fig. 1-2**). Notably, TRIF-dependent responses diverge by either coupling to TRAF6 and RIP1 or to TRAF3 and TBK1/IKKε, leading to delayed activation of NF-κB and MAPK or IRF3, respectively (81). These proteins are dependent on different regions of TRIF for their association with the signaling complex, but their signaling pathways are not entirely separable as some evidence suggests that

TRAF6 and RIP1 binding contribute to TRAF3-dependent responses (82-84, 422). TRIF mediates the activation of IRF3 through recruitment of TRAF3, an E3 ubiquitin ligase that K63-autoubiquitinates to allow downstream signaling (79, 89). The mode of TRAF3 binding to TRIF is poorly defined, but recruitment and K63 autoubiquitinylation provides a scaffold for TBK1 and IKKε (423). TRAF3 has been shown to recruit adaptor proteins upstream of IKK kinases in other contexts, such as TANK, NF-κB-activating kinase-associated protein (NAP1), and similar to NAP1 TBK1 adaptor (SINTBAD), but their role specifically in TLR4-LPS responses is variable (424-426). Recruitment and activation of TBK1 and to a lesser extent IKKε, mediate the phosphorylation, dimerization, and activation of IRF3 for transcriptional responses (85-88). Although IRF3 is found in complex with the upstream signaling partners, the recruitment and the mechanisms defining its cellular distribution are not known (85, 86).

Ubiquitination of TRAF proteins provides a mechanism for signaling regulation, with K48-linked ubiquitination targeting the TRAF protein for degradation and K63-linked ubiquitination leading to downstream signaling responses (**Fig. 1-2**). Several molecules have been implicated in selectively promoting TRAF3 signaling is this context, while negatively regulating the MyD88-TRAF6 pathway. The ubiquitin ligases cell inhibitor of apoptosis 1 (cIAP1) and cIAP2 mediate the degradative K48 ubiquitination of TRAF3 to promote MyD88-dependent signaling. Receptor internalization promotes removal of K48-linked ubiquitination by ubiquitin-specific protease 25 (USP25) allowing for K63 ubiquitinylation, effectively switching the signaling response (316, 427). Syk also promotes intracellular TLR4 signaling via regulation of K63-linked polyubiquitinylation of TRAF3 in addition to promoting

internalization of TLR4 from the plasma membrane, as described previously (428) (**Fig. 1-2, Fig. 1-3**).

The distribution of TLR4 and the necessary signaling proteins is highly important for the functional outputs of activation, but formation of signaling complexes and the distribution of TLR4 signaling proteins has not been examined in the context of BAI1. Immunoprecipitation assays in heterologous cell systems or in primary cells can be used to measure recruitment and signaling complex formation. Imaging studies may provide further refinement to this analysis by allowing for compartment specific analysis (e.g. endosomal versus phagosomal compartments) of critical receptors and signaling partners. As a first approach, examination of TLR4 trafficking using live cell imaging may highlight defects in the recruitment of TLR4 to the phagosomal compartment. Recruitment of additional signaling proteins, including the adaptor proteins TRIF and TRAM could then be assessed, followed by other members of the intracellular TLR4-dependent response (**Fig. 5-3**).

A more detailed examination of TLR4-dependent signaling upstream of IRF3 activation would provide insight into the mechanism through which BAI1 modulates intracellular TLR4 signaling (**Fig. 1-2, Fig. 1-3**). The results presented in Chapter 3 provided a bottom up approach by examining distal TLR4-TRIF signaling outputs. First, the activation of signaling molecules as assessed by critical post-translational modifications can be measured using immunoblotting. In particular, TRAF3 ubiquitination, TBK1 ubiquitination, and TBK1 or IKKε phosphorylation can be analyzed. Activation of the IRF3 dimer is negatively regulated by protein turnover and phosphatases (429, 430). Through similar methods, measuring total protein levels can

assess the relative protein stability of IRF3, while measurement of the activation of protein phosphatases can identify differences in the maintenance of the active IRF3 dimer. Collectively, this would identify the point at which TLR4-dependent responses are attenuated, providing insight into the mechanism of the BAI1-mediated responses.

While TBK1 activation was indirectly analyzed in Chapter 3, the impact of BAI1 on the phosphorylation of TBK1 differed depending on the stimuli used. TBK1 phosphorylation was significantly reduced in BAI1-deficient cells stimulated with non-pathogenic, non-invasive *Salmonella* and *E. coli* BW25113, but not in response to *E. coli* DH5α. The reasons for this discrepancy are not yet clear. It may be explained by differences in the presentation and concentration of LPS and other MAMPs by the representative bacteria and their engagement with cognate PRRs. A more detailed examination of TBK1 and IKKε, such as the assessment of post-translational modifications, subcellular localization, and kinase activity would further resolve this discrepancy.

In general, the parameters defining activation and kinase activity of non-canonical IKK family proteins, TBK1 and IKKε, are poorly understood (317, 324, 326). On one hand, recruitment and oligomerization is thought to trigger activation via trans-phosphorylation (327). Alternatively, some evidence suggests a role for a currently unidentified activating kinase (325). Additionally, the E3 ubiquitin ligase Nrdp1 positively regulates TBK1 by ubiquitination (431), and evidence for negative feedback loops for regulating phosphorylation of TBK1 exist (325, 326). Given the complex regulation and role of TBK phosphorylation, to confirm whether TBK activity is regulated by BAI1 in response to Gram-negative bacteria and soluble LPS, we propose to

measure kinase activity directly. Additionally, TBK1 ubiquitination can be assessed with immunoblotting. It is possible that despite differences in phosphorylation, kinase activity may be attenuated in all contexts, thus placing BAI1 upstream of TBK1 in TLR4 signaling.

Mechanisms of signaling crosstalk between BAI1 and TLR4

Several lines of evidence presented in Chapter 3 indicate that BAI1 actively regulates intracellular TLR4 responses. The intracellular cytoplasmic region of BAI1 is known to couple to several cell signaling pathways in a stimulus- and cell and tissue-specific manner (**Fig. 1-9**). Analysis of the respective signaling pathways may provide insight into the mechanism through which BAI1 promotes IRF3 activation in primary macrophages. Das et al showed that BAI1 signals through the bipartite Rac-GEF, ELMO-Dock to mediate Rac activation in response to Gram-negative bacteria (226). Interestingly, Dock2 mediated activation of Rac is required for TLR7 and TLR9 type-I IFN responses in plasmacytoid dendritic cells (49). Moreover, actin remodeling is important for intracellular trafficking (432). Husebye et al showed that Cytochalasin D inhibited recruitment of TLR4 to bacterial phagosomes, perhaps indicating that actin dynamics modulate trafficking of the ERC pool of TLR4. Actin filaments are also important for delivery of Rab11a-postive vesicles to the plasma membrane (67, 433). Analysis of TLR4 signaling in cells expressing mutant BAI1 lacking the RKR motif coupling to ELMO-Dock-Rac activation may provide insight into the role of Rac activation on IRF3 signaling (**Fig. 5-3**). However, interpretation of these results should be taken with care, as it may be difficult to uncouple phagocytosis-dependent versus phagocytosis-independent effects.

Arf6 has also been implicated in intracellular TLR4 signaling and trafficking (90). Santy et al showed that ELMO-Dock180 promotes downstream Arf6 and Rac1 activation during cell migration (434). The activation of Arf6 can be easily assessed using pulldown assays in wild type and BAI1-deficient cells. Interestingly, Van Acker et al showed that Rab11a and Arf6 colocalize in the ERC with TRAM (90). The authors propose that Arf6 and Rab11a may cooperate in modulating TLR4-TRIF-dependent responses, perhaps in a family of Rab11 interacting protein 3 (FIP3) and FIP4-dependent manner (435). TBK1 and IKKε have been shown to regulate the activation of FIP3, a Rab11 effector, in regulating recycling endosome dynamics, perhaps further potentiating this signaling response and placing these signaling molecules together in space and time (436, 437).

LPS stimulates the expression of regulators of G protein signaling (RGS proteins) in macrophages, suggesting that classical GPCR signaling may be relevant during LPS-driven innate responses (438). Stephenson et al showed that BAI1 activates $G\alpha_{12/13}$ (203, 250). Currently identified downstream targets of $G\alpha_{12/13}$ include RhoGEFs, including p115-RhoGEF, PDZ-RhoGEF, leukemia-associated RhoGEF (LARG), and lymphoid blast crisis (LBC)-RhoGEF (439-441). PDZ-RhoGEF and LARG both contain PDZ domains that may promote efficient and localized signaling through interactions with the PDZ-binding motif at the C-terminus of BAI1. BAI1-dependent $G\alpha_{12/13}$ signaling promoted RhoA activation when expressed in 293T cells, and this pathway was upregulated upon expression of a truncated receptor that mimics cleavage at the GPS motif (**Fig. 1-9, Fig. 5-3**). Interestingly, $G\alpha_{13}$ only associates with the truncated receptor (250). Further analysis indicated that this interaction culminated in nuclear factor of activated T cells (NFAT) activation. CD14 promotes Ca^{+} flux and activation of NFAT in

dendritic cells, prompting further examination of BAI1-dependent modulation of inflammatory signaling in other cell subsets (442). Consistent with the literature, we have not observed receptor cleavage in macrophages or heterologous cell lines, but the regulation of cleavage is poorly understood, and BAI1 may still couple to G proteins after incubation with Gram-negative bacteria.

p120catenin was recently implicated in selectively promoting the activation of TLR4-TRIF-dependent responses (77) (**Fig. 1-3, Fig. 1-9)**. The authors discerned that p120catenin negatively regulated RhoA activation to promote TLR4 internalization from the cell surface based on the relative loss of TLR4-MD2 from the cell surface upon treatment with LPS. However, the antibody used to make this assessment has been shown to recognize TLR4-MD2 in a conformation-dependent manner (443, 444). After LPS binding, antibody recognition is lost, so it is possible that their results do not truly reflect a defect in internalization. This perhaps hints at a role for p120catenin and RhoA in the regulation of intracellular TLR4 signaling responses. Additionally, $G\alpha_{12/13}$ subunits bind p120catenin, perhaps indicating a direct mechanism through which BAI1 may regulate this function (331, 445). Selective deletion of the PDZ binding motif at the extreme C-termini of BAI1 and the use of competitive inhibitors may reveal whether this pathway is relevant for BAI1-dependent early innate inflammatory responses (203, 250, 446) (**Fig. 1-9**). However, other PDZ-domain containing proteins have been shown to couple to this region (e.g. MAGI-3 and Par3-Tiam1) and must be taken into consideration (203, 208, 248).

Stephenson et al also showed that the C-terminus of BAI1 associates with β-arrestin2 resulting in receptor ubiquitination (203). In contrast to the activation of $G\alpha_{12/13,}$

this pathway was negatively regulated by the PDZ-binding motif of BAI1. β-arrestins regulate GPCR signaling by altering signaling responses and driving receptor internalization (447, 448) (**Fig. 1-9, Fig. 5-3**). However, they have also been shown to function in other contexts, including the regulation of TLR responses (332, 449). In this capacity, β-arrestins regulate downstream signaling through regulation of ubiquitination and scaffolding activity. β-arrestin2 physically associates with TRAF6, resulting in the negative regulation of NF-κB and MAPK signaling and the induction of pro-inflammatory cytokines (333, 334, 450). Additionally, β-arrestin2 has been shown to interact with p38 to enhance IL-10 production in response to LPS (451). The effects of β-arrestin2 appear to be cell-type specific, as studies differ when using BMDMs and thioglycollate-elicited PEMs. It is unknown whether BAI1 interacts with β-arrestin2 in macrophages in the context of LPS, but it is unlikely that an interaction with β-arrestin2 in the context of BAI1 impacts ERK or MAPK signaling, as we observed no defect in MAPK phosphorylation in any context. However, given the complex interplay between TRAF6 and TRAF3 on downstream signaling and the ability of β-arrestins to interact with TRAF proteins and to regulate cytokine responses in the context of LPS (79, 316, 428), the interaction of BAI1 with β-arrestin2 should be assessed.

Other BAI1-dependent signaling responses may intersect with TLR4. In addition to Gα signaling, canonical heterotrimeric G protein signaling may also lead to the activation Gβγ subunits, which have been shown to potentiate a number of downstream responses (207, 452). Notably, Gβγ subunits have been shown to interact with Rab11a to regulate trafficking downstream of the LPA receptor within the early and recycling endosomal compartments (335), perhaps directly linking BAI1 to Rab11a in the response

to LPS. Further analysis of the binding partners of the PDZ binding motif and the proline rich region of BAI1 in macrophages may also reveal novel mechanisms of signaling crosstalk and regulation of innate inflammatory and anti-inflammatory machinery.

TLR4 trafficking in the context of BAI1 and phagosome heterogeneity

The work shown in Chapter 3 provided insight into the role of BAI1 in the macrophage innate signaling and inflammatory responses to Gram-negative bacteria and suggested that BAI1 acts as a novel accessory protein for the intracellular TLR4 response. While phagocytosis is appreciated as a necessary component of the microbicidal and antigen processing functions of macrophages, its role in the context of innate inflammatory signaling is less characterized. This advance connects an upstream phagocytic receptor with intracellular signaling responses, further highlighting the unique function and environment of the phagosome as a signaling organelle. This is particularly intriguing, as the data presented in Chapter 3 perhaps suggest that the intracellular compartments mediating intracellular TLR4-dependent responses differ in their signaling outputs (**Fig. 5-3**). For example, TRIF-dependent signaling was not completely ablated as the late activation of NF-κB and MAPK signaling was maintained, irrespective of BAI1 expression. This may be because BAI1 intersects with TLR4 signaling downstream of the TRIF-RIP-TRAF6 signaling pathway, but the increased association of TLR4 with Gram-negative bacteria in the context of BAI1 expression suggests that the interaction occurs upstream of that. BAI1 may define a mechanism through which phagosome and endosome heterogeneity is determined in the context of the innate inflammatory signaling response of macrophages**.**

Recent advances have shed light on the mechanism of internalization of TLR4-MD2 from the cells surface. TLR4 is internalized from the plasma membrane to the early endocytic compartment in a manner dependent on clathrin and dynamin (68, 92) (**Fig. 1-3**). GPI anchored CD14 is required for the internalization of TLR4-MD2 by promoting the activation of tyrosine kinase Syk and the phospholipase PLCγ2, likely through interactions with ITAM-containing molecules (74). In this capacity, Syk and PLCγ2 help mediate the necessary phospholipid changes required for internalization (453-455). This process requires ligand induced structural changes of the extracellular regions of TLR4-MD2 resulting in dimerization and occurs rapidly upon exposure to LPS (within 2 min of exposure) (63).

While the work described in Chapter 3 does not suggest a role for BAI1 in promoting TLR4 internalization, direct analysis of CD14 was not performed. Given the importance of CD14 as a master accessory protein in modulating the intracellular TLR4 response to LPS, further analysis would be of interest (**Fig. 1-3**). We showed that high molecular weight complexes containing TLR4 associate with BAI1 selectively upon exposure to Gram-negative bacteria. It is possible that these higher molecular weight products are complexes containing TLR4 and MD2 or protein dimers, with or without CD14. CD14 associates with TLR4 at the cell surface and at the early endosome (63, 74). The use of siRNA-mediated knockdown would determine if BAI1 requires CD14 for enhancing TLR4-dependent IRF3 responses, perhaps providing evidence for whether BAI1 interacts with TLR4 endocytosed from the cell surface or from another compartment. Alternatively, confirming the importance of CD14 for the BAI1-enhanced IRF3 response may reveal a role for CD14 at the phagosome. BAI1 is expressed in other

cell subsets with varying degrees of CD14 expression (456). Analysis of downstream signaling with and without CD14 in the context of BA11 may highlight the impact of BAI1 on intracellular signaling pathways.

Trafficking of TLR4 within the cell has been largely studied in the context of de novo protein synthesis, where protein is processed and secreted from the ER through the Golgi to the plasma membrane. In this context, the chaperones gp96 and Prat4a are required for processing of TLR4 in the ER (457-459). Transmembrane emp24 protein transport domain containing (TMED) proteins mediate the transport of ER cargo to the cis-Golgi. TMED7 regulates trafficking of TLR4 to and within the Golgi network and is required for surface expression (460), while Rab10 facilitates trafficking of TLR4 from the trans-Golgi to the plasma membrane (461). TLR4-MD2 in the perinuclear ERC serves as an additional source of receptor during innate responses. This pool of protein is selectively delivered to phagosomes containing Gram-negative bacteria to enhance TLR4-TRIF signaling (67). Liaunardy-Jopeace et al supported this concept by showing that loss of TMED7 did not impair TRIF-dependent signaling responses (460). Interestingly, this also suggests that the trafficking to the ERC occurs differently than the trafficking to the cell surface during de novo protein synthesis in a manner that is currently undefined. Husebye et al determined that the intracellular trafficking of TLR4 is mediated by Rab11a GTPase through an unknown upstream signal. They observed an enrichment of Rab11a and TLR4 signal around phagosomes containing Gram-negative *E. coli* particles using microscopy. Moreover, Rab11a-depletion impaired delivery of endosomal TLR4 to bacterial phagosomes and attenuated the TLR4-TRIF-dependent response. Van Acker et al provided evidence supporting a role for Arf6 in regulating

intracellular TLR4 signaling, perhaps by interacting with Rab11a and regulating the trafficking of TRAM (90).

To further examine the mechanism of the impact of BAI1-dependent phagocytosis on TLR4 signaling we preliminarily assessed the distribution of Rab11a in wild type and BAI1-deficient macrophages (**Appendix**). Early, transient recruitment of Rab11a was observed after internalization in cells incubated with non-pathogenic, non-invasive *Salmonella.* Rab11a was also transiently enriched at bacterial phagosomes, reflecting different kinetics and dynamics than that described by Husebye et al. However, this assessment is largely incomplete due to technical reasons. Accordingly, the recruitment of ERC-localized TLR4 and the activation of Rab11a and other proteins regulating membrane trafficking events by BAI1 in response to Gram-negative bacteria remains open for further investigation (**Fig. 5-3**).

Given the importance of intracellular receptor trafficking events in the innate response to Gram-negative bacteria, future research should assess Rab11a recruitment and activation by Gram-negative bacteria. Several measures can be taken to better evaluate Rab11a in wild type and BAI1-deficient macrophages. Contradictory evidence exists on the role of Rab11a in LPS-stimulated intracellular signaling by TLR4. Husebye et al showed that the activation of IRF3 in response to LPS was not impaired when Rab11a was depleted (67), Alternatively, Klein et al reported that Rab11a promotes delivery of TRAM to endosomes and is required for complete activation of TLR4-TRIF-dependent responses to LPS. This suggests that trafficking pathways are shared in the response to soluble and particulate ligands perhaps making these pathways difficult to distinguish (69). Husebye et al utilized *E. coli* containing particles (67), which may differ

in the concentration and isolation of soluble LPS monomers relative to viable bacteria. Analysis of Rab11a recruitment to *E. coli* BioParticles (Molecular Probes) can be done for better comparison. Serum concentration also affects the importance of other PRRs on TLR-dependent responses. Nagaoka et al determined that the impact of SIGNR1 (DC-SIGN) expression on co-receptor formation, oligomerization of TLR4-MD2, and downstream signaling was dependent on serum concentration (275). Accordingly, this parameter may be modified to alter the route of entry for whole bacteria and soluble LPS to further separate these pathways (462, 463). Additionally, the importance of Rab11a in the context of BAI1 expression could be assessed through Rab11a depletion. A comparison of the activation of IRF3 in wild type and BAI1-deficient macrophages in response to *E. coli* would reveal whether Rab11a is relevant for BAI1-dependent responses. Moreover, analysis of LPS signaling under these conditions may indicate whether delivery of TLR4 or TLR4 signaling molecules and signaling crosstalk is important, respectively. The approach presented in the Appendix utilized over-expression of Rab11a, which may have off target effects on GTPase signaling, impairing or altering global cellular responses. Analysis of endogenous Rab11a would avoid this. Examination of the localization of endogenous Rab11a through confocal microscopy would provide insight into the distribution of Rab11a in the context of BAI1, and direct measurement of Rab11a activation through the use of a configuration-specific antibody or pulldown assays (464) would provide evidence for whether BAI1 impacts Rab11a activation. It is also possible that other Rab proteins and GTPases, such as Arf6, contribute to the trafficking and signaling of BAI1 and TLR4 within intracellular compartments.

Potential boons and burdens of BAI1-enhanced innate signaling and transcriptional responses

In Chapter 3, we showed that BAI1 selectively promotes the intracellular signaling and transcriptional response of TLR4-mediated IRF3 activation. However, the impact of this on innate immunity in vivo is unknown. The production of type-I IFNs during bacterial infection has only recently been appreciated, and the importance and impact of TLR4 signaling adaptor TRIF in innate immunity to Gram-negative bacterial pathogens is variable (465-468). Sotolongo et al showed that TRIF-dependent induction of IFN-β was protective during infection with *Yersinia enterocolitica*, a Gram-negative bacterial pathogen (339). This was tied to local activation of inflammatory responses, crosstalk between early innate immune cells, cellular recruitment, and the enhancement of macrophage microbicidal activity. Macrophages deficient in TRIF had attenuated microbicidal activity to several Gram-negative enteric pathogens, including *Salmonella* and *E. coli*. However, a later study from the same group indicated that TRIF-dependent responses during systemic infection were not critical for controlling bacterial load (469). Similarly, our lab showed that TRIF-regulated responses are protective during oral Salmonella infection by potentiating neutrophil influx (470). In contrast, TRIF-dependent IFN-β contributed to macrophage necroptosis and increased susceptibility after intravenous infection with *Salmonella* (471), and in other cases it has been linked to attenuated immunity in the gut (472). However, activation of type-I IFN in the gut through other TLRs is tied to protective immunity and homeostasis (473, 474). The role of IRF3 is similarly complex, showing disparate effects depending on experimental conditions (337, 338, 475). Clearly, the role of TRIF and the type-I IFN response is

context-dependent on the pathogen of interest, the route of infection, and the inflammatory microenvironment.

Studies evaluating the importance and impact of TRIF, IRF3, and type-I IFNs during endotoxin challenge are similarly complex. TRIF, IRF3, and IFN-β knockout mice are more resistant to endotoxin challenge (38, 336, 476, 477), while TBK-mutant mice are more susceptible to endotoxins and exhibit exacerbated inflammatory profiles at steady state (478). Route of infection, tissue tropism, viral co-infection status, and the balance between Type I and Type II interferons and inflammatory cytokines all contribute to downstream consequences and effects. Thus, the local environment and magnitude of pro-inflammatory and interferon signaling can have a drastic impact on host outcome (323, 479, 480). The work presented in Chapter 3 addressed the transcriptional response in wild type and BAI1-deficient macrophages, but the translational response (e.g. the secretion of IFN-β) remains to be assessed. Further analysis of the impact of enhanced IFN-β production, such as increased cellular microbicidal activity and Type-I IFN receptor signaling should also be addressed. Given the diverse innate cellular response that accompanies infection, the use of conditional knockout mouse models will provide further insight.

A significant part of the macrophage innate immune response to Gram-negative bacteria occurs in a MyD88-independent manner (43). Given that BAI1-deficient cells had inefficient IRF3 activation and IRF3-dependent gene transcriptional responses in addition to IFN-β (e.g. CCL5 and IL-10), it is possible that BAI1 regulates the induction of other TRIF-dependent genes. Interestingly, at the level of macrophage signaling and activation, TRIF-dependent signaling has also been associated with pro-survival

pathways in macrophages when balanced with MAPK and NF-κB signaling, and TLR4-TRIF responses are required for endotoxin tolerance (340). Moreover, autocrine and paracrine signaling via type I-IFNs induce ISGs, which include gene products that contribute to antimicrobial activity and may play a role in the transition of macrophages from the M1 to M2 phenotype during resolution of inflammation and infection (479). Collectively, this places the NF-κB and MAPK-independent branch of TRIF in a protective and regulatory role critical for microbial clearance, activation of adaptive responses, and resolution of infection.

IL-10 is a TRIF-dependent anti-inflammatory cytokine that is particularly critical for attenuating deleterious inflammatory responses to LPS (79, 316, 341). The regulation of IL-10 in the context of LPS responsiveness is intimately tied with type I-IFNs, strengthening the connection between these phenotypes (322). The transcription of IL-10 was reduced in cells derived from BAI1 knockout animals, suggesting that BAI1 may be critical for controlling inflammatory responses in addition to any protective effects mediated by IFN-β and chemokine responses.

At the intersection between inflammatory responses and microbicidal activity in the innate immune response—TLR crosstalk with microbicidal activity and NADPH oxidases

PRR signaling and the route of cell entry impacts the fate of the ingested particle (117, 164, 174). However, the role of TLR signaling in modulating microbicidal responses in phagocytes is controversial. As such, further refinement of the intersection between cellular microbicidal activity and innate inflammatory responses is highly sought. The mechanism of TLR-enhanced ROS responses differs according to cell type. Park et al showed that TLR4 directly interacts with NOX4, a homologue to the phagocyte

NADPH oxidase catalytic enzyme gp91phox, in HEK 293 and endothelial cells, and that this interaction promoted ROS responses to LPS (402, 407). TLR4-MyD88 signaling has also been shown to mediate recruitment of mitochondria and the production of mitochondrial ROS at the phagosome (156). Some of the signaling pathways initiated downstream of TLR signaling are known to contribute to the activation of NADPH oxidases, providing the potential for signaling crosstalk (481). Moreover, priming TLRs by pre-treatment with MAMPs can lead to enhanced ROS production in phagocytes and epithelial cells (164, 482).

ROS can perform secondary signaling outputs such as the modification of nucleic acids, sugars, lipids, and proteins, alteration of the redox-potential within a cell, inhibition of protein tyrosine phosphatases, and regulation of survival signaling (291, 406, 483). In this capacity, cellular ROS can act as a second messenger to generate intracellular signaling cascades including MAPK, Syk, and Src family kinase activation. LPS stimulates Rac1 activation that is associated with enhanced ROS and inflammatory cytokine responses, suggesting signaling crosstalk (484, 485), and LPS induced ROS production is involved in TLR MyD88-dependent signal transduction and cytokine production by synergizing with inflammatory signaling and promoting surface expression of TLR4 (486, 487). Additionally, TLR4-NOX4 crosstalk is mediated by activation of apoptosis signal-regulating kinase-1 (ASK1). Park et al and others showed the NOX4 induced ROS promoted p38 activation to drive MyD88-dependent gene transcription downstream of TLR4 in 293T cells, endothelial cells, and a macrophage cell line (402, 407, 485). Finally, another study showed that NOX4-dependent ROS production

contributed to IRF3 activation downstream of p38 MAPK in response to LPS, perhaps synergizing with intracellular TLR4 signaling (488).

The impact of BAI1 on the innate inflammatory response and the induction of ROS merits discussion of how these pathways interact. We did not observe a defect in MyD88-dependent signaling, including p38 MAPK activation, indicating that either the BAI1-dependent ROS response is not required for activation of MAPKs or that the low level ROS response in BAI1-deficient cells is still sufficient to promote effective ROS-dependent ASK1 activation. Furthermore, in our hands loss of gp91phox (e.g. NOX2-dependent machinery) completely eliminated the ROS response to bacteria, and inhibition of mitochondrial ROS activity with MITOTempo had no effect on bactericidal activity. This suggests almost no contribution from other pathways. We also did not see any impairment in IRF3 phosphorylation in macrophages from gp91phox-deficient cells, again suggesting that the NOX4 and NOX2 responses act independently on the overall innate inflammatory response. Collectively, this is consistent with the hypothesis that BAI1 specifically promotes phagocyte NADPH oxidase activity (through NOX2) instead of NOX4-dependent ROS or mitochondrial ROS at the time points analyzed. Instead, it is likely that TLR4 and other receptors act as an upstream signal to kinases that mediate the activation of the cytosolic regulatory subunits of the phagocyte NADPH oxidase complex (p47phox, p67phox, and p40phox), while BAI1 drives Rac activation as a second signal. Although the kinetics of the ROS response and the interaction between BAI1 and TLR4 suggest this is not the case, the physical association between BAI1 and TLR4 may concentrate these two signals in space.

Shared themes regarding the inflammatory response initiated in the context of BAI1

TLR4 signaling must be tightly regulated to avoid aberrant inflammatory responses. Although the precise roles TRIF-dependent responses and type I-IFNs are poorly defined, they have been associated with protective immunity and the activation of regulatory mechanisms that limit inflammatory responses associated with deleterious host outcomes. Perhaps somewhat counterintuitively, phagocyte NADPH oxidase ROS are also associated with anti-inflammatory protective responses. For example, the Parkinson disease (autosomal recessive, early onset) 7 (Park7) protein enhances p47phox activation to promote phagocyte NADPH oxidase ROS responses and was shown to be protective during endotoxin and bacterial challenge (489). Moreover, patients with CGD are pre-disposed to inflammatory disorders, including inflammatory bowel disease (304, 490, 491). The protective effect of the ROS response is in part mediated by the negative regulation of inflammatory signaling via redox sensitive pathways (492, 493), by promoting IL-10 expression (494), and by controlling aberrant neutrophil driven pathology (495, 496).

Our data suggest that BAI1 acts to stimulate cellular microbicidal machinery and to regulate inflammation downstream of bacterial recognition. Accordingly, the increased susceptibility to bacterial challenge observed in BAI1 knockout animals may reflect both a defect in early bacterial clearance, as well as excessive inflammatory responses. The recognition of apoptotic cells is considered an anti-inflammatory event. Macrophages release TGF-β and IL-10 upon apoptotic cell phagocytosis to modulate and control for inappropriate inflammatory responses to self-ligands (497-500). BAI1 initiates the same signaling response during the recognition and phagocytosis of both bacteria and apoptotic cells, indicating that other mechanisms help to define the disparate outcomes associated

with each context. We propose this is likely due to the engagement of and interaction with other inflammatory PRRs, such as TLR4, which alter the global cellular response. The regulation of IL-10 downstream of apoptotic cell recognition is independent of IRF3 and is not known to be associated with the induction of IFN-β. However, given their immunomodulatory properties, it would be interesting to see if BAI1 impacts IRF3 activation or IFN-β secretion in response to phosphatidyl serine or apoptotic cells. Although much remains to be determined regarding BAI1 form and function, these themes connect BAI1 functionally, if not mechanistically, to protective immune responses to Gram-negative bacteria.

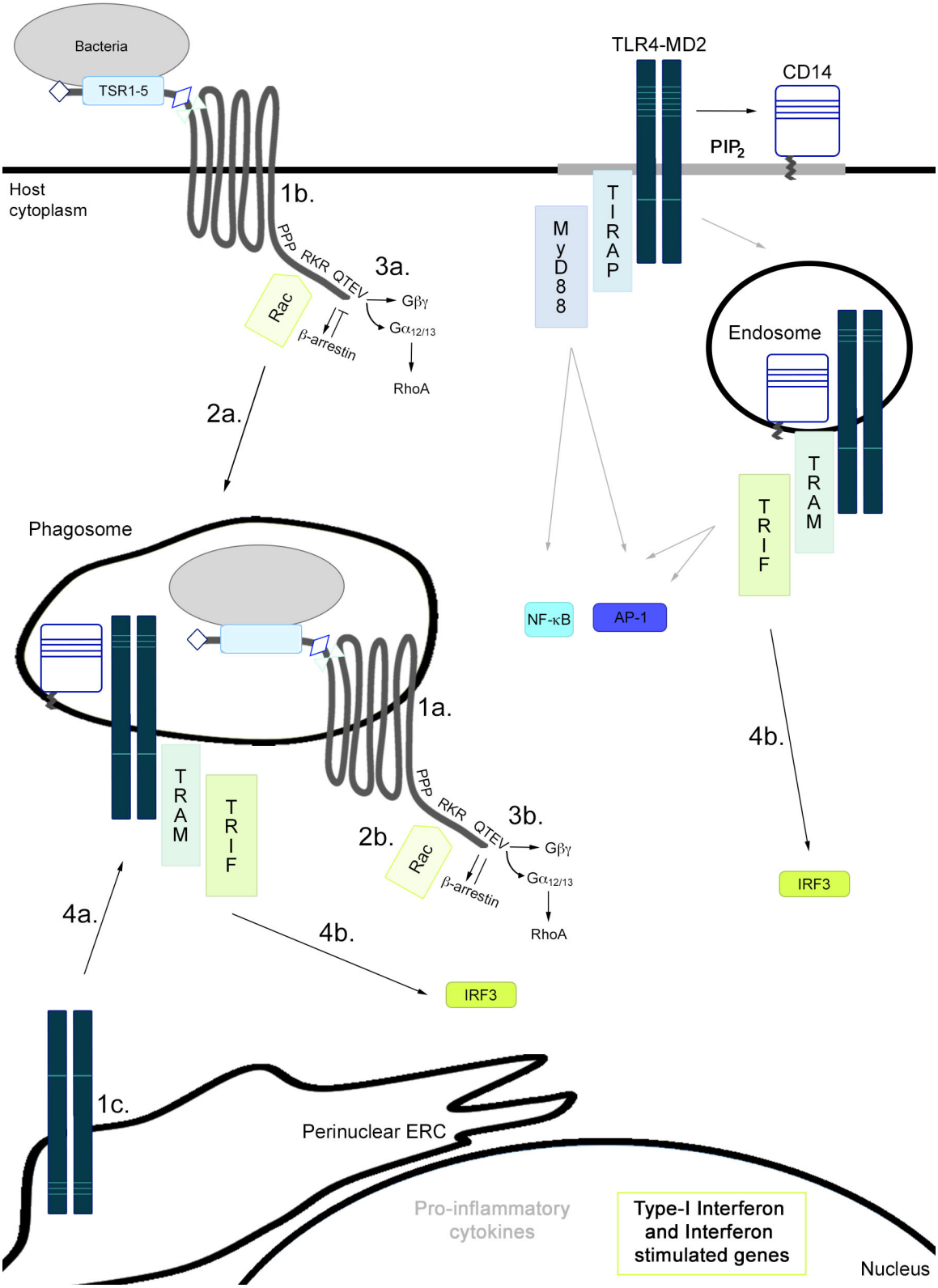
Bacteria
TSR1-5
TLR4-MD2
CD14
PIP2
Host cytoplasm
1b.
PPP RKR QTEV
3a.
Rac
β-arrestin
Gβγ
Gα12/13
RhoA
MyD88
TIRAP
Endosome
TRAM
TRIF
2a.
Phagosome
NF-κB
AP-1
1a.
4b.
TRAM
TRIF
2b.
3b.
PPP RKR QTEV
Rac
β-arrestin
Gβγ
Gα12/13
RhoA
IRF3
4a.
4b.
IRF3
1c.
Perinuclear ERC
Pro-inflammatory cytokines
Type-I Interferon and Interferon stimulated genes
Nucleus

Figure 5-3. Model of BAI1-TLR4 interactions in the early innate response to Gram-negative bacteria

BAI1 selectively promotes intracellular TLR4 signaling leading to IRF3 activation and the induction of TRIF-dependent transcriptional responses (e.g. IFN-β, CCL5, and IL-10). Activation of early, MyD88-dependent, and late, TRIF-dependent, NF-κB and MAPK signaling is unaffected by BAI1 cellular responses in macrophages. TLR4 associates with BAI1 in a manner dependent on the C-terminus of BAI1 from (1a) within the phagosome to regulate with TLR4-TRIF. However, both proteins are found expressed at (1b) the cell surface and within the (1c) ERC and Golgi, so other sites of interaction are possible. Several mechanisms defining the interaction and crosstalk between TLR4 and BAI1 exist. (2a) The BAI1-dependent internalization of bacteria to a phagosome promotes the compartmentalization of ligand enhancing intracellular signaling. (2b) Alternatively, BAI1-dependent Rac activation may promote TLR4 signaling at the phagosome. BAI1 signaling responses independent of Rac (e.g. $G\alpha_{12/13}$, RhoA, Gβγ, or β-arrestin2) may regulate TLR4 at the cell surface (3a) or intracellularly (3b). In this capacity, BAI1 may regulate either the recruitment of TLR4 and TLR4 signaling machinery (4a) or the activity of TLR4 signaling complexes at the phagosome or distally at the endosome (4b).

Summary

Prior to this study, the role of BAI1 in macrophages during the recognition and response to Gram-negative bacteria was largely unknown. The work presented in this thesis provides advances in our understanding of the ligand specificity of the TSR domains, the impact of BAI1-mediated internalization on the fate of the internalized microbe, and the interaction of BAI1 with inflammatory signaling and early transcriptional responses. We found that an interaction between BAI1 and the negatively charged phosphorylated L-glycero-d-manno-heptose sugars in the inner core oligosaccharide of LPS was crucial for BAI1-mediated internalization. This was consistent with the hypothesis that a positively charged groove on the face of the TSR serves as the binding site for LPS, and most importantly indicates that BAI1-mediated recognition is dependent on a motif that is critical for membrane stability and conserved across many Gram-negative bacterial species, commensals and pathogens alike.

The fate of a microbe upon contact with a host cell is determined by the local inflammatory environment and the route of cellular entry. The role and impact of BAI1 mediated recognition in the immune response of macrophages was previously undetermined. Here, we show that BAI1-mediated Rac activation promotes the phagocyte NADPH oxidase-dependent ROS response, resulting in bacterial killing and protection in an in vivo bacterial challenge model. Thus, we provide much needed mechanistic insight into how upstream signals from non-opsonic phagocytic receptors couple to the activation of critical microbicidal machinery in the context of several representative Gram-negative microbes.

Interaction between the limited set of germ-line encoded PRRs contributes to the specificity and magnitude of innate immune responses. We characterized the impact of BAI1 on innate inflammatory signaling pathways and assessed the means of receptor crosstalk and interaction. BAI1 selectively promotes the intracellular TLR4 signaling and transcriptional response by enhancing the phosphorylation and activation of TBK1 and IRF3 downstream of TLR4-MD2. TRIF-dependent type-I IFN-β, IL-10, and CCL5 induction were all reduced in macrophages lacking BAI1, indicating a selective role for BAI1 in critical early innate responses that drive local cellular activation and regulate overly robust inflammatory responses. Moreover, TLR4 and BAI1 physically associate in a manner dependent upon an interaction with the cytoplasmic region of BAI1, and the spatial interaction between Gram-negative bacteria and TLR4 is augmented by BAI1 expression. The direct mechanisms of this interaction remain to be explored, but likely involve BAI1-dependent signaling that modulates the local recruitment and activation of TLR4 signaling partners. Collectively, this highlights the critical and unique specificity and function of BAI1 during TLR4-driven bacterial recognition and early innate responses and suggests that the phagosome serves as a multifunctional and heterogeneous organelle that is distinct from other innate signaling compartments within macrophages.

References

1. Gordon, S. 2008. Elie Metchnikoff: father of natural immunity. *Eur. J. Immunol.* 38: 3257-3264.
2. Kaufmann, S. H. 2008. Immunology's foundation: the 100-year anniversary of the Nobel Prize to Paul Ehrlich and Elie Metchnikoff. *Nat. Immunol.* 9: 705-712.
3. Bayne, C. J. 2003. Origins and evolutionary relationships between the innate and adaptive arms of immune systems. *Integr. Comp. Biol.* 43: 293-299.
4. O'Neill, L. A., D. Golenbock, and A. G. Bowie. 2013. The history of Toll-like receptors - redefining innate immunity. *Nat. Rev. Immunol.* 13: 453-460.
5. Janeway, C. A.,Jr. 1989. Approaching the asymptote? Evolution and revolution in immunology. *Cold Spring Harb. Symp. Quant. Biol.* 54 Pt 1: 1-13.
6. Lemaitre, B., E. Nicolas, L. Michaut, J. M. Reichhart, and J. A. Hoffmann. 1996. The dorsoventral regulatory gene cassette spatzle/Toll/cactus controls the potent antifungal response in Drosophila adults. *Cell* 86: 973-983.
7. Medzhitov, R., P. Preston-Hurlburt, and C. A. Janeway Jr. 1997. A human homologue of the Drosophila Toll protein signals activation of adaptive immunity. *Nature* 388: 394-397.
8. Medzhitov, R., P. Preston-Hurlburt, E. Kopp, A. Stadlen, C. Chen, S. Ghosh, and C. A. Janeway Jr. 1998. MyD88 is an adaptor protein in the hToll/IL-1 receptor family signaling pathways. *Mol. Cell* 2: 253-258.
9. Poltorak, A., X. He, I. Smirnova, M. Y. Liu, C. Van Huffel, X. Du, D. Birdwell, E. Alejos, M. Silva, C. Galanos, M. Freudenberg, P. Ricciardi-Castagnoli, B. Layton, and B. Beutler. 1998. Defective LPS signaling in C3H/HeJ and C57BL/10ScCr mice: mutations in Tlr4 gene. *Science* 282: 2085-2088.
10. Medzhitov, R. and C. A. Janeway Jr. 2002. Decoding the patterns of self and nonself by the innate immune system. *Science* 296: 298-300.
11. Pradeu, T. and E. L. Cooper. 2012. The danger theory: 20 years later. *Front. Immunol.* 3: 287.
12. Stuart, L. M., N. Paquette, and L. Boyer. 2013. Effector-triggered versus pattern-triggered immunity: how animals sense pathogens. *Nat. Rev. Immunol.* 13: 199-206.
13. Tanoue, T., Y. Umesaki, and K. Honda. 2010. Immune responses to gut microbiota-commensals and pathogens. *Gut Microbes* 1: 224-233.
14. Blander, J. M. and L. E. Sander. 2012. Beyond pattern recognition: five immune checkpoints for scaling the microbial threat. *Nat. Rev. Immunol.* 12: 215-225.
15. Brubaker, S. W., K. S. Bonham, I. Zanoni, and J. C. Kagan. 2015. Innate Immune Pattern Recognition: A Cell Biological Perspective. *Annu. Rev. Immunol.*
16. Tan, R. S., B. Ho, B. P. Leung, and J. L. Ding. 2014. TLR cross-talk confers specificity to innate immunity. *Int. Rev. Immunol.* 33: 443-453.
17. Kawai, T. and S. Akira. 2011. Toll-like receptors and their crosstalk with other innate receptors in infection and immunity. *Immunity* 34: 637-650.
18. Hansen, J. D., L. N. Vojtech, and K. J. Laing. 2011. Sensing disease and danger: a survey of vertebrate PRRs and their origins. *Dev. Comp. Immunol.* 35: 886-897.
19. Canton, J., D. Neculai, and S. Grinstein. 2013. Scavenger receptors in homeostasis and immunity. *Nat. Rev. Immunol.* 13: 621-634.
20. Areschoug, T. and S. Gordon. 2009. Scavenger receptors: role in innate immunity and microbial pathogenesis. *Cell. Microbiol.* 11: 1160-1169.

21. Stuart, L. M., J. Deng, J. M. Silver, K. Takahashi, A. A. Tseng, E. J. Hennessy, R. A. Ezekowitz, and K. J. Moore. 2005. Response to Staphylococcus aureus requires CD36-mediated phagocytosis triggered by the COOH-terminal cytoplasmic domain. *J. Cell Biol.* 170: 477-485.
22. Fabriek, B. O., R. van Bruggen, D. M. Deng, A. J. Ligtenberg, K. Nazmi, K. Schornagel, R. P. Vloet, C. D. Dijkstra, and T. K. van den Berg. 2009. The macrophage scavenger receptor CD163 functions as an innate immune sensor for bacteria. *Blood* 113: 887-892.
23. Sankala, M., A. Brannstrom, T. Schulthess, U. Bergmann, E. Morgunova, J. Engel, K. Tryggvason, and T. Pikkarainen. 2002. Characterization of recombinant soluble macrophage scavenger receptor MARCO. *J. Biol. Chem.* 277: 33378-33385.
24. Amiel, E., J. L. Acker, R. M. Collins, and B. Berwin. 2009. Uncoupling scavenger receptor A-mediated phagocytosis of bacteria from endotoxic shock resistance. *Infect. Immun.* 77: 4567-4573.
25. Silverstein, R. L. and M. Febbraio. 2009. CD36, a scavenger receptor involved in immunity, metabolism, angiogenesis, and behavior. *Sci. Signal.* 2: re3.
26. Elinav, E., T. Strowig, J. Henao-Mejia, and R. A. Flavell. 2011. Regulation of the antimicrobial response by NLR proteins. *Immunity* 34: 665-679.
27. Ratsimandresey, R. A., A. Dorfleutner, and C. Stehlik. 2013. An Update on PYRIN Domain-Containing Pattern Recognition Receptors: From Immunity to Pathology. *Front. Immunol.* 4: 440.
28. Chiu, Y. H., J. B. Macmillan, and Z. J. Chen. 2009. RNA polymerase III detects cytosolic DNA and induces type I interferons through the RIG-I pathway. *Cell* 138: 576-591.
29. Schmolke, M., J. R. Patel, E. de Castro, M. T. Sanchez-Aparicio, M. B. Uccellini, J. C. Miller, B. Manicassamy, T. Satoh, T. Kawai, S. Akira, M. Merad, and A. Garcia-Sastre. 2014. RIG-I detects mRNA of intracellular Salmonella enterica serovar Typhimurium during bacterial infection. *MBio* 5: e01006-14.
30. Hornung, V., A. Ablasser, M. Charrel-Dennis, F. Bauernfeind, G. Horvath, D. R. Caffrey, E. Latz, and K. A. Fitzgerald. 2009. AIM2 recognizes cytosolic dsDNA and forms a caspase-1-activating inflammasome with ASC. *Nature* 458: 514-518.
31. Unterholzner, L., S. E. Keating, M. Baran, K. A. Horan, S. B. Jensen, S. Sharma, C. M. Sirois, T. Jin, E. Latz, T. S. Xiao, K. A. Fitzgerald, S. R. Paludan, and A. G. Bowie. 2010. IFI16 is an innate immune sensor for intracellular DNA. *Nat. Immunol.* 11: 997-1004.
32. Kawai, T. and S. Akira. 2009. The roles of TLRs, RLRs and NLRs in pathogen recognition. *Int. Immunol.* 21: 317-337.
33. Pluddemann, A., S. Mukhopadhyay, and S. Gordon. 2011. Innate immunity to intracellular pathogens: macrophage receptors and responses to microbial entry. *Immunol. Rev.* 240: 11-24.
34. Ewald, S. E., B. L. Lee, L. Lau, K. E. Wickliffe, G. P. Shi, H. A. Chapman, and G. M. Barton. 2008. The ectodomain of Toll-like receptor 9 is cleaved to generate a functional receptor. *Nature* 456: 658-662.
35. Lee, B. L. and G. M. Barton. 2014. Trafficking of endosomal Toll-like receptors. *Trends Cell Biol.* 24: 360-369.
36. Barbalat, R., S. E. Ewald, M. L. Mouchess, and G. M. Barton. 2011. Nucleic acid recognition by the innate immune system. *Annu. Rev. Immunol.* 29: 185-214.
37. Yamamoto, M., S. Sato, K. Mori, K. Hoshino, O. Takeuchi, K. Takeda, and S. Akira. 2002. Cutting edge: a novel Toll/IL-1 receptor domain-containing adapter that preferentially activates the IFN-beta promoter in the Toll-like receptor signaling. *J. Immunol.* 169: 6668-6672.
38. Hoebe, K., X. Du, P. Georgel, E. Janssen, K. Tabeta, S. O. Kim, J. Goode, P. Lin, N. Mann, S. Mudd, K. Crozat, S. Sovath, J. Han, and B. Beutler. 2003. Identification of Lps2 as a key transducer of MyD88-independent TIR signalling. *Nature* 424: 743-748.

39. Yamamoto, M., S. Sato, H. Hemmi, S. Uematsu, K. Hoshino, T. Kaisho, O. Takeuchi, K. Takeda, and S. Akira. 2003. TRAM is specifically involved in the Toll-like receptor 4-mediated MyD88-independent signaling pathway. *Nat. Immunol.* 4: 1144-1150.
40. Horng, T., G. M. Barton, and R. Medzhitov. 2001. TIRAP: an adapter molecule in the Toll signaling pathway. *Nat. Immunol.* 2: 835-841.
41. Fitzgerald, K. A., E. M. Palsson-McDermott, A. G. Bowie, C. A. Jefferies, A. S. Mansell, G. Brady, E. Brint, A. Dunne, P. Gray, M. T. Harte, D. McMurray, D. E. Smith, J. E. Sims, T. A. Bird, and L. A. O'Neill. 2001. Mal (MyD88-adapter-like) is required for Toll-like receptor-4 signal transduction. *Nature* 413: 78-83.
42. Brown, J., H. Wang, G. N. Hajishengallis, and M. Martin. 2011. TLR-signaling networks: an integration of adaptor molecules, kinases, and cross-talk. *J. Dent. Res.* 90: 417-427.
43. Bjorkbacka, H., K. A. Fitzgerald, F. Huet, X. Li, J. A. Gregory, M. A. Lee, C. M. Ordija, N. E. Dowley, D. T. Golenbock, and M. W. Freeman. 2004. The induction of macrophage gene expression by LPS predominantly utilizes Myd88-independent signaling cascades. *Physiol. Genomics* 19: 319-330.
44. Hoshino, K., I. Sasaki, T. Sugiyama, T. Yano, C. Yamazaki, T. Yasui, H. Kikutani, and T. Kaisho. 2010. Critical role of IkappaB Kinase alpha in TLR7/9-induced type I IFN production by conventional dendritic cells. *J. Immunol.* 184: 3341-3345.
45. Stack, J., S. L. Doyle, D. J. Connolly, L. S. Reinert, K. M. O'Keeffe, R. M. McLoughlin, S. R. Paludan, and A. G. Bowie. 2014. TRAM is required for TLR2 endosomal signaling to type I IFN induction. *J. Immunol.* 193: 6090-6102.
46. Ip, W. K., A. Sokolovska, G. M. Charriere, L. Boyer, S. Dejardin, M. P. Cappillino, L. M. Yantosca, K. Takahashi, K. J. Moore, A. Lacy-Hulbert, and L. M. Stuart. 2010. Phagocytosis and phagosome acidification are required for pathogen processing and MyD88-dependent responses to Staphylococcus aureus. *J. Immunol.* 184: 7071-7081.
47. Mogensen, T. H. 2009. Pathogen recognition and inflammatory signaling in innate immune defenses. *Clin. Microbiol. Rev.* 22: 240-73, Table of Contents.
48. Kawai, T. and S. Akira. 2010. The role of pattern-recognition receptors in innate immunity: update on Toll-like receptors. *Nat. Immunol.* 11: 373-384.
49. Gotoh, K., Y. Tanaka, A. Nishikimi, R. Nakamura, H. Yamada, N. Maeda, T. Ishikawa, K. Hoshino, T. Uruno, Q. Cao, S. Higashi, Y. Kawaguchi, M. Enjoji, R. Takayanagi, T. Kaisho, Y. Yoshikai, and Y. Fukui. 2010. Selective control of type I IFN induction by the Rac activator DOCK2 during TLR-mediated plasmacytoid dendritic cell activation. *J. Exp. Med.* 207: 721-730.
50. Hoshino, K., O. Takeuchi, T. Kawai, H. Sanjo, T. Ogawa, Y. Takeda, K. Takeda, and S. Akira. 1999. Cutting edge: Toll-like receptor 4 (TLR4)-deficient mice are hyporesponsive to lipopolysaccharide: evidence for TLR4 as the Lps gene product. *J. Immunol.* 162: 3749-3752.
51. Arpaia, N., J. Godec, L. Lau, K. E. Sivick, L. M. McLaughlin, M. B. Jones, T. Dracheva, S. N. Peterson, D. M. Monack, and G. M. Barton. 2011. TLR signaling is required for Salmonella typhimurium virulence. *Cell* 144: 675-688.
52. Sivick, K. E., N. Arpaia, G. L. Reiner, B. L. Lee, B. R. Russell, and G. M. Barton. 2014. Toll-like receptor-deficient mice reveal how innate immune signaling influences Salmonella virulence strategies. *Cell. Host Microbe* 15: 203-213.
53. Vazquez-Torres, A., B. A. Vallance, M. A. Bergman, B. B. Finlay, B. T. Cookson, J. Jones-Carson, and F. C. Fang. 2004. Toll-like receptor 4 dependence of innate and adaptive immunity to Salmonella: importance of the Kupffer cell network. *J. Immunol.* 172: 6202-6208.
54. Noreen, M. and M. Arshad. 2015. Association of TLR1, TLR2, TLR4, TLR6, and TIRAP polymorphisms with disease susceptibility. *Immunol. Res.* 62: 234-252.

55. Agnese, D. M., J. E. Calvano, S. J. Hahm, S. M. Coyle, S. A. Corbett, S. E. Calvano, and S. F. Lowry. 2002. Human toll-like receptor 4 mutations but not CD14 polymorphisms are associated with an increased risk of gram-negative infections. *J. Infect. Dis.* 186: 1522-1525.
56. Torok, H. P., J. Glas, L. Tonenchi, T. Mussack, and C. Folwaczny. 2004. Polymorphisms of the lipopolysaccharide-signaling complex in inflammatory bowel disease: association of a mutation in the Toll-like receptor 4 gene with ulcerative colitis. *Clin. Immunol.* 112: 85-91.
57. Lorenz, E., J. P. Mira, K. L. Frees, and D. A. Schwartz. 2002. Relevance of mutations in the TLR4 receptor in patients with gram-negative septic shock. *Arch. Intern. Med.* 162: 1028-1032.
58. Barber, R. C., L. Y. Chang, B. D. Arnoldo, G. F. Purdue, J. L. Hunt, J. W. Horton, and C. C. Aragaki. 2006. Innate immunity SNPs are associated with risk for severe sepsis after burn injury. *Clin. Med. Res.* 4: 250-255.
59. Borzecka, K., A. Plociennikowska, H. Bjorkelund, A. Sobota, and K. Kwiatkowska. 2013. CD14 mediates binding of high doses of LPS but is dispensable for TNF-alpha production. *Mediators Inflamm.* 2013: 824919.
60. Zanoni, I., C. Bodio, A. Broggi, R. Ostuni, M. Caccia, M. Collini, A. Venkatesh, R. Spreafico, G. Capuano, and F. Granucci. 2012. Similarities and differences of innate immune responses elicited by smooth and rough LPS. *Immunol. Lett.* 142: 41-47.
61. Jiang, Z., P. Georgel, X. Du, L. Shamel, S. Sovath, S. Mudd, M. Huber, C. Kalis, S. Keck, C. Galanos, M. Freudenberg, and B. Beutler. 2005. CD14 is required for MyD88-independent LPS signaling. *Nat. Immunol.* 6: 565-570.
62. Bryant, C. E., M. Symmons, and N. J. Gay. 2015. Toll-like receptor signalling through macromolecular protein complexes. *Mol. Immunol.* 63: 162-165.
63. Tan, Y., I. Zanoni, T. W. Cullen, A. L. Goodman, and J. C. Kagan. 2015. Mechanisms of Toll-like Receptor 4 Endocytosis Reveal a Common Immune-Evasion Strategy Used by Pathogenic and Commensal Bacteria. *Immunity* 43: 909-922.
64. Gay, N. J., M. Gangloff, and L. A. O'Neill. 2011. What the Myddosome structure tells us about the initiation of innate immunity. *Trends Immunol.* 32: 104-109.
65. Song, D. H. and J. O. Lee. 2012. Sensing of microbial molecular patterns by Toll-like receptors. *Immunol. Rev.* 250: 216-229.
66. Latz, E., A. Visintin, E. Lien, K. A. Fitzgerald, B. G. Monks, E. A. Kurt-Jones, D. T. Golenbock, and T. Espevik. 2002. Lipopolysaccharide rapidly traffics to and from the Golgi apparatus with the toll-like receptor 4-MD-2-CD14 complex in a process that is distinct from the initiation of signal transduction. *J. Biol. Chem.* 277: 47834-47843.
67. Husebye, H., M. H. Aune, J. Stenvik, E. Samstad, F. Skjeldal, O. Halaas, N. J. Nilsen, H. Stenmark, E. Latz, E. Lien, T. E. Mollnes, O. Bakke, and T. Espevik. 2010. The Rab11a GTPase controls Toll-like receptor 4-induced activation of interferon regulatory factor-3 on phagosomes. *Immunity* 33: 583-596.
68. Husebye, H., O. Halaas, H. Stenmark, G. Tunheim, O. Sandanger, B. Bogen, A. Brech, E. Latz, and T. Espevik. 2006. Endocytic pathways regulate Toll-like receptor 4 signaling and link innate and adaptive immunity. *EMBO J.* 25: 683-692.
69. Klein, D. C., A. Skjesol, E. D. Kers-Rebel, T. Sherstova, B. Sporsheim, K. W. Egeberg, B. T. Stokke, T. Espevik, and H. Husebye. 2015. CD14, TLR4 and TRAM Show Different Trafficking Dynamics During LPS Stimulation. *Traffic* 16: 677-690.
70. Plociennikowska, A., M. I. Zdioruk, G. Traczyk, A. Swiatkowska, and K. Kwiatkowska. 2015. LPS-induced clustering of CD14 triggers generation of PI(4,5)P2. *J. Cell. Sci.* 128: 4096-4111.
71. Kagan, J. C. and R. Medzhitov. 2006. Phosphoinositide-mediated adaptor recruitment controls Toll-like receptor signaling. *Cell* 125: 943-955.

72. Ruysschaert, J. M. and C. Lonez. 2015. Role of lipid microdomains in TLR-mediated signalling. *Biochim. Biophys. Acta* 1848: 1860-1867.
73. Enokizono, Y., H. Kumeta, K. Funami, M. Horiuchi, J. Sarmiento, K. Yamashita, D. M. Standley, M. Matsumoto, T. Seya, and F. Inagaki. 2013. Structures and interface mapping of the TIR domain-containing adaptor molecules involved in interferon signaling. *Proc. Natl. Acad. Sci. U. S. A.* 110: 19908-19913.
74. Zanoni, I., R. Ostuni, L. R. Marek, S. Barresi, R. Barbalat, G. M. Barton, F. Granucci, and J. C. Kagan. 2011. CD14 controls the LPS-induced endocytosis of Toll-like receptor 4. *Cell* 147: 868-880.
75. Aksoy, E., S. Taboubi, D. Torres, S. Delbauve, A. Hachani, M. A. Whitehead, W. P. Pearce, I. M. Berenjeno, G. Nock, A. Filloux, R. Beyaert, V. Flamand, and B. Vanhaesebroeck. 2012. The p110delta isoform of the kinase PI(3)K controls the subcellular compartmentalization of TLR4 signaling and protects from endotoxic shock. *Nat. Immunol.* 13: 1045-1054.
76. Zhang, S., M. Yu, Q. Guo, R. Li, G. Li, S. Tan, X. Li, Y. Wei, and M. Wu. 2015. Annexin A2 binds to endosomes and negatively regulates TLR4-triggered inflammatory responses via the TRAM-TRIF pathway. *Sci. Rep.* 5: 15859.
77. Yang, Z., D. Sun, Z. Yan, A. B. Reynolds, J. W. Christman, R. D. Minshall, A. B. Malik, Y. Zhang, and G. Hu. 2014. Differential role for p120-catenin in regulation of TLR4 signaling in macrophages. *J. Immunol.* 193: 1931-1941.
78. Rowe, D. C., A. F. McGettrick, E. Latz, B. G. Monks, N. J. Gay, M. Yamamoto, S. Akira, L. A. O'Neill, K. A. Fitzgerald, and D. T. Golenbock. 2006. The myristoylation of TRIF-related adaptor molecule is essential for Toll-like receptor 4 signal transduction. *Proc. Natl. Acad. Sci. U. S. A.* 103: 6299-6304.
79. Hacker, H., V. Redecke, B. Blagoev, I. Kratchmarova, L. C. Hsu, G. G. Wang, M. P. Kamps, E. Raz, H. Wagner, G. Hacker, M. Mann, and M. Karin. 2006. Specificity in Toll-like receptor signalling through distinct effector functions of TRAF3 and TRAF6. *Nature* 439: 204-207.
80. Shibata, T., Y. Motoi, N. Tanimura, N. Yamakawa, S. Akashi-Takamura, and K. Miyake. 2011. Intracellular TLR4/MD-2 in macrophages senses Gram-negative bacteria and induces a unique set of LPS-dependent genes. *Int. Immunol.* 23: 503-510.
81. Sato, S., M. Sugiyama, M. Yamamoto, Y. Watanabe, T. Kawai, K. Takeda, and S. Akira. 2003. Toll/IL-1 receptor domain-containing adaptor inducing IFN-beta (TRIF) associates with TNF receptor-associated factor 6 and TANK-binding kinase 1, and activates two distinct transcription factors, NF-kappa B and IFN-regulatory factor-3, in the Toll-like receptor signaling. *J. Immunol.* 171: 4304-4310.
82. Funami, K., M. Sasai, H. Oshiumi, T. Seya, and M. Matsumoto. 2008. Homo-oligomerization is essential for Toll/interleukin-1 receptor domain-containing adaptor molecule-1-mediated NF-kappaB and interferon regulatory factor-3 activation. *J. Biol. Chem.* 283: 18283-18291.
83. Cusson-Hermance, N., S. Khurana, T. H. Lee, K. A. Fitzgerald, and M. A. Kelliher. 2005. Rip1 mediates the Trif-dependent toll-like receptor 3- and 4-induced NF-{kappa}B activation but does not contribute to interferon regulatory factor 3 activation. *J. Biol. Chem.* 280: 36560-36566.
84. Meylan, E., K. Burns, K. Hofmann, V. Blancheteau, F. Martinon, M. Kelliher, and J. Tschopp. 2004. RIP1 is an essential mediator of Toll-like receptor 3-induced NF-kappa B activation. *Nat. Immunol.* 5: 503-507.
85. Fitzgerald, K. A., D. C. Rowe, B. J. Barnes, D. R. Caffrey, A. Visintin, E. Latz, B. Monks, P. M. Pitha, and D. T. Golenbock. 2003. LPS-TLR4 signaling to IRF-3/7 and NF-kappaB involves the toll adapters TRAM and TRIF. *J. Exp. Med.* 198: 1043-1055.
86. Fitzgerald, K. A., S. M. McWhirter, K. L. Faia, D. C. Rowe, E. Latz, D. T. Golenbock, A. J. Coyle, S. M. Liao, and T. Maniatis. 2003. IKKepsilon and TBK1 are essential components of the IRF3 signaling pathway. *Nat. Immunol.* 4: 491-496.

87. Sharma, S., B. R. tenOever, N. Grandvaux, G. P. Zhou, R. Lin, and J. Hiscott. 2003. Triggering the interferon antiviral response through an IKK-related pathway. *Science* 300: 1148-1151.
88. McWhirter, S. M., K. A. Fitzgerald, J. Rosains, D. C. Rowe, D. T. Golenbock, and T. Maniatis. 2004. IFN-regulatory factor 3-dependent gene expression is defective in Tbk1-deficient mouse embryonic fibroblasts. *Proc. Natl. Acad. Sci. U. S. A.* 101: 233-238.
89. Hacker, H., P. H. Tseng, and M. Karin. 2011. Expanding TRAF function: TRAF3 as a tri-faced immune regulator. *Nat. Rev. Immunol.* 11: 457-468.
90. Van Acker, T., S. Eyckerman, L. Vande Walle, S. Gerlo, M. Goethals, M. Lamkanfi, C. Bovijn, J. Tavernier, and F. Peelman. 2014. The small GTPase Arf6 is essential for the Tram/Trif pathway in TLR4 signaling. *J. Biol. Chem.* 289: 1364-1376.
91. Di Gioia, M. and I. Zanoni. 2015. Toll-like receptor co-receptors as master regulators of the immune response. *Mol. Immunol.* 63: 143-152.
92. Kagan, J. C., T. Su, T. Horng, A. Chow, S. Akira, and R. Medzhitov. 2008. TRAM couples endocytosis of Toll-like receptor 4 to the induction of interferon-beta. *Nat. Immunol.* 9: 361-368.
93. Plociennikowska, A., A. Hromada-Judycka, K. Borzecka, and K. Kwiatkowska. 2015. Co-operation of TLR4 and raft proteins in LPS-induced pro-inflammatory signaling. *Cell Mol. Life Sci.* 72: 557-581.
94. Ozinsky, A., D. M. Underhill, J. D. Fontenot, A. M. Hajjar, K. D. Smith, C. B. Wilson, L. Schroeder, and A. Aderem. 2000. The repertoire for pattern recognition of pathogens by the innate immune system is defined by cooperation between toll-like receptors. *Proc. Natl. Acad. Sci. U. S. A.* 97: 13766-13771.
95. Triantafilou, M., F. G. Gamper, R. M. Haston, M. A. Mouratis, S. Morath, T. Hartung, and K. Triantafilou. 2006. Membrane sorting of toll-like receptor (TLR)-2/6 and TLR2/1 heterodimers at the cell surface determines heterotypic associations with CD36 and intracellular targeting. *J. Biol. Chem.* 281: 31002-31011.
96. Carpenter, S., T. Carlson, J. Dellacasagrande, A. Garcia, S. Gibbons, P. Hertzog, A. Lyons, L. L. Lin, M. Lynch, T. Monie, C. Murphy, K. J. Seidl, C. Wells, A. Dunne, and L. A. O'Neill. 2009. TRIL, a functional component of the TLR4 signaling complex, highly expressed in brain. *J. Immunol.* 183: 3989-3995.
97. Eckert, J. K., Y. J. Kim, J. I. Kim, K. Gurtler, D. Y. Oh, S. Sur, L. Lundvall, L. Hamann, A. van der Ploeg, P. Pickkers, E. Giamarellos-Bourboulis, A. V. Kubarenko, A. N. Weber, M. Kabesch, O. Kumpf, H. J. An, J. O. Lee, and R. R. Schumann. 2013. The crystal structure of lipopolysaccharide binding protein reveals the location of a frequent mutation that impairs innate immunity. *Immunity* 39: 647-660.
98. Gioannini, T. L., A. Teghanemt, D. Zhang, N. P. Coussens, W. Dockstader, S. Ramaswamy, and J. P. Weiss. 2004. Isolation of an endotoxin-MD-2 complex that produces Toll-like receptor 4-dependent cell activation at picomolar concentrations. *Proc. Natl. Acad. Sci. U. S. A.* 101: 4186-4191.
99. Perera, P. Y., S. N. Vogel, G. R. Detore, A. Haziot, and S. M. Goyert. 1997. CD14-dependent and CD14-independent signaling pathways in murine macrophages from normal and CD14 knockout mice stimulated with lipopolysaccharide or taxol. *J. Immunol.* 158: 4422-4429.
100. Tsukamoto, H., K. Fukudome, S. Takao, N. Tsuneyoshi, and M. Kimoto. 2010. Lipopolysaccharide-binding protein-mediated Toll-like receptor 4 dimerization enables rapid signal transduction against lipopolysaccharide stimulation on membrane-associated CD14-expressing cells. *Int. Immunol.* 22: 271-280.
101. Schumann, R. R., S. R. Leong, G. W. Flaggs, P. W. Gray, S. D. Wright, J. C. Mathison, P. S. Tobias, and R. J. Ulevitch. 1990. Structure and function of lipopolysaccharide binding protein. *Science* 249: 1429-1431.

102. Jimenez-Dalmaroni, M. J., N. Xiao, A. L. Corper, P. Verdino, G. D. Ainge, D. S. Larsen, G. F. Painter, P. M. Rudd, R. A. Dwek, K. Hoebe, B. Beutler, and I. A. Wilson. 2009. Soluble CD36 ectodomain binds negatively charged diacylglycerol ligands and acts as a co-receptor for TLR2. *PLoS One* 4: e7411.
103. Hoebe, K., P. Georgel, S. Rutschmann, X. Du, S. Mudd, K. Crozat, S. Sovath, L. Shamel, T. Hartung, U. Zahringer, and B. Beutler. 2005. CD36 is a sensor of diacylglycerides. *Nature* 433: 523-527.
104. Gantner, B. N., R. M. Simmons, S. J. Canavera, S. Akira, and D. M. Underhill. 2003. Collaborative induction of inflammatory responses by dectin-1 and Toll-like receptor 2. *J. Exp. Med.* 197: 1107-1117.
105. Dennehy, K. M., G. Ferwerda, I. Faro-Trindade, E. Pyz, J. A. Willment, P. R. Taylor, A. Kerrigan, S. V. Tsoni, S. Gordon, F. Meyer-Wentrup, G. J. Adema, B. J. Kullberg, E. Schweighoffer, V. Tybulewicz, H. M. Mora-Montes, N. A. Gow, D. L. Williams, M. G. Netea, and G. D. Brown. 2008. Syk kinase is required for collaborative cytokine production induced through Dectin-1 and Toll-like receptors. *Eur. J. Immunol.* 38: 500-506.
106. Gringhuis, S. I., J. den Dunnen, M. Litjens, B. van Het Hof, Y. van Kooyk, and T. B. Geijtenbeek. 2007. C-type lectin DC-SIGN modulates Toll-like receptor signaling via Raf-1 kinase-dependent acetylation of transcription factor NF-kappaB. *Immunity* 26: 605-616.
107. Yu, H., T. Ha, L. Liu, X. Wang, M. Gao, J. Kelley, R. Kao, D. Williams, and C. Li. 2012. Scavenger receptor A (SR-A) is required for LPS-induced TLR4 mediated NF-kappaB activation in macrophages. *Biochim. Biophys. Acta* 1823: 1192-1198.
108. Mukhopadhyay, S., A. Varin, Y. Chen, B. Liu, K. Tryggvason, and S. Gordon. 2011. SR-A/MARCO-mediated ligand delivery enhances intracellular TLR and NLR function, but ligand scavenging from cell surface limits TLR4 response to pathogens. *Blood* 117: 1319-1328.
109. Jozefowski, S., M. Arredouani, T. Sulahian, and L. Kobzik. 2005. Disparate regulation and function of the class A scavenger receptors SR-AI/II and MARCO. *J. Immunol.* 175: 8032-8041.
110. Barton, G. M. and J. C. Kagan. 2009. A cell biological view of Toll-like receptor function: regulation through compartmentalization. *Nat. Rev. Immunol.* 9: 535-542.
111. Underhill, D. M., A. Ozinsky, A. M. Hajjar, A. Stevens, C. B. Wilson, M. Bassetti, and A. Aderem. 1999. The Toll-like receptor 2 is recruited to macrophage phagosomes and discriminates between pathogens. *Nature* 401: 811-815.
112. Stewart, C. R., L. M. Stuart, K. Wilkinson, J. M. van Gils, J. Deng, A. Halle, K. J. Rayner, L. Boyer, R. Zhong, W. A. Frazier, A. Lacy-Hulbert, J. El Khoury, D. T. Golenbock, and K. J. Moore. 2010. CD36 ligands promote sterile inflammation through assembly of a Toll-like receptor 4 and 6 heterodimer. *Nat. Immunol.* 11: 155-161.
113. Ip, W. K., K. Takahashi, K. J. Moore, L. M. Stuart, and R. A. Ezekowitz. 2008. Mannose-binding lectin enhances Toll-like receptors 2 and 6 signaling from the phagosome. *J. Exp. Med.* 205: 169-181.
114. Doyle, S. E., R. M. O'Connell, G. A. Miranda, S. A. Vaidya, E. K. Chow, P. T. Liu, S. Suzuki, N. Suzuki, R. L. Modlin, W. C. Yeh, T. F. Lane, and G. Cheng. 2004. Toll-like receptors induce a phagocytic gene program through p38. *J. Exp. Med.* 199: 81-90.
115. Deng, T., X. Feng, P. Liu, K. Yan, Y. Chen, and D. Han. 2013. Toll-like receptor 3 activation differentially regulates phagocytosis of bacteria and apoptotic neutrophils by mouse peritoneal macrophages. *Immunol. Cell Biol.* 91: 52-59.
116. Kong, L. and B. X. Ge. 2008. MyD88-independent activation of a novel actin-Cdc42/Rac pathway is required for Toll-like receptor-stimulated phagocytosis. *Cell Res.* 18: 745-755.
117. Underhill, D. M. and H. S. Goodridge. 2012. Information processing during phagocytosis. *Nat. Rev. Immunol.* 12: 492-502.

118. Kerrigan, A. M. and G. D. Brown. 2009. C-type lectins and phagocytosis. *Immunobiology* 214: 562-575.
119. Zamze, S., L. Martinez-Pomares, H. Jones, P. R. Taylor, R. J. Stillion, S. Gordon, and S. Y. Wong. 2002. Recognition of bacterial capsular polysaccharides and lipopolysaccharides by the macrophage mannose receptor. *J. Biol. Chem.* 277: 41613-41623.
120. Underhill, D. M., E. Rossnagle, C. A. Lowell, and R. M. Simmons. 2005. Dectin-1 activates Syk tyrosine kinase in a dynamic subset of macrophages for reactive oxygen production. *Blood* 106: 2543-2550.
121. Baranova, I. N., R. Kurlander, A. V. Bocharov, T. G. Vishnyakova, Z. Chen, A. T. Remaley, G. Csako, A. P. Patterson, and T. L. Eggerman. 2008. Role of human CD36 in bacterial recognition, phagocytosis, and pathogen-induced JNK-mediated signaling. *J. Immunol.* 181: 7147-7156.
122. Jing, J., I. V. Yang, L. Hui, J. A. Patel, C. M. Evans, R. Prikeris, L. Kobzik, B. P. O'Connor, and D. A. Schwartz. 2013. Role of macrophage receptor with collagenous structure in innate immune tolerance. *J. Immunol.* 190: 6360-6367.
123. Groves, E., A. E. Dart, V. Covarelli, and E. Caron. 2008. Molecular mechanisms of phagocytic uptake in mammalian cells. *Cell Mol. Life Sci.* 65: 1957-1976.
124. Bohdanowicz, M., G. Cosio, J. M. Backer, and S. Grinstein. 2010. Class I and class III phosphoinositide 3-kinases are required for actin polymerization that propels phagosomes. *J. Cell Biol.* 191: 999-1012.
125. Caron, E. and A. Hall. 1998. Identification of two distinct mechanisms of phagocytosis controlled by different Rho GTPases. *Science* 282: 1717-1721.
126. Flannagan, R. S., V. Jaumouille, and S. Grinstein. 2012. The cell biology of phagocytosis. *Annu. Rev. Pathol.* 7: 61-98.
127. Flannagan, R. S., R. E. Harrison, C. M. Yip, K. Jaqaman, and S. Grinstein. 2010. Dynamic macrophage "probing" is required for the efficient capture of phagocytic targets. *J. Cell Biol.* 191: 1205-1218.
128. Blanchoin, L., K. J. Amann, H. N. Higgs, J. B. Marchand, D. A. Kaiser, and T. D. Pollard. 2000. Direct observation of dendritic actin filament networks nucleated by Arp2/3 complex and WASP/Scar proteins. *Nature* 404: 1007-1011.
129. Machesky, L. M. and R. H. Insall. 1998. Scar1 and the related Wiskott-Aldrich syndrome protein, WASP, regulate the actin cytoskeleton through the Arp2/3 complex. *Curr. Biol.* 8: 1347-1356.
130. Castellano, F., P. Montcourrier, J. C. Guillemot, E. Gouin, L. Machesky, P. Cossart, and P. Chavrier. 1999. Inducible recruitment of Cdc42 or WASP to a cell-surface receptor triggers actin polymerization and filopodium formation. *Curr. Biol.* 9: 351-360.
131. Castellano, F., P. Montcourrier, and P. Chavrier. 2000. Membrane recruitment of Rac1 triggers phagocytosis. *J. Cell. Sci.* 113 (Pt 17): 2955-2961.
132. Massol, P., P. Montcourrier, J. C. Guillemot, and P. Chavrier. 1998. Fc receptor-mediated phagocytosis requires CDC42 and Rac1. *EMBO J.* 17: 6219-6229.
133. Hoppe, A. D. and J. A. Swanson. 2004. Cdc42, Rac1, and Rac2 display distinct patterns of activation during phagocytosis. *Mol. Biol. Cell* 15: 3509-3519.
134. Castellano, F., P. Chavrier, and E. Caron. 2001. Actin dynamics during phagocytosis. *Semin. Immunol.* 13: 347-355.
135. Kheir, W. A., J. C. Gevrey, H. Yamaguchi, B. Isaac, and D. Cox. 2005. A WAVE2-Abi1 complex mediates CSF-1-induced F-actin-rich membrane protrusions and migration in macrophages. *J. Cell. Sci.* 118: 5369-5379.

136. Yamauchi, A., C. Kim, S. Li, C. C. Marchal, J. Towe, S. J. Atkinson, and M. C. Dinauer. 2004. Rac2-deficient murine macrophages have selective defects in superoxide production and phagocytosis of opsonized particles. *J. Immunol.* 173: 5971-5979.
137. Scott, C. C., W. Dobson, R. J. Botelho, N. Coady-Osberg, P. Chavrier, D. A. Knecht, C. Heath, P. Stahl, and S. Grinstein. 2005. Phosphatidylinositol-4,5-bisphosphate hydrolysis directs actin remodeling during phagocytosis. *J. Cell Biol.* 169: 139-149.
138. Bokoch, G. M. 2005. Regulation of innate immunity by Rho GTPases. *Trends Cell Biol.* 15: 163-171.
139. Olazabal, I. M., E. Caron, R. C. May, K. Schilling, D. A. Knecht, and L. M. Machesky. 2002. Rho-kinase and myosin-II control phagocytic cup formation during CR, but not FcgammaR, phagocytosis. *Curr. Biol.* 12: 1413-1418.
140. Colucci-Guyon, E., F. Niedergang, B. J. Wallar, J. Peng, A. S. Alberts, and P. Chavrier. 2005. A role for mammalian diaphanous-related formins in complement receptor (CR3)-mediated phagocytosis in macrophages. *Curr. Biol.* 15: 2007-2012.
141. Lee, W. L., G. Cosio, K. Ireton, and S. Grinstein. 2007. Role of CrkII in Fcgamma receptor-mediated phagocytosis. *J. Biol. Chem.* 282: 11135-11143.
142. Hall, A. B., M. A. Gakidis, M. Glogauer, J. L. Wilsbacher, S. Gao, W. Swat, and J. S. Brugge. 2006. Requirements for Vav guanine nucleotide exchange factors and Rho GTPases in FcgammaR- and complement-mediated phagocytosis. *Immunity* 24: 305-316.
143. Lu, M. and K. S. Ravichandran. 2006. Dock180-ELMO cooperation in Rac activation. *Methods Enzymol.* 406: 388-402.
144. Cox, D., D. J. Lee, B. M. Dale, J. Calafat, and S. Greenberg. 2000. A Rab11-containing rapidly recycling compartment in macrophages that promotes phagocytosis. *Proc. Natl. Acad. Sci. U. S. A.* 97: 680-685.
145. Bajno, L., X. R. Peng, A. D. Schreiber, H. P. Moore, W. S. Trimble, and S. Grinstein. 2000. Focal exocytosis of VAMP3-containing vesicles at sites of phagosome formation. *J. Cell Biol.* 149: 697-706.
146. Mohammadi, S. and R. R. Isberg. 2013. Cdc42 interacts with the exocyst complex to promote phagocytosis. *J. Cell Biol.* 200: 81-93.
147. Munson, M. and P. Novick. 2006. The exocyst defrocked, a framework of rods revealed. *Nat. Struct. Mol. Biol.* 13: 577-581.
148. Niedergang, F., E. Colucci-Guyon, T. Dubois, G. Raposo, and P. Chavrier. 2003. ADP ribosylation factor 6 is activated and controls membrane delivery during phagocytosis in macrophages. *J. Cell Biol.* 161: 1143-1150.
149. Stenmark, H. 2009. Rab GTPases as coordinators of vesicle traffic. *Nat. Rev. Mol. Cell Biol.* 10: 513-525.
150. Patel, P. C. and R. E. Harrison. 2008. Membrane ruffles capture C3bi-opsonized particles in activated macrophages. *Mol. Biol. Cell* 19: 4628-4639.
151. Egami, Y., T. Taguchi, M. Maekawa, H. Arai, and N. Araki. 2014. Small GTPases and phosphoinositides in the regulatory mechanisms of macropinosome formation and maturation. *Front. Physiol.* 5: 374.
152. Kawano, Y., T. Kaneko-Kawano, and K. Shimamoto. 2014. Rho family GTPase-dependent immunity in plants and animals. *Front. Plant. Sci.* 5: 522.
153. Schaefer, A., N. R. Reinhard, and P. L. Hordijk. 2014. Toward understanding RhoGTPase specificity: structure, function and local activation. *Small GTPases* 5: 6.
154. Blander, J. M. and R. Medzhitov. 2006. Toll-dependent selection of microbial antigens for presentation by dendritic cells. *Nature* 440: 808-812.
155. Blander, J. M. and R. Medzhitov. 2004. Regulation of phagosome maturation by signals from toll-like receptors. *Science* 304: 1014-1018.

156. West, A. P., I. E. Brodsky, C. Rahner, D. K. Woo, H. Erdjument-Bromage, P. Tempst, M. C. Walsh, Y. Choi, G. S. Shadel, and S. Ghosh. 2011. TLR signalling augments macrophage bactericidal activity through mitochondrial ROS. *Nature* 472: 476-480.
157. Berger, S. B., X. Romero, C. Ma, G. Wang, W. A. Faubion, G. Liao, E. Compeer, M. Keszei, L. Rameh, N. Wang, M. Boes, J. R. Regueiro, H. C. Reinecker, and C. Terhorst. 2010. SLAM is a microbial sensor that regulates bacterial phagosome functions in macrophages. *Nat. Immunol.* 11: 920-927.
158. Miletic, A. V., D. B. Graham, V. Montgrain, K. Fujikawa, T. Kloeppel, K. Brim, B. Weaver, R. Schreiber, R. Xavier, and W. Swat. 2007. Vav proteins control MyD88-dependent oxidative burst. *Blood* 109: 3360-3368.
159. Flannagan, R. S., G. Cosio, and S. Grinstein. 2009. Antimicrobial mechanisms of phagocytes and bacterial evasion strategies. *Nat. Rev. Microbiol.* 7: 355-366.
160. MacMicking, J., Q. W. Xie, and C. Nathan. 1997. Nitric oxide and macrophage function. *Annu. Rev. Immunol.* 15: 323-350.
161. Fairn, G. D. and S. Grinstein. 2012. How nascent phagosomes mature to become phagolysosomes. *Trends Immunol.* 33: 397-405.
162. Canton, J., R. Khezri, M. Glogauer, and S. Grinstein. 2014. Contrasting phagosome pH regulation and maturation in human M1 and M2 macrophages. *Mol. Biol. Cell* 25: 3330-3341.
163. Kinchen, J. M. and K. S. Ravichandran. 2008. Phagosome maturation: going through the acid test. *Nat. Rev. Mol. Cell Biol.* 9: 781-795.
164. Russell, D. G., B. C. Vanderven, S. Glennie, H. Mwandumba, and R. S. Heyderman. 2009. The macrophage marches on its phagosome: dynamic assays of phagosome function. *Nat. Rev. Immunol.* 9: 594-600.
165. Schroder, B. A., C. Wrocklage, A. Hasilik, and P. Saftig. 2010. The proteome of lysosomes. *Proteomics* 10: 4053-4076.
166. Vernon, P. J. and D. Tang. 2013. Eat-me: autophagy, phagocytosis, and reactive oxygen species signaling. *Antioxid. Redox Signal.* 18: 677-691.
167. VanderVen, B. C., R. M. Yates, and D. G. Russell. 2009. Intraphagosomal measurement of the magnitude and duration of the oxidative burst. *Traffic* 10: 372-378.
168. Weinberg, J. B., M. A. Misukonis, P. J. Shami, S. N. Mason, D. L. Sauls, W. A. Dittman, E. R. Wood, G. K. Smith, B. McDonald, and K. E. Bachus. 1995. Human mononuclear phagocyte inducible nitric oxide synthase (iNOS): analysis of iNOS mRNA, iNOS protein, biopterin, and nitric oxide production by blood monocytes and peritoneal macrophages. *Blood* 86: 1184-1195.
169. Jabado, N., A. Jankowski, S. Dougaparsad, V. Picard, S. Grinstein, and P. Gros. 2000. Natural resistance to intracellular infections: natural resistance-associated macrophage protein 1 (Nramp1) functions as a pH-dependent manganese transporter at the phagosomal membrane. *J. Exp. Med.* 192: 1237-1248.
170. Nunes, P., N. Demaurex, and M. C. Dinauer. 2013. Regulation of the NADPH oxidase and associated ion fluxes during phagocytosis. *Traffic* 14: 1118-1131.
171. Rybicka, J. M., D. R. Balce, M. F. Khan, R. M. Krohn, and R. M. Yates. 2010. NADPH oxidase activity controls phagosomal proteolysis in macrophages through modulation of the lumenal redox environment of phagosomes. *Proc. Natl. Acad. Sci. U. S. A.* 107: 10496-10501.
172. Yang, C. S., J. S. Lee, M. Rodgers, C. K. Min, J. Y. Lee, H. J. Kim, K. H. Lee, C. J. Kim, B. Oh, E. Zandi, Z. Yue, I. Kramnik, C. Liang, and J. U. Jung. 2012. Autophagy protein Rubicon mediates phagocytic NADPH oxidase activation in response to microbial infection or TLR stimulation. *Cell. Host Microbe* 11: 264-276.
173. Martinez, J., R. K. Malireddi, Q. Lu, L. D. Cunha, S. Pelletier, S. Gingras, R. Orchard, J. L. Guan, H. Tan, J. Peng, T. D. Kanneganti, H. W. Virgin, and D. R. Green. 2015. Molecular

characterization of LC3-associated phagocytosis reveals distinct roles for Rubicon, NOX2 and autophagy proteins. *Nat. Cell Biol.* 17: 893-906.
174. Lai, S. C. and R. J. Devenish. 2012. LC3-Associated Phagocytosis (LAP): Connections with Host Autophagy. *Cells* 1: 396-408.
175. Griffiths, G. 2004. On phagosome individuality and membrane signalling networks. *Trends Cell Biol.* 14: 343-351.
176. Henry, R. M., A. D. Hoppe, N. Joshi, and J. A. Swanson. 2004. The uniformity of phagosome maturation in macrophages. *J. Cell Biol.* 164: 185-194.
177. Vieira, O. V., C. Bucci, R. E. Harrison, W. S. Trimble, L. Lanzetti, J. Gruenberg, A. D. Schreiber, P. D. Stahl, and S. Grinstein. 2003. Modulation of Rab5 and Rab7 recruitment to phagosomes by phosphatidylinositol 3-kinase. *Mol. Cell. Biol.* 23: 2501-2514.
178. Lambeth, J. D. 2004. NOX enzymes and the biology of reactive oxygen. *Nat. Rev. Immunol.* 4: 181-189.
179. Bedard, K. and K. H. Krause. 2007. The NOX family of ROS-generating NADPH oxidases: physiology and pathophysiology. *Physiol. Rev.* 87: 245-313.
180. Bylund, J., K. L. Brown, C. Movitz, C. Dahlgren, and A. Karlsson. 2010. Intracellular generation of superoxide by the phagocyte NADPH oxidase: how, where, and what for? *Free Radic. Biol. Med.* 49: 1834-1845.
181. Brown, D. I. and K. K. Griendling. 2009. Nox proteins in signal transduction. *Free Radic. Biol. Med.* 47: 1239-1253.
182. Groemping, Y. and K. Rittinger. 2005. Activation and assembly of the NADPH oxidase: a structural perspective. *Biochem. J.* 386: 401-416.
183. Chessa, T. A., K. E. Anderson, Y. Hu, Q. Xu, O. Rausch, L. R. Stephens, and P. T. Hawkins. 2010. Phosphorylation of threonine 154 in p40phox is an important physiological signal for activation of the neutrophil NADPH oxidase. *Blood* 116: 6027-6036.
184. Ellson, C., K. Davidson, K. Anderson, L. R. Stephens, and P. T. Hawkins. 2006. PtdIns3P binding to the PX domain of p40phox is a physiological signal in NADPH oxidase activation. *EMBO J.* 25: 4468-4478.
185. Tian, W., X. J. Li, N. D. Stull, W. Ming, C. I. Suh, S. A. Bissonnette, M. B. Yaffe, S. Grinstein, S. J. Atkinson, and M. C. Dinauer. 2008. Fc gamma R-stimulated activation of the NADPH oxidase: phosphoinositide-binding protein p40phox regulates NADPH oxidase activity after enzyme assembly on the phagosome. *Blood* 112: 3867-3877.
186. El-Benna, J., P. M. Dang, M. A. Gougerot-Pocidalo, J. C. Marie, and F. Braut-Boucher. 2009. p47phox, the phagocyte NADPH oxidase/NOX2 organizer: structure, phosphorylation and implication in diseases. *Exp. Mol. Med.* 41: 217-225.
187. Geng, J., X. Sun, P. Wang, S. Zhang, X. Wang, H. Wu, L. Hong, C. Xie, X. Li, H. Zhao, Q. Liu, M. Jiang, Q. Chen, J. Zhang, Y. Li, S. Song, H. R. Wang, R. Zhou, R. L. Johnson, K. Y. Chien, S. C. Lin, J. Han, J. Avruch, L. Chen, and D. Zhou. 2015. Kinases Mst1 and Mst2 positively regulate phagocytic induction of reactive oxygen species and bactericidal activity. *Nat. Immunol.* 16: 1142-1152.
188. Swanson, J. A. and A. D. Hoppe. 2004. The coordination of signaling during Fc receptor-mediated phagocytosis. *J. Leukoc. Biol.* 76: 1093-1103.
189. Anderson, K. E., T. A. Chessa, K. Davidson, R. B. Henderson, S. Walker, T. Tolmachova, K. Grys, O. Rausch, M. C. Seabra, V. L. Tybulewicz, L. R. Stephens, and P. T. Hawkins. 2010. PtdIns3P and Rac direct the assembly of the NADPH oxidase on a novel, pre-phagosomal compartment during FcR-mediated phagocytosis in primary mouse neutrophils. *Blood* 116: 4978-4989.

190. Li, X. J., W. Tian, N. D. Stull, S. Grinstein, S. Atkinson, and M. C. Dinauer. 2009. A fluorescently tagged C-terminal fragment of p47phox detects NADPH oxidase dynamics during phagocytosis. *Mol. Biol. Cell* 20: 1520-1532.
191. Tlili, A., M. Erard, M. C. Faure, X. Baudin, T. Piolot, S. Dupre-Crochet, and O. Nusse. 2012. Stable accumulation of p67phox at the phagosomal membrane and ROS production within the phagosome. *J. Leukoc. Biol.* 91: 83-95.
192. van Bruggen, R., E. Anthony, M. Fernandez-Borja, and D. Roos. 2004. Continuous translocation of Rac2 and the NADPH oxidase component p67(phox) during phagocytosis. *J. Biol. Chem.* 279: 9097-9102.
193. Casbon, A. J., L. A. Allen, K. W. Dunn, and M. C. Dinauer. 2009. Macrophage NADPH oxidase flavocytochrome B localizes to the plasma membrane and Rab11-positive recycling endosomes. *J. Immunol.* 182: 2325-2339.
194. Ejlerskov, P., D. P. Christensen, D. Beyaie, J. B. Burritt, M. H. Paclet, A. Gorlach, B. van Deurs, and F. Vilhardt. 2012. NADPH oxidase is internalized by clathrin-coated pits and localizes to a Rab27A/B GTPase-regulated secretory compartment in activated macrophages. *J. Biol. Chem.* 287: 4835-4852.
195. Lambeth, J. D. and A. S. Neish. 2014. Nox enzymes and new thinking on reactive oxygen: a double-edged sword revisited. *Annu. Rev. Pathol.* 9: 119-145.
196. Bourdonnay, E., C. H. Serezani, D. M. Aronoff, and M. Peters-Golden. 2012. Regulation of alveolar macrophage p40phox: hierarchy of activating kinases and their inhibition by PGE2. *J. Leukoc. Biol.* 92: 219-231.
197. Langenhan, T., G. Aust, and J. Hamann. 2013. Sticky signaling--adhesion class G protein-coupled receptors take the stage. *Sci. Signal.* 6: re3.
198. Yona, S., H. H. Lin, W. O. Siu, S. Gordon, and M. Stacey. 2008. Adhesion-GPCRs: emerging roles for novel receptors. *Trends Biochem. Sci.* 33: 491-500.
199. Promel, S., T. Langenhan, and D. Arac. 2013. Matching structure with function: the GAIN domain of adhesion-GPCR and PKD1-like proteins. *Trends Pharmacol. Sci.* 34: 470-478.
200. Wei, W., K. Hackmann, H. Xu, G. Germino, and F. Qian. 2007. Characterization of cis-autoproteolysis of polycystin-1, the product of human polycystic kidney disease 1 gene. *J. Biol. Chem.* 282: 21729-21737.
201. Lin, H. H., G. W. Chang, J. Q. Davies, M. Stacey, J. Harris, and S. Gordon. 2004. Autocatalytic cleavage of the EMR2 receptor occurs at a conserved G protein-coupled receptor proteolytic site motif. *J. Biol. Chem.* 279: 31823-31832.
202. Arac, D., A. A. Boucard, M. F. Bolliger, J. Nguyen, S. M. Soltis, T. C. Sudhof, and A. T. Brunger. 2012. A novel evolutionarily conserved domain of cell-adhesion GPCRs mediates autoproteolysis. *EMBO J.* 31: 1364-1378.
203. Stephenson, J. R., K. J. Paavola, S. A. Schaefer, B. Kaur, E. G. Van Meir, and R. A. Hall. 2013. Brain-specific angiogenesis inhibitor-1 signaling, regulation, and enrichment in the postsynaptic density. *J. Biol. Chem.* 288: 22248-22256.
204. Piao, X., R. S. Hill, A. Bodell, B. S. Chang, L. Basel-Vanagaite, R. Straussberg, W. B. Dobyns, B. Qasrawi, R. M. Winter, A. M. Innes, T. Voit, M. E. Ross, J. L. Michaud, J. C. Descarie, A. J. Barkovich, and C. A. Walsh. 2004. G protein-coupled receptor-dependent development of human frontal cortex. *Science* 303: 2033-2036.
205. Qian, F., A. Boletta, A. K. Bhunia, H. Xu, L. Liu, A. K. Ahrabi, T. J. Watnick, F. Zhou, and G. G. Germino. 2002. Cleavage of polycystin-1 requires the receptor for egg jelly domain and is disrupted by human autosomal-dominant polycystic kidney disease 1-associated mutations. *Proc. Natl. Acad. Sci. U. S. A.* 99: 16981-16986.
206. Krasnoperov, V., M. A. Bittner, R. W. Holz, O. Chepurny, and A. G. Petrenko. 1999. Structural requirements for alpha-latrotoxin binding and alpha-latrotoxin-stimulated secretion. A

study with calcium-independent receptor of alpha-latrotoxin (CIRL) deletion mutants. *J. Biol. Chem.* 274: 3590-3596.
207. Esseltine, J. L. and S. S. Ferguson. 2013. Regulation of G protein-coupled receptor trafficking and signaling by Rab GTPases. *Small GTPases* 4: 132-135.
208. Stephenson, J. R., R. H. Purcell, and R. A. Hall. 2014. The BAI subfamily of adhesion GPCRs: synaptic regulation and beyond. *Trends Pharmacol. Sci.* 35: 208-215.
209. Masuho, I., O. Ostrovskaya, G. M. Kramer, C. D. Jones, K. Xie, and K. A. Martemyanov. 2015. Distinct profiles of functional discrimination among G proteins determine the actions of G protein-coupled receptors. *Sci. Signal.* 8: ra123.
210. Hewavitharana, T. and P. B. Wedegaertner. 2012. Non-canonical signaling and localizations of heterotrimeric G proteins. *Cell. Signal.* 24: 25-34.
211. Gilman, A. G. 1987. G proteins: transducers of receptor-generated signals. *Annu. Rev. Biochem.* 56: 615-649.
212. Siderovski, D. P. and F. S. Willard. 2005. The GAPs, GEFs, and GDIs of heterotrimeric G-protein alpha subunits. *Int. J. Biol. Sci.* 1: 51-66.
213. Iguchi, T., K. Sakata, K. Yoshizaki, K. Tago, N. Mizuno, and H. Itoh. 2008. Orphan G protein-coupled receptor GPR56 regulates neural progenitor cell migration via a G alpha 12/13 and Rho pathway. *J. Biol. Chem.* 283: 14469-14478.
214. Little, K. D., M. E. Hemler, and C. S. Stipp. 2004. Dynamic regulation of a GPCR-tetraspanin-G protein complex on intact cells: central role of CD81 in facilitating GPR56-Galpha q/11 association. *Mol. Biol. Cell* 15: 2375-2387.
215. Brzostowski, J. A. and A. R. Kimmel. 2001. Signaling at zero G: G-protein-independent functions for 7-TM receptors. *Trends Biochem. Sci.* 26: 291-297.
216. Sah, V. P., T. M. Seasholtz, S. A. Sagi, and J. H. Brown. 2000. The role of Rho in G protein-coupled receptor signal transduction. *Annu. Rev. Pharmacol. Toxicol.* 40: 459-489.
217. Cork, S. M. and E. G. Van Meir. 2011. Emerging roles for the BAI1 protein family in the regulation of phagocytosis, synaptogenesis, neurovasculature, and tumor development. *J. Mol. Med. (Berl)* 89: 743-752.
218. Tucker, R. P. 2004. The thrombospondin type 1 repeat superfamily. *Int. J. Biochem. Cell Biol.* 36: 969-974.
219. Olsen, J. G. and B. B. Kragelund. 2014. Who climbs the tryptophan ladder? On the structure and function of the WSXWS motif in cytokine receptors and thrombospondin repeats. *Cytokine Growth Factor Rev.* 25: 337-341.
220. Adams, J. C. and R. P. Tucker. 2000. The thrombospondin type 1 repeat (TSR) superfamily: diverse proteins with related roles in neuronal development. *Dev. Dyn.* 218: 280-299.
221. Kaur, B., D. J. Brat, C. C. Calkins, and E. G. Van Meir. 2003. Brain angiogenesis inhibitor 1 is differentially expressed in normal brain and glioblastoma independently of p53 expression. *Am. J. Pathol.* 162: 19-27.
222. Sokolowski, J. D., S. L. Nobles, D. S. Heffron, D. Park, K. S. Ravichandran, and J. W. Mandell. 2011. Brain-specific angiogenesis inhibitor-1 expression in astrocytes and neurons: implications for its dual function as an apoptotic engulfment receptor. *Brain Behav. Immun.* 25: 915-921.
223. Mori, K., Y. Kanemura, H. Fujikawa, A. Nakano, H. Ikemoto, I. Ozaki, T. Matsumoto, K. Tamura, M. Yokota, and N. Arita. 2002. Brain-specific angiogenesis inhibitor 1 (BAI1) is expressed in human cerebral neuronal cells. *Neurosci. Res.* 43: 69-74.
224. Mazaheri, F., O. Breus, S. Durdu, P. Haas, J. Wittbrodt, D. Gilmour, and F. Peri. 2014. Distinct roles for BAI1 and TIM-4 in the engulfment of dying neurons by microglia. *Nat. Commun.* 5: 4046.

225. Park, D., A. C. Tosello-Trampont, M. R. Elliott, M. Lu, L. B. Haney, Z. Ma, A. L. Klibanov, J. W. Mandell, and K. S. Ravichandran. 2007. BAI1 is an engulfment receptor for apoptotic cells upstream of the ELMO/Dock180/Rac module. *Nature* 450: 430-434.
226. Das, S., K. A. Owen, K. T. Ly, D. Park, S. G. Black, J. M. Wilson, C. D. Sifri, K. S. Ravichandran, P. B. Ernst, and J. E. Casanova. 2011. Brain angiogenesis inhibitor 1 (BAI1) is a pattern recognition receptor that mediates macrophage binding and engulfment of Gram-negative bacteria. *Proc. Natl. Acad. Sci. U. S. A.* 108: 2136-2141.
227. Hochreiter-Hufford, A. E., C. S. Lee, J. M. Kinchen, J. D. Sokolowski, S. Arandjelovic, J. A. Call, A. L. Klibanov, Z. Yan, J. W. Mandell, and K. S. Ravichandran. 2013. Phosphatidylserine receptor BAI1 and apoptotic cells as new promoters of myoblast fusion. *Nature* 497: 263-267.
228. Kee, H. J., J. T. Koh, M. Y. Kim, K. Y. Ahn, J. K. Kim, C. S. Bae, S. S. Park, and K. K. Kim. 2002. Expression of brain-specific angiogenesis inhibitor 2 (BAI2) in normal and ischemic brain: involvement of BAI2 in the ischemia-induced brain angiogenesis. *J. Cereb. Blood Flow Metab.* 22: 1054-1067.
229. Hamoud, N., V. Tran, L. P. Croteau, A. Kania, and J. F. Cote. 2014. G-protein coupled receptor BAI3 promotes myoblast fusion in vertebrates. *Proc. Natl. Acad. Sci. U. S. A.* 111: 3745-3750.
230. Lanoue, V., A. Usardi, S. M. Sigoillot, M. Talleur, K. Iyer, J. Mariani, P. Isope, G. Vodjdani, N. Heintz, and F. Selimi. 2013. The adhesion-GPCR BAI3, a gene linked to psychiatric disorders, regulates dendrite morphogenesis in neurons. *Mol. Psychiatry* 18: 943-950.
231. Nishimori, H., T. Shiratsuchi, T. Urano, Y. Kimura, K. Kiyono, K. Tatsumi, S. Yoshida, M. Ono, M. Kuwano, Y. Nakamura, and T. Tokino. 1997. A novel brain-specific p53-target gene, BAI1, containing thrombospondin type 1 repeats inhibits experimental angiogenesis. *Oncogene* 15: 2145-2150.
232. Duda, D. G., M. Sunamura, L. Lozonschi, T. Yokoyama, T. Yatsuoka, F. Motoi, A. Horii, K. Tani, S. Asano, Y. Nakamura, and S. Matsuno. 2002. Overexpression of the p53-inducible brain-specific angiogenesis inhibitor 1 suppresses efficiently tumour angiogenesis. *Br. J. Cancer* 86: 490-496.
233. Shiratsuchi, T., H. Nishimori, H. Ichise, Y. Nakamura, and T. Tokino. 1997. Cloning and characterization of BAI2 and BAI3, novel genes homologous to brain-specific angiogenesis inhibitor 1 (BAI1). *Cytogenet. Cell Genet.* 79: 103-108.
234. Hatanaka, H., Y. Oshika, Y. Abe, Y. Yoshida, T. Hashimoto, A. Handa, H. Kijima, H. Yamazaki, H. Inoue, Y. Ueyama, and M. Nakamura. 2000. Vascularization is decreased in pulmonary adenocarcinoma expressing brain-specific angiogenesis inhibitor 1 (BAI1). *Int. J. Mol. Med.* 5: 181-183.
235. Fukushima, Y., Y. Oshika, T. Tsuchida, T. Tokunaga, H. Hatanaka, H. Kijima, H. Yamazaki, Y. Ueyama, N. Tamaoki, and M. Nakamura. 1998. Brain-specific angiogenesis inhibitor 1 expression is inversely correlated with vascularity and distant metastasis of colorectal cancer. *Int. J. Oncol.* 13: 967-970.
236. Yoon, K. C., K. Y. Ahn, J. H. Lee, B. J. Chun, S. W. Park, M. S. Seo, Y. G. Park, and K. K. Kim. 2005. Lipid-mediated delivery of brain-specific angiogenesis inhibitor 1 gene reduces corneal neovascularization in an in vivo rabbit model. *Gene Ther.* 12: 617-624.
237. Kaur, B., S. M. Cork, E. M. Sandberg, N. S. Devi, Z. Zhang, P. A. Klenotic, M. Febbraio, H. Shim, H. Mao, C. Tucker-Burden, R. L. Silverstein, D. J. Brat, J. J. Olson, and E. G. Van Meir. 2009. Vasculostatin inhibits intracranial glioma growth and negatively regulates in vivo angiogenesis through a CD36-dependent mechanism. *Cancer Res.* 69: 1212-1220.

238. Kaur, B., D. J. Brat, N. S. Devi, and E. G. Van Meir. 2005. Vasculostatin, a proteolytic fragment of brain angiogenesis inhibitor 1, is an antiangiogenic and antitumorigenic factor. *Oncogene* 24: 3632-3642.
239. Koh, J. T., H. Kook, H. J. Kee, Y. W. Seo, B. C. Jeong, J. H. Lee, M. Y. Kim, K. C. Yoon, S. Jung, and K. K. Kim. 2004. Extracellular fragment of brain-specific angiogenesis inhibitor 1 suppresses endothelial cell proliferation by blocking alphavbeta5 integrin. *Exp. Cell Res.* 294: 172-184.
240. Klenotic, P. A., R. C. Page, W. Li, J. Amick, S. Misra, and R. L. Silverstein. 2013. Molecular basis of antiangiogenic thrombospondin-1 type 1 repeat domain interactions with CD36. *Arterioscler. Thromb. Vasc. Biol.* 33: 1655-1662.
241. Cork, S. M., B. Kaur, N. S. Devi, L. Cooper, J. H. Saltz, E. M. Sandberg, S. Kaluz, and E. G. Van Meir. 2012. A proprotein convertase/MMP-14 proteolytic cascade releases a novel 40 kDa vasculostatin from tumor suppressor BAI1. *Oncogene* 31: 5144-5152.
242. Shiratsuchi, T., M. Futamura, K. Oda, H. Nishimori, Y. Nakamura, and T. Tokino. 1998. Cloning and characterization of BAI-associated protein 1: a PDZ domain-containing protein that interacts with BAI1. *Biochem. Biophys. Res. Commun.* 247: 597-604.
243. Oda, K., T. Shiratsuchi, H. Nishimori, J. Inazawa, H. Yoshikawa, Y. Taketani, Y. Nakamura, and T. Tokino. 1999. Identification of BAIAP2 (BAI-associated protein 2), a novel human homologue of hamster IRSp53, whose SH3 domain interacts with the cytoplasmic domain of BAI1. *Cytogenet. Cell Genet.* 84: 75-82.
244. Fujiwara, T., A. Mammoto, Y. Kim, and Y. Takai. 2000. Rho small G-protein-dependent binding of mDia to an Src homology 3 domain-containing IRSp53/BAIAP2. *Biochem. Biophys. Res. Commun.* 271: 626-629.
245. Shiratsuchi, T., K. Oda, H. Nishimori, M. Suzuki, E. Takahashi, T. Tokino, and Y. Nakamura. 1998. Cloning and characterization of BAP3 (BAI-associated protein 3), a C2 domain-containing protein that interacts with BAI1. *Biochem. Biophys. Res. Commun.* 251: 158-165.
246. Koh, J. T., Z. H. Lee, K. Y. Ahn, J. K. Kim, C. S. Bae, H. H. Kim, H. J. Kee, and K. K. Kim. 2001. Characterization of mouse brain-specific angiogenesis inhibitor 1 (BAI1) and phytanoyl-CoA alpha-hydroxylase-associated protein 1, a novel BAI1-binding protein. *Brain Res. Mol. Brain Res.* 87: 223-237.
247. Lim, I. A., D. D. Hall, and J. W. Hell. 2002. Selectivity and promiscuity of the first and second PDZ domains of PSD-95 and synapse-associated protein 102. *J. Biol. Chem.* 277: 21697-21711.
248. Duman, J. G., C. P. Tzeng, Y. K. Tu, T. Munjal, B. Schwechter, T. S. Ho, and K. F. Tolias. 2013. The adhesion-GPCR BAI1 regulates synaptogenesis by controlling the recruitment of the Par3/Tiam1 polarity complex to synaptic sites. *J. Neurosci.* 33: 6964-6978.
249. Okajima, D., G. Kudo, and H. Yokota. 2010. Brain-specific angiogenesis inhibitor 2 (BAI2) may be activated by proteolytic processing. *J. Recept. Signal Transduct. Res.* 30: 143-153.
250. Kishore, A., R. H. Purcell, Z. Nassiri-Toosi, and R. A. Hall. 2015. Stalk-dependent and stalk-independent signaling by the adhesion G protein-coupled receptors GPR56 (ADGRG1) and BAI1 (ADGRB1). *J. Biol. Chem.*
251. Liebscher, I., J. Schon, S. C. Petersen, L. Fischer, N. Auerbach, L. M. Demberg, A. Mogha, M. Coster, K. U. Simon, S. Rothemund, K. R. Monk, and T. Schoneberg. 2014. A tethered agonist within the ectodomain activates the adhesion G protein-coupled receptors GPR126 and GPR133. *Cell. Rep.* 9: 2018-2026.
252. Demberg, L. M., S. Rothemund, T. Schoneberg, and I. Liebscher. 2015. Identification of the tethered peptide agonist of the adhesion G protein-coupled receptor GPR64/ADGRG2. *Biochem. Biophys. Res. Commun.* 464: 743-747.

253. Stoveken, H. M., A. G. Hajduczok, L. Xu, and G. G. Tall. 2015. Adhesion G protein-coupled receptors are activated by exposure of a cryptic tethered agonist. *Proc. Natl. Acad. Sci. U. S. A.* 112: 6194-6199.
254. Kinchen, J. M., J. Cabello, D. Klingele, K. Wong, R. Feichtinger, H. Schnabel, R. Schnabel, and M. O. Hengartner. 2005. Two pathways converge at CED-10 to mediate actin rearrangement and corpse removal in C. elegans. *Nature* 434: 93-99.
255. Gumienny, T. L., E. Brugnera, A. C. Tosello-Trampont, J. M. Kinchen, L. B. Haney, K. Nishiwaki, S. F. Walk, M. E. Nemergut, I. G. Macara, R. Francis, T. Schedl, Y. Qin, L. Van Aelst, M. O. Hengartner, and K. S. Ravichandran. 2001. CED-12/ELMO, a novel member of the CrkII/Dock180/Rac pathway, is required for phagocytosis and cell migration. *Cell* 107: 27-41.
256. Brugnera, E., L. Haney, C. Grimsley, M. Lu, S. F. Walk, A. C. Tosello-Trampont, I. G. Macara, H. Madhani, G. R. Fink, and K. S. Ravichandran. 2002. Unconventional Rac-GEF activity is mediated through the Dock180-ELMO complex. *Nat. Cell Biol.* 4: 574-582.
257. Patel, M., A. Pelletier, and J. F. Cote. 2011. Opening up on ELMO regulation: New insights into the control of Rac signaling by the DOCK180/ELMO complex. *Small GTPases* 2: 268-275.
258. Lu, M., J. M. Kinchen, K. L. Rossman, C. Grimsley, C. deBakker, E. Brugnera, A. C. Tosello-Trampont, L. B. Haney, D. Klingele, J. Sondek, M. O. Hengartner, and K. S. Ravichandran. 2004. PH domain of ELMO functions in trans to regulate Rac activation via Dock180. *Nat. Struct. Mol. Biol.* 11: 756-762.
259. Lu, M., J. M. Kinchen, K. L. Rossman, C. Grimsley, M. Hall, J. Sondek, M. O. Hengartner, V. Yajnik, and K. S. Ravichandran. 2005. A Steric-inhibition model for regulation of nucleotide exchange via the Dock180 family of GEFs. *Curr. Biol.* 15: 371-377.
260. Das, S., A. Sarkar, K. A. Ryan, S. Fox, A. H. Berger, I. J. Juncadella, D. Bimczok, L. E. Smythies, P. R. Harris, K. S. Ravichandran, S. E. Crowe, P. D. Smith, and P. B. Ernst. 2014. Brain angiogenesis inhibitor 1 is expressed by gastric phagocytes during infection with Helicobacter pylori and mediates the recognition and engulfment of human apoptotic gastric epithelial cells. *FASEB J.* 28: 2214-2224.
261. Fond, A. M., C. S. Lee, I. G. Schulman, R. S. Kiss, and K. S. Ravichandran. 2015. Apoptotic cells trigger a membrane-initiated pathway to increase ABCA1. *J. Clin. Invest.* 125: 2748-2758.
262. Devitt, A. and L. J. Marshall. 2011. The innate immune system and the clearance of apoptotic cells. *J. Leukoc. Biol.* 90: 447-457.
263. Thomas, L., A. Bielemeier, P. A. Lambert, R. P. Darveau, L. J. Marshall, and A. Devitt. 2013. The N-terminus of CD14 acts to bind apoptotic cells and confers rapid-tethering capabilities on non-myeloid cells. *PLoS One* 8: e70691.
264. Rennemeier, C., S. Hammerschmidt, S. Niemann, S. Inamura, U. Zahringer, and B. E. Kehrel. 2007. Thrombospondin-1 promotes cellular adherence of gram-positive pathogens via recognition of peptidoglycan. *FASEB J.* 21: 3118-3132.
265. He, Y. W., H. Li, J. Zhang, C. L. Hsu, E. Lin, N. Zhang, J. Guo, K. A. Forbush, and M. J. Bevan. 2004. The extracellular matrix protein mindin is a pattern-recognition molecule for microbial pathogens. *Nat. Immunol.* 5: 88-97.
266. Tan, K., M. Duquette, J. H. Liu, Y. Dong, R. Zhang, A. Joachimiak, J. Lawler, and J. H. Wang. 2002. Crystal structure of the TSP-1 type 1 repeats: a novel layered fold and its biological implication. *J. Cell Biol.* 159: 373-382.
267. Li, Y., C. Cao, W. Jia, L. Yu, M. Mo, Q. Wang, Y. Huang, J. M. Lim, M. Ishihara, L. Wells, P. Azadi, H. Robinson, Y. W. He, L. Zhang, and R. A. Mariuzza. 2009. Structure of the F-spondin domain of mindin, an integrin ligand and pattern recognition molecule. *EMBO J.* 28: 286-297.

268. Wang, L. W., M. Dlugosz, R. P. Somerville, M. Raed, R. S. Haltiwanger, and S. S. Apte. 2007. O-fucosylation of thrombospondin type 1 repeats in ADAMTS-like-1/punctin-1 regulates secretion: implications for the ADAMTS superfamily. *J. Biol. Chem.* 282: 17024-17031.
269. Tossavainen, H., T. Pihlajamaa, T. K. Huttunen, E. Raulo, H. Rauvala, P. Permi, and I. Kilpelainen. 2006. The layered fold of the TSR domain of P. falciparum TRAP contains a heparin binding site. *Protein Sci.* 15: 1760-1768.
270. Park, B. S., D. H. Song, H. M. Kim, B. S. Choi, H. Lee, and J. O. Lee. 2009. The structural basis of lipopolysaccharide recognition by the TLR4-MD-2 complex. *Nature* 458: 1191-1195.
271. Hagar, J. A., D. A. Powell, Y. Aachoui, R. K. Ernst, and E. A. Miao. 2013. Cytoplasmic LPS activates caspase-11: implications in TLR4-independent endotoxic shock. *Science* 341: 1250-1253.
272. Kayagaki, N., M. T. Wong, I. B. Stowe, S. R. Ramani, L. C. Gonzalez, S. Akashi-Takamura, K. Miyake, J. Zhang, W. P. Lee, A. Muszynski, L. S. Forsberg, R. W. Carlson, and V. M. Dixit. 2013. Noncanonical inflammasome activation by intracellular LPS independent of TLR4. *Science* 341: 1246-1249.
273. Demon, D., L. Vande Walle, and M. Lamkanfi. 2014. Sensing the enemy within: how macrophages detect intracellular Gram-negative bacteria. *Trends Biochem. Sci.* 39: 574-576.
274. Wang, H., J. Head, P. Kosma, H. Brade, S. Muller-Loennies, S. Sheikh, B. McDonald, K. Smith, T. Cafarella, B. Seaton, and E. Crouch. 2008. Recognition of heptoses and the inner core of bacterial lipopolysaccharides by surfactant protein d. *Biochemistry* 47: 710-720.
275. Nagaoka, K., K. Takahara, K. Tanaka, H. Yoshida, R. M. Steinman, S. Saitoh, S. Akashi-Takamura, K. Miyake, Y. S. Kang, C. G. Park, and K. Inaba. 2005. Association of SIGNR1 with TLR4-MD-2 enhances signal transduction by recognition of LPS in gram-negative bacteria. *Int. Immunol.* 17: 827-836.
276. Gonzalez de Peredo, A., D. Klein, B. Macek, D. Hess, J. Peter-Katalinic, and J. Hofsteenge. 2002. C-mannosylation and o-fucosylation of thrombospondin type 1 repeats. *Mol. Cell. Proteomics* 1: 11-18.
277. Hofsteenge, J., K. G. Huwiler, B. Macek, D. Hess, J. Lawler, D. F. Mosher, and J. Peter-Katalinic. 2001. C-mannosylation and O-fucosylation of the thrombospondin type 1 module. *J. Biol. Chem.* 276: 6485-6498.
278. Kumar, H., T. Kawai, and S. Akira. 2011. Pathogen recognition by the innate immune system. *Int. Rev. Immunol.* 30: 16-34.
279. Kawai, T. and S. Akira. 2011. Toll-like receptors and their crosstalk with other innate receptors in infection and immunity. *Immunity* 34: 637-650.
280. Stuart, L. M. and R. A. Ezekowitz. 2005. Phagocytosis: elegant complexity. *Immunity* 22: 539-550.
281. Taylor, P. R., L. Martinez-Pomares, M. Stacey, H. H. Lin, G. D. Brown, and S. Gordon. 2005. Macrophage receptors and immune recognition. *Annu. Rev. Immunol.* 23: 901-944.
282. Medzhitov, R. and T. Horng. 2009. Transcriptional control of the inflammatory response. *Nat. Rev. Immunol.* 9: 692-703.
283. Underhill, D. M. and B. Gantner. 2004. Integration of Toll-like receptor and phagocytic signaling for tailored immunity. *Microbes Infect.* 6: 1368-1373.
284. Greenberg, S. and S. Grinstein. 2002. Phagocytosis and innate immunity. *Curr. Opin. Immunol.* 14: 136-145.
285. Geier, H. and J. Celli. 2011. Phagocytic receptors dictate phagosomal escape and intracellular proliferation of Francisella tularensis. *Infect. Immun.* 79: 2204-2214.
286. Kang, P. B., A. K. Azad, J. B. Torrelles, T. M. Kaufman, A. Beharka, E. Tibesar, L. E. DesJardin, and L. S. Schlesinger. 2005. The human macrophage mannose receptor directs

Mycobacterium tuberculosis lipoarabinomannan-mediated phagosome biogenesis. *J. Exp. Med.* 202: 987-999.
287. Zhang, P., M. Skurnik, S. S. Zhang, O. Schwartz, R. Kalyanasundaram, S. Bulgheresi, J. J. He, J. D. Klena, B. J. Hinnebusch, and T. Chen. 2008. Human dendritic cell-specific intercellular adhesion molecule-grabbing nonintegrin (CD209) is a receptor for Yersinia pestis that promotes phagocytosis by dendritic cells. *Infect. Immun.* 76: 2070-2079.
288. Agramonte-Hevia, J., A. Gonzalez-Arenas, D. Barrera, and M. Velasco-Velazquez. 2002. Gram-negative bacteria and phagocytic cell interaction mediated by complement receptor 3. *FEMS Immunol. Med. Microbiol.* 34: 255-266.
289. Criss, A. K. and J. E. Casanova. 2003. Coordinate regulation of Salmonella enterica serovar Typhimurium invasion of epithelial cells by the Arp2/3 complex and Rho GTPases. *Infect. Immun.* 71: 2885-2891.
290. Bonini, M. G. and A. B. Malik. 2014. Regulating the regulator of ROS production. *Cell Res.* 24: 908-909.
291. Forman, H. J. and M. Torres. 2002. Reactive oxygen species and cell signaling: respiratory burst in macrophage signaling. *Am. J. Respir. Crit. Care Med.* 166: S4-8.
292. Hordijk, P. L. 2006. Regulation of NADPH oxidases: the role of Rac proteins. *Circ. Res.* 98: 453-462.
293. Filippi, M. D., C. E. Harris, J. Meller, Y. Gu, Y. Zheng, and D. A. Williams. 2004. Localization of Rac2 via the C terminus and aspartic acid 150 specifies superoxide generation, actin polarity and chemotaxis in neutrophils. *Nat. Immunol.* 5: 744-751.
294. Noubade, R., K. Wong, N. Ota, S. Rutz, C. Eidenschenk, P. A. Valdez, J. Ding, I. Peng, A. Sebrell, P. Caplazi, J. DeVoss, R. H. Soriano, T. Sai, R. Lu, Z. Modrusan, J. Hackney, and W. Ouyang. 2014. NRROS negatively regulates reactive oxygen species during host defence and autoimmunity. *Nature* 509: 235-239.
295. Gorzalczany, Y., N. Sigal, M. Itan, O. Lotan, and E. Pick. 2000. Targeting of Rac1 to the phagocyte membrane is sufficient for the induction of NADPH oxidase assembly. *J. Biol. Chem.* 275: 40073-40081.
296. Vazquez-Torres, A., J. Jones-Carson, P. Mastroeni, H. Ischiropoulos, and F. C. Fang. 2000. Antimicrobial actions of the NADPH phagocyte oxidase and inducible nitric oxide synthase in experimental salmonellosis. I. Effects on microbial killing by activated peritoneal macrophages in vitro. *J. Exp. Med.* 192: 227-236.
297. Vazquez-Torres, A. and F. C. Fang. 2001. Oxygen-dependent anti-Salmonella activity of macrophages. *Trends Microbiol.* 9: 29-33.
298. Shiloh, M. U., J. D. MacMicking, S. Nicholson, J. E. Brause, S. Potter, M. Marino, F. Fang, M. Dinauer, and C. Nathan. 1999. Phenotype of mice and macrophages deficient in both phagocyte oxidase and inducible nitric oxide synthase. *Immunity* 10: 29-38.
299. Dikalova, A. E., A. T. Bikineyeva, K. Budzyn, R. R. Nazarewicz, L. McCann, W. Lewis, D. G. Harrison, and S. I. Dikalov. 2010. Therapeutic targeting of mitochondrial superoxide in hypertension. *Circ. Res.* 107: 106-116.
300. Mastroeni, P., A. Vazquez-Torres, F. C. Fang, Y. Xu, S. Khan, C. E. Hormaeche, and G. Dougan. 2000. Antimicrobial actions of the NADPH phagocyte oxidase and inducible nitric oxide synthase in experimental salmonellosis. II. Effects on microbial proliferation and host survival in vivo. *J. Exp. Med.* 192: 237-248.
301. Freeman, S. A. and S. Grinstein. 2014. Phagocytosis: receptors, signal integration, and the cytoskeleton. *Immunol. Rev.* 262: 193-215.
302. Park, B. S. and J. O. Lee. 2013. Recognition of lipopolysaccharide pattern by TLR4 complexes. *Exp. Mol. Med.* 45: e66.

303. Greenberg, D. E., J. B. Goldberg, F. Stock, P. R. Murray, S. M. Holland, and J. J. Lipuma. 2009. Recurrent Burkholderia infection in patients with chronic granulomatous disease: 11-year experience at a large referral center. *Clin. Infect. Dis.* 48: 1577-1579.
304. Marciano, B. E., C. Spalding, A. Fitzgerald, D. Mann, T. Brown, S. Osgood, L. Yockey, D. N. Darnell, L. Barnhart, J. Daub, L. Boris, A. P. Rump, V. L. Anderson, C. Haney, D. B. Kuhns, S. D. Rosenzweig, C. Kelly, A. Zelazny, T. Mason, S. S. DeRavin, E. Kang, J. I. Gallin, H. L. Malech, K. N. Olivier, G. Uzel, A. F. Freeman, T. Heller, C. S. Zerbe, and S. M. Holland. 2015. Common severe infections in chronic granulomatous disease. *Clin. Infect. Dis.* 60: 1176-1183.
305. Pizzolla, A., M. Hultqvist, B. Nilson, M. J. Grimm, T. Eneljung, I. M. Jonsson, M. Verdrengh, T. Kelkka, I. Gjertsson, B. H. Segal, and R. Holmdahl. 2012. Reactive oxygen species produced by the NADPH oxidase 2 complex in monocytes protect mice from bacterial infections. *J. Immunol.* 188: 5003-5011.
306. Sousa, S. A., M. Ulrich, A. Bragonzi, M. Burke, D. Worlitzsch, J. H. Leitao, C. Meisner, L. Eberl, I. Sa-Correia, and G. Doring. 2007. Virulence of Burkholderia cepacia complex strains in gp91phox-/- mice. *Cell. Microbiol.* 9: 2817-2825.
307. Panday, A., M. K. Sahoo, D. Osorio, and S. Batra. 2015. NADPH oxidases: an overview from structure to innate immunity-associated pathologies. *Cell. Mol. Immunol.* 12: 5-23.
308. Niedergang, F. and P. Chavrier. 2005. Regulation of phagocytosis by Rho GTPases. *Curr. Top. Microbiol. Immunol.* 291: 43-60.
309. Dong, X., Z. Mo, G. Bokoch, C. Guo, Z. Li, and D. Wu. 2005. P-Rex1 is a primary Rac2 guanine nucleotide exchange factor in mouse neutrophils. *Curr. Biol.* 15: 1874-1879.
310. Utomo, A., X. Cullere, M. Glogauer, W. Swat, and T. N. Mayadas. 2006. Vav proteins in neutrophils are required for FcgammaR-mediated signaling to Rac GTPases and nicotinamide adenine dinucleotide phosphate oxidase component p40(phox). *J. Immunol.* 177: 6388-6397.
311. Baba, T., T. Ara, M. Hasegawa, Y. Takai, Y. Okumura, M. Baba, K. A. Datsenko, M. Tomita, B. L. Wanner, and H. Mori. 2006. Construction of Escherichia coli K-12 in-frame, single-gene knockout mutants: the Keio collection. *Mol. Syst. Biol.* 2: 2006.0008.
312. Ly, K. T. and J. E. Casanova. 2009. Abelson tyrosine kinase facilitates Salmonella enterica serovar Typhimurium entry into epithelial cells. *Infect. Immun.* 77: 60-69.
313. Pishchany, G., S. E. Dickey, and E. P. Skaar. 2009. Subcellular localization of the Staphylococcus aureus heme iron transport components IsdA and IsdB. *Infect. Immun.* 77: 2624-2634.
314. Nunez Miguel, R., J. Wong, J. F. Westoll, H. J. Brooks, L. A. O'Neill, N. J. Gay, C. E. Bryant, and T. P. Monie. 2007. A dimer of the Toll-like receptor 4 cytoplasmic domain provides a specific scaffold for the recruitment of signalling adaptor proteins. *PLoS One* 2: e788.
315. Lin, S. C., Y. C. Lo, and H. Wu. 2010. Helical assembly in the MyD88-IRAK4-IRAK2 complex in TLR/IL-1R signalling. *Nature* 465: 885-890.
316. Tseng, P. H., A. Matsuzawa, W. Zhang, T. Mino, D. A. Vignali, and M. Karin. 2010. Different modes of ubiquitination of the adaptor TRAF3 selectively activate the expression of type I interferons and proinflammatory cytokines. *Nat. Immunol.* 11: 70-75.
317. Hacker, H. and M. Karin. 2006. Regulation and function of IKK and IKK-related kinases. *Sci. STKE* 2006: re13.
318. den Dunnen, J., S. I. Gringhuis, and T. B. Geijtenbeek. 2009. Innate signaling by the C-type lectin DC-SIGN dictates immune responses. *Cancer Immunol. Immunother.* 58: 1149-1157.
319. Ozment, T. R., T. Ha, K. F. Breuel, T. R. Ford, D. A. Ferguson, J. Kalbfleisch, J. B. Schweitzer, J. L. Kelley, C. Li, and D. L. Williams. 2012. Scavenger receptor class a plays a central role in mediating mortality and the development of the pro-inflammatory phenotype in polymicrobial sepsis. *PLoS Pathog.* 8: e1002967.

320. Kagan, J. C. and A. Iwasaki. 2012. Phagosome as the organelle linking innate and adaptive immunity. *Traffic* 13: 1053-1061.
321. Arbibe, L., J. P. Mira, N. Teusch, L. Kline, M. Guha, N. Mackman, P. J. Godowski, R. J. Ulevitch, and U. G. Knaus. 2000. Toll-like receptor 2-mediated NF-kappa B activation requires a Rac1-dependent pathway. *Nat. Immunol.* 1: 533-540.
322. Iyer, S. S., A. A. Ghaffari, and G. Cheng. 2010. Lipopolysaccharide-mediated IL-10 transcriptional regulation requires sequential induction of type I IFNs and IL-27 in macrophages. *J. Immunol.* 185: 6599-6607.
323. Eshleman, E. M. and L. L. Lenz. 2014. Type I interferons in bacterial infections: taming of myeloid cells and possible implications for autoimmunity. *Front. Immunol.* 5: 431.
324. Helgason, E., Q. T. Phung, and E. C. Dueber. 2013. Recent insights into the complexity of Tank-binding kinase 1 signaling networks: the emerging role of cellular localization in the activation and substrate specificity of TBK1. *FEBS Lett.* 587: 1230-1237.
325. Clark, K., L. Plater, M. Peggie, and P. Cohen. 2009. Use of the pharmacological inhibitor BX795 to study the regulation and physiological roles of TBK1 and IkappaB kinase epsilon: a distinct upstream kinase mediates Ser-172 phosphorylation and activation. *J. Biol. Chem.* 284: 14136-14146.
326. Clark, K., M. Peggie, L. Plater, R. J. Sorcek, E. R. Young, J. B. Madwed, J. Hough, E. G. McIver, and P. Cohen. 2011. Novel cross-talk within the IKK family controls innate immunity. *Biochem. J.* 434: 93-104.
327. Ma, X., E. Helgason, Q. T. Phung, C. L. Quan, R. S. Iyer, M. W. Lee, K. K. Bowman, M. A. Starovasnik, and E. C. Dueber. 2012. Molecular basis of Tank-binding kinase 1 activation by transautophosphorylation. *Proc. Natl. Acad. Sci. U. S. A.* 109: 9378-9383.
328. Billings, E. A., C. S. Lee, K. A. Owen, R. S. D'Souza, K. S. Ravichandran, and J. E. Casanova. 2016. The adhesion GPCR BAI1 mediates macrophage ROS production and microbicidal activity against Gram-negative bacteria. *Sci. Signal.* 9: ra14.
329. Duman, J. G., C. P. Tzeng, Y. K. Tu, T. Munjal, B. Schwechter, T. S. Ho, and K. F. Tolias. 2013. The adhesion-GPCR BAI1 regulates synaptogenesis by controlling the recruitment of the Par3/Tiam1 polarity complex to synaptic sites. *J. Neurosci.* 33: 6964-6978.
330. Gotoh, K., Y. Tanaka, A. Nishikimi, R. Nakamura, H. Yamada, N. Maeda, T. Ishikawa, K. Hoshino, T. Uruno, Q. Cao, S. Higashi, Y. Kawaguchi, M. Enjoji, R. Takayanagi, T. Kaisho, Y. Yoshikai, and Y. Fukui. 2010. Selective control of type I IFN induction by the Rac activator DOCK2 during TLR-mediated plasmacytoid dendritic cell activation. *J. Exp. Med.* 207: 721-730.
331. Krakstad, B. F., V. V. Ardawatia, and A. M. Aragay. 2004. A role for Galpha12/Galpha13 in p120ctn regulation. *Proc. Natl. Acad. Sci. U. S. A.* 101: 10314-10319.
332. Jean-Charles, P. Y., L. Zhang, J. H. Wu, S. O. Han, L. Brian, N. J. Freedman, and S. K. Shenoy. 2016. Ubiquitin-specific protease 20 Regulates the Reciprocal Functions of Beta-arrestin2 in Toll-like Receptor 4-promoted NFkappaB Activation. *J. Biol. Chem.*
333. Fan, H., A. Bitto, B. Zingarelli, L. M. Luttrell, K. Borg, P. V. Halushka, and J. A. Cook. 2010. Beta-arrestin 2 negatively regulates sepsis-induced inflammation. *Immunology* 130: 344-351.
334. Fan, H., L. M. Luttrell, G. E. Tempel, J. J. Senn, P. V. Halushka, and J. A. Cook. 2007. Beta-arrestins 1 and 2 differentially regulate LPS-induced signaling and pro-inflammatory gene expression. *Mol. Immunol.* 44: 3092-3099.
335. Garcia-Regalado, A., M. L. Guzman-Hernandez, I. Ramirez-Rangel, E. Robles-Molina, T. Balla, J. Vazquez-Prado, and G. Reyes-Cruz. 2008. G protein-coupled receptor-promoted trafficking of Gbeta1gamma2 leads to AKT activation at endosomes via a mechanism mediated by Gbeta1gamma2-Rab11a interaction. *Mol. Biol. Cell* 19: 4188-4200.

336. Sakaguchi, S., H. Negishi, M. Asagiri, C. Nakajima, T. Mizutani, A. Takaoka, K. Honda, and T. Taniguchi. 2003. Essential role of IRF-3 in lipopolysaccharide-induced interferon-beta gene expression and endotoxin shock. *Biochem. Biophys. Res. Commun.* 306: 860-866.
337. Carrigan, S. O., R. Junkins, Y. J. Yang, A. Macneil, C. Richardson, B. Johnston, and T. J. Lin. 2010. IFN regulatory factor 3 contributes to the host response during Pseudomonas aeruginosa lung infection in mice. *J. Immunol.* 185: 3602-3609.
338. Fischer, H., N. Lutay, B. Ragnarsdottir, M. Yadav, K. Jonsson, A. Urbano, A. Al Hadad, S. Ramisch, P. Storm, U. Dobrindt, E. Salvador, D. Karpman, U. Jodal, and C. Svanborg. 2010. Pathogen specific, IRF3-dependent signaling and innate resistance to human kidney infection. *PLoS Pathog.* 6: e1001109.
339. Sotolongo, J., C. Espana, A. Echeverry, D. Siefker, N. Altman, J. Zaias, R. Santaolalla, J. Ruiz, K. Schesser, B. Adkins, and M. Fukata. 2011. Host innate recognition of an intestinal bacterial pathogen induces TRIF-dependent protective immunity. *J. Exp. Med.* 208: 2705-2716.
340. Biswas, S. K., P. Bist, M. K. Dhillon, T. Kajiji, C. Del Fresno, M. Yamamoto, E. Lopez-Collazo, S. Akira, and V. Tergaonkar. 2007. Role for MyD88-independent, TRIF pathway in lipid A/TLR4-induced endotoxin tolerance. *J. Immunol.* 179: 4083-4092.
341. Fiorentino, D. F., A. Zlotnik, T. R. Mosmann, M. Howard, and A. O'Garra. 1991. IL-10 inhibits cytokine production by activated macrophages. *J. Immunol.* 147: 3815-3822.
342. Means, T. K., E. Mylonakis, E. Tampakakis, R. A. Colvin, E. Seung, L. Puckett, M. F. Tai, C. R. Stewart, R. Pukkila-Worley, S. E. Hickman, K. J. Moore, S. B. Calderwood, N. Hacohen, A. D. Luster, and J. El Khoury. 2009. Evolutionarily conserved recognition and innate immunity to fungal pathogens by the scavenger receptors SCARF1 and CD36. *J. Exp. Med.* 206: 637-653.
343. Plato, A., S. E. Hardison, and G. D. Brown. 2015. Pattern recognition receptors in antifungal immunity. *Semin. Immunopathol.* 37: 97-106.
344. Goodridge, H. S., C. N. Reyes, C. A. Becker, T. R. Katsumoto, J. Ma, A. J. Wolf, N. Bose, A. S. Chan, A. S. Magee, M. E. Danielson, A. Weiss, J. P. Vasilakos, and D. M. Underhill. 2011. Activation of the innate immune receptor Dectin-1 upon formation of a 'phagocytic synapse'. *Nature* 472: 471-475.
345. Yoshimura, A., E. Lien, R. R. Ingalls, E. Tuomanen, R. Dziarski, and D. Golenbock. 1999. Cutting edge: recognition of Gram-positive bacterial cell wall components by the innate immune system occurs via Toll-like receptor 2. *J. Immunol.* 163: 1-5.
346. Trent, M. S., C. M. Stead, A. X. Tran, and J. V. Hankins. 2006. Diversity of endotoxin and its impact on pathogenesis. *J. Endotoxin Res.* 12: 205-223.
347. Nikaido, H. and M. Vaara. 1985. Molecular basis of bacterial outer membrane permeability. *Microbiol. Rev.* 49: 1-32.
348. Nikaido, H. 2003. Molecular basis of bacterial outer membrane permeability revisited. *Microbiol. Mol. Biol. Rev.* 67: 593-656.
349. Whitfield, C., N. Kaniuk, and E. Frirdich. 2003. Molecular insights into the assembly and diversity of the outer core oligosaccharide in lipopolysaccharides from Escherichia coli and Salmonella. *J. Endotoxin Res.* 9: 244-249.
350. Ruiz, N., D. Kahne, and T. J. Silhavy. 2006. Advances in understanding bacterial outer-membrane biogenesis. *Nat. Rev. Microbiol.* 4: 57-66.
351. Raetz, C. R. and C. Whitfield. 2002. Lipopolysaccharide endotoxins. *Annu. Rev. Biochem.* 71: 635-700.
352. Reeves, P. R., M. Hobbs, M. A. Valvano, M. Skurnik, C. Whitfield, D. Coplin, N. Kido, J. Klena, D. Maskell, C. R. Raetz, and P. D. Rick. 1996. Bacterial polysaccharide synthesis and gene nomenclature. *Trends Microbiol.* 4: 495-503.
353. Miller, S. I., R. K. Ernst, and M. W. Bader. 2005. LPS, TLR4 and infectious disease diversity. *Nat. Rev. Microbiol.* 3: 36-46.

354. Gyorfy, Z., E. Duda, and C. Vizler. 2013. Interactions between LPS moieties and macrophage pattern recognition receptors. *Vet. Immunol. Immunopathol.* 152: 28-36.
355. Eder, K., C. Vizler, E. Kusz, I. Karcagi, H. Glavinas, G. E. Balogh, L. Vigh, E. Duda, and Z. Gyorfy. 2009. The role of lipopolysaccharide moieties in macrophage response to Escherichia coli. *Biochem. Biophys. Res. Commun.* 389: 46-51.
356. Needham, B. D. and M. S. Trent. 2013. Fortifying the barrier: the impact of lipid A remodelling on bacterial pathogenesis. *Nat. Rev. Microbiol.* 11: 467-481.
357. Raetz, C. R., C. M. Reynolds, M. S. Trent, and R. E. Bishop. 2007. Lipid A modification systems in gram-negative bacteria. *Annu. Rev. Biochem.* 76: 295-329.
358. Smit, J., Y. Kamio, and H. Nikaido. 1975. Outer membrane of Salmonella typhimurium: chemical analysis and freeze-fracture studies with lipopolysaccharide mutants. *J. Bacteriol.* 124: 942-958.
359. Sanderson, K. E., T. MacAlister, J. W. Costerton, and K. J. Cheng. 1974. Permeability of lipopolysaccharide-deficient (rough) mutants of Salmonella typhimurium to antibiotics, lysozyme, and other agents. *Can. J. Microbiol.* 20: 1135-1145.
360. Frirdich, E. and C. Whitfield. 2005. Lipopolysaccharide inner core oligosaccharide structure and outer membrane stability in human pathogens belonging to the Enterobacteriaceae. *J. Endotoxin Res.* 11: 133-144.
361. Morona, R., C. Daniels, and L. Van Den Bosch. 2003. Genetic modulation of Shigella flexneri 2a lipopolysaccharide O antigen modal chain length reveals that it has been optimized for virulence. *Microbiology* 149: 925-939.
362. Russo, T. A., B. A. Davidson, U. B. Carlino-MacDonald, J. D. Helinski, R. L. Priore, and P. R. Knight 3rd. 2003. The effects of Escherichia coli capsule, O-antigen, host neutrophils, and complement in a rat model of Gram-negative pneumonia. *FEMS Microbiol. Lett.* 226: 355-361.
363. Shi, J., Y. Zhao, Y. Wang, W. Gao, J. Ding, P. Li, L. Hu, and F. Shao. 2014. Inflammatory caspases are innate immune receptors for intracellular LPS. *Nature* 514: 187-192.
364. Crhanova, M., M. Malcova, M. Mazgajova, D. Karasova, A. Sebkova, A. Fucikova, Z. Bortlicek, L. Pilousova, K. Kyrova, M. Dekanova, and I. Rychlik. 2011. LPS structure influences protein secretion in Salmonella enterica. *Vet. Microbiol.* 152: 131-137.
365. Kong, Q., J. Yang, Q. Liu, P. Alamuri, K. L. Roland, and R. Curtiss 3rd. 2011. Effect of deletion of genes involved in lipopolysaccharide core and O-antigen synthesis on virulence and immunogenicity of Salmonella enterica serovar typhimurium. *Infect. Immun.* 79: 4227-4239.
366. Hoare, A., M. Bittner, J. Carter, S. Alvarez, M. Zaldivar, D. Bravo, M. A. Valvano, and I. Contreras. 2006. The outer core lipopolysaccharide of Salmonella enterica serovar Typhi is required for bacterial entry into epithelial cells. *Infect. Immun.* 74: 1555-1564.
367. Ames, G. F., E. N. Spudich, and H. Nikaido. 1974. Protein composition of the outer membrane of Salmonella typhimurium: effect of lipopolysaccharide mutations. *J. Bacteriol.* 117: 406-416.
368. Parker, C. T., A. W. Kloser, C. A. Schnaitman, M. A. Stein, S. Gottesman, and B. W. Gibson. 1992. Role of the rfaG and rfaP genes in determining the lipopolysaccharide core structure and cell surface properties of Escherichia coli K-12. *J. Bacteriol.* 174: 2525-2538.
369. Muhlradt, P. F. 1971. Biosynthesis of Salmonella lipopolysaccharide. Studies on the transfer of glucose, galactose, and phosphate to the core in a cell free system. *Eur. J. Biochem.* 18: 20-27.
370. Yethon, J. A., E. Vinogradov, M. B. Perry, and C. Whitfield. 2000. Mutation of the lipopolysaccharide core glycosyltransferase encoded by waaG destabilizes the outer membrane of Escherichia coli by interfering with core phosphorylation. *J. Bacteriol.* 182: 5620-5623.
371. Valvano, M. A., P. Messner, and P. Kosma. 2002. Novel pathways for biosynthesis of nucleotide-activated glycero-manno-heptose precursors of bacterial glycoproteins and cell surface polysaccharides. *Microbiology* 148: 1979-1989.

372. Sirisena, D. M., K. A. Brozek, P. R. MacLachlan, K. E. Sanderson, and C. R. Raetz. 1992. The rfaC gene of Salmonella typhimurium. Cloning, sequencing, and enzymatic function in heptose transfer to lipopolysaccharide. *J. Biol. Chem.* 267: 18874-18884.
373. Sirisena, D. M., P. R. MacLachlan, S. L. Liu, A. Hessel, and K. E. Sanderson. 1994. Molecular analysis of the rfaD gene, for heptose synthesis, and the rfaF gene, for heptose transfer, in lipopolysaccharide synthesis in Salmonella typhimurium. *J. Bacteriol.* 176: 2379-2385.
374. Lee, N. G., M. G. Sunshine, and M. A. Apicella. 1995. Molecular cloning and characterization of the nontypeable Haemophilus influenzae 2019 rfaE gene required for lipopolysaccharide biosynthesis. *Infect. Immun.* 63: 818-824.
375. Valvano, M. A., C. L. Marolda, M. Bittner, M. Glaskin-Clay, T. L. Simon, and J. D. Klena. 2000. The rfaE gene from Escherichia coli encodes a bifunctional protein involved in biosynthesis of the lipopolysaccharide core precursor ADP-L-glycero-D-manno-heptose. *J. Bacteriol.* 182: 488-497.
376. Jin, U. H., T. W. Chung, Y. C. Lee, S. D. Ha, and C. H. Kim. 2001. Molecular cloning and functional expression of the rfaE gene required for lipopolysaccharide biosynthesis in Salmonella typhimurium. *Glycoconj. J.* 18: 779-787.
377. Muhlradt, P. F. and J. R. Golecki. 1975. Asymmetrical distribution and artifactual reorientation of lipopolysaccharide in the outer membrane bilayer of Salmonella typhimurium. *Eur. J. Biochem.* 51: 343-352.
378. Hasin, M. and E. P. Kennedy. 1982. Role of phosphatidylethanolamine in the biosynthesis of pyrophosphoethanolamine residues in the lipopolysaccharide of Escherichia coli. *J. Biol. Chem.* 257: 12475-12477.
379. Clifton, L. A., M. W. Skoda, E. L. Daulton, A. V. Hughes, A. P. Le Brun, J. H. Lakey, and S. A. Holt. 2013. Asymmetric phospholipid: lipopolysaccharide bilayers; a Gram-negative bacterial outer membrane mimic. *J. R. Soc. Interface* 10: 20130810.
380. Devyatyarova-Johnson, M., I. H. Rees, B. D. Robertson, M. W. Turner, N. J. Klein, and D. L. Jack. 2000. The lipopolysaccharide structures of Salmonella enterica serovar Typhimurium and Neisseria gonorrhoeae determine the attachment of human mannose-binding lectin to intact organisms. *Infect. Immun.* 68: 3894-3899.
381. Keck, M., N. Gisch, H. Moll, F. J. Vorholter, K. Gerth, U. Kahmann, M. Lissel, B. Lindner, K. Niehaus, and O. Holst. 2011. Unusual outer membrane lipid composition of the gram-negative, lipopolysaccharide-lacking myxobacterium Sorangium cellulosum So ce56. *J. Biol. Chem.* 286: 12850-12859.
382. Meredith, T. C., P. Aggarwal, U. Mamat, B. Lindner, and R. W. Woodard. 2006. Redefining the requisite lipopolysaccharide structure in Escherichia coli. *ACS Chem. Biol.* 1: 33-42.
383. Parker, C. T., E. Pradel, and C. A. Schnaitman. 1992. Identification and sequences of the lipopolysaccharide core biosynthetic genes rfaQ, rfaP, and rfaG of Escherichia coli K-12. *J. Bacteriol.* 174: 930-934.
384. Wang, Z., J. Wang, G. Ren, Y. Li, and X. Wang. 2015. Influence of Core Oligosaccharide of Lipopolysaccharide to Outer Membrane Behavior of Escherichia coli. *Mar. Drugs* 13: 3325-3339.
385. Klein, G., S. Muller-Loennies, B. Lindner, N. Kobylak, H. Brade, and S. Raina. 2013. Molecular and structural basis of inner core lipopolysaccharide alterations in Escherichia coli: incorporation of glucuronic acid and phosphoethanolamine in the heptose region. *J. Biol. Chem.* 288: 8111-8127.
386. Yethon, J. A., D. E. Heinrichs, M. A. Monteiro, M. B. Perry, and C. Whitfield. 1998. Involvement of waaY, waaQ, and waaP in the modification of Escherichia coli lipopolysaccharide and their role in the formation of a stable outer membrane. *J. Biol. Chem.* 273: 26310-26316.

387. Yethon, J. A., J. S. Gunn, R. K. Ernst, S. I. Miller, L. Laroche, D. Malo, and C. Whitfield. 2000. Salmonella enterica serovar typhimurium waaP mutants show increased susceptibility to polymyxin and loss of virulence In vivo. *Infect. Immun.* 68: 4485-4491.
388. Balla, E., A. Zamyatina, A. Hofinger, and P. Kosma. 2007. Synthesis of a deoxy analogue of ADP L-glycero-D-manno-heptose. *Carbohydr. Res.* 342: 2537-2545.
389. Delucia, A. M., D. A. Six, R. E. Caughlan, P. Gee, I. Hunt, J. S. Lam, and C. R. Dean. 2011. Lipopolysaccharide (LPS) inner-core phosphates are required for complete LPS synthesis and transport to the outer membrane in Pseudomonas aeruginosa PAO1. *MBio* 2: 10.1128/mBio.00142-11. Print 2011.
390. Zhao, X. and J. S. Lam. 2002. WaaP of Pseudomonas aeruginosa is a novel eukaryotic type protein-tyrosine kinase as well as a sugar kinase essential for the biosynthesis of core lipopolysaccharide. *J. Biol. Chem.* 277: 4722-4730.
391. Loutet, S. A., R. S. Flannagan, C. Kooi, P. A. Sokol, and M. A. Valvano. 2006. A complete lipopolysaccharide inner core oligosaccharide is required for resistance of Burkholderia cenocepacia to antimicrobial peptides and bacterial survival in vivo. *J. Bacteriol.* 188: 2073-2080.
392. Vinogradov, E. and M. B. Perry. 2001. Structural analysis of the core region of the lipopolysaccharides from eight serotypes of Klebsiella pneumoniae. *Carbohydr. Res.* 335: 291-296.
393. St Michael, F., E. Vinogradov, C. Q. Wenzel, B. McIntosh, J. Li, J. C. Hoe, J. C. Richards, and A. D. Cox. 2009. Phosphoethanolamine is located at the 6-position and not at the 7-position of the distal heptose residue in the lipopolysaccharide from Neisseria meningitidis. *Glycobiology* 19: 1436-1445.
394. Gibson, B. W., W. Melaugh, N. J. Phillips, M. A. Apicella, A. A. Campagnari, and J. M. Griffiss. 1993. Investigation of the structural heterogeneity of lipooligosaccharides from pathogenic Haemophilus and Neisseria species and of R-type lipopolysaccharides from Salmonella typhimurium by electrospray mass spectrometry. *J. Bacteriol.* 175: 2702-2712.
395. Nesper, J., A. Kraiss, S. Schild, J. Blass, K. E. Klose, J. Bockemuhl, and J. Reidl. 2002. Comparative and genetic analyses of the putative Vibrio cholerae lipopolysaccharide core oligosaccharide biosynthesis (wav) gene cluster. *Infect. Immun.* 70: 2419-2433.
396. Tennant, I., J. D. Pound, L. A. Marr, J. J. Willems, S. Petrova, C. A. Ford, M. Paterson, A. Devitt, and C. D. Gregory. 2013. Innate recognition of apoptotic cells: novel apoptotic cell-associated molecular patterns revealed by crossreactivity of anti-LPS antibodies. *Cell Death Differ.* 20: 698-708.
397. Herre, J., A. S. Marshall, E. Caron, A. D. Edwards, D. L. Williams, E. Schweighoffer, V. Tybulewicz, C. Reis e Sousa, S. Gordon, and G. D. Brown. 2004. Dectin-1 uses novel mechanisms for yeast phagocytosis in macrophages. *Blood* 104: 4038-4045.
398. Leto, T. L., S. Morand, D. Hurt, and T. Ueyama. 2009. Targeting and regulation of reactive oxygen species generation by Nox family NADPH oxidases. *Antioxid. Redox Signal.* 11: 2607-2619.
399. Zhan, Y., J. V. Virbasius, X. Song, D. P. Pomerleau, and G. W. Zhou. 2002. The p40phox and p47phox PX domains of NADPH oxidase target cell membranes via direct and indirect recruitment by phosphoinositides. *J. Biol. Chem.* 277: 4512-4518.
400. Jancic, C., A. Savina, C. Wasmeier, T. Tolmachova, J. El-Benna, P. M. Dang, S. Pascolo, M. A. Gougerot-Pocidalo, G. Raposo, M. C. Seabra, and S. Amigorena. 2007. Rab27a regulates phagosomal pH and NADPH oxidase recruitment to dendritic cell phagosomes. *Nat. Cell Biol.* 9: 367-378.
401. Lee, C. F., M. Qiao, K. Schroder, Q. Zhao, and R. Asmis. 2010. Nox4 is a novel inducible source of reactive oxygen species in monocytes and macrophages and mediates oxidized low density lipoprotein-induced macrophage death. *Circ. Res.* 106: 1489-1497.

402. Park, H. S., H. Y. Jung, E. Y. Park, J. Kim, W. J. Lee, and Y. S. Bae. 2004. Cutting edge: direct interaction of TLR4 with NAD(P)H oxidase 4 isozyme is essential for lipopolysaccharide-induced production of reactive oxygen species and activation of NF-kappa B. *J. Immunol.* 173: 3589-3593.
403. Gorin, Y., J. M. Ricono, N. H. Kim, B. Bhandari, G. G. Choudhury, and H. E. Abboud. 2003. Nox4 mediates angiotensin II-induced activation of Akt/protein kinase B in mesangial cells. *Am. J. Physiol. Renal Physiol.* 285: F219-29.
404. Inoguchi, T., T. Sonta, H. Tsubouchi, T. Etoh, M. Kakimoto, N. Sonoda, N. Sato, N. Sekiguchi, K. Kobayashi, H. Sumimoto, H. Utsumi, and H. Nawata. 2003. Protein kinase C-dependent increase in reactive oxygen species (ROS) production in vascular tissues of diabetes: role of vascular NAD(P)H oxidase. *J. Am. Soc. Nephrol.* 14: S227-32.
405. Patterson, C., J. Ruef, N. R. Madamanchi, P. Barry-Lane, Z. Hu, C. Horaist, C. A. Ballinger, A. R. Brasier, C. Bode, and M. S. Runge. 1999. Stimulation of a vascular smooth muscle cell NAD(P)H oxidase by thrombin. Evidence that p47(phox) may participate in forming this oxidase in vitro and in vivo. *J. Biol. Chem.* 274: 19814-19822.
406. Jiang, F., Y. Zhang, and G. J. Dusting. 2011. NADPH oxidase-mediated redox signaling: roles in cellular stress response, stress tolerance, and tissue repair. *Pharmacol. Rev.* 63: 218-242.
407. Park, H. S., J. N. Chun, H. Y. Jung, C. Choi, and Y. S. Bae. 2006. Role of NADPH oxidase 4 in lipopolysaccharide-induced proinflammatory responses by human aortic endothelial cells. *Cardiovasc. Res.* 72: 447-455.
408. Grandvaux, N., A. Soucy-Faulkner, and K. Fink. 2007. Innate host defense: Nox and Duox on phox's tail. *Biochimie* 89: 1113-1122.
409. Bae, Y. S., M. K. Choi, and W. J. Lee. 2010. Dual oxidase in mucosal immunity and host-microbe homeostasis. *Trends Immunol.* 31: 278-287.
410. Sommer, F. and F. Backhed. 2015. The gut microbiota engages different signaling pathways to induce Duox2 expression in the ileum and colon epithelium. *Mucosal Immunol.* 8: 372-379.
411. Ha, E. M., C. T. Oh, Y. S. Bae, and W. J. Lee. 2005. A direct role for dual oxidase in Drosophila gut immunity. *Science* 310: 847-850.
412. Hume, D. A. 2011. Applications of myeloid-specific promoters in transgenic mice support in vivo imaging and functional genomics but do not support the concept of distinct macrophage and dendritic cell lineages or roles in immunity. *J. Leukoc. Biol.* 89: 525-538.
413. Chow, A., B. D. Brown, and M. Merad. 2011. Studying the mononuclear phagocyte system in the molecular age. *Nat. Rev. Immunol.* 11: 788-798.
414. Lambeth, J. D., T. Kawahara, and B. Diebold. 2007. Regulation of Nox and Duox enzymatic activity and expression. *Free Radic. Biol. Med.* 43: 319-331.
415. Savina, A., C. Jancic, S. Hugues, P. Guermonprez, P. Vargas, I. C. Moura, A. M. Lennon-Dumenil, M. C. Seabra, G. Raposo, and S. Amigorena. 2006. NOX2 controls phagosomal pH to regulate antigen processing during crosspresentation by dendritic cells. *Cell* 126: 205-218.
416. Mantegazza, A. R., A. Savina, M. Vermeulen, L. Perez, J. Geffner, O. Hermine, S. D. Rosenzweig, F. Faure, and S. Amigorena. 2008. NADPH oxidase controls phagosomal pH and antigen cross-presentation in human dendritic cells. *Blood* 112: 4712-4722.
417. Ling, G. S., J. Bennett, K. J. Woollard, M. Szajna, L. Fossati-Jimack, P. R. Taylor, D. Scott, G. Franzoso, H. T. Cook, and M. Botto. 2014. Integrin CD11b positively regulates TLR4-induced signalling pathways in dendritic cells but not in macrophages. *Nat. Commun.* 5: 3039.
418. Oshiumi, H., M. Sasai, K. Shida, T. Fujita, M. Matsumoto, and T. Seya. 2003. TIR-containing adapter molecule (TICAM)-2, a bridging adapter recruiting to toll-like receptor 4 TICAM-1 that induces interferon-beta. *J. Biol. Chem.* 278: 49751-49762.

419. Piao, W., L. W. Ru, K. H. Piepenbrink, E. J. Sundberg, S. N. Vogel, and V. Y. Toshchakov. 2013. Recruitment of TLR adapter TRIF to TLR4 signaling complex is mediated by the second helical region of TRIF TIR domain. *Proc. Natl. Acad. Sci. U. S. A.* 110: 19036-19041.
420. Hu, Y. H., Y. Zhang, L. Q. Jiang, S. Wang, C. Q. Lei, M. S. Sun, H. B. Shu, and Y. Liu. 2015. WDFY1 mediates TLR3/4 signaling by recruiting TRIF. *EMBO Rep.* 16: 447-455.
421. McGettrick, A. F., E. K. Brint, E. M. Palsson-McDermott, D. C. Rowe, D. T. Golenbock, N. J. Gay, K. A. Fitzgerald, and L. A. O'Neill. 2006. Trif-related adapter molecule is phosphorylated by PKC{epsilon} during Toll-like receptor 4 signaling. *Proc. Natl. Acad. Sci. U. S. A.* 103: 9196-9201.
422. Sasai, M., M. Tatematsu, H. Oshiumi, K. Funami, M. Matsumoto, S. Hatakeyama, and T. Seya. 2010. Direct binding of TRAF2 and TRAF6 to TICAM-1/TRIF adaptor participates in activation of the Toll-like receptor 3/4 pathway. *Mol. Immunol.* 47: 1283-1291.
423. Xie, P. 2013. TRAF molecules in cell signaling and in human diseases. *J. Mol. Signal.* 8: 7-2187-8-7.
424. Ostuni, R., I. Zanoni, and F. Granucci. 2010. Deciphering the complexity of Toll-like receptor signaling. *Cell Mol. Life Sci.* 67: 4109-4134.
425. Gatot, J. S., R. Gioia, T. L. Chau, F. Patrascu, M. Warnier, P. Close, J. P. Chapelle, E. Muraille, K. Brown, U. Siebenlist, J. Piette, E. Dejardin, and A. Chariot. 2007. Lipopolysaccharide-mediated interferon regulatory factor activation involves TBK1-IKKepsilon-dependent Lys(63)-linked polyubiquitination and phosphorylation of TANK/I-TRAF. *J. Biol. Chem.* 282: 31131-31146.
426. Kawagoe, T., O. Takeuchi, Y. Takabatake, H. Kato, Y. Isaka, T. Tsujimura, and S. Akira. 2009. TANK is a negative regulator of Toll-like receptor signaling and is critical for the prevention of autoimmune nephritis. *Nat. Immunol.* 10: 965-972.
427. Zhong, B., X. Liu, X. Wang, X. Liu, H. Li, B. G. Darnay, X. Lin, S. C. Sun, and C. Dong. 2013. Ubiquitin-specific protease 25 regulates TLR4-dependent innate immune responses through deubiquitination of the adaptor protein TRAF3. *Sci. Signal.* 6: ra35.
428. Lin, Y. C., D. Y. Huang, C. L. Chu, Y. L. Lin, and W. W. Lin. 2013. The tyrosine kinase Syk differentially regulates Toll-like receptor signaling downstream of the adaptor molecules TRAF6 and TRAF3. *Sci. Signal.* 6: ra71.
429. Wang, P., W. Zhao, K. Zhao, L. Zhang, and C. Gao. 2015. TRIM26 negatively regulates interferon-beta production and antiviral response through polyubiquitination and degradation of nuclear IRF3. *PLoS Pathog.* 11: e1004726.
430. Long, L., Y. Deng, F. Yao, D. Guan, Y. Feng, H. Jiang, X. Li, P. Hu, X. Lu, H. Wang, J. Li, X. Gao, and D. Xie. 2014. Recruitment of phosphatase PP2A by RACK1 adaptor protein deactivates transcription factor IRF3 and limits type I interferon signaling. *Immunity* 40: 515-529.
431. Wang, C., T. Chen, J. Zhang, M. Yang, N. Li, X. Xu, and X. Cao. 2009. The E3 ubiquitin ligase Nrdp1 'preferentially' promotes TLR-mediated production of type I interferon. *Nat. Immunol.* 10: 744-752.
432. Klein, S., M. Franco, P. Chardin, and F. Luton. 2006. Role of the Arf6 GDP/GTP cycle and Arf6 GTPase-activating proteins in actin remodeling and intracellular transport. *J. Biol. Chem.* 281: 12352-12361.
433. Guichard, A., V. Nizet, and E. Bier. 2014. RAB11-mediated trafficking in host-pathogen interactions. *Nat. Rev. Microbiol.* 12: 624-634.
434. Santy, L. C., K. S. Ravichandran, and J. E. Casanova. 2005. The DOCK180/Elmo complex couples ARNO-mediated Arf6 activation to the downstream activation of Rac1. *Curr. Biol.* 15: 1749-1754.

435. Shiba, T., H. Koga, H. W. Shin, M. Kawasaki, R. Kato, K. Nakayama, and S. Wakatsuki. 2006. Structural basis for Rab11-dependent membrane recruitment of a family of Rab11-interacting protein 3 (FIP3)/Arfophilin-1. *Proc. Natl. Acad. Sci. U. S. A.* 103: 15416-15421.
436. Otani, T., K. Oshima, S. Onishi, M. Takeda, K. Shinmyozu, S. Yonemura, and S. Hayashi. 2011. IKKepsilon regulates cell elongation through recycling endosome shuttling. *Dev. Cell.* 20: 219-232.
437. Gould, G. W. 2011. IKKepsilon: a kinase at the intersection of signaling and membrane traffic. *Sci. Signal.* 4: pe30.
438. Riekenberg, S., K. Farhat, J. Debarry, H. Heine, G. Jung, K. H. Wiesmuller, and A. J. Ulmer. 2009. Regulators of G-protein signalling are modulated by bacterial lipopeptides and lipopolysaccharide. *FEBS J.* 276: 649-659.
439. Siehler, S. 2009. Regulation of RhoGEF proteins by G12/13-coupled receptors. *Br. J. Pharmacol.* 158: 41-49.
440. Buhl, A. M., N. L. Johnson, N. Dhanasekaran, and G. L. Johnson. 1995. G alpha 12 and G alpha 13 stimulate Rho-dependent stress fiber formation and focal adhesion assembly. *J. Biol. Chem.* 270: 24631-24634.
441. Klages, B., U. Brandt, M. I. Simon, G. Schultz, and S. Offermanns. 1999. Activation of G12/G13 results in shape change and Rho/Rho-kinase-mediated myosin light chain phosphorylation in mouse platelets. *J. Cell Biol.* 144: 745-754.
442. Zanoni, I., R. Ostuni, G. Capuano, M. Collini, M. Caccia, A. E. Ronchi, M. Rocchetti, F. Mingozzi, M. Foti, G. Chirico, B. Costa, A. Zaza, P. Ricciardi-Castagnoli, and F. Granucci. 2009. CD14 regulates the dendritic cell life cycle after LPS exposure through NFAT activation. *Nature* 460: 264-268.
443. Akashi, S., S. Saitoh, Y. Wakabayashi, T. Kikuchi, N. Takamura, Y. Nagai, Y. Kusumoto, K. Fukase, S. Kusumoto, Y. Adachi, A. Kosugi, and K. Miyake. 2003. Lipopolysaccharide interaction with cell surface Toll-like receptor 4-MD-2: higher affinity than that with MD-2 or CD14. *J. Exp. Med.* 198: 1035-1042.
444. Kobayashi, M., S. Saitoh, N. Tanimura, K. Takahashi, K. Kawasaki, M. Nishijima, Y. Fujimoto, K. Fukase, S. Akashi-Takamura, and K. Miyake. 2006. Regulatory roles for MD-2 and TLR4 in ligand-induced receptor clustering. *J. Immunol.* 176: 6211-6218.
445. Ardawatia, V. V., M. Masia-Balague, B. F. Krakstad, B. B. Johansson, K. M. Kreitzburg, E. Spriet, A. E. Lewis, T. E. Meigs, and A. M. Aragay. 2011. Galpha(12) binds to the N-terminal regulatory domain of p120(ctn), and downregulates p120(ctn) tyrosine phosphorylation induced by Src family kinases via a RhoA independent mechanism. *Exp. Cell Res.* 317: 293-306.
446. Kozasa, T., X. Jiang, M. J. Hart, P. M. Sternweis, W. D. Singer, A. G. Gilman, G. Bollag, and P. C. Sternweis. 1998. p115 RhoGEF, a GTPase activating protein for Galpha12 and Galpha13. *Science* 280: 2109-2111.
447. Shukla, A. K., K. Xiao, and R. J. Lefkowitz. 2011. Emerging paradigms of beta-arrestin-dependent seven transmembrane receptor signaling. *Trends Biochem. Sci.* 36: 457-469.
448. DeWire, S. M., S. Ahn, R. J. Lefkowitz, and S. K. Shenoy. 2007. Beta-arrestins and cell signaling. *Annu. Rev. Physiol.* 69: 483-510.
449. Jean-Charles, P. Y., V. Rajiv, and S. K. Shenoy. 2016. Ubiquitin-Related Roles of beta-Arrestins in Endocytic Trafficking and Signal Transduction. *J. Cell. Physiol.*
450. Wang, Y., Y. Tang, L. Teng, Y. Wu, X. Zhao, and G. Pei. 2006. Association of beta-arrestin and TRAF6 negatively regulates Toll-like receptor-interleukin 1 receptor signaling. *Nat. Immunol.* 7: 139-147.
451. Li, H., D. Hu, H. Fan, Y. Zhang, G. D. LeSage, Y. Caudle, C. Stuart, Z. Liu, and D. Yin. 2014. beta-Arrestin 2 negatively regulates Toll-like receptor 4 (TLR4)-triggered inflammatory signaling via targeting p38 MAPK and interleukin 10. *J. Biol. Chem.* 289: 23075-23085.

452. Khan, S. M., R. Sleno, S. Gora, P. Zylbergold, J. P. Laverdure, J. C. Labbe, G. J. Miller, and T. E. Hebert. 2013. The expanding roles of Gbetagamma subunits in G protein-coupled receptor signaling and drug action. *Pharmacol. Rev.* 65: 545-577.
453. Botelho, R. J., M. Teruel, R. Dierckman, R. Anderson, A. Wells, J. D. York, T. Meyer, and S. Grinstein. 2000. Localized biphasic changes in phosphatidylinositol-4,5-bisphosphate at sites of phagocytosis. *J. Cell Biol.* 151: 1353-1368.
454. Lau, C., X. Wang, L. Song, M. North, S. Wiehler, D. Proud, and C. W. Chow. 2008. Syk associates with clathrin and mediates phosphatidylinositol 3-kinase activation during human rhinovirus internalization. *J. Immunol.* 180: 870-880.
455. Crowley, M. T., P. S. Costello, C. J. Fitzer-Attas, M. Turner, F. Meng, C. Lowell, V. L. Tybulewicz, and A. L. DeFranco. 1997. A critical role for Syk in signal transduction and phagocytosis mediated by Fcgamma receptors on macrophages. *J. Exp. Med.* 186: 1027-1039.
456. Jersmann, H. P. 2005. Time to abandon dogma: CD14 is expressed by non-myeloid lineage cells. *Immunol. Cell Biol.* 83: 462-467.
457. Takahashi, K., T. Shibata, S. Akashi-Takamura, T. Kiyokawa, Y. Wakabayashi, N. Tanimura, T. Kobayashi, F. Matsumoto, R. Fukui, T. Kouro, Y. Nagai, K. Takatsu, S. Saitoh, and K. Miyake. 2007. A protein associated with Toll-like receptor (TLR) 4 (PRAT4A) is required for TLR-dependent immune responses. *J. Exp. Med.* 204: 2963-2976.
458. Wakabayashi, Y., M. Kobayashi, S. Akashi-Takamura, N. Tanimura, K. Konno, K. Takahashi, T. Ishii, T. Mizutani, H. Iba, T. Kouro, S. Takaki, K. Takatsu, Y. Oda, Y. Ishihama, S. Saitoh, and K. Miyake. 2006. A protein associated with toll-like receptor 4 (PRAT4A) regulates cell surface expression of TLR4. *J. Immunol.* 177: 1772-1779.
459. Randow, F. and B. Seed. 2001. Endoplasmic reticulum chaperone gp96 is required for innate immunity but not cell viability. *Nat. Cell Biol.* 3: 891-896.
460. Liaunardy-Jopeace, A., C. E. Bryant, and N. J. Gay. 2014. The COP II adaptor protein TMED7 is required to initiate and mediate the delivery of TLR4 to the plasma membrane. *Sci. Signal.* 7: ra70.
461. Wang, D., J. Lou, C. Ouyang, W. Chen, Y. Liu, X. Liu, X. Cao, J. Wang, and L. Lu. 2010. Ras-related protein Rab10 facilitates TLR4 signaling by promoting replenishment of TLR4 onto the plasma membrane. *Proc. Natl. Acad. Sci. U. S. A.* 107: 13806-13811.
462. Coats, S. R., T. T. Pham, B. W. Bainbridge, R. A. Reife, and R. P. Darveau. 2005. MD-2 mediates the ability of tetra-acylated and penta-acylated lipopolysaccharides to antagonize Escherichia coli lipopolysaccharide at the TLR4 signaling complex. *J. Immunol.* 175: 4490-4498.
463. Visintin, A., K. A. Halmen, E. Latz, B. G. Monks, and D. T. Golenbock. 2005. Pharmacological inhibition of endotoxin responses is achieved by targeting the TLR4 coreceptor, MD-2. *J. Immunol.* 175: 6465-6472.
464. Garcia-Regalado, A., M. L. Guzman-Hernandez, I. Ramirez-Rangel, E. Robles-Molina, T. Balla, J. Vazquez-Prado, and G. Reyes-Cruz. 2008. G protein-coupled receptor-promoted trafficking of Gbeta1gamma2 leads to AKT activation at endosomes via a mechanism mediated by Gbeta1gamma2-Rab11a interaction. *Mol. Biol. Cell* 19: 4188-4200.
465. Jeyaseelan, S., S. K. Young, M. B. Fessler, Y. Liu, K. C. Malcolm, M. Yamamoto, S. Akira, and G. S. Worthen. 2007. Toll/IL-1 receptor domain-containing adaptor inducing IFN-beta (TRIF)-mediated signaling contributes to innate immune responses in the lung during Escherichia coli pneumonia. *J. Immunol.* 178: 3153-3160.
466. Cai, S., S. Batra, L. Shen, N. Wakamatsu, and S. Jeyaseelan. 2009. Both TRIF- and MyD88-dependent signaling contribute to host defense against pulmonary Klebsiella infection. *J. Immunol.* 183: 6629-6638.
467. Wieland, C. W., S. Florquin, N. A. Maris, K. Hoebe, B. Beutler, K. Takeda, S. Akira, and T. van der Poll. 2005. The MyD88-dependent, but not the MyD88-independent, pathway of TLR4

signaling is important in clearing nontypeable haemophilus influenzae from the mouse lung. *J. Immunol*. 175: 6042-6049.
468. Kelly-Scumpia, K. M., P. O. Scumpia, M. J. Delano, J. S. Weinstein, A. G. Cuenca, J. L. Wynn, and L. L. Moldawer. 2010. Type I interferon signaling in hematopoietic cells is required for survival in mouse polymicrobial sepsis by regulating CXCL10. *J. Exp. Med*. 207: 319-326.
469. Sotolongo, J., S. Kanagavelu, J. Hyun, J. Ruiz, and M. Fukata. 2012. TRIF mobilizes unique primary defense against Gram-negative bacteria in intestinal interface. *Gut Microbes* 3: 437-441.
470. Owen, K. A., C. J. Anderson, and J. E. Casanova. 2016. Salmonella Suppresses the TRIF-Dependent Type I Interferon Response in Macrophages. *MBio* 7: 10.1128/mBio.02051-15.
471. Robinson, N., S. McComb, R. Mulligan, R. Dudani, L. Krishnan, and S. Sad. 2012. Type I interferon induces necroptosis in macrophages during infection with Salmonella enterica serovar Typhimurium. *Nat. Immunol*. 13: 954-962.
472. Perkins, D. J., R. Rajaiah, S. M. Tennant, G. Ramachandran, E. E. Higginson, T. N. Dyson, and S. N. Vogel. 2015. Salmonella Typhimurium Co-Opts the Host Type I IFN System To Restrict Macrophage Innate Immune Transcriptional Responses Selectively. *J. Immunol*. 195: 2461-2471.
473. Kawashima, T., A. Kosaka, H. Yan, Z. Guo, R. Uchiyama, R. Fukui, D. Kaneko, Y. Kumagai, D. J. You, J. Carreras, S. Uematsu, M. H. Jang, O. Takeuchi, T. Kaisho, S. Akira, K. Miyake, H. Tsutsui, T. Saito, I. Nishimura, and N. M. Tsuji. 2013. Double-stranded RNA of intestinal commensal but not pathogenic bacteria triggers production of protective interferon-beta. *Immunity* 38: 1187-1197.
474. Katakura, K., J. Lee, D. Rachmilewitz, G. Li, L. Eckmann, and E. Raz. 2005. Toll-like receptor 9-induced type I IFN protects mice from experimental colitis. *J. Clin. Invest*. 115: 695-702.
475. Walker, W. E., A. T. Bozzi, and D. R. Goldstein. 2012. IRF3 contributes to sepsis pathogenesis in the mouse cecal ligation and puncture model. *J. Leukoc. Biol*. 92: 1261-1268.
476. Yamamoto, M., S. Sato, H. Hemmi, K. Hoshino, T. Kaisho, H. Sanjo, O. Takeuchi, M. Sugiyama, M. Okabe, K. Takeda, and S. Akira. 2003. Role of adaptor TRIF in the MyD88-independent toll-like receptor signaling pathway. *Science* 301: 640-643.
477. Karaghiosoff, M., R. Steinborn, P. Kovarik, G. Kriegshauser, M. Baccarini, B. Donabauer, U. Reichart, T. Kolbe, C. Bogdan, T. Leanderson, D. Levy, T. Decker, and M. Muller. 2003. Central role for type I interferons and Tyk2 in lipopolysaccharide-induced endotoxin shock. *Nat. Immunol*. 4: 471-477.
478. Marchlik, E., P. Thakker, T. Carlson, Z. Jiang, M. Ryan, S. Marusic, N. Goutagny, W. Kuang, G. R. Askew, V. Roberts, S. Benoit, T. Zhou, V. Ling, R. Pfeifer, N. Stedman, K. A. Fitzgerald, L. L. Lin, and J. P. Hall. 2010. Mice lacking Tbk1 activity exhibit immune cell infiltrates in multiple tissues and increased susceptibility to LPS-induced lethality. *J. Leukoc. Biol*. 88: 1171-1180.
479. Coccia, E. M. and A. Battistini. 2015. Early IFN type I response: Larning from microbial evasion strategies. *Semin. Immunol*. 27: 85-101.
480. Trinchieri, G. 2010. Type I interferon: friend or foe? *J. Exp. Med*. 207: 2053-2063.
481. Chen, Q., D. W. Powell, M. J. Rane, S. Singh, W. Butt, J. B. Klein, and K. R. McLeish. 2003. Akt phosphorylates p47phox and mediates respiratory burst activity in human neutrophils. *J. Immunol*. 170: 5302-5308.
482. Kawahara, T., Y. Kuwano, S. Teshima-Kondo, R. Takeya, H. Sumimoto, K. Kishi, S. Tsunawaki, T. Hirayama, and K. Rokutan. 2004. Role of nicotinamide adenine dinucleotide phosphate oxidase 1 in oxidative burst response to Toll-like receptor 5 signaling in large intestinal epithelial cells. *J. Immunol*. 172: 3051-3058.

483. Ray, P. D., B. W. Huang, and Y. Tsuji. 2012. Reactive oxygen species (ROS) homeostasis and redox regulation in cellular signaling. *Cell. Signal.* 24: 981-990.
484. Sanlioglu, S., C. M. Williams, L. Samavati, N. S. Butler, G. Wang, P. B. McCray Jr, T. C. Ritchie, G. W. Hunninghake, E. Zandi, and J. F. Engelhardt. 2001. Lipopolysaccharide induces Rac1-dependent reactive oxygen species formation and coordinates tumor necrosis factor-alpha secretion through IKK regulation of NF-kappa B. *J. Biol. Chem.* 276: 30188-30198.
485. Matsuzawa, A., K. Saegusa, T. Noguchi, C. Sadamitsu, H. Nishitoh, S. Nagai, S. Koyasu, K. Matsumoto, K. Takeda, and H. Ichijo. 2005. ROS-dependent activation of the TRAF6-ASK1-p38 pathway is selectively required for TLR4-mediated innate immunity. *Nat. Immunol.* 6: 587-592.
486. Asehnoune, K., D. Strassheim, S. Mitra, J. Y. Kim, and E. Abraham. 2004. Involvement of reactive oxygen species in Toll-like receptor 4-dependent activation of NF-kappa B. *J. Immunol.* 172: 2522-2529.
487. Kong, X., R. Thimmulappa, P. Kombairaju, and S. Biswal. 2010. NADPH oxidase-dependent reactive oxygen species mediate amplified TLR4 signaling and sepsis-induced mortality in Nrf2-deficient mice. *J. Immunol.* 185: 569-577.
488. Chiang, E., O. Dang, K. Anderson, A. Matsuzawa, H. Ichijo, and M. David. 2006. Cutting edge: apoptosis-regulating signal kinase 1 is required for reactive oxygen species-mediated activation of IFN regulatory factor 3 by lipopolysaccharide. *J. Immunol.* 176: 5720-5724.
489. Liu, W., H. Wu, L. Chen, Y. Wen, X. Kong, and W. Q. Gao. 2015. Park7 interacts with p47(phox) to direct NADPH oxidase-dependent ROS production and protect against sepsis. *Cell Res.* 25: 691-706.
490. Holland, S. M. 2013. Chronic granulomatous disease. *Hematol. Oncol. Clin. North Am.* 27: 89-99, viii.
491. Song, E., G. B. Jaishankar, H. Saleh, W. Jithpratuck, R. Sahni, and G. Krishnaswamy. 2011. Chronic granulomatous disease: a review of the infectious and inflammatory complications. *Clin. Mol. Allergy* 9: 10-7961-9-10.
492. Han, W., H. Li, J. Cai, L. A. Gleaves, V. V. Polosukhin, B. H. Segal, F. E. Yull, and T. S. Blackwell. 2013. NADPH oxidase limits lipopolysaccharide-induced lung inflammation and injury in mice through reduction-oxidation regulation of NF-kappaB activity. *J. Immunol.* 190: 4786-4794.
493. Segal, B. H., W. Han, J. J. Bushey, M. Joo, Z. Bhatti, J. Feminella, C. G. Dennis, R. R. Vethanayagam, F. E. Yull, M. Capitano, P. K. Wallace, H. Minderman, J. W. Christman, M. B. Sporn, J. Chan, D. C. Vinh, S. M. Holland, L. R. Romani, S. L. Gaffen, M. L. Freeman, and T. S. Blackwell. 2010. NADPH oxidase limits innate immune responses in the lungs in mice. *PLoS One* 5: e9631.
494. Deng, J., X. Wang, F. Qian, S. Vogel, L. Xiao, R. Ranjan, H. Park, M. Karpurapu, R. D. Ye, G. Y. Park, and J. W. Christman. 2012. Protective role of reactive oxygen species in endotoxin-induced lung inflammation through modulation of IL-10 expression. *J. Immunol.* 188: 5734-5740.
495. Bagaitkar, J., N. K. Pech, S. Ivanov, A. Austin, M. Y. Zeng, S. Pallat, G. Huang, G. J. Randolph, and M. C. Dinauer. 2015. NADPH oxidase controls neutrophilic response to sterile inflammation in mice by regulating the IL-1alpha/G-CSF axis. *Blood* 126: 2724-2733.
496. Fadeel, B., A. Ahlin, J. I. Henter, S. Orrenius, and M. B. Hampton. 1998. Involvement of caspases in neutrophil apoptosis: regulation by reactive oxygen species. *Blood* 92: 4808-4818.
497. Lucas, M., L. M. Stuart, J. Savill, and A. Lacy-Hulbert. 2003. Apoptotic cells and innate immune stimuli combine to regulate macrophage cytokine secretion. *J. Immunol.* 171: 2610-2615.
498. Fadok, V. A., D. L. Bratton, A. Konowal, P. W. Freed, J. Y. Westcott, and P. M. Henson. 1998. Macrophages that have ingested apoptotic cells in vitro inhibit proinflammatory cytokine

production through autocrine/paracrine mechanisms involving TGF-beta, PGE2, and PAF. *J. Clin. Invest.* 101: 890-898.
499. Chung, E. Y., J. Liu, Y. Homma, Y. Zhang, A. Brendolan, M. Saggese, J. Han, R. Silverstein, L. Selleri, and X. Ma. 2007. Interleukin-10 expression in macrophages during phagocytosis of apoptotic cells is mediated by homeodomain proteins Pbx1 and Prep-1. *Immunity* 27: 952-964.
500. Saraiva, M. and A. O'Garra. 2010. The regulation of IL-10 production by immune cells. *Nat. Rev. Immunol.* 10: 170-181.
501. Sonnichsen, B., S. De Renzis, E. Nielsen, J. Rietdorf, and M. Zerial. 2000. Distinct membrane domains on endosomes in the recycling pathway visualized by multicolor imaging of Rab4, Rab5, and Rab11. *J. Cell Biol.* 149: 901-914.

Appendix

Billings, E. A. performed all experiments and analysis shown in the Appendix. D'Souza, R.S. advised on the design and methods for the microscopy and performed the live cell imaging. Ravichandran, K.S. and Lee, C.S. provided critical reagents. Casanova, J. E. provided intellectual guidance.

Appendix

Preliminary examination of the localization of Rab11a in WT and BAI1-deficient macrophages after exposure to Gram-negative bacteria

TLR4 trafficking and cellular compartmentalization is crucial for downstream signaling and transcriptional responses. Husebye et al showed that Rab11a-mediated delivery of TLR4 from the ERC to the phagosome is required for effective TRIF-dependent cellular responses to Gram-negative bacteria (67). The confocal imaging presented in Chapter 3 indicated that BAI1 expression enhanced the association of TLR4 with *E. coli* (**Fig. 3-13**). However, this was not due to a defect in surface TLR4-MD2 internalization, which was normal in BAI1-deficient cells (**Fig. 3-10**). The mechanism leading to the recruitment of Rab11a is still unknown. This perhaps indicates that BAI1 may regulate the recruitment of Rab11a, and therefore intracellular TLR4, to bacterial phagosomes.

To determine whether BAI1 couples the Rab11a-positive compartment with the bacterial phagosome, we first examined the distribution of Rab11a in wild type and BAI1-knockout macrophages to identify if there were defects in Rab11a association with bacterial phagosomes. To do so, BMDMs from wild type and BAI1-deficient mice were transfected with a plasmid to express exogenous Rab11a-GFP using nucleofection. Cells were infected with either *E. coli* DH5α or the non-pathogenic, non-invasive ΔSPI1ΔSPI2 *Salmonella*, then fixed and stained to assess the recruitment of Rab11a to sites of bacterial association. We did not observe any global differences in the distribution of Rab11a in any conditions assessed (**Fig. A-1**). There appeared to be Rab11a surrounding phagosomes containing *E. coli* (**Fig. A-1A**) and *Salmonella* (**Fig. A-1B**) in wild type and

BAI1-deficient macrophages. The MFI of Rab11a around bacterial phagosomes normalized to the background intensity of the perinuclear region was measured in wild type and BAI1-deficient macrophages infected with both bacterial stimuli. There was no difference in the relative intensity of Rab11a around bacterial phagosomes when BAI1 was absent, moreover there was little enrichment of Rab11a signal relative to the background intensity in general (**Fig. A-1, C and D**). However, given the increased abundance of Rab11a in the perinuclear region and the rapid trafficking of internalized bacteria to that site, it is difficult to reliably assess any enrichment or contact between the Rab11a-positive compartment and bacterial phagosomes.

Rab11a is a master regulator of trafficking within the endosomal compartment. To better assess Rab11a dynamics and trafficking events we utilized live cell imaging. Again, primary BMDMs from wild type and BAI1-knockout mice were nucleofected to exogenously express Rab11a-GFP. Macrophages were infected with either *E. coli* or *Salmonella* and imaged. In both the wild type and BAI1-deficient cells the Rab11a compartment was highly dynamic and mobile (**Movies A, 1 to 4**). We observed Rab11a enriched within the perinuclear region, but its association with the plasma membrane and at membrane ruffles was also apparent. In cells incubated with either *E. coli* (**Fig. A-2, A and B, Movies A-1, A and B, Movies A-2, A and B**) or *Salmonella* (**Fig. A-2, C and D, Movies A-3, A and B, Movies A-4, A and B**) there was a substantial amount of contact and interaction with Rab11a, however enrichment was transient and fluctuated over time. These events differed from that described by Husebye et al, which was more stable and robust. Moreover, the kinetics of this interaction also differed. Husebye et al showed that Rab11a enrichment was detectable after 20 minutes post-infection. This was followed by

a continual enrichment of TLR4 out to 60 minutes after infection. We observed transient contact with the Rab11a compartment more rapidly after uptake, within 5-10 minutes of bacterial internalization. However, this interaction appeared to require trafficking towards the ERC and the perinuclear region. Again, quantification of Rab11a association with bacterial phagosomes in wild type and BAI1-deficient macrophages was not feasible given the transient nature of the interaction and the abundance of Rab11a within the perinuclear region. This may reflect Rab11a-GFP coming in and out of contact with bacterial phagosomes, or may reflect Rab11a enrichment coming in and out of the focal plane.

Interestingly, we saw a transient enrichment in Rab11a signal that occurred just after phagocytosis in macrophages infected with ΔSPI1ΔSPI2 *Salmonella* (**Fig. A-2, E and F, Movies A-5 and A-6**). We did not observe this phenomenon in cells incubated with *E. coli*, suggesting that differences in the route of entry or attachment may impact early Rab11a delivery. This perhaps reflects the previously established role of Rab11a in delivering membrane during phagocytosis. Collectively, it does appear that Rab11a contacts bacterial phagosomes in macrophages, but that the interaction is transient.

The results from theses studies were inconclusive and require additional pursuit. Quantitative analysis of the enrichment and duration of Rab11a in wild type and BAI1-deficient macrophages may be possible with additional work. However, because of the complex and dynamic relationship between the Rab11a-positive compartment and the bacterial phagosome, the techniques proposed in Chapter 5 would better resolve differences in Rab11a activity. Husebye et al showed that TLR4 association with bacterial phagosomes increased over time after phagocytosis and remained associated

with the bacterial phagosomes at the times assessed (67). A more detailed analysis of the TLR4 trafficking and delivery to bacterial phagosomes using live cell imaging may also provide insight into differences between BAI1-deficient and control macrophages.

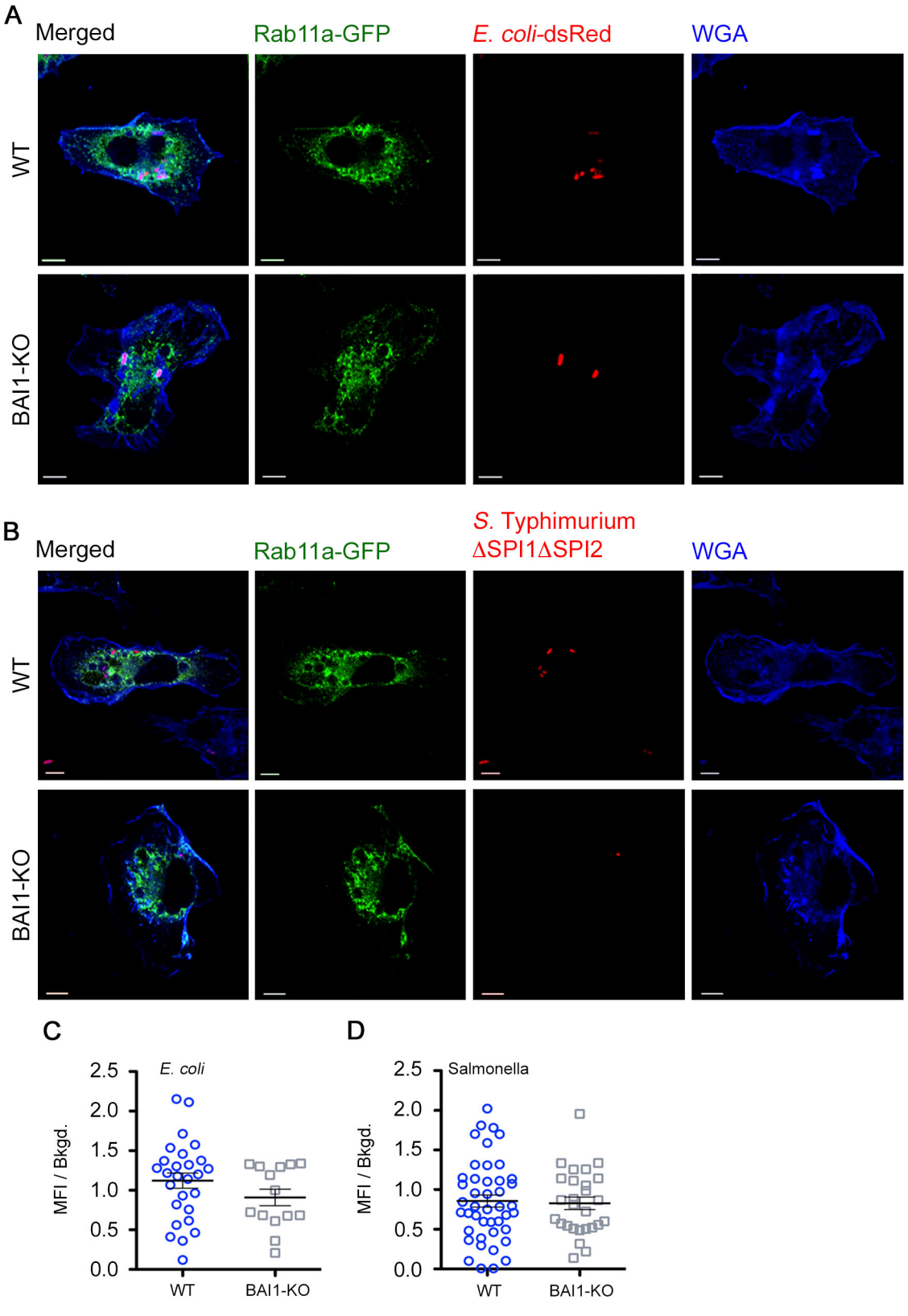
A
Merged
Rab11a-GFP
E. coli-dsRed
WGA
WT
BAI1-KO
B
Merged
Rab11a-GFP
S. Typhimurium
ΔSPI1ΔSPI2
WGA
WT
BAI1-KO
C
E. coli
MFI / Bkgd.
2.5
2.0
1.5
1.0
0.5
0.0
WT
BAI1-KO
D
Salmonella
MFI / Bkgd.
2.5
2.0
1.5
1.0
0.5
0.0
WT
BAI1-KO

Figure A-1. Rab11a is enriched in the perinuclear region near Gram-negative bacteria.

WT and BAI1-KO BMDMs expressing Rab11a-GFP were infected with (**A**) *E. coli* DH5α dsRed (red) or (**B**) ΔSPI1ΔSPI2 *Salmonella* at an MOI of 10. Cells were fixed and stained with anti-GFP antibody (green). The plasma membrane was labeled with wheat germ agglutinin (WGA, blue), and cells were imaged by confocal microscopy. The representative image shows a single confocal section. Scale bar, 5μm. Quantification of the mean fluorescence intensity (MFI) of Rab11a associated with (**C**) *E. coli* or (**D**) *Salmonella*. At least 5 cells per condition were analyzed. A region of interest (ROI) was drawn around each bacterium and the MFI was measured within the ROI (for details see Materials and Methods). Plot shows the MFI ± SEM of Rab11a per ROI after normalizing to an average background MFI (Bkgd). Data was analyzed using the Student's t-test.

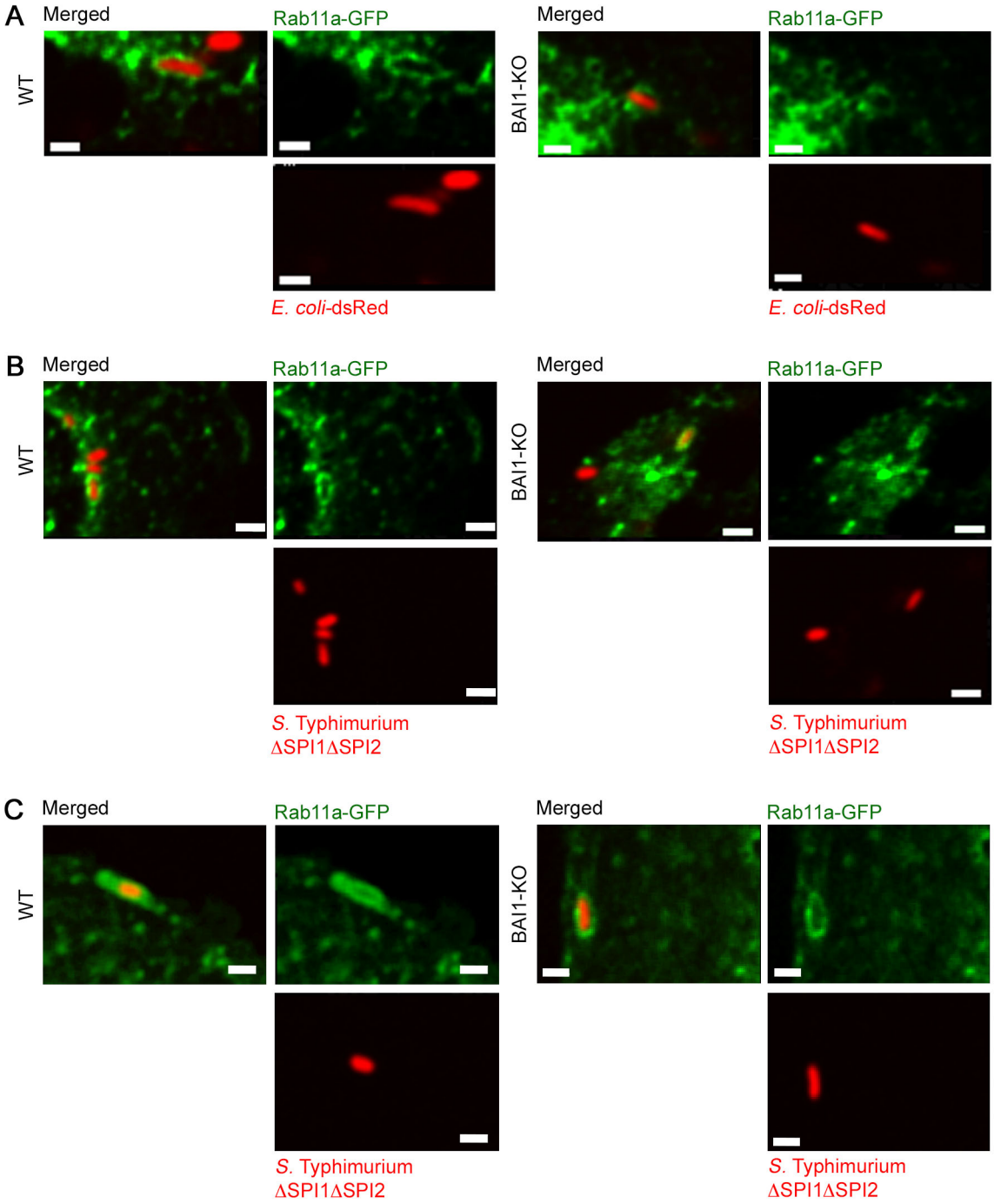
A
Merged
Rab11a-GFP
WT
BAI1-KO
E. coli-dsRed
B
S. Typhimurium
ΔSPI1ΔSPI2
C

Figure 2. Rab11a is transiently enriched around bacterial phagosomes

BMDMs from WT and BAI1-KO mice were incubated with *E. coli* DH5α or ΔSPI1ΔSPI2 *Salmonella* expressing dsRed. Cells were imaged for at least 30 minutes after infection. Movies show a single confocal section and were generated for at least four cells from two separate experiments. Scale bar, 1 μm. (**A**) A single cropped image from representative Movie A-1, A and B, and Movie A-2, A and B, shows Rab11a in WT or BAI1-KO BMDMs in contact with the *E. coli*-containing bacterial phagosome. (**B**) Shows a single image from representative Movie A-3, A and B, and Movie A-4, A and B, of WT or BAI1-KO macrophages infected with ΔSPI1ΔSPI2 *Salmonella*. (**C**) The recruitment of Rab11a-GFP during phagocytosis of ΔSPI1ΔSPI2 *Salmonella* in control and BAI1-KO BMDMs is shown as a single image from representative Movies A-5 and A-6.

Movie A-1, A and B. Rab11a is transiently enriched at bacterial phagosomes containing *E. coli* in wild type macrophages

WT BMDMs exogenously expressing Rab11a-GFP were incubated were incubated with *E. coli* DH5α expressing dsRed. Movies were taken as described in the materials and methods for at least 30 minutes after infection. Movie A-1A shows the entire cell (scale bar, 5 μm), while Movie A-1B shows a cropped movie focused on a limited number of bacteria (scale bar, 1 μm). Note the distribution of Rab11a and the interaction and contact with the Rab11a-compartment at the phagosome.

Movie A-2, A and B. Rab11a is transiently enriched at bacterial phagosomes containing *E. coli* in BAI1-deficient macrophages

BAI1-KO BMDMs exogenously expressing Rab11a-GFP were incubated with *E. coli* DH5α expressing dsRed. Movies were taken as described in the materials and methods for at least 30 minutes after infection. Movie A-2A shows the entire cell (scale bar, 5 μm), while Movie A-2B shows a cropped movie focused on a limited number of bacteria (scale bar, 1 μm). Note the distribution of Rab11a and the interaction and contact with the Rab11a-compartment at the phagosome.

Movie A-3, A and B. Rab11a is transiently enriched at bacterial phagosomes containing *Salmonella* in wild type macrophages

WT BMDMs exogenously expressing Rab11a-GFP were incubated were incubated with ΔSPI1ΔSPI2 *Salmonella* expressing dsRed. Movies were taken as described in the materials and methods for at least 30 minutes after infection. Movie A-1A shows the entire cell (scale bar, 5 μm), while Movie A-1B shows a cropped movie focused on a limited number of bacteria (scale bar, 1 μm). Note the distribution of Rab11a and the interaction and contact with the Rab11a-compartment at the phagosome.

Movie A-4, A and B. Rab11a is transiently enriched at bacterial phagosomes containing *Salmonella* in BAI1-deficient macrophages

BAI1-KO BMDMs exogenously expressing Rab11a-GFP were incubated with ΔSPI1ΔSPI2 *Salmonella* expressing dsRed. Movies were taken as described in the materials and methods for at least 30 minutes after infection. Movie A-2A shows the entire cell (scale bar, 5 μm), while Movie A-2B shows a cropped movie focused on a limited number of bacteria (scale bar, 1 μm). Note the distribution of Rab11a and the interaction and contact with the Rab11a-compartment at the phagosome.

Movie A-5. Rab11a is rapidly enriched and lost at sites of bacterial internalization of *Salmonella* in wild type macrophages

WT BMDMs exogenously expressing Rab11a-GFP were incubated were incubated with ΔSPI1ΔSPI2 *Salmonella* expressing dsRed. Movies were taken as described in the materials and methods for at least 30 minutes after infection. Movie A-5 shows a representative cropped movie of the internalization of a single bacterium (scale bar, 1 μm). Note the enrichment of Rab11a just after uptake.

Movie A-6. Rab11a is rapidly enriched and lost at sites of bacterial internalization of *Salmonella* in BAI1-deficient macrophages

BAI1-KO BMDMs exogenously expressing Rab11a-GFP were incubated were incubated with ΔSPI1ΔSPI2 *Salmonella* expressing dsRed. Movies were taken as described in the materials and methods for at least 30 minutes after infection. Movie A-5 shows a representative cropped movie of the internalization of a single bacterium (scale bar, 1 μm). Note the enrichment of Rab11a just after uptake.

Materials and Methods

Ethics statement

All experiments were performed in accordance with the recommendations in the Guide for the Care and Use of Laboratory Animals of the National institutes of Health. Protocols were approved by the Institutional Animal Care and Use Committee at the University of Virginia (Protocol number 3488).

Plasmids

The pEGFP-C3-Rab11a construct used in this study is from Sönnichsen et al (501).

Mice

Age- and sex-matched C57BL/6 mice between 6 and 10 weeks of age were used for the harvesting of primary macrophages. BAI1 knockout mice have been described previously (227). Mice were housed in pathogen-free conditions.

Isolation and culture of cells

To generate BMDMs, cells were seeded onto non-tissue culture treated plastic plates and cultured in RPMI supplemented with 10% FBS, 10% L929-conditional medium (as a source of colony-stimulating factor-1), and 1% pen-strep. BMDMs were cultured for 6 days ex vivo before use, and the culture medium was changed every 2 days. Macrophage differentiation was confirmed by flow cytometric analysis of the cell surface abundances of F4/80 (eBioscience, clone BM8) and CD11b (eBioscience, clone M1/70).

Bacterial strains and culture

All bacteria, including *Escherichia coli* DH5α (Invitrogen, 18265-017) or *Salmonella* Typhimurium SL1344 ΔorgA ΔspiA (SPI1 and SPI2 double mutant, e.g. ΔSPI1ΔSPI), from Dr. Denise Monack at Stanford University, were cultured overnight in Luria-Bertani

(LB) broth under aerobic conditions before use. Immunofluorescence microscopy was performed using ΔSPI1ΔSPI2 *Salmonella* Typhimurium or *E. coli* expressing dsRed (312).

Immunofluoresence microscopy

1×10^5 transgenic BMDMs, nucleofected with 1μg pRab11a-GFP construct according to the manufacturers instructions (Lonza), were plated on fibronectin-coated coverslips (Sigma). The following day, the cells were incubated with *E. coli* DH5α-dsRed or ΔSPI1ΔSPI2 *Salmonella*-dsRed at an MOI of 10 for 30 min at 37°C. Cells were then fixed with 4% PFA and labeled with Alexa Fluor 647-conjugated wheat germ agglutinin (WGA) (Life Technologies, 5 μg/ml) in Hanks' balanced salt solution (HBSS) for an additional 10 min to label the plasma membrane. After washing, the cells were permeabilized for 30 min in PBS containing 3% BSA, 1% normal goat serum (NGS), and 0.1% Triton X-100. Cells were labeled with Rabbit anti-GFP antibody (Sigma, G1544) followed by Alexa Fluor 488-conjugated anti-rabbit secondary antibody. Regions of interest (ROIs) for *E. coli* or *Salmonella*-treated cells were determined by dsRed signal. Images were captured with a Nikon C1 Plus confocal microscope with Z-stacks at 0.5-μm. Analysis and processing was performed with NIS-Elements software (Nikon). Cell-associated bacteria were defined as regions of interest (ROIs).

Live-cell imaging

BMDMs were nucleofected with 1μg of pRab11a DNA according to the manufacturers instructions (Lonza). Cells were plated on fibronectin-coated Matek dishes (P35G-1.5-14c) 18 hours before imaging. Imaging was performed in imaging media (Molecular Probes, A14291DJ) containing 10% heat-inactivated FBS. Cells were infected with either

E. coli DH5α expressing dsRed or ΔSPI1ΔSPI2 *Salmonella* expressing dsRed and imaged with a 100X objective fitted to a Nikon TE 2000 microscope equipped with a Yokogawa CSU 10 spinning disc and a 512X512 Hamamatsu 9100c-13 EM-BT camera. Movies were captured at a frame rate of 500 ms.